WAR DEPARTMENT
CORPS OF ENGINEERS
ENGINEER DEPARTMENT

HELFERT
DEPARTMENT OF COMMERCE
WEATHER BUREAU
HYDROMETEOROLOGICAL SECTION

MAXIMUM POSSIBLE PRECIPITATION

SACRAMENTO RIVER BASIN

HYDROMETEOROLOGICAL REPORT NO. 3

Department of Commerce
Weather Bureau
Hydrometeorological Section

War Department
Corps of Engineers
Engineer Department

Hydrometeorological Report No. 3

MAXIMUM POSSIBLE PRECIPITATION

OVER THE SACRAMENTO BASIN OF CALIFORNIA

A Study of Meteorological Causes of Record
Storms and Quantitative Estimates of
Critical Precipitation Rates

Prepared by

The Hydrometeorological Section of the Weather Bureau

in cooperation with

The Corps of Engineers, U. S. Army

and submitted

May 15, 1942

Published at
U. S. Waterways Experiment Station
Vicksburg, Mississippi
1943

TABLE OF CONTENTS

INDEX TO TABLES

INDEX TO FIGURES

APPENDIX: SYNOPTIC WEATHER CHARTS

FOREWORD

1. In a letter dated May 21, 1941, the U. S. Engineer Department, Corps of Engineers, requested that "upon completion of the basin studies to determine limiting precipitation rates and snow melt conditions for the tributary areas above Pittsburgh, Pa., . . . the Hydrometeorological Section undertake similar studies for the Sacramento River Basin, California." Work on the new assignment was begun about August 1, 1941.

2. Preliminary investigations by the U. S. Engineer Department had identified nine critical storms of record, from the viewpoint of runoff. Under a cooperative plan the detailed rainfall analysis was prepared by the Sacramento District for five of these storms, by the San Francisco District for one, and by the Hydrometeorological Section for three.

3. This report on the Sacramento Basin follows the publication of two previous reports, now to be given wider distribution, in which certain fundamental hydrometeorological techniques were employed and their theoretical bases developed. These reports (No. 1 and 2, respectively) are "Maximum Possible Precipitation over the Ompompanoosuc Basin above Union Village, Vermont," originally issued March 18, 1940, and "Maximum Possible Precipitation over the Ohio River Basin above Pittsburgh, Pennsylvania," originally issued June 16, 1941, both reports

prepared by the Hydrometeorological Section in cooperation with the U. S. Engineer Department. In the current report many references are made to material developed in the previous reports, which will be called the Ompompanoosuc Report and the Pittsburgh Report, respectively.

4. The report presents, in a logical sequence, the facts and the methods that are the basis for the derivation of the maximum possible storm over the Sacramento Basin. The arrangement of details differs slightly from previous reports. The physical characteristics of the basin are briefly discussed in Chapter I. In treating the climatology of the region a new approach was preferred which justifies the title of Chapter II, "Dynamic Climatology." The usual citation of the averages and extremes of meteorological elements was found to be an inadequate description of the climate of so topographically complex a basin. Furthermore, it was felt that, for the purposes of the report, a clarification of the position of the basin in the general circulation of the atmosphere would lay the proper foundation for the meteorological description of the major storms. It follows, then, that there is more than the usual amount of "meteorology" in the chapter on the climatology, but it is obvious that there can be no sharp demarcation between the two sciences. Naturally, also, the vertical distribution of the climatic elements is stressed.

5. The special methods of rainfall analysis used in this report are explained in Chapter III, with particular emphases on the use of the normal seasonal precipitation map developed by the Sacramento Engineer District and the subdivision of the region into zones of similar rainfall character. In the next chapter the flood record of the Sacramento Valley

is examined exhaustively and tables are presented which make the floods comparable on the basis of representative percentages of normal seasonal precipitation for specific subdivisions of the basin.

6. As a preliminary to the synoptic analyses of the major storms in Chapter V, the Sacramento "storm type" is defined and the use of the normal seasonal precipitation as the basic distribution pattern meteorologically justified. The major storms are found to rank in the same order both in cyclonic intensity and 72-hour maximum depth of rainfall. Because of their historical importance, a short analytical description of the January 1862 storms is included, although the data are scant.

7. In Chapter VI on "Maximum Possible Precipitation" the computation methods developed in previous reports, particularly the Pittsburgh Report, are further refined for use on a basin with high orographic boundaries. Three types of orographic precipitation are defined and it is shown that one combination of types would be most critical for the Sacramento. After development of the basin constants for various directions of inflow, the formula for the computation of maximum precipitation is derived. At this point the validity of the formula is tested by comparison of the intensities of rainfall in each major storm, as computed from the rainfall data and as computed from the formula using the actual wind and dew points observed in the storm. It should be pointed out that the computations were made independently of each other, and were made, in fact, in order to derive a correction coefficient to be applied to the formula. The agreement is good enough, however, to justify the use of the formula without a coefficient. It is necessary only to find the maximum possible values of wind and dew point. This is done before

the maximum possible precipitation is computed.

8. In Chapter VII the snow melt factors are evaluated, the basin constants modifying the theoretical formula determined, and the most critical antecedent distribution of snow cover justified from past records. In the final chapter, the values obtained in the previous two are summed and the distribution of increments in area and time restricted by meteorological considerations. The results are the maximum possible storms for the basin as a whole and for the assigned tributary basins as individuals.

9. The glossary, which follows the last chapter, includes no terms that are not used within the report. Since its readers will include hydrologists, engineers and meteorologists, it was felt that a worthy purpose would be served in acquainting one group with the terminology of the other.

10. A bibliography is added to this report on account of the extraordinary wealth of material available for the region. The list includes, of course, all the works, general or specific, to which reference is made in the text of the report. The textual references are indicated by underlined numbers enclosed within parentheses. In addition, it was decided to include within the bibliography selected material which has specific bearing on the Sacramento Basin.

11. For facility in reading, all the figures appear within the text of the report, except that all synoptic charts (referred to in Chapter V) are relegated to the Appendix.

12. Reports prepared by the Division and District Offices of the

U. S. Engineer Department, containing precipitation data, isohyetal maps, and mass rainfall curves for a large number of major storms have formed a broad basis for the study of storm patterns and precipitation characteristics. In addition to published records, such reports include all precipitation data and miscellaneous information on storms obtainable from the manuscripts of original records, files of municipal agencies, newspapers, testimony of witnesses, and similar sources. Data assembled and organized by the Engineer Offices are reviewed by the Hydrometeorological Section and are supplemented by meteorological analyses. There has been profitable collaboration with representatives of the Office of Chief of Engineers and with personnel visiting the Section from District and Division Offices of the Engineer Department. The following members of the Hydrometeorological Section contributed to the preparation of the final report:

Collaborators

A. K. Showalter, Meteorologist in Charge
P. Light, Assistant Hydrologic Engineer
C. Woo, Assistant Hydrologic Engineer
G. N. Brancato, Assistant Meteorologist
P. R. Jones, Assistant Meteorologist
A. L. Shands, Assistant Meteorologist
S. B. Solot, Assistant Meteorologist
D. J. Stevlingson, Assistant Meteorologist
H. K. Gold, Junior Meteorologist
J. R. Rosenthal, Junior Meteorologist

Consultants

Merrill Bernard, Principal Hydrologist
H. C. S. Thom, Associate Hydrologic Engineer
W. T. Wilson, Assistant Hydrologic Engineer

The above were ably assisted by the sub-professional and clerical staff.

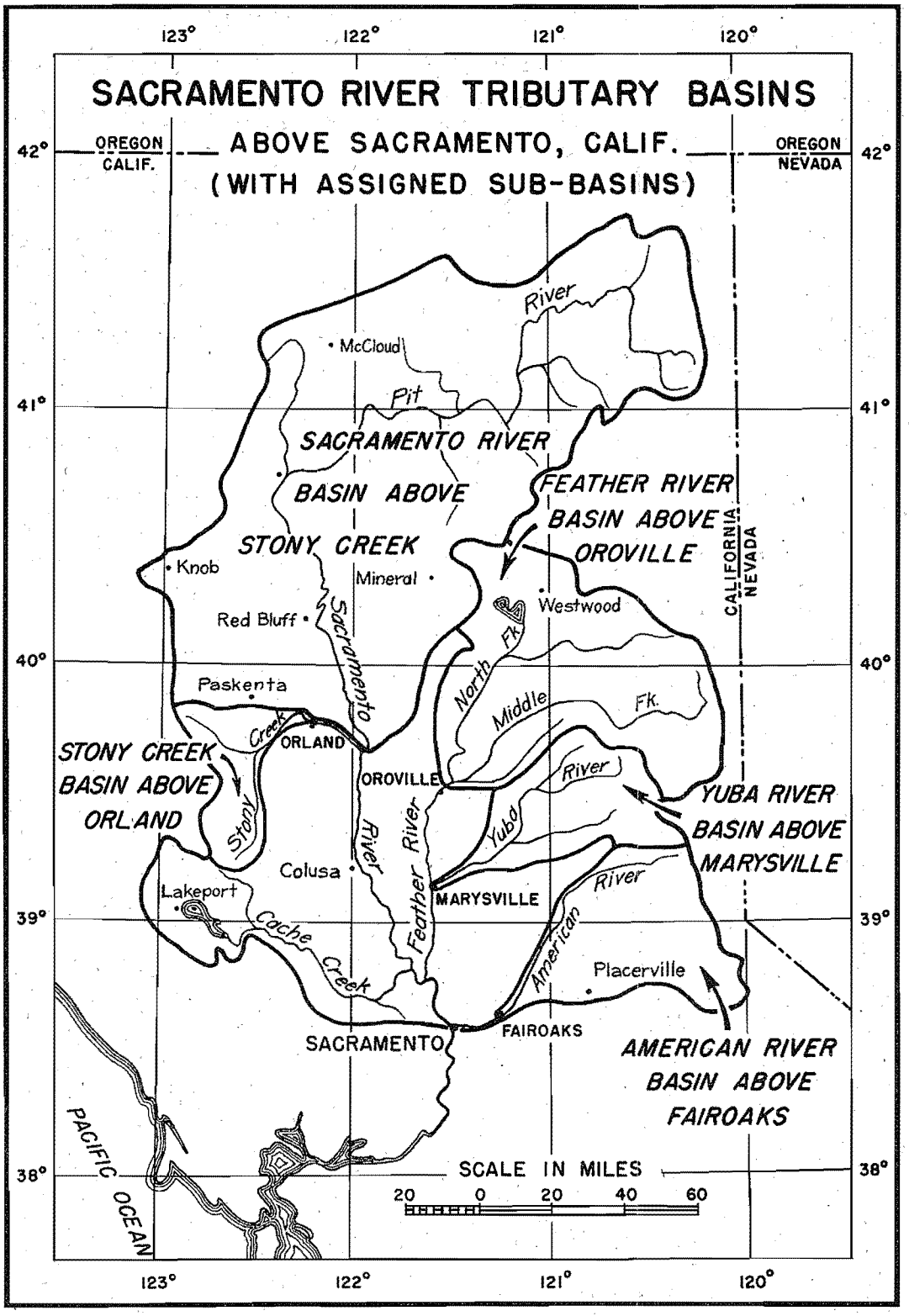
SACRAMENTO RIVER TRIBUTARY BASINS
ABOVE SACRAMENTO, CALIF.
(WITH ASSIGNED SUB-BASINS)
123°
122°
121°
120°
42°
41°
40°
39°
38°
OREGON
CALIF.
OREGON
NEVADA
CALIFORNIA
NEVADA
McCloud
Pit
River
SACRAMENTO RIVER
BASIN ABOVE
STONY CREEK
FEATHER RIVER
BASIN ABOVE
OROVILLE
Knob
Mineral
Red Bluff
Sacramento
Westwood
North Fk.
Middle Fk.
Paskenta
Stony Creek
ORLAND
OROVILLE
STONY CREEK
BASIN ABOVE
ORLAND
Stony
River
Feather River
Yuba
River
YUBA RIVER
BASIN ABOVE
MARYSVILLE
Colusa
Lakeport
MARYSVILLE
Cache Creek
American
River
Placerville
FAIROAKS
SACRAMENTO
AMERICAN RIVER
BASIN ABOVE
FAIROAKS
PACIFIC OCEAN
SCALE IN MILES
20 0 20 40 60

Figure 1

CHAPTER I

PHYSICAL CHARACTERISTICS

13. Location. The Sacramento River Basin occupies the northern third of the Great Central Valley of California, lying between the Coast Range on the west and the Sierra Nevadas on the east. Figure 1 shows the location of the basin and outlines the tributary basins assigned for study. These tributary basins, as well as the total basin, are listed below:

Basin	Above	Area (Sq. Mi.)
Sacramento	Stony Creek	11,500
Stony Creek	Orland	772
Yuba	Marysville	1,330
Feather	Oroville	3,640
American	Fair Oaks	1,921
Sacramento	Latitude of Sacramento	25,200

It should be noted that for the purposes of this report the Goose Lake Basin in the upper Sacramento region is excluded from the total basin area although Goose Lake has been known to flow into the Pit River.

14. Topography. Except for a narrow gap in the Coast Range

through which the San Joaquin and Sacramento Rivers flow into the Pacific Ocean, the Great Central Valley is completely enclosed by mountain ranges. The Tehachapi Mountains, forming the southern limits of the valley, connect the Coast and Sierra Nevada Ranges. The latter, forming respectively the western and eastern borders, converge in the north to complete the mountainous circuit through the Klamath Mountains (including the Trinity group), Mt. Shasta, the upper Pit River Plateau and the Warner Range. Figure 2 shows the location of profiles, plotted in Figures 3 and 4, of the mountains surrounding the Great Central Valley. It should be noted that both profiles begin at Mt. Shasta and end at Double Mountain. The distances indicated are measured from Mt. Shasta along the irregular course of the profile as shown in the plan view of Figure 2. The valley floor is comparatively level, sloping from an elevation of 60 feet at Sacramento in the south to 330 feet at Red Bluff in

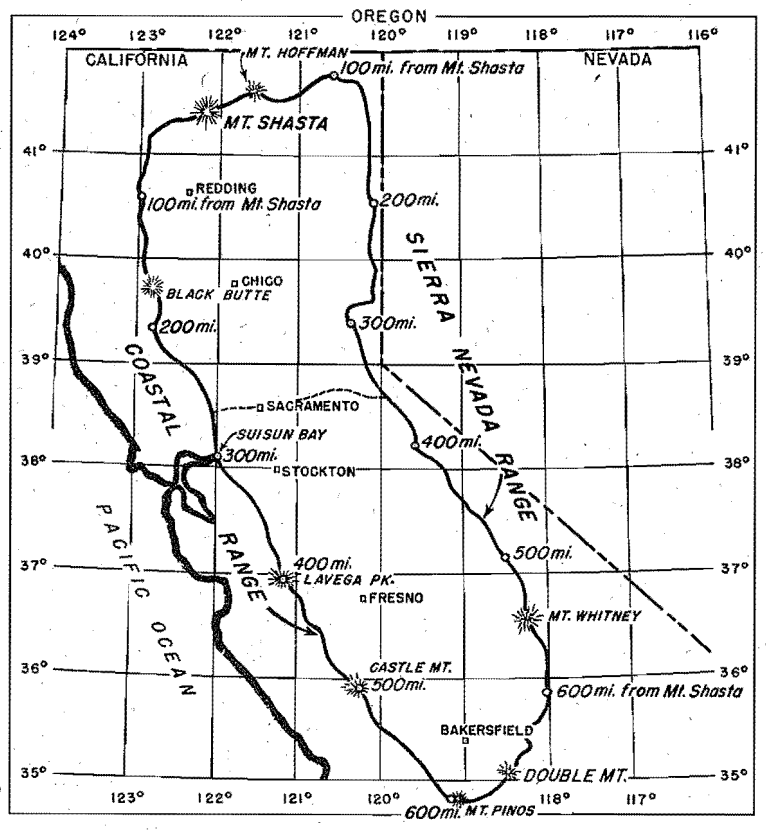

Figure 2

Location of profiles of Sierra Nevada and Coastal Ranges adjoining the Central Valley of California (see Figures 3 and 4)

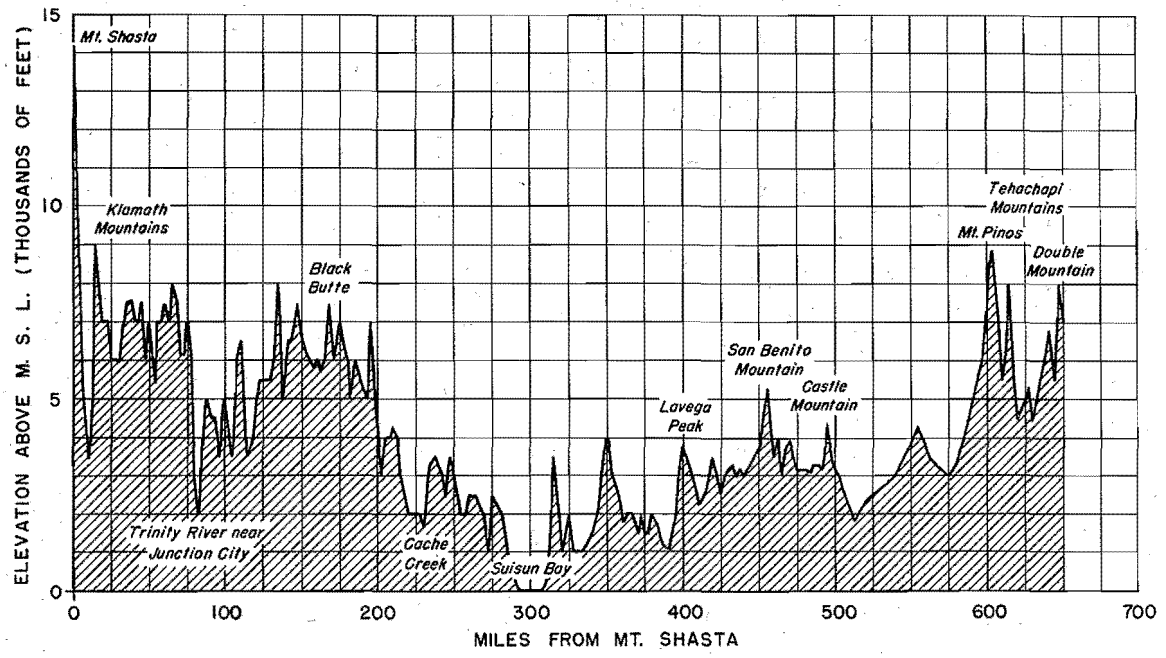

Figure 3

Profile of Coastal Range of the Central Valley of California (see Fig. 2)

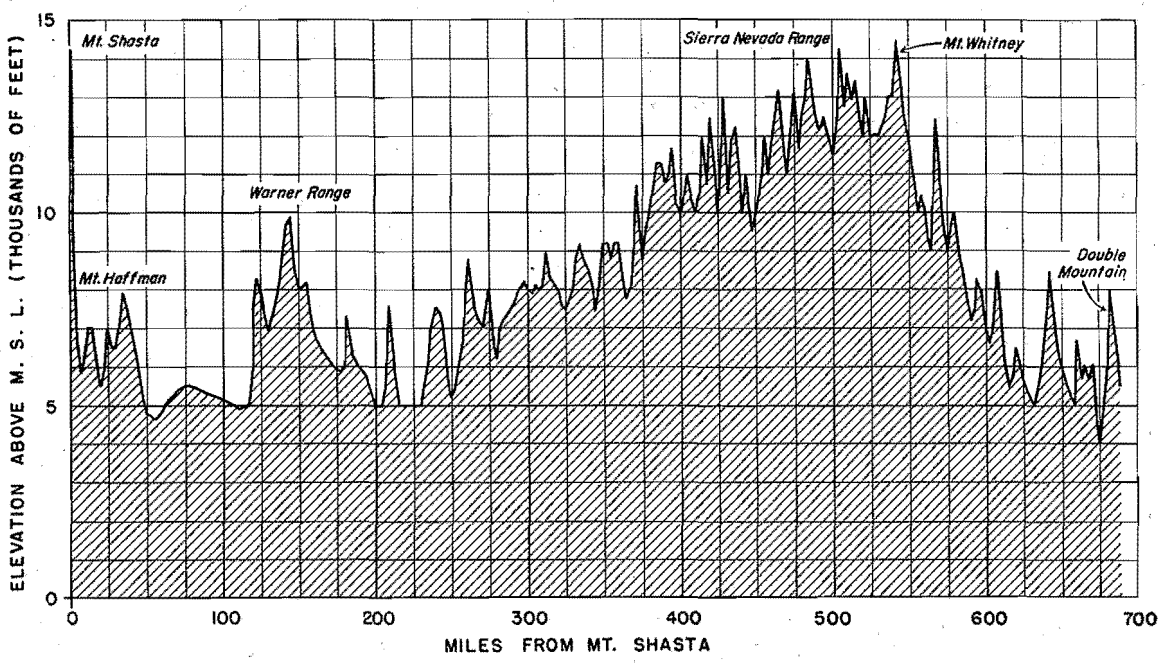

Figure 4

Profile of Sierra Nevada Range of the Central Valley of California (see Fig. 2)

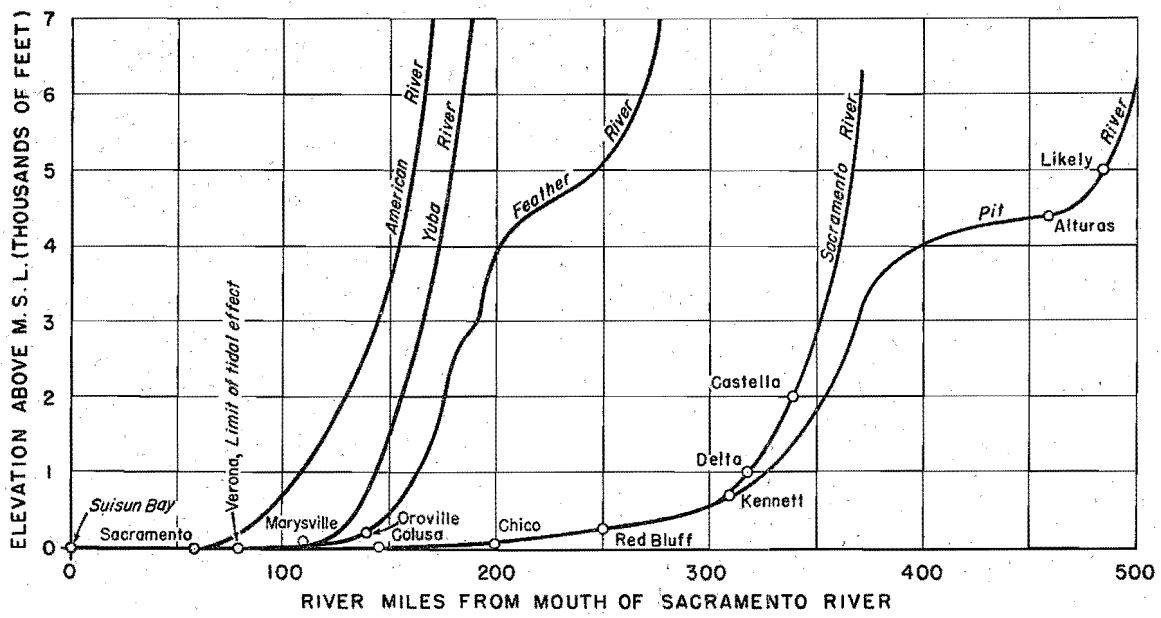

Figure 5

Stream profiles of the Sacramento River System

the north. It is 150 miles long, tapering from an approximate 50-mile width at Sacramento to about a 20-mile width at Redding. The stream profiles are very steep in the mountainous areas and flatten abruptly on reaching the valley floor, as shown in Figure 5.

15. Vegetative Cover. The native vegetative cover in the basin is roughly distributed as follows:

a. Marsh grassland, 20 miles wide, in the valley from Sacramento to Marysville.

b. Bounding the marsh grass, in a large U-shape open at the south, bunch grass -- over-all width 60 miles and extending 150 miles north from Sacramento.

c. On the periphery of the U-shaped area a strip of chaparral, 10 to 30 miles in width, widest on the east.

d. Next a concentric band of Western Pine forest, 20 to 40 miles wide.

e. A region of desert shrub in the upper Pit plateau.

f. Surrounding this desert shrub, a strip of coniferous woodland.

g. Western Pine forest at higher elevations in the northeastern portion of the basin.

Except in the Upper Feather and Pit Basins, the area above 2,500 feet is occupied by dense forest. Below that elevation, excluding the valley floor, the region may be designated as open-forested area and woodland. On the whole, forest density increases with elevation through the zone of maximum precipitation which is roughly between 4,000 and 6,000 feet (45).

16. Hydrologic Features. The Sacramento River Basin is probably unique among basins of its size in its varied hydrologic characteristics and in its hydraulic structures built to control floods. Only a brief description of these features will be presented. For more extensive treatment of the subject the reader is referred to a paper by Otto H. Meyer (66).

17. The main tributary streams of the Sacramento River have their headwaters in the high mountains of the Sierra Nevada and the Coast Range. These streams concentrate their flood flows rapidly and deliver large volumes of water to the main channel of the Sacramento River which flows through the comparatively flat valley bottom. A system of levees and bypasses has been constructed to protect the natural overflow land along the lower reaches of the stream, and several weirs are situated at strategic points to divert water during flood periods from the Sacramento River into the two main bypass channels, Sutter and Yolo.

18. Numerous storage reservoirs for flood control, irrigation, power, navigation, etc., serve to regulate flood runoff. During the December 1937 flood 480,000 acre-feet, or 15% of the total runoff, was

stored in this manner (65). The completion of Shasta Dam on the Sacramento River near Kennett will add 4,500,000 acre-feet to the total artificial storage capacity in the basin. In terms of average depth over area this signifies a potential storage of 12.8 inches for the basin above Shasta Dam and 3.4 inches for the entire basin area.

19. Major inflows into the Sacramento River are contributed by the Upper Sacramento River in the northern portion of the basin, by the Feather, Yuba, Bear, and American River Basins of the Sierra Nevada section in the east, and by the Stony Creek and Cache Creek drainages of the Coast Range in the west. Critical areas from the hydrologic standpoint can therefore be outlined from the above considerations to form a basis for the assembly of flood flows at Sacramento. To facilitate the analysis of storm rainfall, as explained in Chapter III, the basin was further subdivided. These subdivisions are shown in

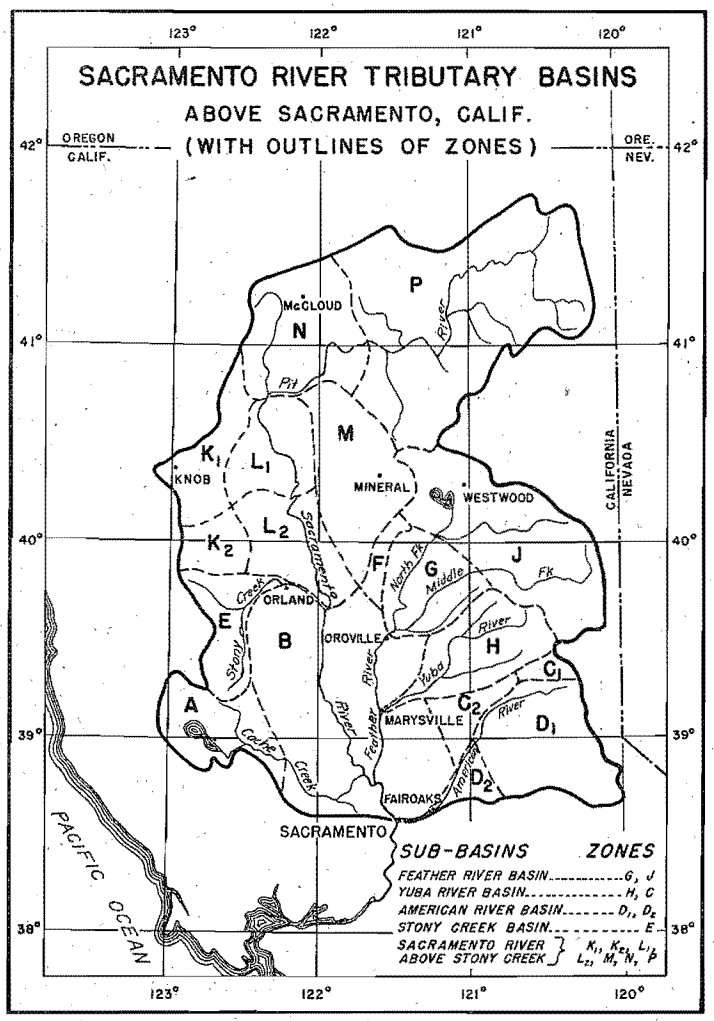

Figure 6

Figure 6 and defined in the following table:

TABLE 1

IDENTIFICATION OF ZONES

Zone A	Area of Cache Creek Basin above the 1000-foot level
Zone B	Lower Sacramento Valley below 1000 feet
Zone C_1	Area of Yuba River Basin above Spaulding Dam
Zone C_2	Area of Bear River Basin above 1000 feet
Zone D_1	American River Basin above 2000 feet
Zone D_2	American River Basin at Fair Oaks below 2000 feet
Zone E	Stony Creek Basin at Orland
Zone F	Area of Butte Creek Basin above 1000 feet
Zone G	Lower portion of Feather River Basin at Oroville
Zone H	Yuba River Basin at Marysville
Zone J	Upper portion of Feather River Basin
Zone K_1	Eastern slope of Coast Range above 1000 feet in Sacramento Basin above Sacramento River gaging station near Red Bluff
Zone K_2	Eastern slope of Coast Range above 1000 feet in Sacramento Basin between Sacramento River gaging station near Red Bluff and Stony Creek
Zone L_1	Upper Sacramento Valley below 1000 feet above Sacramento River gaging station near Red Bluff
Zone L_2	Upper Sacramento Valley below 1000 feet between Sacramento River gaging station near Red Bluff and Stony Creek
Zone M	Western slope of Sierra Nevada in Upper Sacramento Basin above 1000 feet
Zone N	Lower portion of Sacramento Basin above Shasta Dam
Zone P	Upper portion of Sacramento Basin above Shasta Dam

CHAPTER II

DYNAMIC CLIMATOLOGY

20. The Semipermanent Centers of Action. Although it is obviously the topography which is responsible for the specific and varied features of the climate within the confines of the Sacramento Basin, the general and over-all nature of the climate is dependent upon the basin's latitude and position on the west coast of a continent. This is so because the semipermanent pressure centers over the ocean that develop from the general circulation of the atmosphere are the dominating influences on the climate of the entire west coast. In the mean pattern these centers are located within the belts of comparatively low and high pressure that extend around the earth at about latitudes 55° N. and 35° N., respectively. Following the annual march of solar altitude, the pressure belts are farthest south in the winter of the Northern Hemisphere, farthest north in the summer. The number of anticyclonic and cyclonic systems (chiefly the latter) within each belt depends largely on the mean speed of the westerlies between the two latitudes (83). Characteristic of ocean areas lying to the west of continental masses in the Northern Hemisphere are the Aleutian Low and the Pacific (sometimes called the California or Hawaiian) High of the North Pacific Ocean.

21. The "permanence" of these two centers is statistical, rather than actual, but of the two, the Pacific anticyclone is more nearly permanent. Most Highs are the cold type, thermal in origin and migratory, with anticyclonic circulation seldom extending upward beyond three kilometers. The Pacific High, however, is chiefly dynamic in origin (83), remaining approximately stationary for long periods of time and retaining its anticyclonic circulation throughout the troposphere. Its center generally persists in the region between 140°-150° W. longitude and 30°-40° N. latitude. Gradually increasing in strength and extent during the summer months, a maximum is reached in August, with the center then displaced farthest north and west. This is followed by a decline to a minimum in January when the center is usually farthest southeast. Occasionally in winter months the anticyclone exhibits an eastward extension past the Sierra Nevada Range, where it is reinforced by radiational cooling and resultant air drainage to form the Great Basin High (42, 83).

22. The development of the Aleutian Low is dependent upon the outflow of cold polar air from its source over the interior of Asia (83). It follows that this Low attains its maximum intensity and geographical expanse during January when it is displaced farthest southward. As a center of action it is practically nonexistent during the summer and not an important factor in California weather between May and September.

23. It is of course possible that the summer distribution of these centers of action may occur during the winter or vice versa. The latter situation does not persist because the source of cold air is limited; but when the former anomaly occurs and persists throughout the major portion of the season, an abnormally dry winter over California ensues. It is

also interesting to note that the final clearing front which ends a series of winter rains in this region is often followed by the re-establishment of the Pacific anticyclone in midsummer strength and position.

24. The normally dry summer of the Sacramento Basin results, then, from the basin's position beneath the deep current rounding the northeast side of the Pacific anticyclone. Over the mainland the current is from the northwest up to 1500 meters, but above that level it backs to southwest as it travels around the upper-air standing wave that is troughed at approximately 130° W. (72, pp. 152-153; 107). Regardless of the direction from which it crosses the coast line the current is, nevertheless, generally from the north side of the anticyclone, traveling down slope and diverging as it approaches the eastern edge of the cell. The result is a dry and stable air mass (72, p. 147). In the more southern latitudes the trades have moved northward for the season. The winds aloft at Pearl Harbor, for example, are northeast to high levels. Tropical air from this source, or polar air modified by a sojourn over this region, is thus excluded from the California coast. Occasionally a simultaneous westward shift of the centers of the Pacific High and the summer continental high-level anticyclone (71, 75, 76) brings tropical air aloft to California from the Atlantic source. But even this air, sometimes found in San Diego soundings (14), has been partially dehydrated in its westward passage across the mountains of Mexico and stabilized by subsequent down-slope motion toward the Sacramento Valley. In New Mexico and Arizona and northward it is this current, as Reed has shown (76), that is responsible for the summer rains of that region. In southern California it is the cause of the so-called Sonora summer rains (93, pp. 151-152;

15). Local in character, the convective showers occurring in this air are generally confined to the area south of the Tehachapis and east of the Sierras. In the Great Central Valley of California rain rarely occurs during the summer months.

25. The southward displacement of both semipermanent centers in the winter alters the prevailing air flow over the Sacramento Basin. While the Aleutian Low has deepened and strengthened, the anticyclone has diminished not only in central pressure but also in size. The trade winds have followed the thermal equator southward, as have the polar front and the mean storm track. The southwest current preceding each storm now travels around the western side of the anticyclone, up slope and direct from tropical latitudes (72, p. 147). During this season California thus appears more often in the path of tropical (or polar becoming tropical) maritime air aloft and, by the same token, also more often in the path of the cyclonic systems moving inland from the Pacific. The result is the rainy season.

26. Proximity of the Pacific Ocean. The nearness of the basin to the ocean, in conjunction with the prevailing westerly direction of the wind, means that the most frequently recurrent air masses are brought in from the ocean and will, hence, usually exhibit maritime characteristics. As shown in the Ompompanoosuc Report (1), the temperature of the water in the source region over which the air mass obtains its moisture properties will determine the upper limit of the amount of precipitable water in a moist column of air over that region. For the tropical maritime air affecting the Sacramento Basin, the southern limit of the Pacific source can be considered to be latitude 25° N. For the area extending 5° north

of that latitude, and bounded by the meridians 145° and 165° W., the mean sea surface temperature for the months of December to March, inclusive, is 69 F (59). That would be the average surface dew point of a saturated air mass over that region during the bulk of the Sacramento Basin's rainy season. Its maximum value would limit the maximum value over the basin. However, a more adequate determination of the maximum dew point temperatures and their distribution, applicable to the basin, was obtained from land station observations made through the tropical air masses. The data used are presented in Chapter VI, entitled "Maximum Possible Precipitation." During the colder season of the year the isotherms of water temperature of the North Pacific Ocean are parallel to the circles of latitude, with gradient directed northward. In the summer months this gradient is disturbed by the upwelling of the cold bottom water along the coast, an effect that extends westward about 370 miles off Cape Mendocino and 1300 miles off San Diego, California (21, 56). The stabilizing effect in the region of these water surface temperatures is therefore greatest in summer when the ocean temperatures are comparatively lower, and least during the winter season.

27. In general, cold polar air masses invading the Pacific Ocean from continental areas are made unstable and increasingly moist by warming from below. Tropical air masses moving northward are cooled from below, becoming stabilized in their lower layers and losing some slight moisture by condensation into surface fog. The amount of modification undergone by a k-type air mass varies directly with the length of its trajectory over the water, but the most convectively unstable air mass will not be the one with the longest trajectory. Byers, in his "Air

Masses of the North Pacific" (18, p. 320) states: "... the rate of change of θ_E (equivalent potential temperature) with elevation varies inversely as the length of the maritime trajectory." Since the lapse rate of equivalent potential temperature is the index of convective instability, the short trajectory of arctic or polar continental air from British Columbia to north and central California by way of the ocean results in the creation of the most convectively unstable air and often provides the last sharp cold front rainfall of the winter storms over the basin. At the other extreme, an air mass with a long sojourn over lower latitudes will develop a lapse rate of θ_E that is not as steep, and consequently less convectively unstable. Most of the storm rainfall over the Sacramento Basin falls from air, often designated as mPk becoming mTk (see Chapter V), whose properties are between the two extremes.

28. In the modification of the cold polar air masses as they pass southward over the warmer waters of the Pacific Ocean, the air temperatures in the lower layers are raised to such an extent that freezing temperatures in this air do not on the average occur below four thousand feet. The mean elevation of the snow line on the Sierra Nevada slope thus becomes a function of the oceanic modification. It is obvious that in the most intense type of storm, however, the freezing isotherm can be at so high a level that rain will fall at almost all elevations in the basin, with flood consequences that are fully discussed in Chapter V on "Major Storms" and Chapter VII on "Snow Melt."

29. Topography. The large-scale factors already discussed determine the basin's general climate. For the specific variations in that climate within the basin, the variations in the topography are

responsible. The nature of that topography has already been discussed in the previous chapter (see Figures 2, 3, and 4). It should be pointed out that while the profiles in Figures 3 and 4 generally follow the drainage divide, they also indicate the elevations to which air must rise on entering and leaving the Sacramento Valley. These profiles show that the prevailing westerlies can enter the valley at sea level only by way of the Golden Gate; therefore the delta region of the basin experiences somewhat cooler summer temperatures (see Figure 9) than the remote areas. Deflected northward over the Sacramento Basin, this stream of maritime air becomes the prevailing low level south wind.

30. The elevation of a station within its surrounding air mass will largely determine its temperature. In other words, the station temperature will correspond, more or less closely, to the temperature of the free air at the station's altitude. Some effective modification of the expected mean value will result from the leeward or windward position of the station, from sheltering afforded by mountains and, as shown above, from nearness to the San Francisco Bay area. Air masses moving up the slopes of the Coast Range will be cooled by adiabatic expansion. Moving down slope into the basin they will undergo a rise in temperature due to adiabatic compression. Were these the only effects, the resulting temperatures would be the same on either side of the ridge, level for level. But if enough moisture is present, as it often is, it will be condensed in the lifting process and the rate of cooling after saturation decreased by the release of the latent heat of condensation. In short, the process will be partly pseudo-adiabatic and the potential temperature will be increased. On the down-slope side the process will remain adiabatic, and

the temperature will increase at the dry adiabatic rate. The result is that, level for level, there will be higher temperatures in the lee of the mountains. The down-slope effect, sometimes known as foehn, is especially noticeable in the infrequent cases when continental air, initially of low relative humidity, is forced to flow into the basin from the east and north. This produces the dessicating heat waves of summer in the valley.

31. The secluding effect of the surrounding ranges allows stagnation of the air trapped in the basin. During some winter situations, cold continental air pours into the basin from the north and east and, if the atmospheric flow pattern is favorable, helps maintain a quasi-stationary front along its southern limits. During the summer the effect of continuous solar heating of the trapped air is the "heat low" which elongates as a pressure trough northward from the southern deserts, following the valley contours with surprising exactness.

32. The topography practically determines the distribution of precipitation. The mean seasonal precipitation over the basin increases with elevation and is greatest above four thousand feet. The orographic effect is such, however, that it varies not only with elevation but also with slope, air flow, and the thermodynamic characteristics of the air masses in each synoptic situation. The distribution of orographic effects in the idealized storm will be discussed in Chapter V, "Major Storms," and the theoretical aspects of orographic rain in Chapter VI, "Maximum Possible Precipitation." Here we can consider the orographic influences imposed upon the moisture-bearing winds as those effects are made visible in the mean seasonal isohyetal pattern (Figure 7), or, as

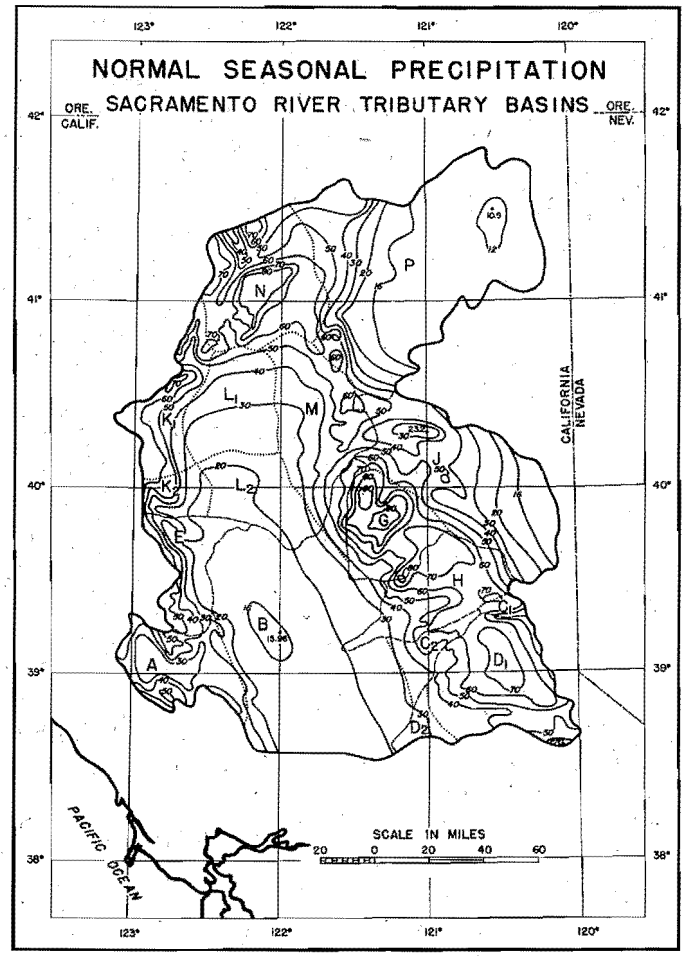

Figure 7

will be shown later, in the individual storm's isohyetal pattern. From the well-marked windward isohyetal maxima of the Coast Range there is a rapid decline on the eastern, leeward slopes. Within the basin the principal points of maximum rainfall are found on the west slopes of the Sierra Nevada Range. Over these areas, drained by the American, Yuba, and Feather Rivers, the mean seasonal isohyets clearly show the lifting effect of the high mountains on the moist southwesterly winds which have crossed the comparatively low hills in the vicinity of San Francisco Bay with only slight loss of precipitable moisture. Farther north, where southwesterly winds are lifted to moderate elevations over the higher ridges of the Coast Range, a greater depletion of moisture occurs and rainfall diminishes somewhat along that portion of the west slopes of the Sierras which lies in the path of this part of the southwesterly current. Over the upper reaches of the Sacramento Valley, and particularly above the confluence of the Pit and

Sacramento Rivers, other rainfall peaks are apparent on the isohyetal charts. They result from the combined orographic and convergent effects upon the air at lower levels which has been deflected from its northeastward path by the Sierra Nevada Range and is forced northward along the rising floor of the valley. This air is "piled up" toward the northern end of the valley where its escape is impeded by the relatively high mountains. A "dome" is built up, over which southwesterly winds at higher levels must gradually rise, producing the relatively high rainfall in the low-lying Red Bluff-Redding sector of the Sacramento Valley.

33. Distribution of Climatic Elements. While the qualitative distribution of temperature and precipitation has already been discussed, the quantitative variations in climatic elements can best be described over such a heterogeneous region by the classification of the basin into regions climatically similar. Since it was necessary to divide the basin into zones in order to make the rainfall analyses (see Figure 6), combinations of these zones have been grouped into such climatic regions. Data for a comprehensive study of any one climatic element do not exist, but the data are more nearly adequate for precipitation than for any other element.

34. Because the California rainfall regime occurs during the winter months, the precipitation that falls during the twelve-month period, July through June, is referred to as the seasonal precipitation. The mean seasonal isohyets for the basin, shown in Figure 7, are based on data gathered by the Sacramento District Office of the U. S. Engineer Department (4). The areal distribution of the average depth of normal seasonal precipitation for each of the five climatic regions is plotted

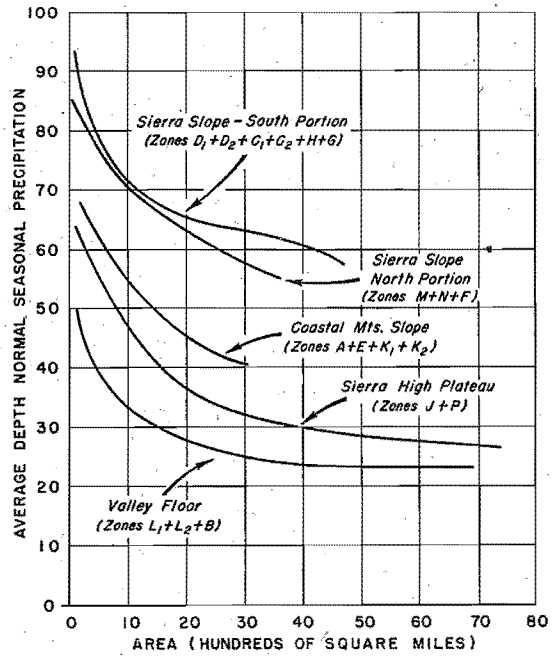

Figure 8

Area-depth curves, normal seasonal precipitation Sacramento Basin (divided into climatic regions by zone grouping)

on Figure 8. The general nature of the curves, indicating marked differences in average precipitation within each region, may be ascribed to the effect of elevation. Similarly, differences between the regional curves can be attributed to the effects of the unique elevation characteristics and topographic aspects of the different regions. However, areal variations of seasonal precipitation cannot be expressed exclusively in terms of elevation. The curve representing the "high plateau" of the Sierra Nevadas should, for instance, plot higher than it does, if considered solely on the basis of the region's mean elevation. Along the Sierra slope regions, the "high plateau" has a high frequency of precipitation due to showers and thunderstorms during the summer months. The regions of least frequency are the coastal slope and the valley floor, where summer showers rarely occur.

35. Snow surveys of the basin have been too few to permit description of the specific regional variations of this element. Generally, however, that portion of the mean seasonal precipitation which falls as snow is naturally distributed with elevation, the greater depths at the

higher elevations. The greatest annual amount occurs over the Sierra Nevada slope regions. Summit in 1879-80 recorded a total seasonal fall of 783 inches. Except in the shaded portions of the higher peaks, deep ravines and canyons, and on the northern slopes of the higher mountains, where snow is found in the late summer and early fall, the mountains as a whole are not covered with snow the year round. A more detailed discussion of normal and critical distribution of snow cover within the basin is contained in Chapter VII on "Snow Melt."

36. Although during the winter months the temperature is practically uniform throughout the valley, there are probably few places in the world where there exists so marked a temperature gradient as obtains during the summer months over the Sacramento Basin. The July averages are 25 F higher in the valley bottom than in the high Sierras. As elsewhere in the state, the isotherms have mostly a north-south instead of the usual east-west trend, following topographic contours rather than the parallels of latitude (90). Average temperature values for January, July, and the year, have therefore been plotted against elevation for each of the climatic regions on Figures 9 to 13. Again, because of the paucity of data and the diversified nature of exposure, no temperature-elevation

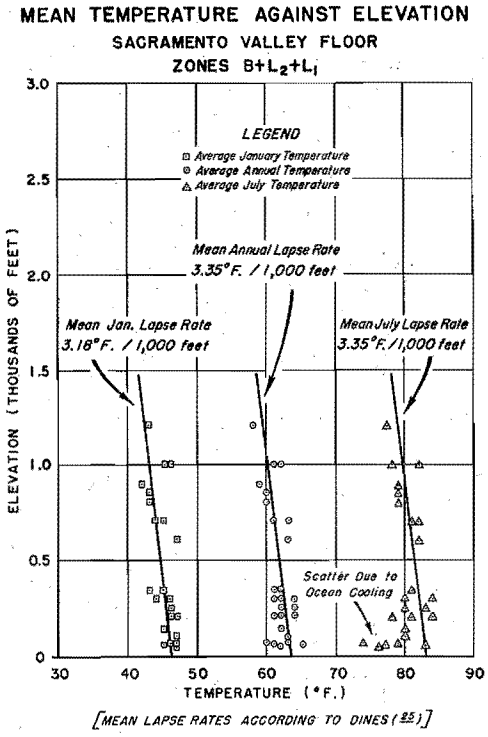

Figure 9

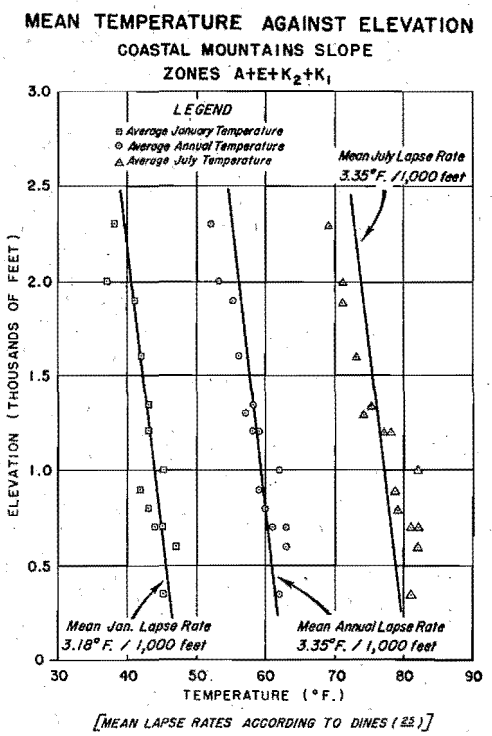

Figure 10

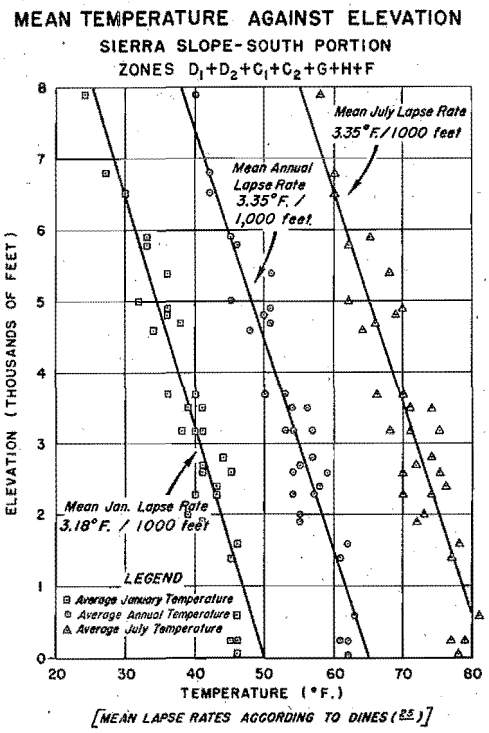

Figure 11

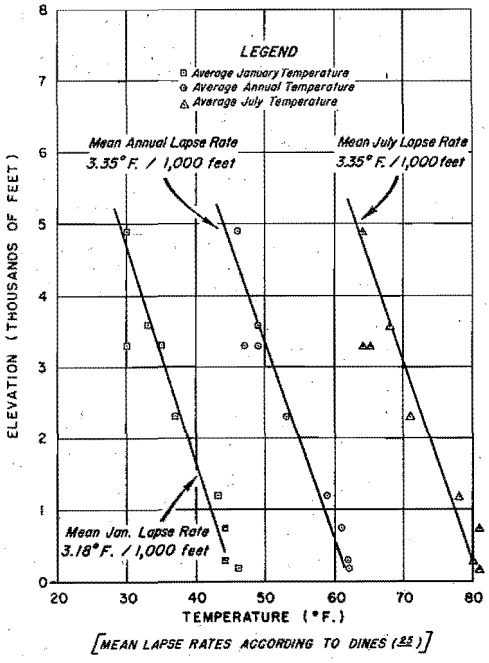

Figure 12

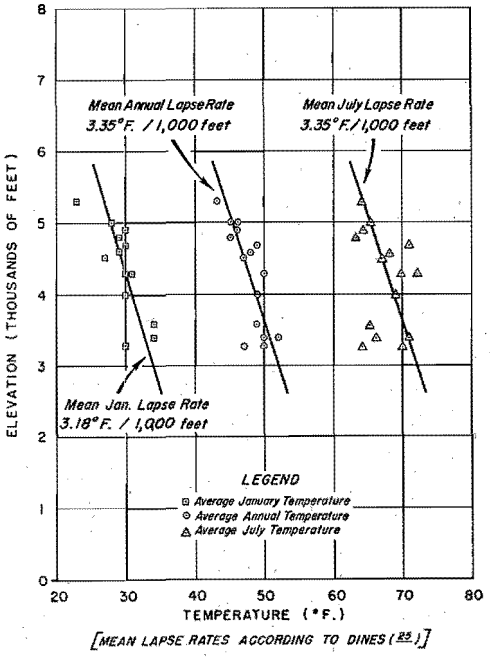

Figure 13

correlation has been attempted. The mean temperature lapse rate in the free air, as given by Dines (25, p. 258), has been plotted on each figure as a guide. It will be noted that the data fit the curves fairly well in every case except for July in Figures 9 and 13. In the former, the lowest elevation represents stations in and near the delta region, where the maritime cooling effect is felt. In the latter case, the most probable explanation is that the station temperatures are not representative of the free air. It should also be noted that the vertical scale is changed between Figures 10 and 11 to accommodate the higher elevations.

37. The general movement of the air over the basin is southerly in the lower layers, shifting to westerly with elevation. Strong southerly indrafts at all elevations occur during the months of November, December, January, February and March, whenever strong cyclonic disturbances approach the coast. Of the elements, sunshine, humidity, and wind, there is unfortunately no adequate continuous and systematic record from which to compute the regional variations, which are obviously great. The maximum values of the wind and humidity constitute a separate problem, which is treated in Chapter VI.

CHAPTER III

RAINFALL ANALYSIS

38. In this study, rainfall is analyzed in order to discover its distribution in area and time within the storm period. From such an analysis it is possible to derive the maximum depth-duration-area values for the various subdivisions of the basin. To accomplish this, the procedure described in supplementary bulletins of the U. S. Engineer Department (5) was utilized. In brief, the process involves the following steps:

a. Compilation of basic precipitation data.

b. Preparation of mass-rainfall curves.

c. Preparation of total isohyetal map.

d. Tabulation of contemporaneous rainfall quantities scaled from mass-rainfall curves.

e. Computation of accumulated precipitation values representing average depth of rainfall over selected areas.

f. Computation of maximum depth-duration-area data.

As applied to the Sacramento study, the method requires the construction of average mass curves of precipitation for segments of the basin area and then adjustment of the curves to give total storm values that correspond to average rainfall amounts from the total isohyetal map. The

mass curves may be determined by an arithmetic average of station rainfall within the sub-area, if sufficient gages are present, or by averaging station rainfall weighted according to area derived from the Thiessen polygon surrounding each station (96). Such a procedure makes the storm isohyetal map and areal breakdown of the basin especially important. These items will therefore be discussed in detail.

39. The Total Storm Isohyetal Map. The usual method of preparing an isohyetal map is to plot all the rainfall values and draw isopleths by linear interpolation between neighboring stations. The available meteorological information is then used to refine the precipitation pattern in areas sparsely covered by rain gages. However, in the area under study, the precipitation is so irregular that spatial interpolation with the present density of gages is wholly inadequate. The topography influences the precipitation to a marked degree and rainfall is intimately related to elevation within a given area, although a sufficient number of anomalies exist to discourage the use of rainfall depth-elevation relationships exclusively.

40. A study of a number of storms revealed the existence of a recurring characteristic rainfall pattern in the basin. Since seasonal precipitation is the summation of successive storms during the rainy period, it was decided to use a normal or mean seasonal precipitation map as a guide in defining the precipitation pattern of the individual storm. The meteorological justification for such a practice is developed in Chapter V. The normal seasonal map (Figure 7), developed by the Sacramento District Office from considerations of precipitation, runoff, and physiographic data (4), was introduced in Chapter II in connection

with the over-all precipitation features of the basin. It is hereinafter referred to as the N.S.P. map.

41. To develop the total storm isohyetal map from the observed rainfall values and the N.S.P. values, the procedure is as follows: Both values are tabulated for each station and ratios of storm rainfall to N.S.P. calculated in percentages. Isopercental lines are then drawn on the N.S.P. map. The N.S.P. values are multiplied by corresponding percentages at unmeasured key points and translated to an isohyetal plotting map together with the observed rainfall values. Both the implied and actual rainfall amounts are then used to plot storm isohyetal lines which are drawn so as to be consistent with the N.S.P. map, topography, and the meteorology of the storm.

42. Zonal Subdivisions. The usual procedure in rainfall analysis requires a breakdown of the storm area into contiguous sub-areas or zones, and separate maximum depth-duration-area computations for each zone. In this study each assigned basin is divided into zones having homogeneous rainfall characteristics. These zones, identified in Table 1 and located as shown in Figure 6, are fixed and form the basis of all rainfall computations for the major storms studied. The zones may be roughly grouped as follows: C_1, C_2, D_1, D_2, F, G, H, and M represent the western slope of the Sierra Nevadas, showing a marked increase of precipitation with elevation. The eastern slope of the Coast Range consists of A, E, K_1, and K_2, also characterized by rapid increase of precipitation with elevation. J and P form the Sierra Nevada plateau section where the rainfall is deficient. B, L_1, and L_2 are the light rainfall areas of the valley, and N is the mountainous area of heavy

rainfall in the northwest section of the basin. As the study progressed it became apparent that some of the subdivisions could be combined without the sacrifice of accuracy. In making such changes, listed below, the original nomenclature was adhered to as far as possible, in order to avoid confusion in future storm studies:

H was combined with C_1 to form HC_1

D_1 was combined with D_2 to form D

K_1 was combined with K_2 to form K

L_1 was combined with L_2 to form L.

CHAPTER IV

HYDROLOGIC HISTORY

43. The Available Data. There is no accurate basis for comparing the early floods in the Sacramento Valley with those of the present day. Records of river stages prior to 1853 do not exist. Between 1853 and 1879 casual and unrelated gage readings were made along the Sacramento River. By that time the Signal Corps began such observations but not until May 1906, when the Weather Bureau established an organized river service, did any accurate reference marks become available.

44. Slickens accumulations caused by uncontrolled hydraulic mining operations prior to 1893 constituted a changing factor in the channel structure. Since the occupation of the valley, levee construction, first sporadic but later organized, has acted to raise the water plane. For such reasons river gage heights, even if accurate by themselves, are unreliable for comparative purposes. It was decided therefore that, within the limits of available data, representative rainfall depths would serve as the most useful index.

45. Historical Notes (1805-1862). For records of the earliest floods, however, it was necessary to resort to historical references. These allowed a tabulation of dates and occasionally provided information

for an estimate of the flood's severity. In the notes that follow, all gage readings, unless otherwise identified, are of the Sacramento River at Sacramento. Also, unless otherwise specified, the "river" referred to is the Sacramento River and the "city" mentioned is Sacramento.

46. (1805) The earliest flood mentioned by historians occurred in 1805. The exact dates are not known but Willis (109) states that "... the great flood of 1805 formed an epoch in Indian history from which they still speak of subsequent events." Traditionally, this flood is said to have covered "the entire Sacramento Valley except the Marysville Buttes."

47. (1824-25) The winter season of 1824-25 was marked by an "unprecedented" fall of rain. Flood damage was extensive throughout the populated areas of that time. Historical accounts describe only the coastal region from San Francisco to San Diego and the interior of the southern portion of the state as sustaining extremely severe flood damages, but it can be assumed that flooding conditions prevailed throughout the Great Central Valley. The simultaneous occurrence of a Sacramento River flood is further indicated by evidence, in Bancroft's account (47), of stages in the lower San Joaquin higher even than those of 1861-62. Only an approximate date is given, but Willis (109) also mentions a flood of 1825 which "is often referred to by the older Indians."

48. (1846-47) The winter of 1846-47 is mentioned by Willis (109) as a period during which the Sacramento River overflowed. At that time the only white settlement in the valley was at New Helvetia (Sacramento). No information as to severity or extent of the flood is available.

49. (December 1849) Not until the following winter season was the first Smithsonian observer, Dr. T. M. Logan, established at Sacramento; however, it is from his quotations of the California State Medical Journal that the following description is paraphrased (53). The entire winter season was one of almost continuous precipitation, with the first rain occurring on September 23. The rain continued more or less regularly through October, November, and December, increasing in average intensity and accompanied by somewhat colder temperatures. The culmination was the flooding of the lower portion of the city of Sacramento on December 25.

50. (January 10-17, 1850) On January 8, 1850 the Sacramento River rose rapidly and from the 10th to about the 17th nearly the entire city was flooded. During this period the Sacramento River reached a stage of 20.3 feet above low water.

51. (April 7, 1850) After subsiding from the January overflow the river apparently remained within its natural banks until April 7, when another rise caused flooding of the lower part of Sacramento. A temporary levee system was promptly constructed to protect the city from further damage.

52. (March 7, 1852) During the first part of the 1851-52 winter season, conditions were like those of 1849-50. About ten inches of rain fell at Sacramento during the last four months of 1851, contemporaneous rainfall over the basin raising the Sacramento River to within four feet of its natural banks by December 30. However, the first flood of the season occurred during the heavy rains of the first week of March 1852. As a result of breaks in the levee system at Sutter's Lake, as well as a

crevasse in the American River system, part of the city was flooded on March 7. The inundation covered practically the whole city before subsiding about a week later. The highest stage reached on the Sacramento during this period was 20.0 feet above low water.

53. (December 25, 1852) The basin's December rainfall, of which Sacramento's twelve inches was representative, caused the Sacramento River to rise "seventeen inches higher than the flood of 1850" (53). The city remained almost entirely submerged from December 25, 1852 to January 24, 1853, when the flood waters began to recede. Willis (109) lists December 19 as the date on which the first flooding occurred, stating that the city was flooded to a depth of several inches by the water that came through breaks in the levee on the American River.

54. (January 1, 1853) Thompson and West (97) give January 1, 1853, as the date the city was next flooded. A stage of 21.7 feet above low water was recorded and it was assumed that the major discharge was from the American River.

55. (April 2, 1853) During March 1853 rainfall was heavy once more and the Sacramento rose rapidly during the latter part of the month. On March 29 the river rose about twelve feet in 24 hours, soon overflowed its natural banks and then, from a break in the levee at Sutterville, again inundated the greater portion of Sacramento on April 2. Some portions of the city remained flooded from the first of April until the last of May. Seventeen inches of rain fell at Sacramento during the first five months of 1853.

56. (March 1854) A stage of 20.3 feet above low water was recorded during March 1854 by Logan (53) but no mention was made of the

city's being flooded.

57. (March 28, 1861) On March 28, 1861, the Sacramento rose at the rate of 7 feet in 24 hours. The highest stage reached was 21.7 feet above low water. The lowlands were flooded but the city was apparently untouched. A consideration of the precipitation and temperature records at Sacramento indicates that snow melt must have been the major contributing factor.

58. (December 9, 1861) All historians consulted agree that the floods that occurred during the winter season of 1861-62 were by far the greatest and most disastrous on record. As in prior floods, the winter rains set in early. The first storm period began at Sacramento on November 9, 1861, and rainfall was quite persistent through December 7. On this date the rainfall was described by the observer as "almost tropical." Two and one-half inches fell in 36 hours at Sacramento and Logan (53) estimated that the fall in the mountains was nearly six times as great. Critical snow melt conditions accompanied the rainfall. With the Sacramento River already at a high level, the American rose very rapidly, overflowed its banks and caused severe flooding in the foothills and valley. The American rose to 22.7 feet above the low water mark, and a break in the levee system at Burns' Slough caused nearly all portions of the city of Sacramento to be inundated.

59. (December 28, 1861) Precipitation was light and intermittent from December 9 to the 21st; however, on the 22nd, steady rain began again and on the 26th 2.44 inches fell in 18 hours at Sacramento. This was the highest intensity of rainfall that had ever been recorded at the station. The American River again rose very rapidly and the lower

portion of Sacramento was flooded. On December 28 a stage of 22.6 feet above low water was recorded at Sacramento, exceeding all prior flood stages.

60. (January 9-12, 1862) Precipitation over the basin had ceased shortly before the December 28 stage was reached but began again on the morning of January 5. Moderately intense precipitation occurred on the 5th and 6th over the lower portion of the basin, falling as rain showers over valley stations but as severe snow showers over the foothill regions. Although all the precipitation fell as rain at Sacramento, 12 to 30 miles to the northwest, in a region seldom accumulating snow, there were snow depths ranging from 6 to 12 inches. Warm and heavy general rains followed during the period from the 8th to 11th, the Sacramento River reflecting each period of heavy rain. The highest stage reached was 24 feet above low water, on the 9th. The Alta Californian described the resulting flooded areas as "extending from Tehama, 80 miles above Marysville, to a point in the San Joaquin at least 50 miles south of Stockton, forming a lake 20 miles wide by some 250 miles long."

61. (January 15-17, 1862) The preceding storm's meteorological pattern, although it can only be inferred from meager data, is of special interest in the consideration of conditions antecedent to major floods and will be discussed in that connection in Chapter V, "Major Storms." The pattern was apparently reproduced during the period January 15-17, 1862, resulting in similar precipitation intensities and distribution. The effect was to prolong the severe flooding of the lower portion of the basin, and to extend flood conditions over the

upper basin near Red Bluff.

62. The available precipitation data for the 1861-62 flood period are tabulated below:

TABLE 2

PRECIPITATION - FLOODS OF 1861-62

Station	Jan. 5-11, 1862 Total Inches	Jan. 5-11, 1862 % of Mean Seasonal	Jan. 5-22, 1862 Total Inches	Jan. 5-22, 1862 % of Mean Seasonal	Dec. 21, 1861, to Jan. 22, 1862 Total Inches	Dec. 21, 1861, to Jan. 22, 1862 % of Mean Seasonal
Sacramento	6.54	38	14.78	86	20.65	121
Marysville	3.88	19	8.23	40	-	-
Benecia	6.22	40	10.52	68	12.70	82
San Francisco	12.72	58	23.01	101	-	-
Alcatraz	4.17	19	11.74	53	12.51	62
Ft. Crook	3.19	7	8.14	18	13.46	30
Ft. Gaston	13.00	24	24.55	45	39.95	73

Additional untabulated amounts are:

Nevada City, Dec. 26 to Jan. 12 - 26.00 inches, 54% of mean seasonal;
Red Dog Jan. 10-11 - 11.32 inches (48 hours).

63. Storm Tabulation (1864-1940). The selection of the storm periods chronologically listed in Tables 3 and 4, which follow, was based on California precipitation records used in conjunction with Sacramento River stage and discharge records. During some of the periods the primary flood factor was snow melt, and those cases are so designated. In doubtful instances the rainfall values were tabulated.

64. The actual precipitation values in all cases were converted into percentages of the mean seasonal amounts. In the tables this conversion is called the "storm index." On the assumption that station rainfall can be representative of its region's rainfall, the storm index was computed for a station in each of the indicated sub-basins. The station was chosen because of its location, exposure, elevation, and

length of record. For the storms occurring prior to 1900 such a selection could not be made for each sub-basin on account of the limited data available. In Table 3, which is for the period 1864-1899, the index values are merely such as are available and cannot be considered particularly representative. In Table 4, for the period 1900-1941, the stations selected represent basin features and appear under sub-basin headings. Whenever the record became discontinuous, a proper substitution was made, if possible, and the substitution indicated in the table.

TABLE 3

STORMS AND FLOODS: 1864–99

Storm Period	Station and Storm Index
1864 Nov. 25–27	Meadow Valley 18 Sacramento 23
1864 Dec. 11–13	Meadow Valley 7 Sacramento 30
1864 Dec. 24–26	Meadow Valley 8 Sacramento 5
1866 Jan. 18–21	No adequate data available
1866 Dec. 19–21	Ft. Bidwell 6 Ft. Crook 13 Sacramento 30
1867 Dec. 17–19	No adequate data available
1868 Jan. –	No adequate data available
1871 Dec. 19–21	No adequate data available
1875 Jan. –	No adequate data available
1878 Feb. 14–17	No adequate data available
1880 April 19–21	Ft. Bidwell 7 Red Bluff 20 Sacramento 52
1881 Jan. 28–30	Red Bluff 36 Sacramento 29
1881 Feb. –	No adequate data available
1885 Nov. 7–9	Ft. Bidwell 14 Red Bluff 28
1889 Dec. –	No definite storm period -- evenly distributed monthly rainfall
1891 Feb. 28–Mar. 2	Ft. Bidwell 4 Red Bluff 5 Sacramento 10 Georgetown 14

TABLE 3 (Cont.)

Storm Period		Station and Storm Index									
1892	May --30	Snow melt									
1892	Nov. 28-Dec. 1	Ft. Bidwell	23	Red Bluff	27	Sacramento	36	Susanville	56	Nevada City	22
1892	Dec. 24-27	Ft. Bidwell	5	Red Bluff	4	Nevada City	13				
1893	Mar. 19-21	Red Bluff	1	Sacramento	6	Nevada City	10	Placerville	15		
1894	Dec. 2-7	Cedarville	5	Red Bluff	6	Nevada City	10				
1894	Dec. 2-22	Cedarville	3	Red Bluff	9	Nevada City	5				
1896	Jan. 25-27	Red Bluff	14	Quincy	10	Sacramento	17	Nevada City	8		
1897	Jan. 28-30	Snow melt									
1897	Feb. 3-5	Cedarville	5	Red Bluff	10	Nevada City	7				
1899	Mar. 22-24	Sisson	2	Cedarville	6	Orland	14	Red Bluff	14	Colfax	17
1899	Nov. 27-29	Snow melt									
1899	Dec. 13-15	Snow melt									

TABLE 4

STORMS AND FLOODS: 1900-40

BASIN AND REPRESENTATIVE STATION'S STORM INDEX

		Sacramento Basin above Stony Creek		Stony Creek Basin	Feather River Basin	Yuba and American Basins
	Storm Period	Sisson	Cedarville	Orland	Quincy	Colfax
1900	Jan. 30-Feb. 1	Snow melt				
1900	Mar. 6-8	6	3	5	12	8
1900	Nov. 20-21	2	14	18	11	16
1900	Dec. 19-21	2	1	2	3	2
				Fruto		
1901	Jan. 3-5	18	3	24	19	13
1901	Feb. 18-20	9	4	9	10	12
1901	Dec. 2-5	4	9	2	8	8
1902	Feb. 24-26	20	4	29	13	11
1902	Mar. 7-9	3	1	2	3	6
1902	Apr. 5-7	7	4	8	4	4
1902	Nov. 8-10	24	2	17	9	5
1902	Dec. 25-27	-	4	0.4	8	6
1903	Jan. 24-26	0.8	7	3	8	5
						Nevada City
1903	Mar. 2-5	Snow melt				
1903	Mar. 28-30	7	2	5	13	12
						Colfax
1903	Nov. 19-21	8	5	20	18	12

TABLE 4 (Cont.)

Storm Period	Sacramento Basin above Stony Creek		Stony Creek Basin	Feather River Basin	Yuba and American Basins
	Sisson	Cedarville	Fruto	Quincy	Nevada City
1903 Dec. 16-17	0.6	2	0.8	9	4
				La Porte	
1904 Feb. 14-16	3	8	5	7	8
					Colfax
1904 Feb. 22-24	3	13	11	15	4
				Quincy	
1904 Mar. 8-10	8	2	14	6	2
1904 Mar. 17-19	3	7	-	8	18
1904 April -- -14	Snow melt				
1904 May -- -13	Snow melt				
					Nevada City
1904 Oct. 8-11	15	4	16	10	11
					Colfax
1904 Dec. 29-31	8	6	11	18	7
1905 Jan. 21-23	12	1	15	9	6
1905 Jan. 31-Feb. 2	2	8	2	4	6
					Nevada City
1905 Mar. 12-14	12	2	10	5	3

TABLE 4 (Cont.)

Storm Period	Sisson	Cedarville	Fruto	Quincy	Nevada City
1905 Mar. 18-20	0.9	3	3	7	5
1905 Mar. -- -29	Snow melt				
1905 April -- -24	Snow melt				
					Colfax
1906 Jan. 16-18	14	8	18	21	21
					Nevada City
1906 Feb. 21-23	3	2	3	5	4
					Colfax
1906 Mar. 22-24	7	2	6	5	8
1906 Mar. 30-31	7	5	10	6	8
1906 April -- -23	Snow melt				
1906 May 26-28	1	10	5	10	12
1906 June 2-5	Snow melt				
1906 July -- -2	Snow melt				
1906 Dec. 25-27	11	4	12	13	12
					Nevada City
1907 Jan. 3-4	5	4	4	5	5
1907 Jan. 27-29	8	0.5	3	4	4
					Colfax
1907 Feb. 1-3	1	21	1	6	12

TABLE 4 (Cont.)

Storm Period		Sisson	Cedarville	Fruto	Quincy	Colfax
1907	Mar. 17-19	14	10	6	43	15
1907	April 4-6	Snow melt				
1907	April -- -19	Snow melt				
						Nevada City
1907	June 11-13	2	6	0	8	6
						Colfax
1908	Jan. 19-21	9	2	2	5	5
1908	Feb. 1-3	5	2	20	6	5
1908	Feb. 6-8	15	0	11	0.9	2
1908	April 13-15	Snow melt				
1909	Jan. 13-15	7	-	4	20	24
					Inskip	
1909	Feb. 2-4	24	1	15	7	2
1909	Feb. 10-12	4	3	5	9	8
1909	Mar. 3-4	3	-	0.8	6	3
1909	April -- -19	Snow melt				
1909	May - -5	Snow melt				
1909	June - -4	Snow melt				
1909	Nov. 21-23	4	8	0.8	5	6
1909	Dec. 7-9	7	2	5	12	9
1910	Jan. 22-24	6	3	5	7	4
1910	Feb. 22-24	4	1	2	7	2
1910	Mar. 21-23	2	6	17	7	9
1910	April -- -11	Snow melt				
1911	Jan. 12-14	3	14	16	8	21

TABLE 4 (Cont.)

Storm Period		Sisson	Cedarville	East Park	Inskip	Colfax
1911	Jan. 28-31	4	4	13	18	16
1911	Jan. 31-Feb. 2	3	4	6	9	7
1911	Feb. 11-13	2	3	1	6	2
1911	March 5-7	14	2	19	13	11
1911	April 4-5	3	9	2	8	7
1911	May - -5	Snow melt				
1911	June - -3	Snow melt				
1912	Jan. 25-27	5	4	4	12	5
1913	Jan. 16-18	5	5	6	12	2
1913	April -- -27	Snow melt				
1913	May 8-9	Snow melt				
1913	Dec. 29-31	13	20	17	22	6
1914	Jan. 24-26	3	6	9	12	10
1914	Feb. 19-21	12	-	18	16	12
1914	March -- -19	Snow melt				
1914	April 4-5	0.7	1	4	3	2
1914	May -- -5	Snow melt				
1915	Jan. 7-9	4	2	18	8	8
1915	Jan. 31-Feb. 2	5	0.6	24	15	10
1915	March 27-29	14	2	17	10	5
1915	April - -3	Snow melt				
1915	April -- -20	Snow melt				
1915	May 9-11	Snow melt				
1915	June - -8	Snow melt				
1915	Dec. 12-14	2	1	15	11	11
1916	Jan. 2-3	7	11	13	13	10
1916	Jan. 22-24	8	0	13	13	9
1916	Feb. 9-10	5	0.8	0.6	7	2
1916	March 4-5	2	0	2	5	6
1916	April -- -11	Snow melt				

TABLE 4 (Cont.)

Storm Period		Sisson	Cedarville	East Park	Inskip	Colfax
1916	May - -6	Snow melt				
1916	Dec. 2-3	8	7	8	12	9
1917	Feb. 23-24	11	-	15	23	11
1917	March 29-30	Snow melt				
		McCloud				
1917	April 22-23	2	1	0.6	8	4
1917	May - -9	Snow melt				
1917	June - -9	Snow melt				
1918	Feb. 5-7	7	3	10	8	4
1918	March 18-19	8	-	-	7	7
1918	March 25-26	2	4	-	6	1
1918	April 8-9	3	1	-	3	2
			Ft. Bidwell			
1918	Sept. 12-14	4	5	-	6	10
			Madeline			
1918	Oct. 1-2	4	2	-	2	0.5
		Sisson				
1919	Jan. 19-20	5	2	-	6	6
1919	Feb. 9-11	10	11	-	14	15
1919	Feb. 28-Mar. 2	2	3	-	7	5
1919	April 4-5	Snow melt				
1919	May - -2	Snow melt				

TABLE 4 (Cont.)

Storm Period		Sisson	Ft. Bidwell	East Park	Inskip	Colfax
1920	April 14-15	2	10	-	7	8
1920	Nov. 17-19	11	4	-	15	5
1920	Nov. 25-26	-	2	-	5	2
1920	Dec. 9-11	4	3	-	8	7
1920	Dec. 18-19	4	5	-	9	4
1921	Jan. 17-19	8	13	-	14	12
1921	Jan. 29-30	2	3	-	9	3
1921	Feb. 14-15	-	-	-	4	2
1921	Feb. 20-21	1	7	-	6	4
1921	March 12-13	3	2	-	5	5
1921	April - -3	Snow melt				
1921	May -- -15	Snow melt				
1922	Feb. 17-19	6	5	-	11	9
1922	April -- -27	Snow melt				
1922	May 19-20	3	1	-	2	3
1922	June - -5	Snow melt				
1922	Dec. 10-13	3	4	-	10	13
1923	April 4-6	3	4	-	7	9
1923	May - -10	Snow melt				
1924	Feb. 6-8	3	7	-	14	7
1924	April 3-4	3	4	-	2	3
1925	Feb. 3-5	5	3	-	11	16
1925	Feb. 11-12	6	1	-	6	4
1925	April 15-16	5	1	-	2	1
		Mt. Shasta				
1926	Feb. 2-4	8	2	-	16	11
1926	April 5-8	12	7	-	15	16
1926	Nov. 22-25	15	11	-	21	14
1926	Nov. 26-29	12	9	-	10	9

TABLE 4 (Cont.)

Storm Period		Mt. Shasta	Ft. Bidwell	East Park	Inskip	Colfax
1926	Dec. 1-3	6	10	-	2	1
1927	Feb. 19-21	5	3	-	8	9
1927	March 13-14	1	5	-	4	4
1927	Mar. 31-April 2	9	5	-	9	12
1927	May -- -16	Snow melt				
1927	June - -7	Snow melt				
1927	Dec. 27-28	-	1	-	4	7
1928	Feb. 1-3	8	2	-	5	5
1928	March 23-26	10	11	-	22	22
1928	April 1-3	4	1	-	6	6
1928	May -- -1	Snow melt				
1929	Feb. 2-4	8	4	10	9	6
			Cedarville			
1929	Dec. 12-15	12	5	12	23	7
1930	March 3-5	8	-	10	9	13
1931	Dec. 24-27	16	6	18	17	13
1932	Feb. 5-6	1	4	5	2	5
1932	Mar. 14-20	Snow melt				
1932	May -- -12	Snow melt				
1933	March 26-28	13	-	1	3	5
1933	May -- -30	Snow melt				
1933	Dec. 28-30	9	2	19	7	6
1934	Mar. 27-29	3	4	2	4	3
1935	April 6-8	5	7	4	2	12
1935	May - -9	Snow melt				
1935	May -- -23	Snow melt				
1936	Jan. 13-15	7	30	2	10	10
1936	Feb. 19-21	7	5	6	11	4
1936	April -- -17	Snow melt				

TABLE 4 (Cont.)

Storm Period	Mt. Shasta	Cedarville	East Park	Inskip	Colfax
1936 May -- -14	Snow melt				
1936 June 6-7	4	1	5	3	3
1937 Feb. 11-13	3	6	13	3	9
1937 Mar. 10-12	5	1	11	4	3
1937 Mar. 19-21	7	1	3	7	1
1937 April 13-15	3	2	-	3	-
1937 April -- -22	Snow melt				
1937 May -- -14	Snow melt				
1937 Nov. 18-20	8	2	8	10	1
1937 Dec. 9-12	16	42	26	30	19
1938 Feb. 10-13	16	4	-	18	14
1938 Mar. 11-13	5	2	12	5	5
1938 Mar. 17-19	1	6	1	4	3
1938 April 4-5	2	6	4	3	4
1938 April -- -21	Snow melt				
1938 May 14-16	Snow melt				
1938 May -- -June 1	Snow melt				
1939 March -- -13	Snow melt				
1940 Jan. 24-26	8	4	15	9	7
1940 Feb. 26-28	18	6	28	28	16
1940 March 28-30	11	2	8	18	15
1940 Dec. 21-23	7	1	9	7	8
1940 Dec. 24-26	16	1	16	9	8

CHAPTER V

MAJOR STORMS

65. The Sacramento Storm Type. The rainfall of flood-producing storms over the Sacramento Basin is released from moist unstable air which originates over the polar regions of the northwest Pacific area, travels southeastward across progressively warmer waters to about the vicinity of the Hawaiian Islands and then northeastward over somewhat cooler waters and onto the continent. Heat and moisture are rapidly added to the air from the sea surface during much of its journey. The instability, produced by the rapid increase in temperature of the air at the surface, results in vertical motions which carry heat and moisture to greater and greater heights. In flood-producing storms the height to which this moist unstable layer extends is approximately 10,000 feet before moving inland. In the final stages of its movement toward the coast the air passes over cooler water and becomes stable in a shallow layer next to the sea surface. This stable layer retards release of the potential energy in the moist air until orographic, frontal or isentropic lifting is encountered. As the air is borne inland from the southwest it is acted upon by the unchanging and efficient rain-producing mechanism of the Sacramento Basin's topography. Because the circulation

described is impossible with summer pressure distribution the storms are naturally confined to the colder half of the year.

66. The weather maps analyzed, the theoretical and statistical climatology of the region, the opinions of authorities consulted -- all point to the paramount importance of the southwest current. Storms of flood magnitude have occurred in which the pressure gradient necessary for a strong southwest current was not often discernible, but during most storms the rains were usually heaviest when the gradient was strongest. And, for the basin as a whole, the greatest rains have occurred with the strongest and most sustained southwest winds. For that reason it would not be improper to call the critical Sacramento storm type the "Southwest Type" but, if so named, it should not be confused with the type similarly designated by Reed (79) in his discussion of weather types of the northeast Pacific Ocean. Because he was considering the entire west coast of the United States, his "Southwest Type" was restricted to the storms of Oregon northward. With Reed's theoretical pressure distribution and his lobe or "head" of the Pacific anticyclone displaced southward, the type adequately describes the Sacramento storm. In the next chapter it will be shown that the particular constraints imposed by the basin serve to magnify the rainfall effectiveness of the southwest wind, apart from any considerations purely meteorological.

67. Once the southwesterly current of moist unstable air is established over the basin the occurrence of a flood is dependent on the persistence and intensity of this flow. A duration of two or more days is necessary. Minor fluctuations in trajectory are unimportant as long

as the general northeastward movement of the air remains undisturbed. Frontal passages across the region during flood rains may be frequent, but they are relatively unimportant when they do not appreciably disturb the southwesterly current of air. The passage of a well-marked front, bringing a definite shift in wind to west or northwest, is often the immediate precursor of the storm's ending. It is followed by comparatively cold and dry, subsiding air which settles in the region of the mean position of the California-Hawaii anticyclone. Though the dynamics of the process are debatable, it is apparent from purely synoptic studies that the new cold anticyclone now establishes itself as the dynamic, stationary type which results in cessation of rainfall for the Sacramento Basin. It is of special importance in the theoretical consideration of the maximum possible storm that the cold thrust responsible for the re-establishment of such a control is most likely to follow shortly after the strong southwest current. The pressure gradient required for the latter is part of the intense cyclone that, by virtue of its intensity, must also have a strong gradient on its west and northwest side which will produce the rapid influx of new cold air. The maximum rainfall intensity, in other words, tends to limit its own duration.

68. It was pointed out in Chapter II, "Dynamic Climatology," that the distribution of rainfall within the basin, as shown by the isohyetal pattern, is the result of the orographic effect. However, the occurrence of the rainfall maxima, although primarily orographic in origin, is nevertheless not simultaneous. If we consider the idealized storm it can be seen that the orographic intensities and their

contemporaneous distribution will vary with the storm sector. At any selected point, that is, the orographic effect will reach its peak of efficiency at a particular stage of the storm's progress or development. The sequence can begin with a relatively cold but stable air mass filling the valley, overrun by air that has become maritime tropical over the Pacific, with the warm sector of the cyclone visible on the surface somewhere southwest of San Francisco. As the surface warm front, or its occluded phase, approaches the coast, the cold air in the valley becomes a current from the south or southeast. Above it the trajectory of the overrunning warm air is from the southwest. The cold air in the basin will flow fairly parallel to both coast and Sierra ridges but, as previously indicated, definitely up slope in the northern part of the basin. In that portion the warm air is not only moving up slope along the frontal surface but is being given additional lift because the cold wedge beneath is being lifted. To the warm air aloft in this section there will be imparted an additional upward displacement not present in the warm air to the south. The rainfall intensity will be increased (12). Some moisture may be precipitated out of the cold wedge itself as a result of lifting and convergence.

69. The warm sector of the cyclone will rarely move inland, but when it does, it is likely to occlude against or straddle the coastal chain. According to Bjerknes it is in this section that the "pure" orographic effect will be most noticeable and the intensities of the very highest kind (12). However, the orographic effect of the Coast Range on the warm sector air will be one that cannot be observed in the deeply occluded storm. Depending on the velocity of the wind in the

warm sector there will be some carry-over to the Sacramento side of the coast ridge. (Precipitation sometimes attributed to carry-over may actually be caused by convergence of valley air against the leeward mountain slope.) At this point in the sequence, though, the cold air in the valley will be at its shallowest, and the warm air can flow from the southwest across the exceptionally low ridges east of the Golden Gate (around 2,000 feet) and impinge directly against the Sierras in the Bowman-Fordyce area, accounting for another peak of intensity.

70. The final frontal effects in this schematic outline will also vary. In a warm type occlusion the warm sector will be lifted along the old cold wedge -- which is itself lifted in the north, the flow in it being from the south or southeast. Added to this will be the effect of orographic slope on the air in the warm sector aloft. A cold type occlusion, however, will lift the old cold air against the north-south ridge as well, imparting an added lift to the warm air. Along the frontal zone in either type dynamic convergence in the warm air will add to the rain's intensity. The movement of this final front is from the west or northwest, its orientation usually being north-northeast to south-southwest, and it is this compounding of factors that causes the late, heavy rain in the headwaters of the American. This is usually the last important rain of the individual cyclone, what follows being mostly snow in the high Sierras. The new cold air becomes quickly stabilized by mechanical and dynamic subsidence. The re-establishment of the Pacific High follows. Since such a reappearance of a stable pressure distribution rarely follows the warm front type occlusion, it is possible to say that the meteorological sequence just schematically outlined is

more likely to be repeated if the occlusion is of the warm type. Any one total storm can consist of one or more such sequences, although the only demonstrable evidence of the entire sequence may be the occluded or upper front.

71. For all storms of the Pacific Coast of the United States, the sequence of fronts is similar. The air masses involved do not differ greatly, and then only by reason of the varying lengths of trajectory from their source region, resulting in more or less modification. In origin and structure the storms are all essentially one type. What distinguishes the Sacramento storm is first, of course, the migration of the semipermanent centers of action so as to superpose upon the Sacramento Basin air of the optimum moisture content and velocity of flow. But the true individuality of the storm is the result of the physical structure of the basin. In other reports the Hydrometeorological Section has usually been concerned with the effect of the storm upon the region. Here the concern is with the effect of the region upon the storm. The isohyetal pattern is the imprint of the basin on the storm. It is a characteristic function of the Sacramento Basin. It cannot be transposed from the basin, nor can any other pattern be transposed to the basin.

72. In every such storm there occur practically all the frontal and air-mass types that can occur in any other Sacramento storm of moderate magnitude. Differences in pressure distribution and greater variations in speed of air flow do not change its basic character. It follows then that, except for negligible instances of unimportant magnitude, the Sacramento storms are all essentially of the same type, differing only in orientation and intensity. Because the rainy season consists

of a series of such storms it can, for practical purposes, be considered as one continuous storm differing chiefly in duration from the individual storms of which it is the summation. This is why the isohyetal pattern of the individual total storm can be considered as representative of the mean seasonal pattern. It is important to note that such representativeness cannot be true of the one-day rainfall pattern, or of the isohyetal pattern for any period less than the total storm period. Use of any fraction of the storm period will naturally stress frontal activity or air-mass characteristics at that stage in the storm's existence -- minor variations in the general northeastward movement of the air. Only consideration of the total life of the storm will properly weight all the factors of all its stages.

73. In the following sections of this chapter the major storms of the basin are treated individually. Since the source of all the storms is the Pacific Ocean, the reliability of the meteorological analyses was dependent on the density and accuracy of ship observations. Although never ideal in number or distribution, these observations were considered adequate from March 1928. Synoptic charts for the four storms from that date are included in the appendix. Symbols used are explained in Figures 68A and 68B. No maps have been reproduced for the storms occurring prior to March 1928, but the analyses are briefly discussed except in the case of the 1911 storm, which was not considered important. For each storm, except 1911, there are presented three tables of rainfall values. Two are for accumulated precipitation -- one by zones and the other by combinations of zones representing assigned sub-basins. These can be considered average mass curves of rainfall. The third table shows maximum

duration-depth values, representing average depth of rainfall for maximum periods within the storm. The times indicated in the tabulations are Pacific Standard while all map times are Eastern Standard.

74. Before proceeding to the individual analyses it should be stated that the air masses which usually produce flood rains in the Sacramento Basin may properly be called modified polar air which has acquired tropical characteristics, as distinguished from the more stable tropical or equatorial air which sometimes visits the region. In considering the synoptic charts reproduced in conjunction with the meteorological analyses it should be remembered that the air masses variably designated on the charts as mPk or mTk often have very much the same character. The first is being modified into the second. In the borderline circumstances which these charts usually depict, the distinction between mPk and mTk becomes more or less arbitrary. It should also be borne in mind that even when the air mass is labelled mTw, it is stable only in the lowest layers and identical with mTk aloft. The important fact is that a pressure distribution which permits extensive modification of polar air, and then persists so as to produce continuous southwesterly winds over the basin for a period of two or more days, is requisite for storms of the Sacramento type.

75. Storm of February 24-29, 1940. The excessive rainfall which resulted in the Sacramento floods of February 27-March 6, 1940, was confined to the five-day period, February 25-29. However, the antecedent rainfall, snow cover, and ground condition over the basin were important contributing factors to the flood. During January and February intense cyclonic systems developed at frequent intervals over the Pacific Ocean

far south of the normal position in the vicinity of the Aleutian Islands. These centers moved eastward over the ocean but curved northeastward as they approached the Pacific Coast. This sequence of events resulted in the intermittent invasion of the area by warm moist air which produced moderate rains to high elevations. It accounts for the deficiency of snow cover over the mountains and the high elevation (about 5,000 feet) of the snow line. Thus, prior to the beginning of the period of excessive rainfall, conditions favoring rapid runoff and the development of a flood prevailed. The soil was thoroughly saturated, stream and bypass levels were high, and runoff up to over 5,000 feet in the mountains was unimpeded by the presence of the normal snow pack.

76. The five intense cyclonic disturbances which developed over the western Pacific and then moved eastward and northeastward toward the Pacific Coast during the period February 25-29, Figures 69 to 73, were similar to the intermittent storms which occurred during January and the earlier part of February. The close succession of these centers, each associated with a well-marked frontal system, produced almost unbroken southwesterly flow of moist unstable air over the basin. In general each frontal passage was preceded and accompanied by a temporary increase in rainfall intensity and followed by a temporary decrease. Owing to the fact, however, that the air following the fronts, like the air in advance, was also moist and unstable after its long trajectory over warm water, continued orographic lifting caused practically continuous rain over much of the basin.

77. The weather map for February 25, Figure 69, was characterized by the cold continental anticyclone that usually follows or accompanies

a period of low zonal circulation (8). The high pressure and cold air extended from Alaska through central United States to the Gulf of Mexico. Such a stage in the circulation pattern is fairly typical of the major Sacramento storms in their early stages. A belt of low pressure with four intense centers stretched along middle latitudes from the Pacific Coast westward and northwestward toward the Aleutians. South of these centers mPk air was being transformed into mTk as it traversed the warmer waters. The thrusts of cold air (more apparent on the isentropic charts, Figures 74 to 78) behind the low centers in the trough maintained the temperature contrast which, supplemented by the realized heat of condensation, supplied the energy necessary for the individual developments. As they began to occlude, the potential energy of mass distribution was released to intensify the centers. The maps for the following days indicate that each center moved northeastward toward the coast, became completely occluded and then began to fill. Their close succession served to maintain, except for short intervals, the steep pressure gradient along the coast.

78. The isentropic charts, Figures 74 to 78, show the passage of each front accompanied by a northward surge of warm moist air, accounting for the increased intensity of rainfall. The isentropic charts are not synoptic with the surface weather maps, but the proper position of each front is indicated and the front identified by letter. The solid isobars are similar to the contours of a topographic map and indicate the elevations of the isentropic surface. The dotted lines represent saturation pressures, which means that the air along such a line would have to be lifted to the indicated pressure before saturation could occur. They are

therefore also lines of equal specific humidity or mixing ratio and thus outline the moisture distribution along the isentropic surface (20). The value of mixing ratio for each condensation pressure is shown in the table included in each chart. These charts portray each tongue or valley of up-gliding warm moist air associated with a front followed by a ridge of colder, drier air. Noteworthy, too, is the steep slope of the final cold dome advancing into California on the morning of the 29th (Figure 78).

79. The surface pressure gradient over the Sacramento Basin was steepest between February 26 and 28, Figures 70 to 72. It was during this period, with the passage inland of fronts B, C and D that an average of about 7 inches of rain fell over the entire basin. From the isentropic charts for February 27 and 28, Figures 76 and 77, the saturated condition of the air preceding fronts C and D can be noted. Convergence, plus orographic lifting of this air which was flowing into the basin at a rapid rate, resulted in 12.51 inches of rain at Kennett in 48 hours, 16.55 inches at Hobergs, and 15.20 inches at Stirling City.

80. It will be shown from thermodynamic considerations in the following chapter that the winds aloft in such deeply occluded systems as occurred in February 1940 are likely to be of the strongest kind. Nevertheless, a comparison of the surface pressure gradient with the pressure gradient at five kilometers as indicated on the five charts, Figures 79 to 83, demonstrates that even then the gradient decreased with altitude. The fact should not, of course, be interpreted to mean that the wind velocity decreased with elevation, since wind speed would also be inversely proportional to the air density which naturally decreases aloft. Apart from this, the fixed-level charts, which are synoptic with the

isentropic, show the characteristic flow pattern to be maintained to higher levels.

81. The storm ended with the passage of front E on February 28, Figure 72. The wind shifted to a westerly direction, the flow of moist air into the intense cyclonic system was cut off, the pressure gradient along the northern California coast decreased considerably as the system filled and moved northeastward, and rain ended except for a few scattered instability showers. Figure 73 for February 29 shows the re-establishment of the Pacific High following the invasion of the area by colder air. By the evening of that day the pressure at the center rose to 1028 mb. Tables 5, 6, and 7 give the rainfall values of this storm, whose maximum 72-hour value is exceeded only by the 1937 storm.

82. Storm of December 9-11, 1937. Of all the major storms studied, the most truly representative of the maximum Sacramento type is that of December 1937. It was characterized by the persistence of a steep southeast-northwest gradient that produced southwest winds of nearly gale velocities over the basin for about two days. With the exception of the final clearing front, the frontal passages over the basin were not as well-marked as in the February 1940 storm. The procession of moist tongues, in other words, was so briefly and immaterially interrupted by the colder and drier tongues that the storm could be described as characterized by the persistence of a moist tongue over the basin. As in the February 1940 storm, the region of principal activity was between a cold, occluded Low and the warm, southeastwardly displaced Pacific High. Between the two the temperature contrast was great but, as will be indicated in the next chapter's section on maximum winds,

still not great enough to cause an increase of pressure gradient with height in the critical first 10,000 feet.

83. The weather map for December 9 (Figure 84) bears a close resemblance to the first map of the February 1940 series (Figure 69). The cold continental anticyclone extending by way of the central states from Alaska to the Gulf was again in evidence. Westward and northwestward from the coast were two intense cyclonic centers dominating the circulation over the Pacific. South of the centers mPk air was being transformed to mTk. During the day the centers advanced eastward and continued to deepen and strengthen. So far south did the huge cyclonic circulation expand that the temperature and moisture content of the air brought over the basin were near the maximum values for December. On the 10th, in fact, San Francisco reported its maximum dew point for any winter season of record.

84. The combined result of the persistent gradient, the southwest wind and the high moisture content is presented in the rainfall tabulations of Tables 8, 9, 10. Except during a short period following the passage of the occluded front on the morning of December 10 (Figure 85), there was little diminution of rainfall intensity throughout the storm. For the maximum 72-hour duration over the whole basin, it is the most intense of record. Although of comparatively short total duration its total accumulated rainfall exceeds that of many flood-producing storms of much longer duration. The greatest amounts fell in the Feather-Yuba section at elevations between 3,000 and 6,000 feet. Except on a few of the higher peaks, the precipitation was entirely in the form of rain. In the 48 hours ending at 6 p.m. (P.S.T.) of the 11th about 19 inches of

rain fell at Scales on the North Fork of the Yuba and about 18 inches at Inskip and Brush Creek Ranger Station in the North and Middle Forks of the Feather respectively.

85. Snow conditions antecedent to the storm period were somewhat like those preceding the February 1940 storm. Heavy rains had occurred over the upper Sacramento Basin as early as the first week in October and a long-protracted heavy rainfall followed in November. Snow cover had receded to high elevations, the ground was well saturated, but stream channels and bypasses were not carrying much water. On account of the abnormally high temperatures and heavy rainfall of the storm, most of the prior snow cover that did exist, such as the 12 inches above the 6,000-foot level in the headwaters of the American, melted during December 10, releasing two to three inches of water. Following the passage inland of the cold front on the morning of December 11, Figure 87, the heavy rainfall ended and the Pacific High was re-established with the influx of colder air.

86. Storm of December 8-16, 1929. Of all the storms subjected to synoptic analysis in this chapter, the storm of December 1929 was the only one which did not produce a major flood. However, antecedent conditions, not the lack of prolonged heavy rains, were the chief factors acting to prevent flooding of the Sacramento River and its tributaries. During the month of November, only one California station, out of a total of more than 250, reported measurable precipitation, and during the first week in December only scattered light rains were reported. Summit (elevation 7017 ft.) in Placer County reported no snow on the ground on December 7, 16 inches on the 12th, and 11 inches on the 16th. McCloud

(3270 ft.) in Siskiyou County reported no snow on the ground during the entire month and Portola (4832 ft.) in Plumas County reported snow on the ground on one day only, 2 inches on December 10.

87. The circulation pattern which had resulted in the drought conditions and which was characterized by the persistence of high pressure along the west coast, suddenly gave way to a new pattern on December 8. By the morning of the 9th the synoptic chart showed the familiar cold continental High, this time farther east in the United States than in the first days of the storms previously described. Again this High stretched northward into Canada and Alaska, but from Alaska it bulged southward to the 45th parallel in a large anticyclonic wedge. South of the wedge a comparatively narrow belt of low pressure extended from mid-continent westward into the far Pacific. The warm, semipermanent Pacific High, somewhat stronger and more extensive than in the 1940 and 1937 storms, rested southeast of its mean position.

88. Under the new regime the gradient winds over northern California settled into southwest, there to remain for several days, little disturbed by the passing fronts. The polar front, with its family of wave cyclones, lay in the belt of low pressure. Although most of these waves occluded, none occluded as completely as the major developments in 1940 and 1937. Some persisted as stable waves throughout the period while others were damped out (Figure 89) as they entered the field of the warm, dynamic anticyclone. The basic temperature contrast across the front in this storm, it is important to note, was often between warm air in the low pressure along the front and the cold anticyclone to the northwest. In such a situation, as will be shown in the next chapter,

the pressure gradient must decrease with height.

89. In advance of the first of the cyclones to approach the coast, the air flowing into northern California was tropical Pacific, i.e., air which had traveled around the periphery of the semipermanent Pacific anticyclone. The current of tropical air remained undisturbed by the passage inland of this cyclone as its portion of the polar front recurved sharply westward from the Low center over Washington and reached the Siskiyou Mountains as the southern limit of its movement. The second wave cyclone, partially occluded and more intense, swung its portion of the polar front directly across northern California on December 10 (Figure 88) as the center moved into the region off Vancouver Island and stagnated. Heavy rains fell during the period from the evening of December 9 to about noon (P.S.T.) of the 10th as nearly every factor which can act to produce intense rainfall was brought into play -- increased southwesterly winds in advance of the front, convergence in the frontal trough, and the lifting action of the cold front itself. Only the inherent stability of the tropical air prevented the higher rainfall intensities possible for the given temperature and moisture conditions.

90. There followed next a period of light rains as the isobaric pattern changed temporarily to anticyclonic, but the rate of fall increased again during the afternoon of December 11 and continued strong until the next front (a rather weak occlusion of limited extent) passed across the basin by the early morning of the 12th (Figure 89). Air flowing over the basin was now predominantly modified polar air. During the following two days another pair of occlusions, moving toward the coast, dissipated before reaching the continent as they entered the southwesterly

current of the Pacific High. Gradually the tropical air returned to northern California as the primary scene of action shifted to the cyclone which had stagnated off the northwest coast. Temporarily the head of the Pacific High extended northward to cause a cessation of rain over the southern portion of the basin. It is interesting to note the influence of this anticyclonic circulation in producing marked stability. Not only did the rain cease, but cloudiness decreased noticeably despite dew point readings of 60 F or more at San Francisco and Sacramento on the afternoon of the 13th.

91. Southwestward from the cyclonic center near Vancouver Island the low pressure trough became on December 11 the scene of frontogenesis between the fresh polar air and the modified polar air to the south. The newly formed front moved into Washington and Oregon and trailed westward along the 40th parallel (Figure 89). A wave on this front moved northeastward on December 13 into the region so recently vacated by the parent disturbance, but its influence was not felt in California where the southwest winds around the high ridge still held sway. On the 13th frontogenesis again occurred in the southwestward extension of the low pressure, this time intensifying the cyclone and producing a well-marked front which rapidly moved inland to northern Idaho by the evening of December 14 (Figure 90). Once again wave development over the ocean prevented a marked frontal passage in California, the southward advance of the cold front being checked just south of the Siskiyous. Rains continued spasmodically for another four or five days as pressure fell in the Aleutian-Gulf of Alaska region and the Pacific anticyclone simultaneously but gradually resumed a more normal size and position. The

major part of the rain had fallen by the evening of the 14th. Table 11 shows that the maximum 72-hour rainfall for the entire basin occurred up to 6:00 a.m. (P.S.T.) of the 12th and also indicates the percentage of the mean seasonal rainfall to be substantially below the 1940 and 1937 values. Tables 12 and 13 give accumulated precipitation amounts by zones and combined zones, respectively. The Feather and Yuba basins received the highest amounts, although Kennett in Shasta County recorded the heaviest total point rainfall for the storm period: 35.29 inches from December 8 to December 16, inclusive. The explanation for this extremely large total in the Kennett area probably lies in the relative stability of the air, which in this storm was predominantly tropical Pacific. Because stable air resists lifting, there is a very marked tendency for the air to be deflected northward along the valley floor rather than to escape across the Sierras. Eventually, of course, its movement is blocked in the landlocked upper portion of the basin and, with the force of the pressure gradient continuously feeding the air into that bottleneck, ascent must take place with the consequent condensation and precipitation.

92. Storm of March 22-27, 1928. It is only by coincidence that the four most recent major storms, and therefore the four for which synoptic charts are reproduced in this report, can be ranked in such a manner as to make their synoptic and rainfall values significantly comparable. On the basis of 72-hour maximum duration-depths for the total basin, they rank in the following descending order: 1937, 1940, 1929, 1928. An examination of the synoptic charts will show that the intensity of occlusion, as exhibited by the depth of the cyclonic center and the

surface pressure gradient, varies in exactly the same order. The storm of March 1928, in both categories, is at the bottom of the list. It is, in fact, at the bottom of a list which includes the major, basin-wide storms yet to be discussed.

93. As shown in Figures 91 and 92, throughout most of the storm period under consideration the polar front was quasi-stationary from the Great Lakes to the vicinity of Hawaii. From March 22 to March 25, several non-occluding waves traveled along the front across northern California resulting in variations in position and orientation of the front (87) over the Sacramento Basin. Until the passage of the final front (Figure 93) on March 26, the surface pressure gradient was never steep and, since the temperature contrast across the front was from warm Low to cold High, the pressure gradient aloft could not increase. The southwesterly winds therefore did not attain great velocities except for the brief period preceding the final front which accompanied the only occluded system of the series. It is instructive to compare the map of March 26, 1928 (Figure 93) with the a.m. map for December 10, 1937 (Figure 85) and see that during this final period the 1928 storm was a smaller version of the 1937.

94. Despite the presence of a quasi-stationary polar front across the basin during much of the period, this storm did not differ essentially from the Sacramento storm type. The rain-bearing winds were from the southwest and the air had acquired its moisture and instability in about the usual manner, with the difference that the air had remained longer in the more southern latitudes. It had thus acquired a character more nearly tropical maritime than usual, like the air in the prefrontal

incursions of the 1929 storm. Scattered rains began over the northern portion of the state on March 21, following a week when little or no rain occurred throughout the state. On the 22nd rains became general over the basin and continued with varying intensity through March 27. With the passage of each wave, rainfall intensities increased as the attendant convergence augmented the orographic influences in producing the vertical motions which wring from the air its load of moisture. It can be assumed that an upper trough and warm moist tongue accompanied each wave crest along the front, much like the tongues accompanying the occluded fronts of the February 1940 storm, as shown on the isentropic charts. In the non-occluded case, such as 1928, the tongues would be smaller and the rainfall of lesser magnitude.

95. The weather map for 8:00 p.m., March 23 (Figure 91) illustrates the large number of waves on the polar front. Another interesting feature of this map is the appearance of an incipient cyclone at about latitude 33° N. and longitude 148° W., which later developed into a vigorous center and carried with it the cold front that swept across the basin to end the flood-producing rains. The path of this Low is plotted on all the maps. The a.m. map of March 25 (Figure 92) shows a later stage in its development. Following this, the Low deepened rapidly and moved with increased speed into the region off Vancouver Island. The attendant cold front moved across the basin on March 26 (Figure 93) and the colder air following it displaced the moist southwesterly current. Immediately in advance of the cold front the southwesterly winds reached maximum velocities for the storm and during the period from noon to 6 p.m. (P.S.T.) of the 26th the greatest 6-hourly increments of rainfall were

recorded for the entire basin. Instability showers continued for some time in the unstable cold air but, as usual, the definite shift to westerly winds ended the storm.

96. The rainfall records (Tables 14, 15, and 16) and river stages clearly indicate concentration of precipitation along the west slope of the Sierras in this storm. The Feather, Yuba, and particularly the American drainage systems contributed heavily to the flooding of the lower Sacramento River. The isohyetal peak at Kennett, common to most of the other storms and to the N.S.P., was missing in this storm. The cold air at low levels in the basin, especially the northern portion, was partly responsible for this departure. It prevented the northward deflection of low level air from the south and its subsequent convergence and lifting in the landlocked northern end of the valley. The usual circumstances in the Sacramento storm type have been described in the first section of this chapter. In March 1928, with a quasi-stationary front across the basin, the low-level winds to the north of the front were actually northerly whereas in the usual storm they would have a southerly component. In addition, as has already been noted, the southwest winds were seldom as strong in this storm as in some of the others studied. Also acting to prevent the heavier rains in the upper portion of the basin and producing a concentration along the Sierras was the anticyclonic deflection of the overrunning moist air (22, pp. 112-114).

97. Snow melt contributed very little to the runoff in this flood. According to Taylor (95), "at no time during the high waters was there any snow on the flanks of the mountains, and that on the ground was confined to the extreme altitudes, where there was much less than usually

has accumulated at this season of the year."

98. Before ending the discussion of the March 1928 storm it is well to point out that it illustrates another feature of the Sacramento storm type. Those acquainted with previous reports of the Hydrometeorological Section should be struck by the resemblance between the chief synoptic feature of the March 1928 storm and the chief feature of many other major storms that have occurred elsewhere in the country. In particular, a comparison can be made of the p.m. map for March 23, 1928 (Figure 91) with the maps for March 24-26, 1913, reproduced in the Pittsburgh Report (2). The latter was, of course, an Ohio Valley storm, but both storms are distinctly the quasi-stationary frontal type. In the Ohio Valley, and in other regions where the orographic influence is not marked, this type produces a definite and recognizable isohyetal pattern. The isohyets are elongated ellipses with their major axes parallel to the mean position of the front. In the case of the Sacramento Basin, however, the occurrence of the quasi-stationary front does not produce its characteristic pattern. The general isohyetal pattern of the March 1928 storm is the pattern of all the other Sacramento storms. In this storm, as in all the others, it is the basin that produces the isohyetal pattern -- which is a variant of the N.S.P. map.

99. Storm of December 29, 1913, to January 3, 1914. In its general meteorological aspects this storm was similar to the February 1940 storm. The number of days in the storm period was six in each case. The number of fronts was four in this storm and five in 1940, which accounts in part for the difference in total storm rainfall. The patterns of the frontal and cyclonic systems were markedly similar,

although an analysis of the few ship reports available indicates that the cyclonic centers were approximately 5° farther north in the 1913-14 storm than in 1940. This greater distance between the basin and the Low centers resulted in lower average gradient winds over the critical area and alsc in a northward displacement of the warm sectors of the cyclones which, on one or two days during the storm, were far enough north to permit an ingress of tropical air at the surface.

100. An examination of Tables 18 and 19 reveals that the total storm rainfall, although smaller, was distributed in much the same manner as in February 1940. Figures for percentage of N.S.P. of the maximum 72-hour rainfall (Tables 5 and 17) follow much the same pattern, zone by zone, for the two storms. In only two of the zones did the 1913-14 storm exceed that of 1940. Prior to the general, heavy rains of the storm period there had been widespread precipitation of moderate intensity over northern California from about the 20th to the 25th of December, followed by widely scattered small amounts of rainfall on the 27th and 28th. It is reasonable to suppose then that the ground over the drainage basin was nearly saturated and, with river stages at relatively high levels, conditions were favorable for high runoff and resultant flood stages during the storm period. The snow mantle had been increased during the period December 20 to 25. Records indicate an accumulation of snow at elevations somewhat below 5000 feet in the southeastern portion of the basin and at considerably lower elevations in the northern end of the drainage system where McCloud (3270 ft.) reported a depth on the ground of 23 inches on the 29th. This snow cover at McCloud decreased to 5 inches during the storm period and at Emigrant Gap (5230 ft.) a snow

depth of 46 inches on the 29th decreased to 9 inches by January 1. The records show that even at Summit (7017 ft.) in Placer County there was a marked diminution of the cover during the height of the storm. A depth of 101 inches was reported on December 30, and 80 inches on December 31 and January 1. The observer's notes indicate that rain fell on the 31st.

101. Storm of January 23-31, 1911. This was a minor storm in comparison with others studied. It was not critical for the basin as a whole. The heaviest rainfall and flood conditions were confined to the southeastern portion. Two tables of precipitation data (Tables 20 and 21) are reproduced and both are limited to the southern zones. Although total storm rainfall was high for these zones, the 72-hour amounts were relatively light, as shown by percentage of the mean seasonal which in this storm averaged considerably below other storms in this series. On account of the limited area of critical rainfall there is no table of accumulated precipitation by combined zones.

102. Storm of January 12-16, 1909. The month of January 1909 was one of almost continuous rain in California, the average precipitation for the state being 6 inches above the normal of 10.17 inches. The interval January 12-16 was selected for study, not because the flood rains had so definite a beginning or ending, but rather because the highest stages on the Sacramento River were reached during that period. The rainfall for the five days ranged from 20 to 40 per cent of the monthly total.

103. Both in rainfall values and principal synoptic features the storm ranks between the 1940 and the 1929. Just as in the others, its opening phase was characterized by the cold continental High extending

in an arc from the Gulf of Mexico to Alaska and then, as in 1929, bulging southward over the Pacific. In the orientation of the polar front and the number of systems on it, the 1909 storm most closely resembles the 1929 pattern, with the important difference that the front is farther south and the occlusions on it more intense. The warm Pacific High was naturally farther southeast. As a result of such a displacement the "tip" of each occlusion (i.e., the apex of each occluding warm sector) generally passed a short distance south of the basin. The successive passage of such crests, which are areas of maximum convergence and accompanied by the usual moist tongue aloft, made the concentration of rainfall greatest over the southern part of the critical area, particularly in such a basin as the American. In this item the storm differed from the 1929 storm, which had an exceptional peak at Kennett in the north. An additional factor causing the 1909 distribution was the southward displacement, along with the other synoptic features, of the Canadian portion of the continental High. Extremely cold air flowed southward into Washington and Oregon and appeared, though modified, in northern California with northerly winds, as in the 1928 storm which also lacked the northern isohyetal peak.

104. At the beginning of the storm period a belt of low pressure lay approximately along the 40th parallel, extending from Colorado westward into mid-Pacific. Within this belt there were two cyclonic centers, each associated with an occlusion on the polar front which lay along the 30th parallel. A developing wave appeared southwest of the second cyclonic center. By the morning of January 13 both occlusions had passed eastward beyond the basin and the wave, having deepened rapidly and

reached the occluding stage, was moving northeastward toward the Puget Sound region. The following 24 hours saw increasing southwesterly winds across the basin as this third system reached its maximum intensity and the occlusion approached the coast. Rainfall diminished in intensity for a time after the occluded front had crossed the basin and caused a slight veering of the winds, but resumed its greater rate during the evening of the 14th as the winds backed slightly and increased in speed with the approach of still another frontal system. This time the Low center moved inland even farther north than its predecessor. The front, oriented northeast-southwest, crossed northern California during the night of the 15th and early morning of the 16th. The winds veered sharply and brought the familiar cessation of continuous torrential rains. Frontal activity continued for some days after the 16th but, at least for several succeeding days, rainfall was lighter because the polar front gradually moved farther north and the air following each cyclonic disturbance had not been carried southward far enough to attain maximum moisture content.

105. Snowfall records from Emigrant Gap (elevation 5230 ft.) indicate on January 11 an accumulation of 10 inches which disappeared completely by the 15th. Summit (7017 ft.) reported an accumulation of 121 inches on the 11th which increased to 127 inches on January 14 and fell to 89 inches by the 17th. These records, coupled with a knowledge of temperature conditions (average of 5 degrees above normal from January 11 to 17 for six stations selected at random) indicate a large contribution of snow melt to the storm runoff. The precipitation values are given in Tables 22, 23, and 24.

106. Storm of March 16 to 20, 1907. Several prolonged periods of

precipitation during January, February, and the early part of March had produced some flood stages on the Sacramento and its tributaries. Each succeeding storm added considerably to the accumulation of snow in the high Sierras above an elevation of about 6000 feet. Most significant was the deposition onto bare ground of a fresh snow cover down to an elevation of about 2500 feet during the period from March 8 to 12. Snow depths slowly diminished during the next three days but, when the heavy rains set in on the 16th, rapid melting of the fresh snow cover began. Outstanding among records examined were those of Deer Creek (3700 ft.) and Emigrant Gap (5230 ft.). At the former station a snow cover of 29 inches on the 12th disappeared by the 18th, and at the latter station 49 inches of snow on the 12th diminished to a trace by the 19th. On the basis of available records it can be conservatively estimated that the snow line, which was near 2500 feet at the beginning of the storm period, receded to an elevation of about 5500 feet by the 19th. No attempt was made to determine the contribution of this snow melt to the runoff for the basin because snow depth records are concentrated mainly in the American and Yuba drainage systems while little is definitely known about other portions of the basin. Nevertheless, it is certain that the contribution of snow melt to runoff was far greater in this storm than in any of the other storms studied, with the possible exception of the 1861-62 storm for which even fewer records are available.

107. In orientation and position of the major frontal system the 1907 storm resembled the storm of March 1928. On March 15 the polar front moved southeastward across the coastal states and by the morning of the 16th had become practically stationary across California near the

southern end of the San Joaquin Valley. Rain began early on the 16th as tropical Pacific air overran the cooler air north of the front. Three wave cyclones moved directly across the Sacramento Basin between the evening of the 16th and the night of the 19th. As each partly occluded wave crossed the basin the frontal rains augmented the continuing orographic rainfall, producing peaks in intensity. With the approach of each cyclonic center the surface tropical air moved into the southern end of the Sacramento Valley and with the passage of the cyclone was replaced by modified polar air which had traveled southward to about 30° latitude before returning as a southwesterly wind behind the occluding wave. In this storm a considerable amount of rain fell from tropical Pacific air, although maximum rainfall intensities occurred whenever the modified polar Pacific air followed the occluding waves across the basin.

108. According to Scarr (86), this period of heavy rainfall "... was accompanied by unusually warm weather, especially at the higher altitudes, causing rapid melting of the soft snow and a runoff probably the heaviest since these valleys have been inhabited by civilized people .... All previous high-water records were surpassed at all points on the Feather, Yuba, and Bear Rivers, also at all points on the Sacramento River, except Red Bluff and Sacramento.... Undoubtedly this flood was the greatest since the lowlands of the Sacramento and San Joaquin Valleys have been reclaimed to any considerable extent. It is probable that the volume of water discharged was equal to if not greater than that of 1862, referred to as the 'great flood'." The storm's rainfall values are given in Tables 25, 26, and 27.

109. Storm of January 11-19, 1906. During this storm period

phenomenal amounts of rain fell over much of the Sacramento Basin. The stations reporting the largest amounts were: Helen Mine 38.13, Magalia 35.29, Stirling City 33.32, La Porte 29.32, Fordyce Dam 28.08, Pilot Creek 27.56, and Brush Creek 27.06 inches. These are totals for the entire storm period which, it can be seen, was uncommonly long. The 72-hour maximum depth's percentage of N.S.P. was only 15.6 for the total basin (Table 28). Only the March 1928 storm has a lower corresponding value.

110. Prior to the storm period the season had been unusually dry and cold and conditions were not favorable for rapid runoff. In addition, above the 5000-foot level, most of the storm precipitation occurred in the form of snow. In the American Basin, from January 10 to 19 the snow depth increased from 23 inches to 157 inches at Summit (7017 ft.) but at Blue Canyon (4695 ft.) it increased from 5 to 12 inches and then decreased to 2 inches. At Fordyce Dam (6500 ft.), in the Yuba, it increased from 31 to 99 inches and from 28.5 to 40 inches at La Porte (5000 ft.), also in the Yuba. The antecedent conditions, the small contribution from melting snow, and the storm snowfall at the higher elevations prevented more than moderate flooding of the basin.

111. Because of the scarcity of oceanic and Canadian observations the meteorological pattern of this storm is not too clearly defined. The usual cold anticyclone in the central states was evident in the early stages. It is also apparent that during most of the storm period the persistence of a low pressure center of varying intensity off the Washington coast governed the circulation over the coastal states. The air generally flowing over northern California was moist unstable polar air

which had assumed tropical characteristics and its direction was predominantly southwesterly.

112. From the 11th through the 16th three periods of extended light to moderate precipitation preceded frontal passages on the morning of the 12th, the evening of the 13th, and the morning of the 16th. Precipitation started well in advance of each of the fronts but, as usual, was heaviest for several hours just prior to the frontal passage due to increased transport and convergence of the moist unstable air. At each passage the wind shifted to a more westerly direction and, as in the other storms, the precipitation ceased temporarily except for light amounts due to the orographic lifting over some of the high regions. During the 17th and 18th a wave on the front which then lay southwest of the Sacramento Basin developed into a major cyclonic system. The pressure gradient over the basin steepened considerably and with the usual results — 5 to 10 inches of precipitation in 24 hours over the western slopes of the Sierra Nevada Mountains. The increments by zone are contained in Tables 28, 29, and 30. The rain period ended on the morning of January 19 with the passage of a well-marked cold front and the invasion of the area by cold air that re-established the Pacific High.

113. Storms of January 1862. In the preceding chapter an account was given of the rains of the winter of 1861-62. In this section an attempt is made to reconstruct the meteorological pattern of the January storms which were responsible for the highest stages observed at Sacramento up to that date. Meteorological data were, of course, extremely limited. Tridaily observations were available from eight California stations, located from San Francisco northward, and operated by the

Smithsonian Institution and the Surgeon General's Office. Supplementary information was obtained from accounts of travelers through the Sacramento Basin and from histories of the period. From these meager clues it is possible to infer certain broad features of the meteorological situation.

114. On January 5, 1862, the polar front was located some distance south of San Francisco, extending east-northeastward and westward as a quasi-stationary front much like the one in the March 1928 storm (see Figures 91 and 92). The important differences between the two storms are that in 1862 the front was farther south and the temperatures north of it, particularly in the Sacramento Basin, were lower. Between January 5 and 7, 1862, wave action on the quasi-stationary front caused rain near Sacramento and snow to moderate depths but a short distance northward. By the 7th a cyclone had developed on the polar front over the Pacific. As a result there was increased overrunning of moist air northeastward. Warm rains and rising temperatures occurred over the basin as the polar front east of the new cyclone receded northward in advance of the cyclone's northeastward progress. This final sequence also bears a close resemblance to the final stages of the March 1928 storm (Figures 91 to 93).

115. As in the 1928 storm, there is little evidence of a strong southwesterly current except in the latter stages of the final cyclonic development. In both storms the quasi-stationary frontal pattern is sharp enough to induce northerly winds in the cold air in the valley, always an unusual circumstance. The most important conclusion to be drawn from the 1862 sequence of events is the possibility of rapid transition from significant snow cover over most of the basin — with the

concomitant of saturated or frozen soil -- to warm, heavy rains. Following stages already bankful, such a combination of events will naturally produce an extreme flood.

116. By the morning of January 15, colder stable air had again invaded the basin. The polar front was again displaced southward and, so far as can be determined, the frontal and cyclonic pattern of the earlier storm repeated -- at least between the 15th and 17th. For this period no snowfall information is available. However, as late as January 29, a snowfall of three inches in 18 hours was recorded at Sacramento. Up to that date there was no definite cessation of either precipitation or flooding.

TABLE 5

SACRAMENTO BASIN STUDY

MAXIMUM DURATION-DEPTH VALUES

February 1940 Storm

(Duration--Hours)

	6	12	18	24	36	48	72	96	120	N.S.P.	Percentage N.S.P. (72 hrs. ending 6A/29, P.S.T.)
A	1.9	3.3	4.7	4.9	7.4	9.3	10.3	10.5	10.8	35.4	28.5
B	0.8	1.5	2.0	2.3	3.1	3.8	4.1	4.6	4.7	20.7	19.8
C_2	1.1	2.0	2.8	3.8	4.9	5.7	7.6	8.8	9.4	49.6	15.3
D	1.6	2.8	4.2	5.4	6.7	7.6	9.8	10.8	11.6	51.8	18.9
E	1.9	3.7	4.8	5.0	6.8	8.4	9.0	9.5	9.5	31.6	27.2
F	2.5	4.7	6.4	7.5	10.4	12.3	14.2	15.7	16.7	59.6	23.8
G	2.3	4.1	5.6	7.0	9.7	12.1	14.5	15.8	16.6	71.3	20.3
J	1.3	2.0	3.0	3.8	5.5	6.6	8.3	8.6	9.0	33.2	25.0
K	2.8	4.4	5.5	5.7	8.8	10.2	10.8	11.6	11.8	49.7	21.1
L	0.9	1.7	2.4	2.5	3.8	4.6	4.9	5.3	5.4	27.4	17.5
M	1.3	2.4	3.3	3.8	5.6	6.7	7.5	8.2	8.8	43.8	17.1
N	2.4	4.0	5.6	5.9	8.9	10.8	12.2	13.4	14.4	63.7	18.7
P	0.7	1.3	1.6	1.7	2.7	3.1	3.5	3.7	4.0	22.9	15.3
HC_1	1.6	3.1	4.1	5.2	7.0	8.4	11.0	12.3	13.2	57.8	19.0
GJ	1.5	2.5	3.6	4.6	6.5	8.1	10.0	10.7	11.1	43.9	22.8
KLMNP	1.3	2.1	2.8	3.0	4.9	5.8	6.4	6.9	7.4	31.6	19.9
Total	1.1	2.0	2.8	3.4	5.1	6.4	7.4	7.9	8.4	37.1	19.9
Max. Period Ending* (P.S.T.)	M/26	6A/27	6A/27	6P/27	6A/28	6A/28	6A/29	M/28	N/29		

* Applicable only to the total basin.

TABLE 6

SACRAMENTO BASIN STUDY

ACCUMULATED PRECIPITATION BY ZONES

February 24-29, 1940 Storm
(6-Hour Periods)

Zone	A	B	C_2	D	E	F	G	J	K	L	M	N	P
Period Ending (P.S.T.)													
N/24	0	0	0	0	0	0	0	0	0	0	0	0.2	0
6P/24	0.1	0	0	0	0.2	0	0	0	0.3	0.1	0.1	0.8	0.2
M/24	0.3	0.1	0.1	0	0.4	0.3	0.2	0	0.5	0.3	0.3	1.3	0.3
6A/25	0.3	0.3	0.5	0.5	0.5	0.9	0.7	0.2	0.7	0.3	0.6	1.5	0.3
N/25	0.4	0.5	1.3	1.1	0.5	1.3	1.2	0.4	1.0	0.6	0.7	1.9	0.5
6P/25	0.4	0.6	1.5	1.2	0.7	1.6	1.6	0.5	1.1	0.6	0.9	2.0	0.5
M/25	0.4	0.6	1.6	1.4	0.7	1.8	1.7	0.5	1.2	0.6	1.0	2.1	0.5
6A/26	0.7	0.6	1.7	1.5	0.9	2.4	2.0	0.6	1.3	0.6	1.3	2.5	0.5
N/26	1.5	0.9	2.0	2.0	1.4	3.5	3.2	1.3	1.6	0.7	1.7	3.0	0.6
6P/26	2.6	1.4	2.8	2.8	2.5	5.2	4.7	1.8	3.4	1.5	2.8	4.4	1.2
M/26	4.1	2.1	3.8	4.0	3.9	7.7	6.5	2.4	5.2	2.3	4.1	6.5	1.9
6A/27	5.1	2.9	4.8	5.6	4.5	9.9	8.8	3.7	5.8	2.7	5.0	7.4	2.2
N/27	5.3	3.1	5.5	6.6	4.5	10.9	9.9	4.4	6.0	2.8	5.5	7.7	2.3
6P/27	6.7	3.7	6.6	8.2	5.6	12.4	11.7	5.4	7.6	3.6	6.3	9.3	2.6
M/27	8.6	3.8	6.8	8.5	7.5	13.9	12.8	6.2	10.4	4.5	7.3	11.7	3.3
6A/28	10.0	4.4	7.4	8.9	9.3	14.7	14.1	7.2	11.5	5.2	8.0	13.3	3.6
N/28	10.1	4.4	7.7	9.6	9.5	15.2	15.0	7.9	11.6	5.3	8.2	13.3	3.6
6P/28	10.3	4.5	8.1	9.8	9.5	15.3	15.3	8.1	11.7	5.3	8.3	14.2	3.7
M/28	10.7	4.7	8.8	10.6	9.5	15.8	15.7	8.4	11.8	5.4	8.5	14.3	4.0
6A/29	10.8	4.7	9.3	11.3	9.5	16.6	16.5	8.9	11.8	5.4	8.8	14.4	4.0
N/29	10.8	4.7	9.4	11.6	9.5	16.7	16.6	9.0	11.8	5.4	8.8	14.4	4.0

TABLE 7

SACRAMENTO BASIN STUDY

ACCUMULATED PRECIPITATION BY COMBINED ZONES

February 24-29, 1940 Storm

(6-Hour Periods)

Period Ending (P.S.T.)	Yuba (HC_1)	Feather (GJ)	Upper Sac. (KLMNP)	Entire Basin
N/24	0	0	0	0
6P/24	0	0	0.3	0.1
M/24	0.1	0.1	0.5	0.3
6A/25	0.7	0.3	0.6	0.5
N/25	1.4	0.6	0.8	0.8
6P/25	1.7	0.8	0.9	0.9
M/25	1.9	0.8	0.9	0.9
6A/26	2.0	1.0	1.1	1.0
N/26	2.8	1.8	1.3	1.5
6P/26	3.8	2.6	2.2	2.3
M/26	5.3	3.6	3.4	3.4
6A/27	6.9	5.1	3.9	4.3
N/27	7.4	5.9	4.1	4.7
6P/27	9.0	7.2	4.9	5.7
M/27	9.8	8.0	6.2	6.6
6A/28	10.4	9.1	6.9	7.4
N/28	10.7	9.9	6.9	7.6
6P/28	11.4	10.1	7.2	7.8
M/28	12.3	10.4	7.3	8.2
6A/29	13.0	11.0	7.4	8.4
N/29	13.2	11.1	7.4	8.4

TABLE 8

SACRAMENTO BASIN STUDY

MAXIMUM DURATION-DEPTH VALUES

December 1937 Storm

(Duration--Hours)

	6	12	18	24	36	48	72	96	N.S.P.	Percentage N.S.P. (72 hrs. ending 6A/12, P.S.T.)
A	2.7	4.2	5.9	7.4	10.0	11.1	11.5	11.5	35.4	32.5
B	0.8	1.5	1.7	2.3	3.2	3.9	4.2	4.2	20.7	19.8
C_2	1.4	2.6	3.8	4.2	6.3	7.7	8.4	8.4	49.6	15.7
D	1.9	3.6	5.0	5.6	8.3	10.5	11.5	11.6	51.8	21.4
E	1.7	3.4	3.8	5.0	6.8	9.0	9.5	9.5	31.6	29.8
F	2.7	5.4	6.4	7.3	11.5	14.1	14.9	15.0	59.6	25.0
G	2.9	5.0	6.8	8.3	12.9	15.4	16.7	16.8	71.3	23.3
J	1.3	2.5	3.8	4.6	6.3	8.0	8.7	8.7	33.2	26.2
K	1.6	2.9	4.1	5.2	6.9	8.2	8.9	8.9	49.7	17.7
L	1.5	2.4	3.1	3.7	5.2	6.0	6.1	6.1	27.4	22.3
M	2.7	4.6	6.2	8.1	10.8	12.2	12.7	12.7	43.8	29.0
N	2.0	3.7	5.5	7.0	9.1	10.8	11.3	11.7	63.7	18.0
P	1.2	2.1	3.1	4.2	5.4	6.0	6.2	6.2	22.9	26.2
HC_1	1.9	3.9	4.6	5.7	8.7	10.4	11.3	11.4	57.8	19.0
GJ	1.6	3.1	4.5	5.4	8.2	10.0	10.8	11.0	43.9	24.6
KLMNP	1.3	2.5	3.6	4.8	6.8	7.8	8.1	8.2	31.6	25.6
Total	1.3	2.4	3.5	4.6	6.8	7.9	8.5	8.6	37.1	22.9
Max. Period Ending* (P.S.T.)	N/10	N/10	N/10	6A/11	6A/11	N/11	6A/12	N/12		

*Applicable only to the total basin.

TABLE 9

SACRAMENTO BASIN STUDY

ACCUMULATED PRECIPITATION BY ZONES

December 9-12, 1937 Storm
(6-Hour Periods)

Zone	A	B	C_2	D	E	F	G	J	K	L	M	N	P
Period Ending (P.S.T.)													
6A/9	0	0	0	0	0	0	0.1	0.1	0	0	0	0.2	0
N/9	0.1	0.2	0.1	0.1	0.7	0.1	0.4	0.4	0.5	0.3	0.4	0.7	0
6P/9	0.9	0.7	0.4	0.5	2.2	1.0	1.5	1.2	1.4	0.8	1.2	2.0	0.2
M/9	2.3	1.1	1.6	1.9	2.8	3.7	4.0	2.5	2.5	1.5	2.9	3.5	1.0
6A/10	3.5	1.6	3.0	3.8	4.0	6.4	6.5	3.7	3.7	2.4	4.8	5.3	1.4
N/10	5.2	2.3	4.2	5.5	5.2	7.4	8.3	5.0	5.0	3.9	6.4	7.0	2.5
6P/10	6.7	2.4	4.6	6.1	5.6	8.0	9.8	5.8	6.6	4.5	8.3	9.0	3.5
M/10	9.4	3.1	5.7	7.0	7.3	9.9	11.5	6.6	7.4	5.2	11.0	9.8	4.4
6A/11	10.9	3.9	6.7	8.9	9.0	12.5	14.4	7.5	8.2	6.0	12.0	11.0	5.6
N/11	11.2	4.1	7.8	10.3	9.1	14.2	15.8	8.4	8.7	6.1	12.6	11.4	6.0
6P/11	11.2	4.1	7.8	11.0	9.1	14.6	16.3	8.6	8.8	6.1	12.6	11.5	6.0
M/11	11.5	4.1	7.8	11.1	9.4	14.9	16.6	8.7	8.8	6.1	12.7	11.5	6.0
6A/12	11.5	4.2	8.4	11.5	9.5	14.9	16.8	8.7	8.9	6.1	12.7	11.6	6.0
N/12	11.5	4.2	8.4	11.6	9.5	15.0	16.8	8.7	8.9	6.1	12.7	11.7	6.2

TABLE 10

SACRAMENTO BASIN STUDY

ACCUMULATED PRECIPITATION BY COMBINED ZONES

December 9-12, 1937 Storm
(6-Hour Periods)

Period Ending (P.S.T.)	Yuba (HC_1)	Feather (GJ)	Upper Sac. (KLMNP)	Entire Basin
6A/9	0	0.1	0	0
N/9	0.2	0.4	0.3	0.3
6P/9	0.8	1.2	1.0	0.9
M/9	2.6	2.8	1.9	2.0
6A/10	4.5	4.3	3.0	3.1
N/10	5.4	5.7	4.2	4.4
6P/10	6.5	6.6	5.5	5.4
M/10	7.9	7.8	6.7	6.4
6A/11	9.5	9.4	7.8	7.7
N/11	10.6	10.4	8.1	8.2
6P/11	10.7	10.7	8.1	8.4
M/11	11.0	10.8	8.1	8.4
6A/12	11.3	10.9	8.1	8.5
N/12	11.4	11.0	8.2	8.6

TABLE 11

SACRAMENTO BASIN STUDY

MAXIMUM DURATION-DEPTH VALUES

December 1929 Storm

(Duration--Hours)

	6	12	18	24	36	48	72	96	120	N.S.P.	Percentage N.S.P. (72 hrs. ending 6A/12, P.S.T.)
A	1.6	1.9	2.8	3.2	4.2	4.5	6.2	7.2	8.3	35.4	17.5
B	1.0	1.2	1.4	1.7	2.4	2.5	3.0	4.0	4.4	20.7	12.6
C_2	1.6	2.7	3.3	3.6	5.6	6.6	7.6	9.7	11.3	49.6	13.9
D	1.6	2.8	3.3	3.8	5.1	6.8	7.8	10.1	11.6	51.8	13.3
E	1.6	2.0	2.4	2.6	3.1	3.2	5.0	5.8	6.8	31.6	15.8
F	2.1	3.9	4.8	5.6	7.7	8.5	13.2	15.4	16.7	59.6	22.1
G	3.2	5.6	6.8	7.4	9.0	10.3	15.4	19.1	21.3	71.3	21.6
J	1.5	2.6	3.0	3.8	4.6	5.7	8.7	10.2	11.9	33.2	26.2
K	1.5	2.3	3.0	3.3	3.6	4.4	7.1	8.2	9.1	49.7	14.3
L	0.8	1.0	1.2	1.4	2.1	2.4	3.0	3.5	4.1	27.4	11.0
M	0.9	1.6	2.3	2.7	4.1	4.4	6.2	7.3	9.0	43.8	14.2
N	2.5	3.5	4.5	4.8	5.8	7.1	10.3	12.6	13.9	63.7	16.2
P	0.5	0.7	1.0	1.2	1.5	1.7	2.2	2.6	2.9	22.9	9.2
HC_1	2.4	4.1	5.0	5.8	8.4	9.9	11.2	14.3	16.3	57.8	18.5
GJ	1.8	3.4	4.1	4.7	5.8	6.7	10.6	12.9	14.5	43.9	24.1
KLMNP	0.8	1.2	1.7	2.0	2.4	2.7	4.7	5.4	6.2	31.6	14.9
Total	1.1	1.6	2.1	2.6	3.4	4.0	5.9	7.1	8.2	37.1	15.9
Max. Period Ending* (P.S.T.)	M/11	6A/12	6A/10	6A/10	6A/10	6P/10	6A/12	6A/12	6A/13		

* Applicable only to the total basin.

TABLE 12

SACRAMENTO BASIN STUDY

ACCUMULATED PRECIPITATION BY ZONES

December 8-16, 1929 Storm
(6-Hour Periods)

Zone	A	B	C_2	D	E	F	G	J	K	L	M	N	P
Period Ending (P.S.T.)													
6A/8	0	0	0	0	0	0.1	0.2	0	0.1	0	0	0.1	0
N/8	0.2	0.2	0.2	0.6	0.3	0.3	0.8	0.2	0.5	0.2	0.4	0.4	0.2
6P/8	0.8	0.3	0.6	0.9	0.3	0.3	0.8	0.4	0.6	0.2	0.4	0.7	0.2
M/8	0.8	0.6	1.4	2.1	0.8	1.4	2.1	1.3	0.9	0.4	0.8	1.1	0.4
6A/9	0.9	0.7	2.8	3.1	0.8	1.4	2.4	1.5	1.0	0.4	0.9	1.4	0.5
N/9	1.4	0.8	3.2	3.4	1.2	1.9	3.0	1.9	2.0	1.0	1.4	2.5	0.8
6P/9	2.6	1.0	3.5	3.9	2.5	3.7	5.4	3.4	3.0	1.4	2.2	3.7	1.0
M/9	3.0	1.2	4.6	4.4	3.2	5.8	8.6	4.5	3.6	1.6	3.0	4.4	1.5
6A/10	3.9	1.8	6.2	6.0	3.2	6.7	9.8	4.9	3.8	1.7	3.3	5.0	1.7
N/10	4.0	2.0	6.8	7.2	3.2	6.8	10.0	5.7	4.1	1.8	3.4	5.7	1.7
6P/10	4.0	2.0	7.1	7.7	3.2	6.9	10.2	6.1	4.5	1.8	3.6	6.5	1.8
M/10	4.8	2.1	7.2	7.7	3.2	7.5	10.9	6.4	4.6	1.9	3.8	6.6	1.9
6A/11	5.1	2.1	7.4	7.8	3.2	9.1	12.5	7.0	4.8	2.0	4.4	6.9	1.9
N/11	5.5	2.2	7.4	7.8	3.5	10.4	13.3	7.4	5.1	2.2	5.1	7.2	2.2
6P/11	5.6	2.4	7.8	8.4	4.0	11.1	14.1	7.9	5.8	2.4	5.5	8.2	2.4
M/11	6.4	3.1	9.0	9.4	5.2	13.1	16.6	9.4	7.3	3.2	6.4	10.7	2.5
6A/12	7.1	3.3	9.7	10.1	5.8	14.6	17.8	10.2	8.1	3.4	7.1	11.7	2.6
N/12	7.4	3.3	9.8	10.2	5.8	15.0	18.3	10.2	8.3	3.4	7.2	11.9	2.7
6P/12	7.4	3.4	10.0	10.4	5.9	15.0	18.3	10.3	8.5	3.5	7.2	12.1	2.7
M/12	7.7	3.8	11.0	11.4	6.0	16.0	19.9	11.3	9.0	3.5	7.8	12.1	2.8
6A/13	7.7	3.9	11.3	11.6	6.0	16.8	21.5	11.9	9.2	3.5	8.2	14.0	2.9
N/13	7.8	3.9	11.3	11.6	6.0	16.9	21.6	11.9	9.3	3.6	8.2	14.1	2.9

TABLE 12 (Cont.)

Zone	A	B	C_2	D	E	F	G	J	K	L	M	N	P
Period Ending (P.S.T.)													
6P/13	7.8	3.9	11.3	11.6	6.0	16.9	21.6	11.9	9.3	3.6	8.2	14.1	2.9
M/13	8.1	3.9	11.3	11.6	6.0	16.9	21.6	11.9	9.3	3.6	8.2	14.1	2.9
6A/14	8.8	4.0	11.4	11.7	6.4	16.9	21.6	12.0	10.1	4.0	8.5	14.7	3.0
N/14	9.2	4.5	11.4	11.7	8.0	17.8	23.4	12.3	11.1	4.6	9.4	16.1	3.2
6P/14	10.1	4.8	11.5	11.7	8.2	19.6	25.5	13.2	11.5	4.7	10.0	16.8	3.4
M/14	10.4	5.0	11.5	11.7	8.6	21.1	26.4	13.6	11.6	5.0	10.8	16.8	3.5
6A/15	12.0	5.2	11.5	11.7	8.8	21.5	27.0	13.9	12.1	5.3	11.1	17.6	3.8
N/15	12.2	6.2	11.9	12.1	9.1	22.9	28.8	14.3	12.9	5.7	12.0	19.0	4.1
6P/15	12.3	6.4	12.7	13.0	9.2	23.6	30.0	14.8	13.2	5.9	12.6	19.6	4.2
M/15	12.3	6.4	12.8	13.2	9.2	23.7	30.2	14.9	13.2	6.0	12.6	19.7	4.5
6A/16	12.3	6.4	12.8	13.2	9.4	23.7	30.2	14.9	13.3	6.0	12.6	19.8	4.6
N/16	12.3	6.4	12.8	13.2	9.4	23.7	30.2	14.9	13.3	6.0	12.6	19.8	4.6
6P/16	12.3	6.4	12.8	13.2	9.4	23.7	30.2	14.9	13.3	6.0	12.6	19.8	4.6
M/16	12.4	6.4	12.8	13.2	9.4	23.7	30.2	14.9	13.3	6.0	12.6	19.8	4.7

TABLE 13

SACRAMENTO BASIN STUDY

ACCUMULATED PRECIPITATION BY COMBINED ZONES

December 8-16, 1929 Storm

(6-Hour Periods)

Period Ending (P.S.T.)	Yuba (HC_1)	Feather (GJ)	Upper Sac. (KIMNP)	Entire Basin
6A/8	0	0.1	0	0
N/8	0.1	0.4	0.3	0.3
6P/8	0.8	0.5	0.4	0.4
M/8	1.6	1.5	0.6	0.9
6A/9	3.4	1.7	0.7	1.2
N/9	4.2	2.2	1.3	1.7
6P/9	5.0	4.0	1.9	2.4
M/9	6.7	5.6	2.4	3.2
6A/10	9.1	6.3	2.7	3.8
N/10	10.0	6.9	2.9	4.2
6P/10	10.2	7.2	3.1	4.4
M/10	10.3	7.7	3.2	4.5
6A/11	10.7	8.5	3.4	4.8
N/11	10.7	9.0	3.8	5.1
6P/11	11.0	9.6	4.2	5.5
M/11	12.8	11.4	5.0	6.6
6A/12	14.1	12.3	5.4	7.1
N/12	14.4	12.5	5.6	7.2
6P/12	14.6	12.5	5.6	7.3
M/12	15.8	13.7	5.8	7.8
6A/13	16.3	14.6	6.2	8.2
N/13	16.4	14.6	6.3	8.2
6P/13	16.4	14.6	6.3	8.2
M/13	16.4	14.6	6.3	8.2
6A/14	16.4	14.7	6.6	8.5
N/14	16.4	15.4	7.3	9.0
6P/14	17.1	16.6	7.6	9.5
M/14	17.3	17.2	7.8	9.8
6A/15	17.4	17.6	8.3	10.1
N/15	18.3	18.4	8.9	10.8
6P/15	19.3	19.0	9.2	11.2
M/15	19.6	19.2	9.3	11.3
6A/16	19.6	19.2	9.4	11.4
N/16	19.6	19.2	9.4	11.4
6P/16	19.6	19.2	9.4	11.4
M/16	19.6	19.2	9.4	11.4

TABLE 14

SACRAMENTO BASIN STUDY

MAXIMUM DURATION-DEPTH VALUES

March 1928 Storm

(Duration--Hours)

	6	12	18	24	36	48	72	96	120	N.S.P.	Percentage N.S.P. (72 hrs. ending 6P/26, P.S.T.)
A	1.4	1.8	1.9	2.2	2.6	3.2	4.2	5.3	6.1	35.4	11.3
B	0.6	1.0	1.3	1.5	1.9	2.1	2.5	2.9	3.5	20.7	7.7
C_2	2.6	3.3	3.9	4.1	5.7	7.0	9.1	10.9	12.5	49.6	17.7
D	2.7	3.6	4.4	4.8	6.2	7.8	9.9	12.1	13.7	51.8	16.8
E	1.9	2.2	2.2	2.5	2.8	3.5	4.0	5.2	5.7	31.6	12.7
F	2.0	2.5	2.9	3.7	5.4	6.8	8.9	11.7	13.3	59.6	14.1
G	2.3	3.3	4.3	4.8	6.6	8.4	11.1	15.2	17.6	71.3	15.6
J	1.2	1.9	2.4	2.6	3.5	4.5	5.8	6.9	8.0	33.2	16.6
K	1.2	1.6	1.7	2.4	2.9	3.4	4.2	5.0	6.0	49.7	8.4
L	0.8	0.9	0.9	1.2	1.5	1.7	2.5	3.2	3.9	27.4	9.1
M	1.8	2.3	2.4	3.0	4.3	5.3	6.6	8.3	9.5	43.8	15.1
N	1.9	2.3	2.4	4.2	4.6	5.3	5.7	7.8	9.2	63.7	8.9
P	1.5	1.8	1.9	2.0	2.6	2.7	3.4	3.9	4.5	22.9	14.0
HC_1	1.9	3.2	4.1	4.3	6.1	8.4	10.8	13.5	15.2	57.8	17.1
GJ	1.5	2.2	2.8	3.0	4.4	5.6	7.1	9.2	10.7	43.9	16.2
KLMNP	1.4	1.7	1.9	2.4	3.0	3.4	4.1	5.1	6.0	31.6	13.0
Total	1.2	1.5	1.8	2.1	2.9	3.8	5.1	6.6	7.4	37.1	13.7
Max. Period Ending* (P.S.T.)	6P/26	6P/26	M/26	6P/26	M/26	6P/26	6P/26	M/26	M/26		

* Applicable only to the total basin.

TABLE 15
SACRAMENTO BASIN STUDY
ACCUMULATED PRECIPITATION BY ZONES

March 21-28, 1928 Storm
(6-Hour Periods)

Zone Period Ending (P.S.T.)	A	B	C_2	D	E	F	G	J	K	L	M	N	P
6P/21	0	0	0	0	0	0	0	0	0.1	0.1	0	0.2	0
M/21	0	0	0	0	0	0	0	0	0.2	0.1	0.2	0.3	0.1
6A/22	0.1	0.1	0.1	0.1	0.3	0.3	0.5	0.3	0.7	0.4	0.5	0.9	0.3
N/22	0.3	0.2	0.5	0.3	0.4	1.2	1.3	0.5	1.1	0.8	1.2	1.5	0.5
6P/22	0.7	0.4	1.2	1.1	0.5	1.5	1.7	0.6	1.1	0.8	1.2	1.6	0.5
M/22	0.8	0.6	1.5	1.5	0.5	1.8	2.4	1.1	1.2	0.9	1.3	2.0	0.7
6A/23	1.0	0.8	1.9	1.8	0.6	2.3	2.9	1.3	1.5	1.1	1.6	2.6	0.8
N/23	1.7	1.1	2.5	2.5	1.1	3.2	3.9	1.3	1.5	1.1	2.1	3.2	0.8
6P/23	2.0	1.7	3.6	3.8	1.7	4.8	5.8	1.8	1.9	1.5	2.9	3.7	1.1
M/23	2.0	2.1	4.7	4.8	1.8	5.5	7.2	2.3	2.1	1.9	3.4	3.9	1.2
6A/24	2.0	2.2	4.8	4.9	1.8	5.7	7.5	2.4	2.1	1.9	3.4	3.9	1.2
N/24	2.0	2.2	5.0	5.2	1.8	5.8	7.7	2.4	2.1	1.9	3.4	3.9	1.2
6P/24	2.8	2.4	5.6	6.0	2.2	6.4	8.5	2.8	2.7	2.3	4.2	4.1	1.6
M/24	3.4	2.5	8.2	8.7	2.8	7.6	9.5	3.9	3.2	2.6	5.1	4.8	1.9
6A/25	3.5	2.6	8.9	9.6	2.9	7.8	10.5	4.3	3.3	2.6	5.2	4.9	2.0
N/25	3.5	2.6	9.0	10.0	2.9	8.2	11.0	4.5	3.3	2.6	5.3	4.9	2.0
6P/25	3.8	2.6	9.5	10.6	3.2	9.5	12.4	5.2	3.7	2.8	6.5	5.2	2.3
M/25	4.2	2.7	10.6	11.4	3.5	10.7	13.4	5.6	4.5	3.1	7.2	7.1	2.7
6A/26	4.2	2.7	10.6	11.4	3.5	10.8	13.7	5.6	4.5	3.1	7.2	7.1	2.7
N/26	4.6	2.7	11.1	11.7	3.8	11.2	14.6	6.1	4.9	3.2	7.7	7.7	2.8
6P/26	6.0	3.3	11.7	12.5	5.7	13.2	16.9	7.3	6.1	4.0	9.5	9.4	4.3
M/26	6.1	3.5	12.4	13.6	5.7	13.3	17.6	8.0	6.2	4.0	9.6	9.5	4.6
6A/27	6.1	3.5	12.6	13.6	5.7	13.5	17.8	8.2	6.2	4.0	9.8	9.5	4.6
N/27	6.2	3.5	12.6	14.0	5.8	13.5	18.1	8.2	6.2	4.0	9.8	9.6	4.6
6P/27	6.3	3.5	12.7	14.1	5.8	13.5	18.1	8.3	6.4	4.1	9.9	9.8	4.8
M/27	6.3	3.5	12.7	14.2	5.8	13.5	18.2	8.3	6.4	4.1	9.9	9.8	4.9
6A/28	6.3	3.5	12.7	14.2	5.8	13.5	18.2	8.3	6.4	4.1	9.9	9.8	4.9
N/28	6.3	3.5	12.7	14.2	5.8	13.5	18.2	8.3	6.4	4.1	9.9	9.8	4.9

TABLE 16

SACRAMENTO BASIN STUDY

ACCUMULATED PRECIPITATION BY COMBINED ZONES

March 21-28, 1928 Storm

(6-Hour Periods)

Period Ending (P.S.T.)	Yuba (HC_1)	Feather (GJ)	Upper Sac. (KLMNP)	Entire Basin
6P/21	0	0	0.1	0
M/21	0	0	0.2	0.1
6A/22	0.2	0.4	0.5	0.3
N/22	0.7	0.7	0.8	0.6
6P/22	1.4	0.9	0.9	0.8
M/22	1.7	1.5	1.1	0.9
6A/23	2.1	1.7	1.3	1.4
N/23	3.2	2.0	1.5	1.7
6P/23	4.7	2.9	1.9	2.1
M/23	6.0	3.7	2.2	2.8
6A/24	6.2	3.8	2.2	2.9
N/24	6.4	3.9	2.2	2.9
6P/24	7.3	4.4	2.6	3.4
M/24	9.2	5.5	3.1	4.1
6A/25	10.5	6.0	3.2	4.5
N/25	10.7	6.3	3.2	4.6
6P/25	11.6	7.3	3.6	5.1
M/25	12.5	7.8	4.3	5.6
6A/26	12.8	7.9	4.3	5.7
N/26	13.8	8.5	4.6	6.0
6P/26	14.6	10.0	6.0	7.2
M/26	15.2	10.7	6.2	7.5
6A/27	15.4	10.9	6.2	7.6
N/27	15.6	11.0	6.2	7.7
6P/27	15.8	11.0	6.4	7.8
M/27	15.8	11.1	6.4	7.8
6A/28	15.9	11.1	6.4	7.8
N/28	15.9	11.1	6.4	7.8

TABLE 17

SACRAMENTO BASIN STUDY

MAXIMUM DURATION-DEPTH VALUES

December 1913-January 1914 Storm

	(Duration--Hours)										Percentage N.S.P. (72 hrs. ending 6A/2, P.S.T.)
	6	12	18	24	36	48	72	96	120	N.S.P.	
A	1.5	2.9	3.5	4.2	6.1	6.4	7.0	7.9	8.1	35.4	19.8
B	0.9	1.6	2.0	2.2	2.9	3.2	3.8	4.0	4.2	20.7	16.4
C_2	2.1	3.2	3.9	4.7	6.3	7.2	8.4	9.1	9.5	49.6	16.1
D	1.5	3.0	4.1	4.8	7.4	8.0	9.6	10.3	10.8	51.8	17.4
E	1.9	3.7	4.7	5.0	5.5	6.4	6.7	7.5	7.7	31.6	19.3
F	3.9	6.0	7.5	8.6	10.6	11.6	14.6	15.7	15.9	59.6	24.5
G	3.9	6.1	7.9	9.2	11.3	12.7	15.6	17.1	17.5	71.3	21.9
J	1.1	2.0	3.1	3.8	4.9	5.5	6.6	7.3	7.6	33.2	19.9
K	2.5	4.6	6.3	6.5	7.6	7.9	10.2	11.5	11.9	49.7	20.5
L	1.1	2.1	2.7	2.8	3.3	3.4	4.2	4.8	5.0	27.4	15.3
M	2.0	3.6	4.1	4.4	5.5	5.9	7.7	8.9	9.2	43.8	17.1
N	2.8	4.9	6.0	6.4	7.5	8.6	10.3	11.7	12.3	63.7	16.2
P	1.2	1.9	2.3	2.3	2.5	2.5	3.7	3.8	3.9	22.9	14.8
HC_1	2.6	4.0	5.2	6.1	8.3	9.2	10.1	11.4	11.7	57.8	17.5
GJ	1.8	3.0	4.2	5.2	6.7	7.5	8.9	10.0	10.4	43.9	20.7
KLMNP	1.4	2.9	3.5	3.8	4.4	4.7	5.9	6.8	7.0	31.6	18.6
Total	1.4	2.7	3.3	3.9	5.0	5.5	6.6	7.5	7.7	37.1	17.8
Max. Period Ending* (P.S.T.)	M/30	M/30	M/30	6A/31	6P/31	M/31	6A/2	N/2	6A/3		

* Applicable only to the total basin.

TABLE 18

SACRAMENTO BASIN STUDY

ACCUMULATED PRECIPITATION BY ZONES

December 29, 1913 - January 3, 1914 Storm
(6-Hour Periods)

Zone	A	B	C_2	D	E	F	G	J	K	L	M	N	P
Period Ending (P.S.T.)													
N/29	0.2	0.2	0	0.3	0.6	0.2	0.2	0.2	0.4	0.2	0.3	0.6	0
6P/29	0.4	0.4	0.4	0.8	1.4	0.8	0.8	0.4	1.1	0.6	1.0	1.3	0.1
M/29	0.5	0.5	0.5	0.8	1.4	0.8	0.9	0.5	1.1	0.6	1.1	1.4	0.1
6A/30	0.6	0.6	0.5	0.8	1.4	1.1	1.3	0.6	1.3	0.6	1.2	1.4	0.1
N/30	2.1	1.0	0.7	1.0	2.4	2.2	2.6	1.0	3.0	1.6	1.5	2.5	0.1
6P/30	3.5	1.9	1.4	2.4	4.2	4.3	4.8	1.7	5.5	2.7	3.1	5.3	0.8
M/30	4.1	2.6	3.5	3.6	6.1	8.2	8.7	2.8	7.6	3.3	5.1	7.4	2.0
6A/31	4.8	2.8	4.6	4.3	6.4	9.7	10.5	3.7	7.8	3.4	5.6	7.8	2.4
N/31	5.7	3.1	5.0	5.4	6.6	10.4	11.3	4.8	8.3	3.6	5.9	8.1	2.4
6P/31	6.7	3.5	6.1	6.9	6.7	11.7	12.6	5.5	8.9	3.9	6.7	8.9	2.6
M/31	6.9	3.7	7.0	8.4	6.7	12.4	13.6	5.9	9.0	3.9	7.0	9.7	2.6
6A/1	7.0	3.8	7.7	8.8	6.7	12.5	13.8	6.1	9.0	3.9	7.0	10.0	2.6
N/1	7.0	3.8	7.8	9.0	6.7	12.7	14.0	6.2	9.0	3.9	7.0	10.1	2.6
6P/1	7.1	3.8	7.9	9.0	6.7	13.5	14.9	6.4	9.4	4.1	7.2	10.2	2.7
M/1	7.3	3.9	8.1	9.0	7.3	15.0	16.2	6.7	10.4	4.4	7.9	10.7	3.1
6A/2	7.6	4.0	8.5	9.8	7.5	15.7	16.9	7.2	11.5	4.8	8.7	11.7	3.5
N/2	8.1	4.2	9.1	10.6	7.7	15.9	17.3	7.5	11.8	5.0	9.2	12.2	3.8
6P/2	8.1	4.2	9.4	10.8	7.7	15.9	17.4	7.6	11.8	5.0	9.2	12.2	3.8
M/2	8.1	4.2	9.4	10.8	7.7	15.9	17.4	7.6	11.8	5.0	9.2	12.2	3.8
6A/3	8.1	4.2	9.4	10.8	7.7	15.9	17.4	7.6	11.9	5.0	9.2	12.3	3.8
N/3	8.4	4.2	9.5	10.8	7.7	16.1	17.7	7.6	12.2	5.2	9.5	12.9	3.9

TABLE 19

SACRAMENTO BASIN STUDY

ACCUMULATED PRECIPITATION BY COMBINED ZONES

December 29, 1913 - January 3, 1914 Storm

(6-Hour Periods)

Period Ending (P.S.T.)	Yuba (HC_1)	Feather (GJ)	Upper Sac. (KLMNP)	Entire Basin
N/29	0.1	0.2	0.2	0.2
6P/29	0.5	0.5	0.6	0.6
M/29	0.6	0.6	0.6	0.6
6A/30	0.7	0.8	0.7	0.7
N/30	1.3	1.4	1.3	1.3
6P/30	2.7	2.6	2.7	2.6
M/30	5.3	4.4	4.2	4.0
6A/31	6.5	5.6	4.5	4.6
N/31	7.3	6.6	4.6	5.0
6P/31	8.8	7.5	5.1	5.7
M/31	9.6	8.1	5.3	6.1
6A/1	9.9	8.3	5.3	6.2
N/1	9.9	8.4	5.3	6.2
6P/1	10.0	8.8	5.5	6.4
M/1	10.3	9.4	6.0	6.8
6A/2	10.8	9.9	6.6	7.3
N/2	11.5	10.2	7.0	7.7
6P/2	11.6	10.4	7.0	7.7
M/2	11.6	10.4	7.0	7.7
6A/3	11.6	10.4	7.0	7.7
N/3	11.8	10.4	7.2	7.9

TABLE 20

SACRAMENTO BASIN STUDY

MAXIMUM DURATION-DEPTH VALUES

January 1911 Storm

(Duration--Hours)

	6	12	18	24	36	48	72	96	120	N.S.P.	Percentage N.S.P. (72 hrs. ending 6A/31, P.S.T.)
B	0.5	0.9	1.1	1.3	1.8	2.0	2.8	3.6	3.8	20.7	13.5
C_2	1.2	2.0	2.6	3.4	4.2	5.4	6.6	7.9	8.2	49.6	13.1
D	1.4	2.0	2.6	3.5	4.6	5.7	6.9	8.4	8.9	51.8	13.3
F	1.6	2.4	3.2	3.9	4.5	5.1	7.0	9.8	11.2	59.6	10.9
G	1.8	3.3	4.4	5.3	5.7	6.4	8.0	10.4	11.8	71.3	11.2
J	0.8	1.4	1.7	2.2	2.9	3.6	4.5	5.4	6.1	33.2	13.6
HC_1	1.3	2.5	3.6	4.3	5.0	5.8	7.8	9.4	10.0	57.8	13.2
GJ^1	1.0	1.9	2.6	2.9	3.5	4.3	5.5	6.8	7.7	43.9	12.5

TABLE 21

SACRAMENTO BASIN STUDY

ACCUMULATED PRECIPITATION BY ZONES

January 23-31, 1911 Storm
(6-Hour Periods)

Zone	B	C_2	F	G	J	D	HC_1	GJ
Period Ending (P.S.T.)								
6P/23	0.2	0.1	0.3	0.2	0.1	0.1	0.1	0.1
M/23	0.7	0.6	1.0	1.1	0.5	0.2	0.8	0.4
6A/24	1.1	1.4	1.8	2.2	1.0	1.6	1.9	1.3
N/24	1.2	2.2	3.4	4.0	1.6	2.1	3.1	2.3
6P/24	1.5	3.1	4.2	5.5	2.1	2.8	4.4	3.0
M/24	1.8	4.0	4.3	5.7	2.1	3.7	5.0	3.1
6A/25	1.8	4.2	4.3	5.7	2.1	4.0	5.0	3.1
N/25	1.8	4.3	4.3	5.7	2.1	4.0	5.0	3.1
6P/25	1.9	4.6	4.6	6.0	2.3	4.5	5.4	3.3
M/25	2.0	5.0	4.6	6.1	2.6	5.4	6.0	3.6
6A/26	2.0	5.0	4.6	6.2	2.6	5.5	6.0	3.6
N/26	2.0	5.0	5.0	6.5	2.6	5.7	6.0	3.7
6P/26	2.0	5.1	5.1	6.6	2.7	5.8	6.0	3.8
M/26	2.1	5.2	5.3	6.9	3.1	6.2	6.4	4.2
6A/27	2.2	5.3	6.0	7.6	3.3	6.2	6.5	4.5
N/27	2.3	5.3	6.9	8.0	3.4	6.2	6.6	4.7
6P/27	2.5	5.4	7.2	8.2	3.5	6.4	6.6	4.8
M/27	2.9	5.7	7.8	8.9	3.8	6.8	7.2	5.2
6A/28	3.0	6.2	9.3	10.0	4.2	7.3	7.7	5.8
N/28	3.1	6.6	9.8	10.3	4.3	7.7	8.2	6.0
6P/28	3.2	6.6	9.8	10.4	4.3	7.8	8.2	6.0
M/28	3.7	7.1	10.3	11.1	4.7	8.3	9.1	6.5
6A/29	4.0	7.6	10.8	11.7	5.2	8.6	9.9	7.0
N/29	4.1	7.8	10.9	11.9	5.4	8.9	10.1	7.2
6P/29	4.5	8.5	11.3	12.5	5.9	9.6	11.0	7.8
M/29	4.5	9.4	11.8	13.2	6.2	10.9	11.6	8.2
6A/30	4.8	10.3	12.7	14.4	7.0	11.4	12.4	9.1
N/30	5.0	10.6	13.8	15.7	7.6	12.0	13.4	9.9
6P/30	5.2	10.7	13.9	16.0	7.8	12.4	13.7	10.1
M/30	5.7	11.5	14.8	17.0	8.3	13.3	14.2	10.7
6A/31	5.8	12.7	15.8	18.0	8.7	14.2	15.3	11.3
N/31	5.8	13.2	16.0	18.3	8.7	14.6	15.9	11.4
6P/31	5.8	13.2	16.0	18.3	8.7	14.6	16.0	11.4

TABLE 22

SACRAMENTO BASIN STUDY

MAXIMUM DURATION-DEPTH VALUES

January 1909 Storm

(Duration--Hours)

	6	12	18	24	36	48	72	96	120	N.S.P.	Percentage N.S.P. (72 hrs. ending N/16, P.S.T.)
A	1.4	1.7	2.4	3.1	4.8	6.1	8.3	9.2	9.2	35.4	23.4
B	0.4	0.6	0.8	1.0	1.5	1.9	2.3	2.9	2.9	20.7	11.1
C_2	1.4	2.6	3.5	4.5	6.4	7.8	10.5	12.2	12.3	49.6	21.2
D	2.4	4.7	5.8	6.4	9.4	10.8	14.1	17.3	17.7	51.8	27.2
E	0.9	1.5	1.8	2.3	3.3	3.9	5.7	6.1	6.2	31.6	18.0
F	1.7	3.3	4.1	4.7	6.7	8.8	12.5	14.7	14.9	59.6	21.0
G	2.0	3.8	5.2	6.3	9.4	12.0	15.8	18.8	19.2	71.3	22.2
J	1.3	1.9	2.6	3.3	4.6	5.7	7.3	7.9	8.1	33.2	22.0
K	1.0	1.7	2.1	2.6	4.1	4.8	6.9	8.0	8.1	49.7	13.9
L	0.7	0.9	1.1	1.4	2.0	2.4	2.9	3.4	3.5	27.4	10.6
M	0.8	1.4	2.1	2.4	3.6	4.6	6.0	7.2	7.2	43.8	13.7
N	1.6	2.5	2.6	3.4	4.3	5.7	8.0	9.3	9.4	63.7	12.6
P	0.9	1.0	1.2	1.3	2.1	2.2	2.8	3.3	3.3	22.9	12.2
HC_1	1.8	3.2	4.3	6.0	8.0	10.5	13.6	15.9	16.1	57.8	22.8
GJ	1.5	2.3	2.9	3.9	5.9	7.4	9.7	11.0	11.2	43.9	22.1
KLMNP	0.8	1.1	1.5	1.7	2.7	3.3	4.5	5.3	5.4	31.6	14.2
Total	0.9	1.5	1.9	2.5	3.8	4.7	6.4	7.5	7.7	37.1	17.2
Max. Period Ending* (P.S.T.)	M/13	M/13	6A/14	N/14	6A/15	N/15	N/16	N/16	N/16		

* Applicable only to the total basin.

TABLE 23

SACRAMENTO BASIN STUDY

ACCUMULATED PRECIPITATION BY ZONES

January 11-16, 1909 Storm
(6-Hour Periods)

Zone	A	B	C_2	D	E	F	G	J	K	L	M	N	P
Period Ending (P.S.T.)													
6P/11	0	0	0	0	0	0	0	0	0	0	0	0	0
M/11	0	0	0.1	0.4	0.1	0.2	0.2	0.2	0	0	0	0	0
6A/12	0	0	0.1	0.4	0.1	0.2	0.3	0.2	0	0	0	0	0
N/12	0	0	0.1	0.4	0.1	0.2	0.3	0.2	0	0	0	0	0
6P/12	0.1	0.3	0.4	1.6	0.2	0.4	0.6	0.2	0.2	0.1	0.1	0.1	0
M/12	0.8	0.6	1.7	3.4	0.5	1.5	2.2	0.6	1.0	0.4	0.8	1.2	0.5
6A/13	0.9	0.6	1.8	3.5	0.5	2.3	3.0	0.8	1.1	0.5	1.2	1.3	0.5
N/13	0.9	0.6	1.8	3.6	0.5	2.4	3.3	0.8	1.1	0.5	1.2	1.3	0.5
6P/13	1.5	0.9	3.2	5.9	1.3	3.2	4.4	1.2	1.8	0.5	1.5	1.8	0.6
M/13	2.6	1.0	4.2	8.3	2.0	4.9	6.4	2.5	2.7	0.9	2.3	2.9	1.5
6A/14	2.8	1.0	4.7	9.4	2.0	6.5	8.2	2.9	2.7	1.1	2.9	3.4	1.6
N/14	3.5	1.4	6.0	10.0	2.3	7.1	9.6	3.2	3.2	1.4	3.6	4.3	1.8
6P/14	4.5	1.4	7.3	11.5	2.9	7.6	10.7	4.2	3.7	1.4	3.8	4.3	1.9
M/14	5.2	1.8	8.2	13.0	3.8	9.1	12.5	5.1	4.7	1.9	4.5	5.2	2.3
6A/15	5.9	2.0	9.2	14.0	4.0	9.9	13.8	5.8	5.3	2.2	5.1	6.0	2.7
N/15	6.2	2.1	9.6	14.4	4.3	11.1	15.3	6.5	5.6	2.4	5.6	6.1	2.7
6P/15	7.6	2.3	10.3	15.5	5.2	12.0	16.1	6.8	6.5	2.6	6.1	7.0	2.8
M/15	7.9	2.5	11.1	15.9	5.4	13.1	17.1	7.1	7.3	3.3	6.6	8.6	3.0
6A/16	8.3	2.9	12.0	17.2	5.8	14.3	18.4	7.4	7.5	3.4	6.9	8.6	3.2
N/16	9.2	2.9	12.3	17.7	6.2	14.9	19.1	8.1	8.0	3.4	7.2	9.3	3.3
6P/16	9.2	2.9	12.3	17.7	6.2	14.9	19.2	8.1	8.1	3.5	7.2	9.4	3.3

TABLE 24

SACRAMENTO BASIN STUDY

ACCUMULATED PRECIPITATION BY COMBINED ZONES

January 11-16, 1909 Storm

(6-Hour Periods)

Period Ending (P.S.T.)	Yuba (HC_1)	Feather (GJ)	Upper Sac. (KLMNP)	Entire Basin
6P/11	0	0	0	0
M/11	0.2	0.2	0	0.1
6A/12	0.2	0.2	0	0.1
N/12	0.2	0.2	0	0.1
6P/12	0.5	0.3	0.1	0.3
M/12	2.1	1.0	0.7	1.0
6A/13	2.9	1.4	0.8	1.2
N/13	2.9	1.5	0.8	1.2
6P/13	4.4	2.1	1.0	1.8
M/13	5.7	3.6	1.8	2.7
6A/14	6.4	4.4	2.1	3.1
N/14	8.2	5.0	2.5	3.7
6P/14	9.6	6.0	2.6	4.2
M/14	10.7	7.2	3.2	4.9
6A/15	12.4	8.0	3.7	5.6
N/15	13.2	8.9	3.9	5.9
6P/15	13.9	9.4	4.3	6.4
M/15	14.7	9.9	4.9	6.9
6A/16	15.7	10.5	5.1	7.3
N/16	16.1	11.2	5.3	7.6
6P/16	16.1	11.2	5.4	7.7

TABLE 25

SACRAMENTO BASIN STUDY

MAXIMUM DURATION-DEPTH VALUES

March 1907 Storm

(Duration--Hours)

	6	12	18	24	36	48	72	96	120	N.S.P.	Percentage N.S.P. (72 hrs. ending 6A/19, P.S.T.)
A	1.6	3.1	3.5	3.7	4.2	5.4	6.8	7.6	7.6	35.4	18.4
B	0.6	1.0	1.3	1.4	1.6	1.9	3.0	3.5	3.6	20.7	14.5
C_2	1.7	2.3	3.5	4.3	5.5	6.6	8.6	9.9	10.3	49.6	16.5
D	1.9	3.1	4.3	5.2	6.3	7.5	9.7	11.4	12.5	51.8	18.7
E	1.3	2.4	2.6	2.8	3.2	4.1	5.1	5.8	5.8	31.6	15.5
F	2.0	3.9	5.7	6.7	9.4	11.4	16.0	18.2	19.1	59.6	26.2
G	2.2	4.3	6.2	7.6	10.6	13.7	18.8	22.5	22.8	71.3	26.4
J	1.4	2.3	3.2	3.9	5.7	6.9	8.9	10.4	10.4	33.2	26.2
K	1.3	2.3	2.8	3.2	4.4	5.2	7.0	8.0	8.3	49.7	12.9
L	0.7	0.9	1.0	1.1	1.4	1.8	2.4	2.7	2.8	27.4	8.0
M	1.1	2.1	3.1	3.5	4.9	6.3	9.0	10.0	10.5	43.8	19.6
N	1.7	3.1	3.7	4.5	5.4	7.5	9.7	11.5	12.4	63.7	12.9
P	0.7	1.2	1.5	2.1	2.9	3.4	3.8	4.1	4.3	22.9	16.6
HC_1	1.7	3.4	5.0	6.2	8.0	9.5	12.7	15.0	15.8	57.8	21.8
GJ	1.6	2.8	4.0	4.8	7.1	8.8	11.7	13.9	13.9	43.9	26.2
KLMNP	0.7	1.3	1.7	2.1	3.2	4.0	5.3	6.2	6.5	31.6	16.1
Total	1.0	1.8	2.4	2.8	3.9	4.9	6.6	7.9	8.2	37.1	17.8
Max. Period Ending* (P.S.T.)	6P/18	6P/18	M/18	6P/18	M/18	M/18	6A/19	M/19	M/20		

* Applicable only to total basin.

TABLE 26

SACRAMENTO BASIN STUDY

ACCUMULATED PRECIPITATION BY ZONES

March 15-27, 1907 Storm
(6-Hour Periods)

Zone	A	B	C_2	D	E	F	G	J	K	L	M	N	P
Period Ending (P.S.T.)													
6P/15	0	0	0	0	0	0	0	0	0	0	0	0	0
M/15	0	0	0	0	0	0	0	0	0	0	0	0	0
6A/16	0.3	0.2	0.2	0.2	0.2	0.8	0.4	0	0.2	0.2	0.6	0.1	0
N/16	0.8	0.6	0.5	0.7	0.5	2.3	1.3	0.1	0.5	0.4	1.5	0.3	0.1
6P/16	1.1	1.0	0.9	1.4	0.8	3.7	2.8	0.5	0.8	0.6	2.4	0.7	0.2
M/16	1.4	1.2	1.8	2.4	1.0	4.7	4.6	1.4	1.0	0.8	3.0	1.3	0.4
6A/17	2.2	1.5	2.7	3.2	1.7	5.7	6.2	2.1	1.7	1.1	3.8	1.6	0.7
N/17	2.8	1.6	3.2	3.8	2.1	7.0	7.7	2.6	2.1	1.4	4.7	2.1	0.9
6P/17	3.1	1.6	3.3	3.9	2.2	8.4	9.1	3.5	2.6	1.6	5.2	3.8	1.4
M/17	3.1	1.7	3.3	3.9	2.3	9.4	10.7	4.7	3.2	1.6	5.6	5.2	2.1
6A/18	3.3	1.7	4.1	4.8	2.5	11.3	12.1	5.1	3.4	1.7	6.6	5.4	2.3
N/18	4.8	2.1	5.3	6.4	3.8	13.3	14.3	6.0	4.4	1.9	7.6	5.4	2.8
6P/18	6.4	2.6	6.4	7.9	4.9	15.1	16.4	7.4	5.7	2.4	8.7	5.9	3.5
M/18	6.8	3.0	7.6	9.1	5.1	16.0	18.3	8.3	6.2	2.4	9.0	6.9	3.8
6A/19	6.8	3.2	8.4	9.9	5.1	16.4	19.2	8.7	6.6	2.4	9.2	8.3	3.8
N/19	6.8	3.2	8.8	10.2	5.1	16.7	19.9	9.0	7.0	2.4	9.3	9.6	3.8
6P/19	7.5	3.4	9.5	10.9	5.6	17.6	21.0	9.6	7.8	2.6	9.7	10.4	4.0
M/19	7.6	3.5	9.9	11.4	5.8	18.2	22.5	10.2	8.0	2.7	10.0	10.8	4.1
6A/20	7.6	3.6	9.9	11.5	5.8	18.4	22.7	10.4	8.1	2.7	10.0	11.0	4.1
N/20	7.6	3.6	9.9	11.7	5.8	18.4	22.7	10.4	8.3	2.8	10.1	11.8	4.1

(Continued)

TABLE 26 (Cont.)

Zone	A	B	C_2	D	E	F	G	J	K	L	M	N	P
Period Ending (P.S.T.)													
6P/20	7.6	3.6	10.2	12.3	5.8	18.8	22.8	10.4	8.3	2.8	10.4	11.9	4.3
M/20	7.6	3.6	10.3	12.5	5.8	19.1	22.8	10.4	8.3	2.8	10.5	11.9	4.3
6A/21	7.9	3.6	10.3	12.5	5.9	19.1	22.8	10.4	8.4	2.8	10.5	11.9	4.3
N/21	8.4	3.6	10.3	12.5	6.0	19.1	22.9	10.4	8.8	2.9	10.6	12.7	4.3
6P/21	8.4	3.8	10.8	13.3	6.1	20.4	24.0	10.8	8.9	3.0	11.3	12.8	4.3
M/21	8.4	3.9	11.3	13.7	6.1	20.4	24.3	11.0	8.9	3.0	11.4	12.8	4.3
6A/22	8.4	3.9	11.3	13.7	6.1	20.4	24.3	11.0	8.9	3.0	11.4	12.8	4.3
N/22	8.4	3.9	11.3	13.7	6.1	20.4	24.3	11.0	8.9	3.0	11.4	12.8	4.3
6P/22	8.5	3.9	11.3	13.9	6.1	20.7	24.6	11.0	9.6	3.1	11.5	13.4	4.3
M/22	9.0	4.2	11.5	14.2	6.6	22.0	26.4	11.7	10.5	3.8	12.6	14.7	4.5
6A/23	10.1	4.8	11.9	14.8	7.7	22.7	27.7	12.2	11.4	4.0	12.9	15.1	5.0
N/23	10.6	5.2	13.6	16.7	7.8	22.9	28.6	12.4	11.8	4.0	12.9	15.5	5.3
6P/23	10.9	5.3	13.8	17.0	8.0	23.3	29.8	13.0	12.1	4.2	13.2	16.1	5.6
M/23	11.0	5.4	14.0	17.3	8.2	23.3	30.4	13.3	12.5	4.2	13.2	16.5	5.6
6A/24	11.4	5.5	14.4	17.8	8.4	23.3	30.6	13.5	12.6	4.3	13.2	16.5	5.6
N/24	11.5	5.6	14.7	18.5	8.6	23.6	31.0	13.8	12.8	4.3	13.3	16.5	5.7
6P/24	11.8	5.8	15.1	19.1	8.7	24.1	31.3	13.9	12.9	4.4	13.5	17.1	6.0
M/24	12.0	5.8	15.4	19.5	8.7	24.2	31.6	14.4	13.1	4.4	13.5	17.1	6.1
6A/25	12.0	5.8	15.6	20.1	8.7	24.2	31.9	14.6	13.1	4.4	13.6	17.1	6.1
N/25	12.0	5.8	15.8	20.4	8.7	24.2	32.2	14.6	13.1	4.4	13.6	17.1	6.1
6P/25	12.1	5.8	16.1	20.6	8.7	24.5	32.3	14.6	13.1	4.4	13.7	17.1	6.1
M/25	12.1	5.8	16.2	20.8	8.7	24.7	32.5	14.6	13.3	4.5	13.8	17.7	6.1
6A/26	12.1	5.8	16.4	20.8	8.7	24.7	32.6	14.6	13.3	4.5	13.8	17.7	6.1
N/26	12.1	5.8	16.5	21.0	8.7	24.8	32.8	14.6	13.3	4.5	13.8	17.7	6.1
6P/26	12.1	5.8	16.7	21.2	8.7	24.8	32.9	14.6	13.3	4.6	13.9	17.7	6.1
M/26	12.3	5.8	16.7	21.2	8.7	24.8	32.9	14.6	13.4	5.0	14.2	17.9	6.1
6A/27	12.3	5.8	16.7	21.2	8.7	24.8	32.9	14.7	13.4	5.1	14.2	17.9	6.1
N/27	12.3	5.8	16.7	21.2	8.7	24.8	32.9	14.7	13.4	5.1	14.2	17.9	6.1

TABLE 27

SACRAMENTO BASIN STUDY

ACCUMULATED PRECIPITATION BY COMBINED ZONES

March 15-27, 1907 Storm

(6-Hour Periods)

Period Ending (P.S.T.)	Yuba (HC_1)	Feather (GJ)	Upper Sac. (KLMNP)	Entire Basin
6P/15	0	0	0	0
M/15	0	0	0	0
6A/16	0.3	0.1	0.2	0.2
N/16	0.8	0.4	0.4	0.5
6P/16	1.4	1.1	0.7	1.0
M/16	2.7	2.3	1.0	1.5
6A/17	4.0	3.2	1.4	2.1
N/17	5.0	4.0	1.8	2.5
6P/17	5.2	5.1	2.5	3.0
M/17	5.5	6.4	3.1	3.6
6A/18	6.7	7.1	3.4	4.0
N/18	8.4	8.3	3.9	4.8
6P/18	10.1	9.9	4.6	5.8
M/18	11.7	11.1	5.0	6.4
6A/19	12.9	11.6	5.3	6.8
N/19	13.5	12.0	5.6	7.1
6P/19	14.0	12.8	6.0	7.5
M/19	15.0	13.6	6.2	7.9
6A/20	15.2	13.9	6.2	8.0
N/20	15.4	13.9	6.4	8.1
6P/20	15.8	13.9	6.5	8.2

(Continued)

TABLE 27 (Cont.)

Period Ending (P.S.T.)	Yuba (HC_1)	Feather (GJ)	Upper Sac. (KIMNP)	Entire Basin
M/20	15.8	13.9	6.5	8.2
6A/21	16.0	13.9	6.5	8.3
N/21	16.1	13.9	6.7	8.4
6P/21	16.6	14.5	6.9	8.7
M/21	17.2	14.7	6.9	8.8
6A/22	17.2	14.7	6.9	8.8
N/22	17.2	14.7	6.9	8.8
6P/22	17.3	14.8	7.1	8.9
M/22	17.9	15.8	7.8	9.6
6A/23	18.7	16.6	8.2	10.1
N/23	20.3	16.9	8.4	10.6
6P/23	20.9	17.7	8.8	11.0
M/23	21.3	18.1	8.9	11.2
6A/24	21.6	18.3	8.9	11.4
N/24	21.9	18.6	9.0	11.5
6P/24	22.1	18.8	9.2	11.8
M/24	22.2	19.2	9.3	12.0
6A/25	22.6	19.4	9.3	12.1
N/25	23.0	19.5	9.3	12.1
6P/25	23.4	19.6	9.3	12.2
M/25	23.5	19.6	9.5	12.3
6A/26	23.7	19.6	9.5	12.3
N/26	23.8	19.7	9.5	12.3
6P/26	23.8	19.7	9.5	12.4
M/26	23.8	19.7	9.7	12.4
6A/27	23.8	19.8	9.7	12.5
N/27	23.8	19.8	9.7	12.5

TABLE 28

SACRAMENTO BASIN STUDY

MAXIMUM DURATION-DEPTH VALUES

January 1906 Storm

(Duration--Hours)

	6	12	18	24	36	48	72	96	120	N.S.P.	Percentage N.S.P. (72 hrs. ending M/18, P.S.T.)
A	1.8	2.9	3.3	3.7	5.0	5.1	6.8	9.1	10.0	35.4	17.5
B	0.8	1.5	1.5	1.5	2.3	2.5	3.5	4.6	5.0	20.7	16.9
C_2	1.5	2.6	3.4	3.7	5.4	6.3	9.1	11.3	12.6	49.6	18.3
D	2.1	3.7	5.1	6.1	6.6	8.3	9.3	11.9	15.1	51.8	18.0
E	1.9	3.1	3.7	4.9	5.7	5.8	7.0	9.0	9.5	31.6	20.2
F	3.0	4.2	5.1	6.3	9.0	9.3	13.5	17.8	18.3	59.6	20.4
G	2.9	4.8	6.1	7.1	10.3	10.6	14.4	19.4	20.5	71.3	20.2
J	1.2	2.1	2.5	3.2	4.0	4.2	5.9	7.6	8.1	33.2	17.8
K	1.2	2.0	2.8	3.6	4.9	5.0	5.9	8.0	9.0	49.7	11.9
L	0.9	1.3	1.4	1.7	2.6	2.7	3.3	4.4	4.9	27.4	12.0
M	1.5	2.3	2.6	3.4	5.0	5.1	7.0	9.4	9.8	43.8	16.0
N	2.2	4.0	4.8	5.2	5.8	6.1	9.4	11.5	12.2	63.7	13.5
P	0.8	1.4	1.4	1.5	1.9	2.1	2.8	3.4	4.2	22.9	9.6
HC_1	1.8	3.1	4.3	4.6	6.9	8.4	10.2	13.5	15.5	57.8	17.5
GJ^1	1.4	2.5	3.4	4.1	5.8	6.0	8.2	10.9	11.6	43.9	18.7
KLMNP	0.9	1.5	1.9	2.2	3.1	3.4	4.7	6.0	6.7	31.6	13.6
Total	0.9	1.8	2.1	2.8	4.2	4.3	5.8	7.8	8.3	37.1	15.6
Max. Period Ending* (P.S.T.)	6P/18	M/18	M/18	M/18	M/18	6A/19	M/18	M/18	M/18		

* Applicable only to the total basin.

TABLE 29

SACRAMENTO BASIN STUDY

ACCUMULATED PRECIPITATION BY ZONES

January 11-19, 1906 Storm
(6-Hour Periods)

Zone	A	B	C_2	D	E	F	G	J	K	L	M	N	P
Period Ending (P.S.T.)													
N/11	0	0	0	0	0	0	0	0	0	0	0	0	0
6P/11	0.4	0.2	0.1	0	0.4	0.2	0.1	0	0.7	0.2	0.2	0.4	0.1
M/11	0.8	0.4	0.5	0.4	0.9	1.6	1.2	0.4	1.3	0.6	1.1	1.7	0.3
6A/12	2.6	1.0	1.0	1.1	2.6	2.3	2.0	0.8	2.4	1.1	1.7	2.9	0.8
N/12	2.9	1.5	2.4	2.2	2.7	4.2	4.2	1.7	2.6	1.1	2.4	2.9	1.0
6P/12	3.0	1.5	2.9	2.5	2.8	4.6	5.0	1.9	2.9	1.2	2.7	2.9	1.0
M/12	3.7	1.5	3.0	2.6	3.5	4.6	5.0	2.0	3.1	1.3	2.7	3.3	1.1
6A/13	3.9	1.8	3.9	4.0	3.7	4.8	5.6	2.4	3.3	1.4	2.8	3.5	1.4
N/13	4.7	2.3	5.4	6.1	4.1	5.4	7.1	3.2	3.7	1.7	3.3	3.9	1.4
6P/13	5.0	2.4	6.4	7.7	4.3	6.1	8.3	3.8	4.1	1.9	3.7	4.6	2.0
M/13	5.0	2.4	6.7	8.7	4.3	6.5	8.8	4.0	4.1	1.9	4.0	4.8	2.1
6A/14	5.0	2.5	6.8	8.9	4.3	6.5	8.9	4.1	4.1	1.9	4.0	4.8	2.1
N/14	5.0	2.5	6.8	8.9	4.3	6.5	8.9	4.2	4.1	1.9	4.0	4.8	2.1
6P/14	5.5	2.5	6.8	8.9	4.6	6.5	8.9	4.2	4.5	2.0	4.0	4.9	2.3
M/14	5.9	2.8	7.2	9.1	4.8	6.8	9.8	4.4	5.0	2.3	4.3	5.3	2.6
6A/15	5.9	3.3	8.1	9.7	4.8	7.2	11.4	5.0	5.2	2.7	4.6	5.5	2.7
N/15	6.4	3.6	8.8	10.8	5.0	8.7	12.3	5.5	5.5	2.9	5.1	5.5	2.8
6P/15	7.7	3.8	8.9	11.2	6.0	10.5	13.0	5.6	6.3	3.1	6.0	5.9	2.8
M/15	8.7	3.9	9.4	11.7	7.2	12.4	14.8	6.1	7.1	3.4	6.7	8.1	3.6

(Continued)

TABLE 29 (Cont.)

Zone	A	B	C_2	D	E	F	G	J	K	L	M	N	P
Period Ending (P.S.T.)													
6A/16	9.1	3.9	10.3	12.1	7.4	13.3	16.3	6.7	7.6	3.5	7.1	9.9	4.2
N/16	9.7	4.4	11.1	12.4	8.0	14.9	17.9	7.3	8.0	4.0	8.1	10.7	4.2
6P/16	9.8	4.9	12.1	13.7	8.0	15.4	18.7	7.9	8.1	4.1	8.6	10.9	4.2
M/16	9.8	4.9	12.5	14.4	8.0	15.4	18.8	8.0	8.1	4.1	8.7	10.9	4.2
6A/17	9.8	4.9	12.6	14.4	8.0	15.5	18.8	8.0	8.1	4.1	8.7	10.9	4.2
N/17	9.9	5.1	13.3	14.8	8.1	15.6	18.9	8.0	8.1	4.1	8.7	10.9	4.2
6P/17	10.8	5.6	14.6	16.2	8.1	16.8	20.2	8.4	8.6	4.6	9.5	11.4	4.4
M/17	11.6	5.9	15.6	17.7	9.9	19.8	23.1	8.8	9.6	5.0	10.6	12.2	4.8
6A/18	11.6	5.9	15.8	18.5	9.9	20.7	25.0	10.0	10.2	5.3	11.3	13.4	5.1
N/18	12.7	5.9	15.9	18.6	11.1	21.1	25.8	10.9	11.0	5.4	11.4	13.5	5.1
6P/18	14.5	6.7	17.2	19.5	13.0	23.1	27.3	11.1	12.2	6.3	12.9	15.3	5.4
M/18	14.9	7.4	18.5	21.0	13.6	24.6	29.2	12.0	13.0	6.7	13.7	16.7	5.8
6A/19	15.0	7.4	18.7	21.1	13.8	24.8	29.4	12.2	13.1	6.8	13.8	17.0	6.0
N/19	15.0	7.4	18.7	21.1	13.8	24.8	29.4	12.2	13.1	6.8	13.8	17.0	6.0
6P/19	15.0	7.4	18.7	21.1	13.8	24.8	29.4	12.2	13.1	6.8	13.8	17.0	6.0
M/19	15.0	7.4	18.7	21.1	13.8	24.8	29.4	12.2	13.1	6.8	13.8	17.0	6.0

TABLE 30

SACRAMENTO BASIN STUDY

ACCUMULATED PRECIPITATION BY COMBINED ZONES

January 11-19, 1906 Storm

(6-Hour Periods)

Period Ending (P.S.T.)	Yuba (HC_1)	Feather (GJ)	Upper Sac. (KLMNP)	Entire Basin
N/11	0	0	0	0
6P/11	0.1	0	0.2	0.2
M/11	0.6	0.6	0.8	0.7
6A/12	1.1	1.1	1.5	1.4
N/12	2.2	2.4	1.7	2.0
6P/12	2.7	2.8	1.8	2.1
M/12	2.8	2.8	1.9	2.3
6A/13	3.5	3.3	2.1	2.6
N/13	5.1	4.3	2.4	3.3
6P/13	6.6	5.1	2.8	3.9
M/13	7.3	5.4	3.0	4.1
6A/14	7.5	5.4	3.0	4.2
N/14	7.5	5.5	3.0	4.2
6P/14	7.5	5.5	3.1	4.3
M/14	8.0	5.9	3.5	4.6
6A/15	9.3	6.8	3.7	5.1
N/15	10.0	7.4	3.9	5.4
6P/15	10.2	7.7	4.2	5.8
M/15	11.4	8.6	5.1	6.6
6A/16	12.1	9.4	5.7	7.1
N/16	12.8	10.3	6.1	7.6
6P/16	13.8	10.9	6.3	8.1
M/16	14.3	11.0	6.3	8.2
6A/17	14.5	11.0	6.3	8.2
N/17	14.6	11.0	6.3	8.2
6P/17	15.9	11.7	6.7	8.9
M/17	17.7	12.8	7.3	9.6
6A/18	18.9	14.2	7.9	10.3
N/18	19.2	15.1	8.0	10.6
6P/18	20.2	15.6	8.9	11.5
M/18	21.5	16.8	9.4	12.4
6A/19	21.9	17.0	9.7	12.5
N/19	23.0	17.0	9.7	12.5
6P/19	23.0	17.0	9.7	12.5
M/19	23.0	17.0	9.7	12.5

CHAPTER VI

MAXIMUM POSSIBLE PRECIPITATION

117. The General Theory. A theoretical method of determining the maximum possible precipitation over an area in a given time was developed in Chapters I and II of the Pittsburgh Report (2). In the Sacramento study the theory must be modified to take into account the effect of the orographic barrier. However, in its most general terms the theory states that the volume of precipitation over an area in a given time is not greater than the product of the total number of unit columns entering the area and the amount of moisture which can be precipitated out of each column. Assuming that all of the air crossing a given line normal to the inflow direction will flow over the area, the average depth of precipitation R may be expressed by:

$$R \leq \frac{xvMt}{A} \qquad (1)$$

where x is the length of the line normal to the inflow direction, v the velocity of flow, M the amount of moisture which can be precipitated out of each unit column, t time and A area.* It is obvious that the solution of this equation must be geometrical as well as meteorological.

* The symbols used in this chapter are recapitulated on page 160.

The geometrical portion of the equation is x/A, which may be called the basin constant K.

118. It is possible to circumscribe a rectangle about any basin, such that one pair of sides is normal and the other pair parallel to a given inflow direction. Let A_r be the area of the rectangle, A_b the area of the basin, and x the length of the side normal to inflow. If we assume all of the precipitation confined within the rectangle, then $K = \frac{x}{A_r}$; but if the further restriction be imposed that all of the precipitation fall within the basin, then $K = \frac{x}{A_b}$. (See Figure 14.) The true value of K will therefore lie between $\frac{x}{A_r}$ and $\frac{x}{A_b}$, depending on the individual case. In the special case of a basin with high outflow boundaries, however, it is permissible to use the latter value provided

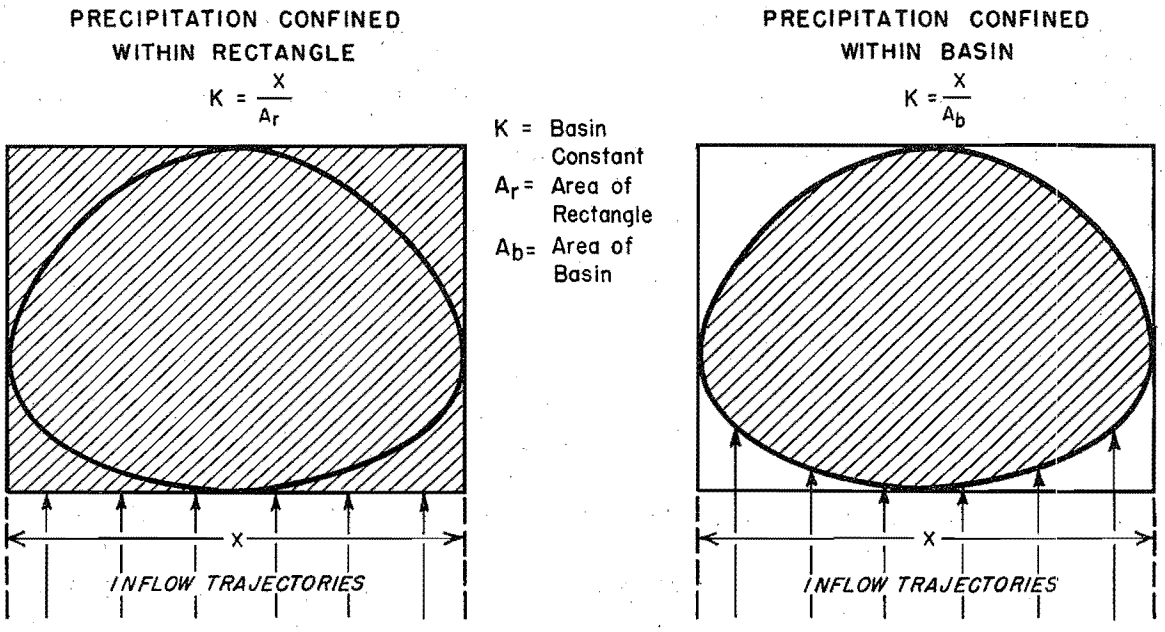

Figure 14

Schematic diagram illustrating computation of basin constant

the inflow boundary does not have too odd a shape.

119. There are two limitations on the application of the above analysis. The first is that the basin length parallel to the inflow direction must be great enough to allow sufficient time for the complete precipitation process to occur within the basin. There is some doubt as to the minimum value of such a length, but it is safe to say that the dimensions of the Pittsburgh and Sacramento Basins far exceed this limit. For small basins a different type of treatment might be necessary, e.g., an equation of radial inflow or the application of a correction factor. The other limitation on the use of the analysis is that the basin width normal to inflow must be somewhat less than the width of moist tongues. The upper limit of such a basin width is probably not less than 250 to 300 miles. Wider basins would have to be dealt with by subdivision into two or more portions.

120. Since K is a function of inflow direction, which may vary with time, and since, as will be shown later, both v and M may also be functions of time, (1) can be rewritten in analytic form:

$$R \leqq \int KvMdt \qquad (2)$$

The critical inflow directions, from a meteorological standpoint, must be determined from synoptic studies such as presented in Chapter V. For the evaluation of v the maximum possible wind velocity from these directions must be considered. The variation of the maximum wind with height and duration, as well as with season, must be determined. The treatment of this problem, appearing later in this chapter, depends to a large extent on the data available.

121. It is still necessary to evaluate M, the amount of moisture

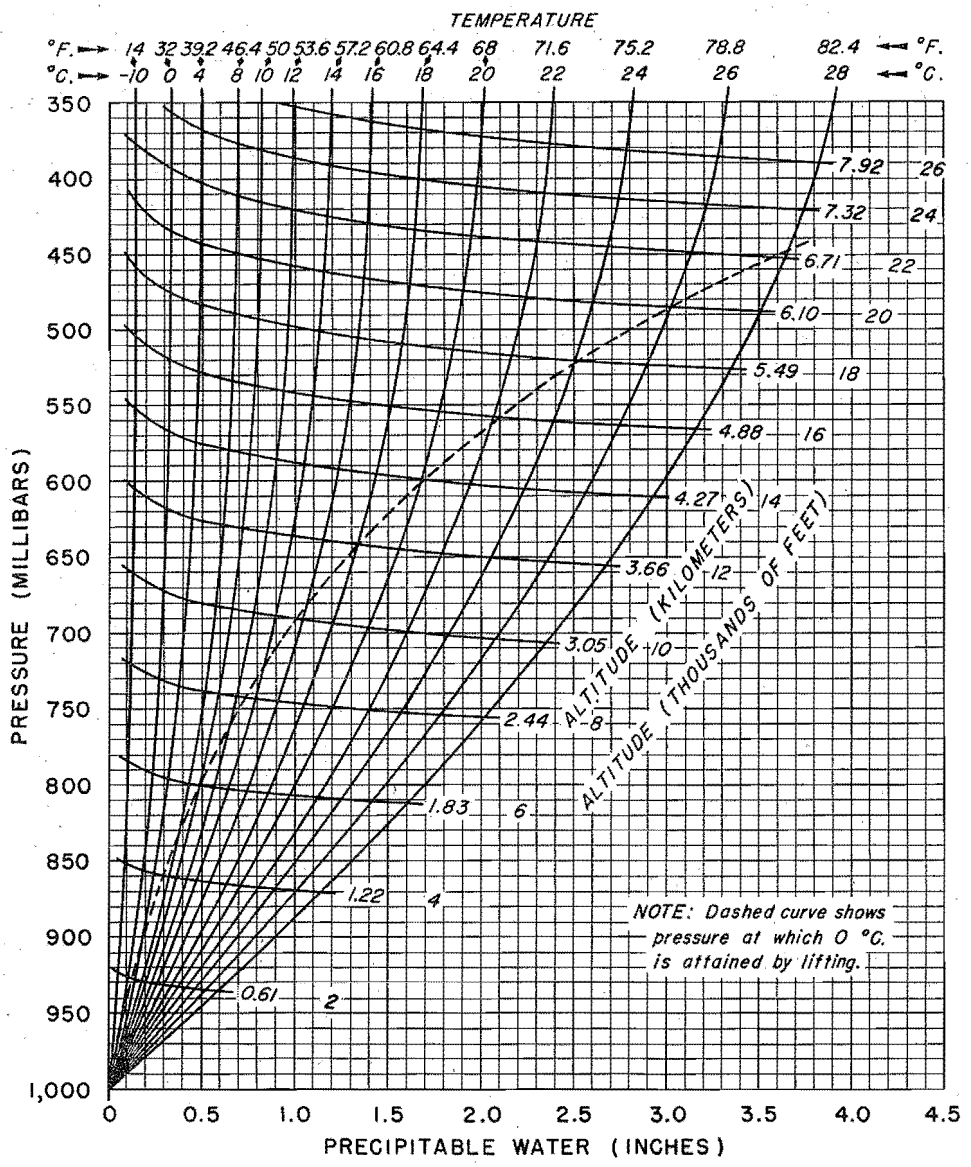

Figure 15

Depths of precipitable water in a column of air of given height above 1,000 millibars assuming saturation with a pseudo-adiabatic lapse rate for the indicated surface temperatures

which can be precipitated out of each unit column. The total precipitable water in the air column (89) is defined by $\int q\, dp$ multiplied by a constant, where q is specific humidity and p pressure. Figure 15 is a chart for the computation of depth of precipitable water in a saturated

column. In Figure 16, where p and q are linear coordinates, the precipitable water Wp_1 of the column at the lower level is equal to the area between p_o and p_1. If the base of the column were lifted to p_2 and the top to p_3, the precipitable water Wp_2 remaining in the column would be equal to the area between p_2 and p_3, and M the amount precipitated would be equal to $Wp_1 - Wp_2$. Thus, it is evident that M is a function of p_o, p_1, p_2, p_3, and G.

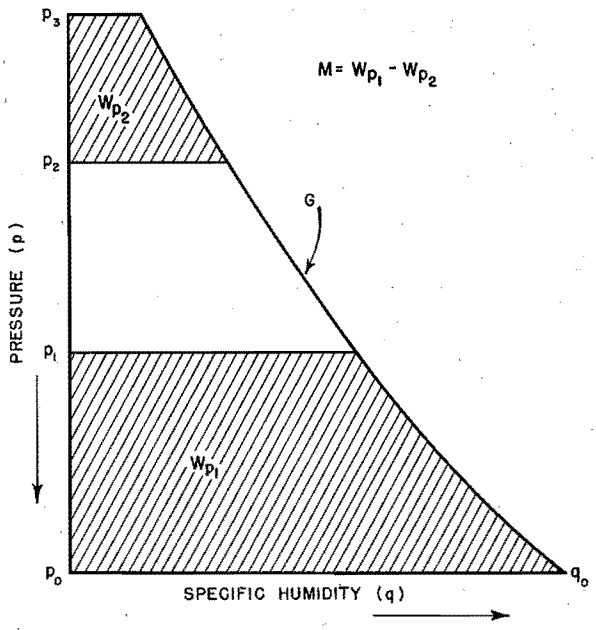

Figure 16

Schematic diagram illustrating the determination of M

122. In the Pittsburgh Report (2) it was shown that for a maximum convective process all of the above variables are uniquely determined by the point q_o. This point, in terms of temperature, will be called the reduced dew point D_r, and is the dew point reduced along the pseudo-adiabat to 1000 mb. In saturated air it is obviously the actual dew point at 1000 mb. The function M, thus determined, is called the effective precipitable water W_E, as explained in the Pittsburgh Report. It is the greatest amount of moisture that can be precipitated from a saturated column of air by complete convective overturning. Since the latter is the most efficient natural process for producing rainfall, W_E is used in the computation of maximum rainfall. The way in which the variables

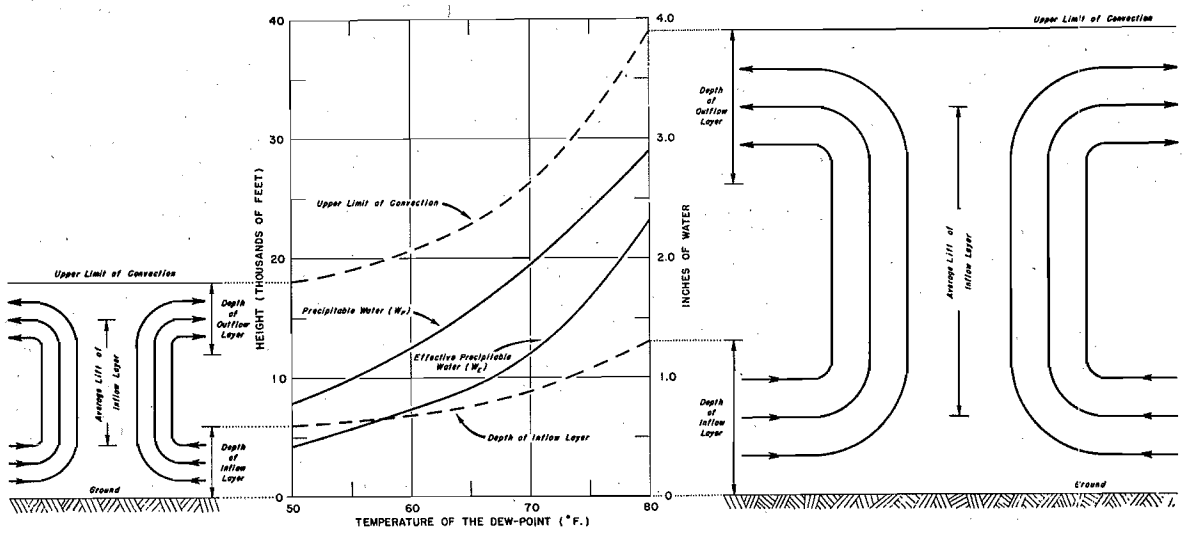

Figure 17

Effect of moisture charge on the structure of a convective cell

p_o, p_1, p_2, and p_3 depend on the value of D_r, and thus determine W_E, is shown in Figure 17. The pressure levels p_o and p_1 (of Figure 16) are now the base and top of the inflow layer, and p_2 and p_3 the base and top of the outflow layer. G is assumed to be a pseudo-adiabat. For a basin, the interpretation of the theory is that every unit column of saturated air entering the basin will undergo a definite lift before leaving it. This will cause a certain amount of water W_E to be deposited within the basin. The lifting mechanism is the convective cell, whose size is determined by the D_r value of the air. It becomes essential, then, to determine the maximum reduced dew point D_r and its variation with time.

123. In the equation for maximum rainfall it is assumed that the inequality sign may be removed, and the equation thus becomes

$$R_{max} = \int K v_{max} W_{E_{max}} dt \qquad (3)$$

where v_{max} refers to the maximum possible velocities from the most

critical wind directions and $W_{E_{max}}$ is the effective precipitable water for the maximum possible reduced dew points, both occurring in the most persistent pattern appropriate to the season. K is a function of wind direction and, as will be shown later, also a function of reduced dew point in the particular case of a basin in the lee of an orographic barrier.

124. Orographic Precipitation. It has already been pointed out that in applying the general method outlined above to the Sacramento Basin, it would be necessary to take into account the effects of topography, i.e., the orographic effect. The term "orographic precipitation" includes a complex of meteorological phenomena. It is obvious, for example, that the same orographic barrier which is a rain-producing agent on its windward side acts as a rain-inhibiting agent on the leeward. Both effects are orographic. Furthermore, either is as much orographic in origin as the distribution of precipitation intensity along the slope, although we may be concerned with but one of all three effects. In general, it may be said that the effect of orography on precipitation will depend on the following factors other than elevation and slope: stability of the air mass, amount and vertical distribution of water vapor, wind velocity and shear, and inflow direction. The usual type of rainfall-elevation correlation is inadequate, since it neglects important variables.

125. Pockels (73, 74) and J. Bjerknes (12) have analyzed the dynamics of air currents ascending over a mountain barrier. The following principles can be inferred from the conclusions of both authors:

a. Rainfall intensity is a direct function of slope.

b. One effect of elevation is to reduce the moisture available farther up slope, so that, if the raindrops fell vertically, intensity would be an inverse function of elevation.

c. Another effect of elevation, however, is to increase the slanting trajectory of raindrops.

d. The net effect of b. and c. is to produce a zone of maximum intensity some distance up the slope, at approximately 4,000 feet above the base.

e. The higher the condensation level, the farther toward the mountain top will the zone of maximum intensity be shifted.

It should be noted that the base mentioned in d. is sea level, or practically so, for the Coast Range. For the Sierra Nevada Range, however, the base becomes, in effect, the top of the coastal barrier to the windward. It is therefore to be expected that the zone of maximum intensity is at a higher elevation on the Sierras than on the Coast Range. Later it will be shown that, with respect to the Sierra Range, the effective condensation level is also no lower than the top of the coastal chain.

126. In computing the distribution of intensities along the slope of the Sierra Madres, Bjerknes assumed that the air was in neutral equilibrium with respect to the pseudo-adiabatic process. If the lapse rate of the air column were less than the pseudo-adiabatic, however, there would be a tendency toward suppression of vertical motions, so that the rainfall intensity would be less than that computed by Bjerknes. On the other hand, if the lapse rate were greater than the pseudo-adiabatic, there would be an additional upward component, so that the actual intensities would be greater than those computed by Bjerknes. Thus, in general, the intensity at a point on the slope will depend in part on the stability of the air mass, and, as Bjerknes states, it may even be incalculable for extreme instability. By taking stability into account it is

possible to distinguish three types of orographic rain in terms of the assumptions made in computing effective precipitable water. These are:

a. Stable orographic rain -- when the lapse rate is less than the pseudo-adiabatic. The upper limit of intensities for this type of rain could be computed from Bjerknes' analysis.

b. Incomplete convective orographic rain -- when the air mass is slightly unstable. In addition to the lift computed from the Bjerknes model there is a convective component, but the convective process is incomplete in the sense that not all the effective precipitable water is realized.

c. Complete convective rain -- when all of the W_E is realized. This would be the case when an unstable column undergoes extreme convergence. The rainfall would be the same as in a non-orographic convective process, the mountain merely acting as a "trigger" in setting off the convection.

127. Although knowledge of the distribution of intensities is not necessary to the development of the theoretical precipitation formula for the Sacramento Basin, it is of interest to compare some calculable intensities in the orographic types. As a preliminary, certain further deductions from the fundamental assumptions involved in the concept of W_E should be made. It was previously shown that the effective precipitable water is equal to $W_{p_1} - W_{p_2}$, where the subscripts 1 and 2 refer to initial and final states, respectively, of a saturated column. The numerical values of W_E were computed on the assumption that initially the base of the column was at 1000 mb. If the base of the column were initially at any elevation H, or if the column became saturated just when the base of the column was lifted to H, the effective precipitable water for such a case, designated by $(W_E)_H$, could also be computed. Figure 18 shows the values of the ratio $\frac{(W_E)_H}{W_E}$ in percent, for various values of D_r and H. The ratio is called the lift coefficient L. If

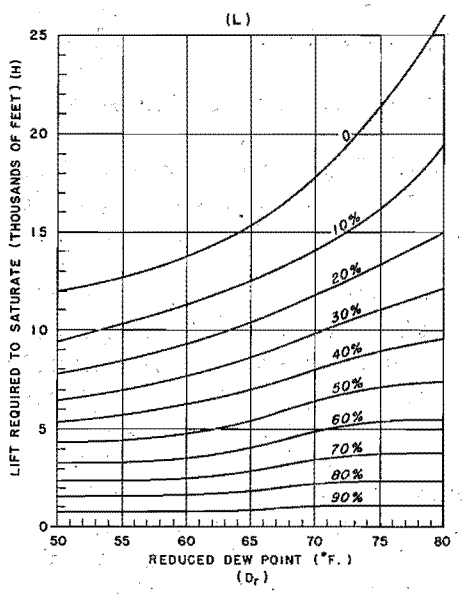

Figure 18

The percentage of effective precipitable water remaining in a column of air

H were the height of an inflow barrier, $(W_E)_H$ would be the greatest amount of effective precipitable water that could enter a basin lying in the lee of the barrier (neglecting re-evaporation), and W_E minus $(W_E)_H$ could be deposited on the windward side by the incomplete convective orographic rain process. Computing the maximum rainfall intensity in the situation described by Bjerknes (12), using his basic data and comparing, the results are:

For incomplete convective orographic rain; 2.9 in. per hr.

For stable orographic rain (computed by Bjerknes): 1.3 in. per hr.

The incomplete convective orographic intensity is 2-1/4 times as great as the stable orographic. It should be pointed out, however, that the higher the top of the barrier the more nearly will the stable orographic intensity approach that of the incomplete convective.

128. Development of Basin Constants. The synoptic studies of the preceding chapter have already confined the possible inflow directions of the potentially flood-producing air to the quadrant from south to west. It remains to determine which direction within this quadrant is geometrically the most effective. For different inflow directions the basin width normal to the inflow will of course be different. It should be obvious, too, that if the inflow boundaries are also high, not all of the

effective precipitable water can reach the basin. The Coast Range must necessarily release a portion of the effective precipitable water in the inflow layer. The problem is to discover what process will combine these effects to permit the maximum moisture to flow into the basin.

129. Three distinct assumptions will be made and their results compared by computing the resultant constants for a reduced dew point of 63 F. Figure 19 shows the functional relationship between L and H for that dew point. It will be recalled that in the preceding section L was shown to be a function of H. In the figure and in future discussion H will be called the "effective height," defined as the height to which the base of a narrow column of air must be lifted in order to enter the basin from a given direction. By the use of topographic charts, effective heights for five directions within the significant southwest quadrant

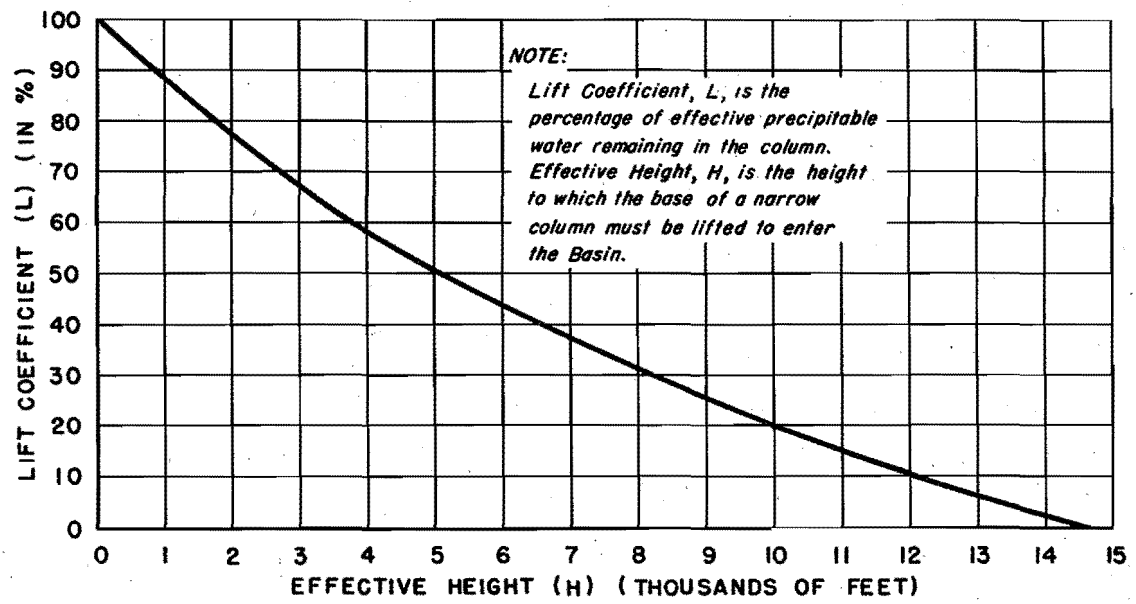

Figure 19

Relation between lift coefficient and effective height for a reduced dew point of 63 F

were found for five-mile intervals between parallel lines running from the Pacific Ocean to the basin boundaries. The inflow L values, based on these values of H and a reduced dew point of 63 F, appear in Table 31 which has been arranged in ascending order of effective heights. Constants for the following assumptions were then computed.

130. Assumption I is that incomplete convective rain occurs both on the Coast Range and in the basin. The air flowing across the inflow barrier will enter the basin with a certain lift coefficient L, but at the higher outflow barrier its lift coefficient will be lower. The difference between the two values, ΔL, will determine the W_E released over the basin. Given the inflow direction, however, the outflow lift coefficient, and therefore ΔL, will vary with the flow pattern over the basin. Several patterns were assumed and the constants computed for each:

a. Straight line flow. Example: inflow from west, outflow from west.

b. Cyclonic rotation of 22.5°. Example: inflow from west, outflow from west-southwest.

c. Cyclonic rotation of 45°. Example: inflow from west, outflow from southwest.

Anticyclonic flow was not considered since, aside from meteorological considerations, the constants have lower values. The profiles plotted on Figures 3 and 4 indicate roughly how ΔL is decreased in such a flow, but it should be remembered that the profile heights are not necessarily effective heights. For all patterns, however, the geometrical constant will be equal to:

$$\frac{\text{Width of Inflow} \quad (\text{Mean Inflow L} - \text{Mean Outflow L})}{\text{Area of Basin}}$$

Table 32 shows the computations of the constants for Assumption I. They

TABLE 31

TABULATION OF DATA FOR BASIN CONSTANTS (D_r = 63 F)

(A) = Accumulated Width (miles) (L) = Lift Coefficient
(H) = Effective Height (hundreds of feet)

Flow From:	S		SSW		SW		WSW		W	
(A)	(H)	(L)	(H)	(L)	(H)	(L)	(H)	(L)	(H)	(L)
5	20	.78	11	.88	5	.94	22	.75	22	.75
10	20	.78	12	.87	5	.94	22	.75	31	.66
15	29	.68	12	.87	12	.87	22	.75	32	.65
20	30	.67	20	.78	12	.87	23	.74	32	.65
25	30	.67	20	.78	13	.85	23	.74	32	.65
30	30	.67	23	.74	14	.84	31	.66	32	.65
35	31	.66	23	.74	18	.80	31	.66	39	.59
40	31	.66	23	.74	19	.79	31	.66	40	.58
45	31	.66	23	.74	20	.78	32	.65	41	.57
50	32	.65	28	.69	20	.78	32	.65	41	.57
55	32	.65	28	.69	20	.78	32	.65	48	.52
60	33	.64	28	.69	21	.76	41	.57	51	.50
65	36	.61	30	.67	21	.76	45	.54	51	.50
70	37	.60	30	.67	22	.75	48	.52	51	.50
75	37	.60	31	.66	22	.75	50	.51	51	.50
80	39	.59	31	.66	22	.75	51	.50	51	.50
85	39	.59	31	.66	23	.74	51	.50	51	.50
90	39	.59	31	.66	23	.74	51	.50	52	.50
95	40	.58	32	.65	24	.73	51	.50	52	.50
100	40	.58	32	.65	28	.69	51	.50	53	.49
105	41	.57	33	.64	30	.67	52	.50	54	.48
110	41	.57	33	.64	32	.65	54	.48	60	.44
115	43	.55	34	.63	32	.65	55	.48	60	.44
120	43	.55*	39	.59	32	.65	57	.46	60	.44
125	51	.50	40	.58	33	.64*	59	.45	60	.44
130	54	.48	51	.50	41	.57	60	.44	62	.43
135	58	.45	58	.45	48	.52	60	.44	62	.43
140	66	.40	61	.43	50	.51	60	.44	63	.42
145	68	.39	62	.43	51	.50	61	.43	65	.41
150	76	.34	62	.43	53	.49	62	.43	68	.39
155			62	.43*	55	.48	63	.42	70	.38
160			64	.41	58	.45	65	.41	70	.38
165			69	.38	59	.45	69	.38	70	.38
170			73	.35	60	.44	70	.38	70	.38
175			76	.34	61	.43	71	.37	71	.37*
180			80	.31	62	.43	71	.37*	75	.34
185					63	.42	72	.36	80	.31
190					64	.41	80	.31	90	.25
195					67	.39	80	.31	90	.25
200					70	.38	82	.30	100	.20
205					70	.38	120	.10		
210					71	.37				
215					72	.36				
Total		17.71		22.03		27.15		20.56		18.89
Mean		.590		.612		.631		.501		.472

* Optimum value for Assumption II.

TABLE 32

COMPUTATION OF BASIN CONSTANTS (D_r = 63 F)

Inflow From:		S	SSW	SW	WSW	W
Assumption I. $K = \frac{\text{total inflow width (mean inflow L - mean outflow L)}}{25,200}$						
I(a)	Mean Inflow L	.590	.612	.631	.501	.472
	Mean Outflow L	.374	.339	.351	.338	.326
	Δ L	.116	.273	.280	.163	.146
	K	.00129	.00195	.00239	.00133	.00116
I(b)	Mean Inflow L		.612	.631	.501	.472
	Mean Outflow L		.374	.339	.351	.338
	Δ L		.238	.292	.150	.134
	K		.00165	.00249	.00122	.00106
I(c)	Mean Inflow L			.631	.501	.472
	Mean Outflow L			.374	.339	.351
	Δ L			.257	.162	.121
	K			.00219	.00132	.00096

Assumption II. $K = \frac{\text{Maximum (L x A)}}{25,200}$

L	.55	.43	.64	.37	.37
A	120.0	155.0	125.0	180.0	175.0
LXA	66.0	66.65	80.0	66.60	64.75
K	.00262	.00264	.00317	.00264	.00257

Assumption III. $K = \frac{5\Sigma L}{25,200}$

ΣL	17.71	22.03	27.15	20.56	18.89
K	.00351	.00437	.00539	.00408	.00375

are based on the values in Table 31 where, however, tabulations of H and L for outflow have been omitted to save space.

131. Assumption II is that complete convective rain occurs both on the Coast Range and in the basin. Under this assumption, if the column of air were saturated at sea level, there would be no rain whatsoever reaching the basin, except that which "spilled over" the coastal barrier. On the other hand, if the saturation level were at some higher elevation, every column whose effective height is below the saturation level would contribute to the rainfall in the basin, and every column whose effective height is above the saturation elevation would not contribute. Theoretically, a saturation level can be selected that will exceed all effective heights but, since L decreases as the saturation level increases (Figure 18), such an occurrence would not necessarily be productive of the most rainfall over the basin. What is needed for maximum precipitation is a saturation level which will result in the maximum product of L and the total number of columns undergoing complete convection within the basin. Table 32 outlines the manner in which the constants for Assumption II are computed, using H and L values of Table 31. In column H of Table 31 the effective heights are tabulated in ascending order. Each entry represents an air column five miles wide. Column (A) represents the accumulated width of all air columns whose effective heights are equal to or less than the corresponding saturation level. Column (L) contains the corresponding values of the lift coefficient. The maximum constant will therefore be the maximum product of columns (A) and (L), divided by the area of the basin.

132. Assumption III is that incomplete convective orographic rain occurs on the Coast Range and complete convective rain in the basin. As it

flows inland the air is assumed to be saturated and slightly unstable. As it passes over the Coast Range, incomplete convective orographic rain will fall. After it clears the barrier, the remaining W_E is realized within the basin by the process of complete convection which is finally achieved with the aid of convergence produced by the basin. As has been previously mentioned, the constraints imposed by the basin are such that the air in the lowest layers can enter only through the Golden Gate. The valley floor is roughly triangular in shape with the apex near Redding and Kennett. The effect is to cause horizontal convergence in the lower layers in two ways. First, the wind is constrained to a more northerly course, thus acquiring a greater cyclonic vorticity. Second, as the air flows toward the apex it is restricted to a progressively narrower space. Both of these effects are compensated for in part by vertical stretching. The vertical motions cause decreasing stability to greater and greater heights, until finally convective overturning takes place. The value of the constant for Assumption III will thus be controlled by the width of inflow times the sum of the L values of the inflow columns. The formula becomes

$$K = \frac{5\Sigma L}{\text{Area of Basin}}$$

The computations are shown in Table 32, the H and L values in Table 31.

133. The assumption of stable orographic rain on the Coast Range and complete convective rain in the basin would of course give even higher values of the constant. There are, however, two serious objections to this assumption. It is extremely doubtful whether saturated air with the assumed maximum dew points would have a stable lapse rate. Secondly, if

the air were both conditionally and convectively stable to begin with it could not later become unstable by dynamic means.

134. The results of the three assumptions for a dew point of 63 F are shown in Figure 20. It is evident that Assumption III produces the greatest depth of rain in the basin, and that a southwest flow is the most critical for any assumption.

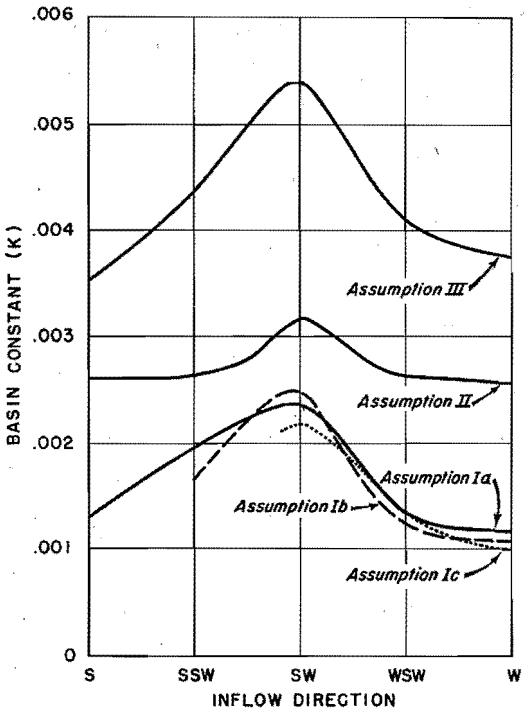

Figure 20

Relation between basin constant and inflow direction for a reduced dew point of 63 F

135. Theoretical Analysis of Major Storms. It is logical at this point to test the validity of the hypothetical storm which forms the basis for Assumption III, or, in other words, to discover whether storms observed in nature approximate the assumed conditions. This can best be accomplished by comparing the rainfall of individual storms computed on the basis of the above theory with the rainfall computed from isohyetal charts.

136. To expedite the computations, some adjustment can be made in the precipitation formula. It has already been shown that the basin constant for Assumption III is $\frac{5\Sigma L}{25,200}$, and that L is a function of H and D_r. By making use of the computed data in the preceding section, the basin constant K may be expressed as a function of D_r and inflow direction. Thus, in the formula $R = \int KW_E v dt$, both K and W_E are

functions of D_r, so that they may be combined into one term

$$f = KW_E$$

where f is called the moisture index and is a function of D_r and inflow direction (see Table 33). The precipitation formula can now be written

$$R = \int f v dt$$

TABLE 33

VALUES OF MOISTURE INDEX ($f \times 10^4$) FOR VARIOUS INFLOW DIRECTIONS

D_r(°F)	W	WSW	SW	SSW	S
40	4	4	7	5	4
41	5	5	8	6	5
42	5	6	8	7	6
43	6	6	9	8	6
44	6	7	10	9	7
45	7	8	12	10	8
46	8	9	13	11	9
47	9	10	14	12	9
48	10	11	16	13	10
49	11	12	17	14	11
50	12	13	19	15	12
51	13	14	20	16	13
52	14	15	22	18	14
53	15	17	23	19	15
54	16	18	25	20	16
55	17	19	27	22	17
56	18	20	28	23	18
57	19	22	30	24	19
58	21	24	32	26	21
59	23	25	34	28	22
60	24	27	36	29	23
61	27	29	39	32	25
62	29	31	42	34	27
63	31	33	44	36	29
64	33	35	47	38	31
65	35	38	50	41	33
66	39	42	54	44	35
67	42	45	59	47	38
68	45	49	63	51	42
69	50	54	69	56	46
70	55	60	76	61	50

Strictly, since both f and v in the inflow layers vary also with height, their products should be integrated through height. However, it was found that the error involved in using the product of the total f and the velocity at the mean height of the inflow layer was negligible. This is not surprising, since moisture decreases and v increases with height; the two curves tend to be reflections.

137. The observed values required for the theoretical computation are the dew point and wind velocity that may be used to characterize the storm. On account of their exposures, Mount Tamalpais and Donner Summit were chosen as dew point index stations. San Francisco was also used because data from this station were available in every storm. Point Reyes was chosen as a wind velocity index station. For reasons given in the section on maximum wind, Point Reyes data were assumed to be representative of the 4000-foot free-air wind, or the mean velocity of the inflow layer. Because this assumption was found to work best for southwest inflow directions, and also because the inflow directions were difficult to determine accurately, it was decided to use the f values for southwest winds exclusively.

138. With but one station used as wind index, the results obtained will differ only because of the variation in dew points at the index stations. Values of f from dew point observations at these stations were plotted against time and smooth curves were drawn through them. Hourly values of v were taken from the autographic records at Point Reyes. The products of fv were then integrated with respect to time by numerical integration (see Tables 34 to 41). In Table 42 maximum duration-depth values for the whole basin, as computed from the rainfall

TABLE 34

STORM COMPUTATION

January 12-19, 1906

Date	Period (P.S.T.)	(v)	$(f)_1$	$(R)_1$	$(f)_3$	$(R)_3$
12	0430-0730	114	24	.27	22	.25
	0730-1030	108	22	.24	20	.22
	1030-1330	96	19	.18	18	.17
	1330-1630	78	16	.12	16	.12
	1630-1930	66	14	.09	15	.10
	1930-2230	60	13	.08	15	.09
13	2230-0130	57	14	.08	17	.10
	0130-0430	63	19	.12	21	.13
	0430-0730	84	25	.21	28	.24
	0730-1030	117	28	.33	31	.36
	1030-1330	126	26	.33	31	.39
	1330-1630	111	25	.28	29	.32
	1630-1930	87	22	.19	26	.23
	1930-2230	75	20	.15	22	.16
14	2230-0130	69	17	.12	19	.13
	0130-0430	66	14	.09	15	.10
	0430-0730	48	12	.06	11	.05
	0730-1030	36	10	.04	9	.03
	1030-1330	30	8	.02	10	.03
	1330-1630	30	7	.02	12	.04
	1630-1930	39	9	.04	15	.06
	1930-2230	57	13	.07	21	.12
15	2230-0130	72	18	.13	25	.18
	0130-0430	87	23	.20	27	.24
	0430-0730	102	26	.27	27	.28
	0730-1030	108	26	.28	27	.29
	1030-1330	108	25	.27	26	.28
	1330-1630	102	25	.26	25	.26
	1630-1930	102	26	.27	25	.26
	1930-2230	111	27	.30	26	.29
16	2230-0130	132	25	.33	25	.33
	0130-0430	141	21	.30	23	.32
	0430-0730	141	17	.24	20	.28
	0730-1030	129	15	.19	16	.21
	1030-1330	93	13	.12	13	.12
	1330-1630	57	11	.06	10	.06
	1630-1930	33	10	.03	10	.03
	1930-2230	21	10	.02	9	.02
17	2230-0130	21	11	.02	11	.02
	0130-0430	21	12	.03	13	.03
	0430-0730	24	15	.04	16	.04
	0730-1030	27	19	.05	20	.05
	1030-1330	45	21	.09	23	.10
	1330-1630	78	22	.17	25	.20
	1630-1930	96	22	.21	25	.24
	1930-2230	105	21	.22	24	.25
18	2230-0130	111	21	.23	23	.26
	0130-0430	114	20	.23	23	.26
	0430-0730	117	20	.23	23	.27
	0730-1030	123	21	.26	25	.31
	1030-1330	123	22	.27	26	.32
	1330-1630	123	23	.28	27	.33
	1630-1930	114	22	.25	26	.30
	1930-2230	108	17	.18	22	.24
19	2230-0130	120	6	.07	10	.12

(v)=3-hour wind movement (Point Reyes) (f)=Moisture index x 10^4
(R)=(v) x moisture index = rainfall intensity

NOTE: Subscripts refer to index station used for dew points:
1 = San Francisco, 2 = Donner Summit, 3 = Mt. Tamalpais

TABLE 35

STORM COMPUTATION

March 16-19, 1907

Date	Period (P.S.T.)	(v)	$(f)_1$	$(R)_1$	$(f)_3$	$(R)_3$
16	0430-0730	39	20	.08	20	.08
	0730-1030	51	21	.11	22	.11
	1030-1330	66	22	.15	23	.15
	1330-1630	78	22	.17	24	.19
	1630-1930	81	24	.19	25	.20
	1930-2230	81	25	.20	26	.21
17	2230-0130	90	24	.22	25	.22
	0130-0430	108	23	.25	24	.26
	0430-0730	114	21	.24	23	.26
	0730-1030	117	18	.21	22	.26
	1030-1330	117	15	.18	22	.26
	1330-1630	114	13	.15	23	.26
	1630-1930	111	13	.14	24	.27
	1930-2230	108	14	.15	24	.26
18	2230-0130	114	17	.19	25	.28
	0130-0430	120	21	.25	27	.32
	0430-0730	111	23	.26	27	.30
	0730-1030	99	25	.25	28	.28
	1030-1330	96	27	.26	28	.27
	1330-1630	93	28	.26	28	.26
	1630-1930	87	28	.24	28	.24
	1930-2230	84	27	.23	27	.23
19	2230-0130	81	26	.21	26	.21
	0130-0430	81	27	.22	27	.22
	0430-0730	84	28	.24	28	.24
	0730-1030	87	30	.26	30	.26
	1030-1330	105	31	.33	32	.34
	1330-1630	114	30	.34	31	.35
	1630-1930	102	24	.24	25	.26
	1930-2230	51	17	.09	18	.09

(v) = 3-hour wind movement (Point Reyes)
(f) = Moisture index x 10^4
(R)=(v) x moisture index = rainfall intensity

NOTE: Subscripts refer to index station used for dew points:
1 = San Francisco
2 = Donner Summit
3 = Mt. Tamalpais

TABLE 36

STORM COMPUTATION

January 12-16, 1909

Date	Period (P.S.T.)	(v)	$(f)_1$	$(R)_1$	$(f)_3$	$(R)_3$
12	0430-0730	81	6	.05	9	.07
	0730-1030	63	7	.04	12	.08
	1030-1330	33	8	.03	14	.05
	1330-1630	18	9	.02	18	.03
	1630-1930	33	12	.04	20	.07
	1930-2230	60	15	.09	23	.14
13	2230-0130	84	20	.17	25	.21
	0130-0430	90	25	.22	27	.24
	0430-0730	78	27	.21	30	.23
	0730-1030	63	30	.19	31	.20
	1030-1330	75	28	.22	30	.22
	1330-1630	96	24	.27	30	.29
	1630-1930	99	30	.30	32	.32
	1930-2230	102	30	.31	32	.33
14	2230-0130	102	29	.30	30	.31
	0130-0430	105	28	.29	28	.29
	0430-0730	114	27	.31	28	.32
	0730-1030	120	27	.32	28	.34
	1030-1330	90	27	.24	28	.25
	1330-1630	72	28	.20	28	.20
	1630-1930	84	28	.24	28	.24
	1930-2230	102	28	.29	28	.29
15	2230-0130	99	28	.28	28	.28
	0130-0430	99	27	.27	27	.27
	0430-0730	105	27	.28	27	.28
	0730-1030	111	27	.30	27	.30
	1030-1330	102	27	.28	27	.28
	1330-1630	93	27	.25	27	.25
	1630-1930	87	28	.24	28	.24
	1930-2230	84	28	.24	28	.24
16	2230-0130	81	28	.23	28	.23
	0130-0430	72	28	.20	28	.20
	0430-0730	57	29	.17	29	.17
	0730-1030	45	29	.13	29	.13
	1030-1330	45	29	.13	29	.13
	1330-1630	45	30	.14	30	.14
	1630-1930	42	30	.13	31	.13
	1930-2230	36	29	.10	31	.11

(v)=3-hour wind movement (Point Reyes) (f)=Moisture index x 10^4

(R)=(v) x moisture index = rainfall intensity

NOTE: Subscripts refer to index station used for dew points:
1 = San Francisco, 2 = Donner Summit, 3 = Mt. Tamalpais

TABLE 37

STORM COMPUTATION

December 29, 1913-January 2, 1914

Date	Period (P.S.T.)	(v)	$(f)_1$	$(R)_1$	$(f)_3$	$(R)_3$
29	0600-0900	94	15	.14	19	.18
	0900-1200	119	19	.23	22	.26
	1200-1500	94	21	.20	22	.21
	1500-1800	99	20	.20	20	.20
	1800-2100	39	17	.07	18	.07
	2100-0000	39	15	.06	18	.07
30	0000-0300	53	15	.08	19	.10
	0300-0600	73	16	.12	21	.15
	0600-0900	95	20	.19	25	.24
	0900-1200	109	25	.27	27	.29
	1200-1500	119	28	.33	28	.33
	1500-1800	117	30	.35	28	.33
	1800-2100	123	32	.39	29	.36
	2100-0000	135	33	.45	30	.41
31	0000-0300	134	30	.40	29	.39
	0300-0600	138	27	.37	28	.39
	0600-0900	149	24	.36	24	.36
	0900-1200	140	21	.29	21	.29
	1200-1500	73	22	.16	22	.16
	1500-1800	42	25	.11	23	.10
	1800-2100	35	26	.09	26	.09
	2100-0000	67	27	.18	27	.18
1	0000-0300	72	26	.19	28	.20
	0300-0600	49	25	.12	28	.14
	0600-0900	49	24	.12	28	.14
	0900-1200	75	23	.17	29	.22
	1200-1500	94	24	.23	30	.28
	1500-1800	99	25	.35	32	.32
	1800-2100	112	27	.30	32	.36
	2100-0000	130	27	.35	31	.40
2	0000-0300	136	25	.34	27	.37
	0300-0600	81	23	.19	23	.19
	0600-0900	91	21	.19	23	.21
	0900-1200	88	21	.18	24	.21

(v)=3-hour wind movement (Point Reyes) (f)=Moisture index x 10^4
(R)=(v) x moisture index = rainfall intensity

NOTE: Subscripts refer to index station used for dew points:
1 = San Francisco, 2 = Donner Summit, 3 = Mt. Tamalpais

TABLE 38

STORM COMPUTATION
March 22-27, 1928

Date	Period (P.S.T.)	(v)	$(f)_1$	$(R)_1$
22	0430-0730	42	27	.11
	0730-1030	42	26	.11
	1030-1330	51	25	.13
	1330-1630	63	24	.15
	1630-1930	75	23	.17
	1930-2230	81	23	.19
23	2230-0130	69	24	.17
	0130-0430	42	26	.11
	0430-0730	33	28	.09
	0730-1030	30	28	.08
	1030-1330	51	28	.14
	1330-1630	72	30	.22
	1630-1930	69	33	.23
	1930-2230	69	32	.22
24	2230-0130	69	26	.18
	0130-0430	66	25	.16
	0430-0730	45	12	.05
	0730-1030	33	7	.02
	1030-1330	30	13	.04
	1330-1630	30	20	.06
	1630-1930	60	31	.19
	1930-2230	102	34	.35
25	2230-0130	105	34	.36
	0130-0430	99	31	.31
	0430-0730	69	30	.21
	0730-1030	36	30	.11
	1030-1330	33	30	.10
	1330-1630	45	30	.14
	1630-1930	60	30	.18
	1930-2230	75	30	.23
26	2230-0130	84	29	.24
	0130-0430	93	27	.25
	0430-0730	117	24	.28
	0730-1030	132	23	.30
	1030-1330	123	20	.25
	1330-1630	102	17	.17
	1630-1930	75	20	.15
	1930-2230	51	14	.07
27	2230-0130	48	10	.05
	0130-0430	48	6	.03

(v) = 3-hour wind movement (Point Reyes) (f)=Moisture index x 10^4
(R)=(v) x moisture index = rainfall intensity

NOTE: Subscripts refer to index station used for dew points:
1 = San Francisco, 2 = Donner Summit, 3 = Mt. Tamalpais

TABLE 39

STORM COMPUTATION

December 9-13, 1929

Date	Period (P.S.T.)	(v)	$(f)_1$	$(R)_1$
9	0430-0730	105	21	.22
	0730-1030	114	24	.27
	1030-1330	126	25	.32
	1330-1630	138	24	.33
	1630-1930	147	22	.32
	1930-2230	156	21	.33
10	2230-0130	153	21	.32
	0130-0430	147	21	.31
	0430-0730	111	23	.26
	0730-1030	75	26	.20
	1030-1330	66	28	.18
	1330-1630	60	30	.18
	1630-1930	63	30	.19
	1930-2230	66	29	.19
11	2230-0130	69	27	.19
	0130-0430	72	25	.18
	0430-0730	69	25	.17
	0730-1030	66	27	.18
	1030-1330	72	28	.20
	1330-1630	84	28	.24
	1630-1930	105	28	.29
	1930-2230	120	29	.35
12	2230-0130	117	31	.26
	0130-0430	99	33	.33
	0430-0730	90	34	.31
	0730-1030	84	35	.29
	1030-1330	78	36	.28
	1330-1630	72	36	.26
	1630-1930	72	35	.25
	1930-2230	72	34	.24
13	2230-0130	69	33	.23
	0130-0430	66	32	.21
	0430-0730	69	33	.23

(v)= 3-hour wind movement (Point Reyes)
(f)= Moisture index x 10^4
(R)=(v) x moisture index = rainfall intensity

NOTE: Subscripts refer to index station used for dew points:
1 = San Francisco, 2 = Donner Summit, 3 = Mt. Tamalpais

TABLE 40

STORM COMPUTATION

December 9-12, 1937

Date	Period (P.S.T.)	(v)	$(f)_1$	$(R)_1$	$(f)_2$	$(R)_2$
9	0130-0430	93	17	.16	12	.11
	0430-0730	99	18	.18	13	.13
	0730-1030	105	19	.20	12	.13
	1030-1330	117	22	.26	22	.26
	1330-1630	129	25	.32	25	.32
	1630-1930	135	29	.39	30	.40
	1930-2230	132	32	.42	30	.40
10	2230-0130	126	36	.45	30	.38
	0130-0430	123	41	.50	28	.34
	0430-0730	132	46	.61	39	.51
	0730-1030	147	49	.72	42	.62
	1030-1330	150	50	.75	39	.58
	1330-1630	150	50	.75	44	.66
	1630-1930	153	49	.75	44	.67
	1930-2230	153	45	.69	39	.60
11	2230-0130	132	40	.53	36	.48
	0130-0430	99	36	.36	39	.39
	0430-0730	102	34	.35	39	.40
	0730-1030	108	35	.38	34	.37
	1030-1330	84	36	.30	30	.25
	1330-1630	66	30	.20	25	.16
	1630-1930	60	25	.15	25	.15
	1930-2230	54	22	.12	22	.12
12	2230-0130	51	20	.10	20	.10

(v) = 3-hour wind movement (Point Reyes)
(f) = Moisture index x 10^4
(R)=(v) x moisture index = rainfall intensity

NOTE: Subscripts refer to index station used for dew points:
1 = San Francisco
2 = Donner Summit
3 = Mt. Tamalpais

TABLE 41

STORM COMPUTATION

February 25-29, 1940

Date	Period (P.S.T.)	(v)	$(f)_1$	$(R)_1$	$(f)_2$	$(R)_2$
25	0430-0730	54	30	.16	27	.15
	0730-1030	54	30	.16	25	.14
	1030-1330	45	30	.14	25	.11
	1330-1630	36	29	.10	27	.10
	1630-1930	33	27	.09	25	.08
	1930-2230	36	24	.09	25	.09
26	2230-0130	45	23	.10	25	.11
	0130-0430	69	22	.15	25	.17
	0430-0730	96	23	.22	24	.23
	0730-1030	120	25	.30	22	.26
	1030-1330	114	27	.31	22	.25
	1330-1630	117	28	.33	22	.26
	1630-1930	132	28	.37	22	.29
	1930-2230	150	28	.42	22	.33
27	2230-0130	150	28	.42	22	.33
	0130-0430	135	28	.38	22	.30
	0430-0730	108	28	.30	22	.24
	0730-1030	87	29	.25	23	.20
	1030-1330	99	30	.30	27	.27
	1330-1630	132	28	.37	25	.33
	1630-1930	150	27	.40	25	.38
	1930-2230	159	26	.41	27	.43
28	2230-0130	162	25	.40	25	.40
	0130-0430	156	25	.39	17	.26
	0430-0730	123	24	.30	23	.28
	0730-1030	90	20	.18	23	.21
	1030-1330	96	16	.15	22	.21
	1330-1630	114	16	.18	22	.25
	1630-1930	99	17	.17	19	.19
	1930-2230	75	15	.11	19	.14
29	2230-0130	63	13	.08	11	.07
	0130-0430	54	10	.05	11	.06

(v) = 3-hour wind movement (Point Reyes)
(f) = Moisture index x 10^4
(R)=(v) x moisture index = rainfall intensity

NOTE: Subscripts refer to index station used for dew points:
1 = San Francisco
2 = Donner Summit
3 = Mt. Tamalpais

TABLE 42

MAXIMUM DURATION-DEPTH VALUES FROM FORMULA AND FROM PRECIPITATION DATA

Sacramento Basin above Sacramento (Synchronized at 72 hours)

Duration	Depth in Inches 6	12	18	24	36	48	72
January 1906-A							
By Formula (SF)	0.6	1.2	1.7	2.4	2.6	3.2	4.2
" " (MT)	0.7	1.3	1.8	2.3	3.1	3.3	4.6
From Precip. Data	0.9	1.8	2.1	2.8	4.2	4.3	5.8
January 1906-B							
By Formula (SF)	0.7	1.2	1.7	2.3	3.0	3.3	4.6
" " (MT)	0.8	1.3	1.7	2.3	3.2	3.6	5.0
From Precip. Data (*)	0.8	1.3	1.8	2.3	3.0	3.8	4.5
March 1907							
By Formula (SF)	0.7	1.2	1.6	2.1	3.1	3.8	5.5
" " (MT)	0.7	1.2	2.0	2.2	3.2	4.3	6.3
From Precip. Data	1.0	1.8	2.4	2.8	3.9	4.9	6.6
January 1909							
By Formula (SF)	0.6	1.2	1.8	2.3	3.4	4.5	6.3
" " (MT)	0.6	1.2	1.9	2.4	3.4	4.6	6.4
From Precip. Data	0.9	1.5	1.9	2.5	3.8	4.7	6.4
December 1913							
By Formula (SF)	0.8	1.6	2.3	2.9	3.7	4.0	6.4
From Precip. Data	1.4	2.7	3.3	3.9	5.0	5.5	6.6
March 1928							
By Formula (SF)	0.7	1.2	1.6	1.9	2.8	3.7	4.7
From Precip. Data	1.2	1.5	1.8	2.1	2.9	3.8	5.1
December 1929							
By Formula (SF)	0.6	1.3	1.9	2.5	3.2	4.0	6.2
From Precip. Data	1.1	1.6	2.1	2.6	3.4	4.0	5.9
December 1937							
By Formula (SF)	1.5	3.0	4.3	5.3	6.9	8.3	9.6
" " (DS)	1.3	2.4	3.6	4.5	6.0	7.4	8.5
From Precip. Data	1.3	2.4	3.5	4.6	6.8	7.9	8.5
February 1940							
By Formula (SF)	0.8	1.6	2.3	2.8	4.7	5.6	6.9
From Precip. Data	1.1	2.0	2.8	3.4	5.1	6.4	7.4
February 1942							
By Formula (SF)							4.0
Estimated from Precip. Data							4.4

(*) Ending 6 p. of the 16th, P.S.T. SF - San Francisco Dew Point Data
MT - Mt. Tamalpais Dew Point Data DS - Donner Summit Dew Point Data

data, are compared with the values for the same periods from the theoretical formula. The comparison is graphically illustrated in Figure 21. It will be seen that, in general, there is better agreement as the duration increases. Undoubtedly, this is partly explained by the uncertainty attached to short-period breakdowns. It was also found that the synchronization between the two sets of data was quite good, although the theoretical values in most cases exhibited less abrupt changes in intensity. Perhaps it would be too much, in view of the various possible sources of error in both sets of data, to expect closer agreement. A critical analysis seemed to indicate that lack of agreement, in some cases, was caused by a time lag in dew points at index stations and also by the smoothing inherent in the computation method, although in other cases the cause might have been the inevitable approximations involved in construction of mass rainfall curves for non-recording stations. It will be noted, for example, that in the 1929 storm the 48-hour values agree perfectly, but the theoretical 72-hour values are higher. An examination of the data revealed that this discrepancy resulted from a persistence of high dew points after the rain had ended over most of the basin (see Chapter V). In storms like the 1906 the maximum 72-hour value (period A) represents a somewhat artificial combination of two rain periods separated by a

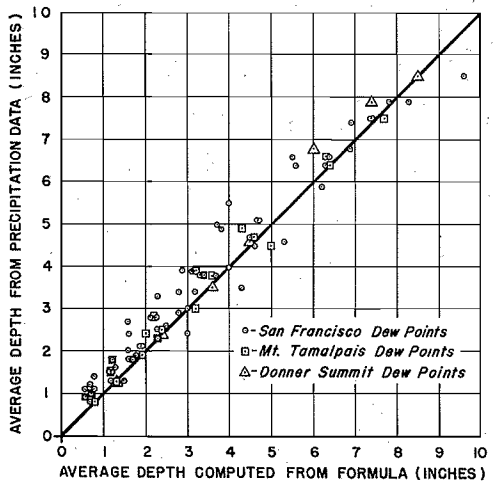

Figure 21

Average precipitation data over total basin

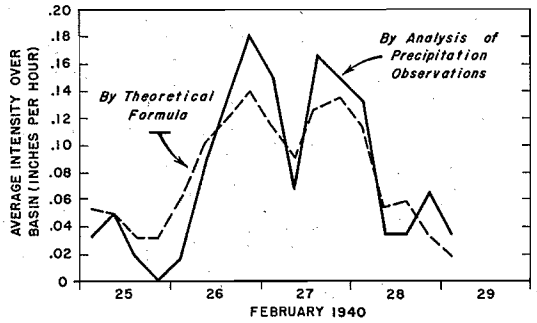

Figure 22

Computed precipitation intensity average over total basin storm of February 25-29, 1940

lull. In such a case the agreement is not likely to be very good. The period B (see Table 42), which is a more continuous rain period in the 1906 storm, shows a much better agreement than A. The best synchronization was obtained in the 1940 storm (see Figure 22) during which the greatest number of recording gages were in operation. The storm of February 1942 occurred while this study was in progress and a comparison of 72-hour values computed from formula and from data is included in Table 42. Rainfall data from only selected key stations were used since most other data were unavailable. The storm did not appear to be of comparatively major importance. Table 43 compares the relative magnitude of the major storms, as computed from formula and from rainfall data.

TABLE 43

SACRAMENTO STORMS ARRANGED IN DESCENDING ORDER OF MAGNITUDE

Maximum 72-Hour Average Depths

	From Precip. Data	By Formula (San Francisco Dew Points)
1.	1937	1937
2.	1940	1940
3.	1913-14	1913-14
4.	1907	1907
5.	1909	1909
6.	1929	1929
7.	1906-A	1928
8.	1928	1906-B
9.	1906-B	1906-A

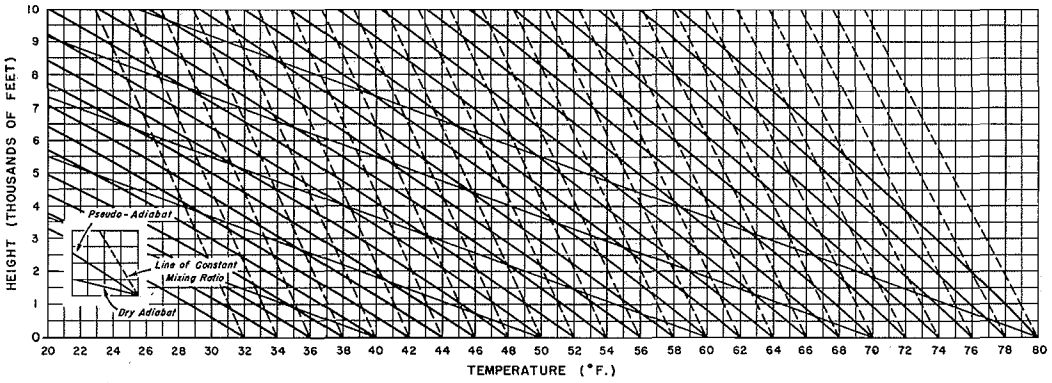

Figure 23

Pseudo-adiabatic diagram adapted for dew-point computations

139. The results seem to support the conclusion that Assumption III is an adequate description of a major storm over the Sacramento Basin. In order to compute the maximum possible precipitation it will thus be necessary to determine the maximum dew points and the maximum winds, and then to apply the formula developed above.

140. Maximum Dew Points. A survey was made of the maximum observed dew points for all months at nine stations in and near the Sacramento Basin. From these values reduced dew point temperatures were computed by the use of Figure 23. The results of the study are summarized in Table 44. Account having been taken of the relative degree of saturation, composite seasonal enveloping curves of the maximum reduced dew points were constructed. They are shown in Figure 24. It is evident from a study of the figure that the dew point maxima at low

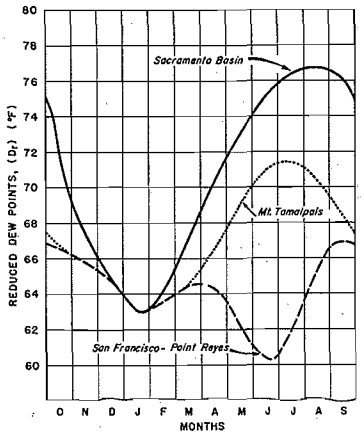

Figure 24

Seasonal variation of maximum possible reduced dew points

TABLE 44

MAXIMUM DEW POINT DATA

Stations		Jan.	Feb.	Mar.	Apr.	May	June	July	Aug.	Sept.	Oct.	Nov.	Dec.
Donner Summit	(a)	25	10,28	29	3	12	26	15	26	15	6	12	10,31
7200 ft.	(b)	38	37	42	47	51	56	57	57	54	51	45	45
1932-41	(c)	58.5	57.5	61.5	65.5	68.5	73	73.5	73.5	70.5	68.5	64	64
Fresno	(a)	14,29	25,28	3,11	4	28	30	22	27,28	25	22	2	11
330 ft.	(b)	60	59	64	68	69	61	67	66	69	67	63	61
1899-1941	(c)	61	60	65	69	70	62	68	67	70	68	64	62
Independence	(a)	12	16	11	26	29	17	21	14	28	10	9	15
3957 ft.	(b)	52	47	57	56	56	63	65	68	68	64	50	45
1899-1924	(c)	62	58	67	66	66	72	74	77	77	73	60.5	56
Mt. Tamalpais	(a)	16	26	3	22	15	20	6	24	16	22	9	3,9
2375 ft.	(b)	52	56	56	60	63	60	66	64	60	60	58	54
1899-1921	(c)	58.5	62	62	66	69	66	71	70	66	66	64	60
Point Reyes	(a)	1	16	21	1	24	23	15	11	12	19	1,7,19	2,30
490 ft.	(b)	58	61	64	60	57	58	60	60	64	63	58	56
1902-26	(c)	59	62	65	61	58	59	61	61	65	64	59	57
Red Bluff	(a)	14	16,24	2	16,30	26	8	26	7	21	2	12	1
334 ft.	(b)	58	59	61	65	67	68	68	69	75	64	67	59
1893-1934	(c)	59	60	62	66	68	69	69	70	76	65	68	60
Reno	(a)	2,28	7	22	10	15	16	24	27	26	1	26	11
4532 ft.	(b)	43	45	52	49	60	59	63	61	58	54	47	49
1906-1941	(c)	56	57.5	64	61	70.5	70	73	71.5	69	65	59	61
Sacramento	(a)	1	15	28	14	12	16	19	15	30	9	1	10
71 ft.	(b)	58	62	63	66	67	70	74	73	67	71	64	62
1893-1941													
San Francisco	(a)	2	19	12,28	22	9	6,24	1	26	12	3,25	12	10
153 ft.	(b)	59	63	60	64	63	60	60	66	66	62	62	65
1893-1941													

(a) Day of month (b) Dew Point (c) Reduced Dew Point

coastal stations are dependent on the sea surface temperatures. While the San Francisco-Point Reyes curve has a minimum value in mid-June, the curve for Mt. Tamalpais (elevation 2,375 ft. and only 14 miles from San Francisco) is climbing toward a maximum in July. Such extreme stability could occur only if the air in contact with the sea surface were being cooled. It is evident, of course, that such a state does not favor the production of flood rainfall. The pattern of the general circulation which is responsible for this stability and the dry summer of the region has already been discussed in Chapter II. It is obvious that the summer dew points described by the uppermost curve cannot, therefore, be considered representative in a storm or rain situation.

141. The observations considered must be representative in two respects: vertically of an unstable saturated column of air, and horizontally of an area comparable to that of the basin. From this point of view, the midwinter portion of the curve can be 100% representative, whereas the midsummer values, as has been just indicated, are not at all representative. There is no reason to believe, however, that the representativeness changes abruptly. It is much more reasonable to assume a more or less gradual transition. In such a case, it would be illogical to assume a definite rain season and then to choose dew point maxima at its beginning or end, because these values would be less representative than the ones nearer the middle of the period. It might be decided, for example, that the rain period extends from November 1 to April 1, 69 F being the maximum dew point during this period. But 69 would not be as representative a dew point as 63, the value at the middle of the assumed rain season. The true representative maximum dew point should therefore

lie between 63 and 69. Referring again to Figure 24, it can be seen that in the winter the three curves merge into one. In this region the maximum dew point values may be said to be 100% representative. The dew point value at the highest point of concurrence is 65. It is reasonable, therefore, to choose 65 F as the maximum possible representative dew point. It so happens that 65 was the maximum San Francisco dew point in the December 1937 storm, although the San Francisco dew points in that situation were not quite as representative as the reduced dew points at Donner Summit, which were somewhat lower. However, it may be assumed that in the maximum possible storm the San Francisco values would be representative of the inflow layer.

142. It is necessary also to consider the possible duration of maximum dew points. Meteorologically, it is not reasonable to assume that a dew point of 65 F could persist for 72 hours in a Sacramento storm. As a measure of dew point persistence on a scale 0 to 1, the ratio of the average 72-hour value of f to the maximum f was computed for the major storms. Figure 25 shows, as might be expected, that the relationship is

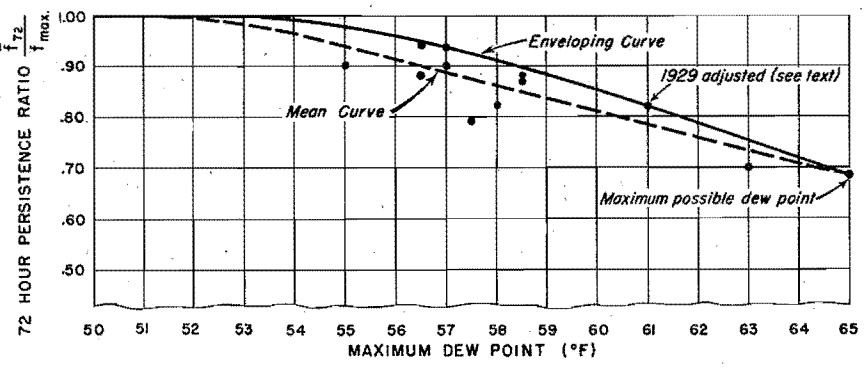

Figure 25

72-hour persistence of dew points during storm periods

an inverse one. In other words, it is generally true that the higher the maximum dew point the shorter its duration. In the case of the December 1929 storm the persistence ratio was originally .89 but, since this value included a period of high dew points when there was no rain (see Chapter V), it was not properly applicable to the storm period. This fact was allowed for by excluding 8 hours of duration, and the adjusted value was found to be .82, which lies on the enveloping curve. Duration curves of maximum average values of moisture index (f) were constructed for all the major storms. From these curves and from Figure 25, the curves on Figure 26 were drawn. The average values of moisture index for the various durations of the maximum possible storm are shown in the following table:

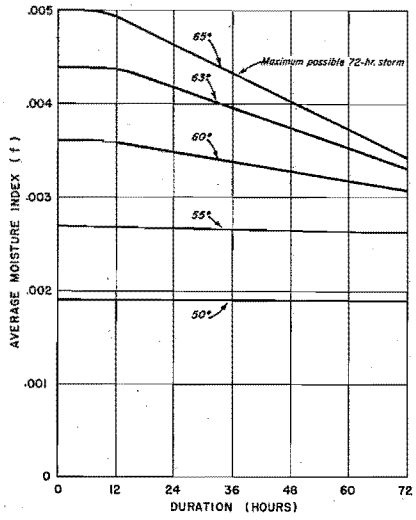

Figure 26

Duration curves of average moisture index for various maximum dew points

TABLE 45

AVERAGE MOISTURE INDEX FOR VARIOUS DURATIONS IN THE MAXIMUM POSSIBLE STORM

Duration (hours)	f x 10^4
12	49.5
24	46.6
36	43.5
48	40.4
72	34.2

143. Maximum Wind. Figure 27 shows the mean southwest wind at Oakland for the winter season, December to March, for the period of record

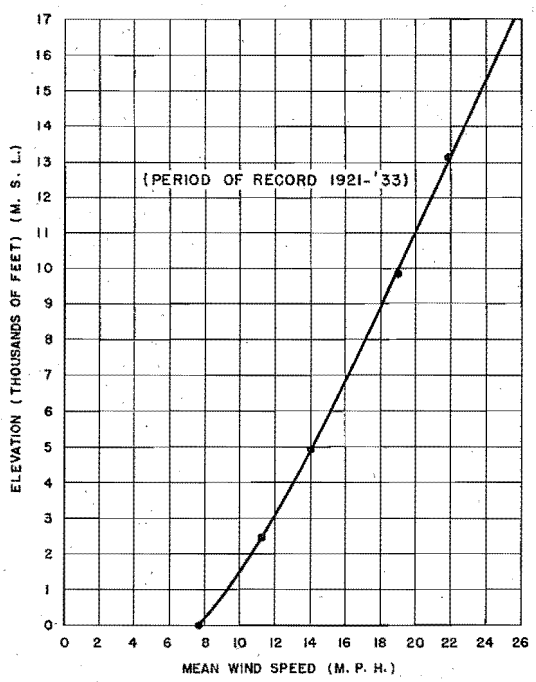

Figure 27

Mean southwest wind, December-March season, Oakland, California

1921-33. It will be noted that, except for the surface layer, the assumption of a linear velocity variation with height is valid. Assuming geostrophic flow as a first approximation, the wind velocity may be expressed as follows:

$$V = \frac{G}{F\rho}$$

where V is the geostrophic wind velocity, G the pressure gradient, F the parameter due to the earth's rotation -- constant for any given latitude, ρ the density of the air. The ratio of the velocity at five kilometers to the velocity at one kilometer is:

$$\frac{V_5}{V_1} = \frac{\rho_1 G_5}{\rho_5 G_1}$$

the subscripts referring to the levels. Since the density from one to five kilometers decreases by one third over a considerable range of conditions, the ratio $\frac{\rho_1}{\rho_5}$ may here be used as a constant with the value 3/2. For the assumption that the pressure gradient does not vary with height, $\frac{G_5}{G_1}$ will equal unity and $\frac{V_5}{V_1} = 3/2$ or 1.5. Summarizing three possible values of $\frac{V_5}{V_1}$:

	V_5/V_1
Pressure gradient constant with height	1.50
Velocity distribution assumed by Bjerknes (12)	1.82
Mean southwest wind (Figure 27)	2.08

Since $\frac{V_5}{V_1} = \frac{3}{2}\frac{G_5}{G_1}$ or $\frac{G_5}{G_1} = \frac{2}{3}\frac{V_5}{V_1}$

it is evident that the second case implies an increase in pressure gradient with height of 21% and the third case an increase of 39%. To determine the conditions of maximum wind movement, then, it is necessary to consider the types of pressure distribution which will produce the strongest winds both surface and aloft.

144. The most critical wind direction is southwest; therefore, for maximum conditions, we must assume pressure decreasing to the northwestward off the California coast. This is possible with (1) a quasi-stationary front off the coast and an anticyclone northwest of the front (as in March 1928), i.e., warm air in the low pressure and cold air in the high pressure; or (2) pressure decreasing continuously to a deep Low over the ocean (as in December 1937), i.e., cold air in the low pressure and warm air in the high pressure.

145. From the hydrostatic equation and equation of state we can conclude, as a first approximation, that

$$(p_0 - p_z)_c = K_1\rho_c = K_2\left(\frac{p_c}{T_c}\right)$$

$$(p_0 - p_z)_w = K_1\rho_w = K_2\left(\frac{p_w}{T_w}\right)$$

where p, ρ, and T are the pressure, density and temperature respectively, the subscript 0 refers to the surface and z to a fixed upper level a short distance above the surface, and c and w refer to cold and warm air; K_1 and K_2 are positive constants. In the first case (warm air in low pressure and cold air in high pressure -- curve ABC, Figure 28)

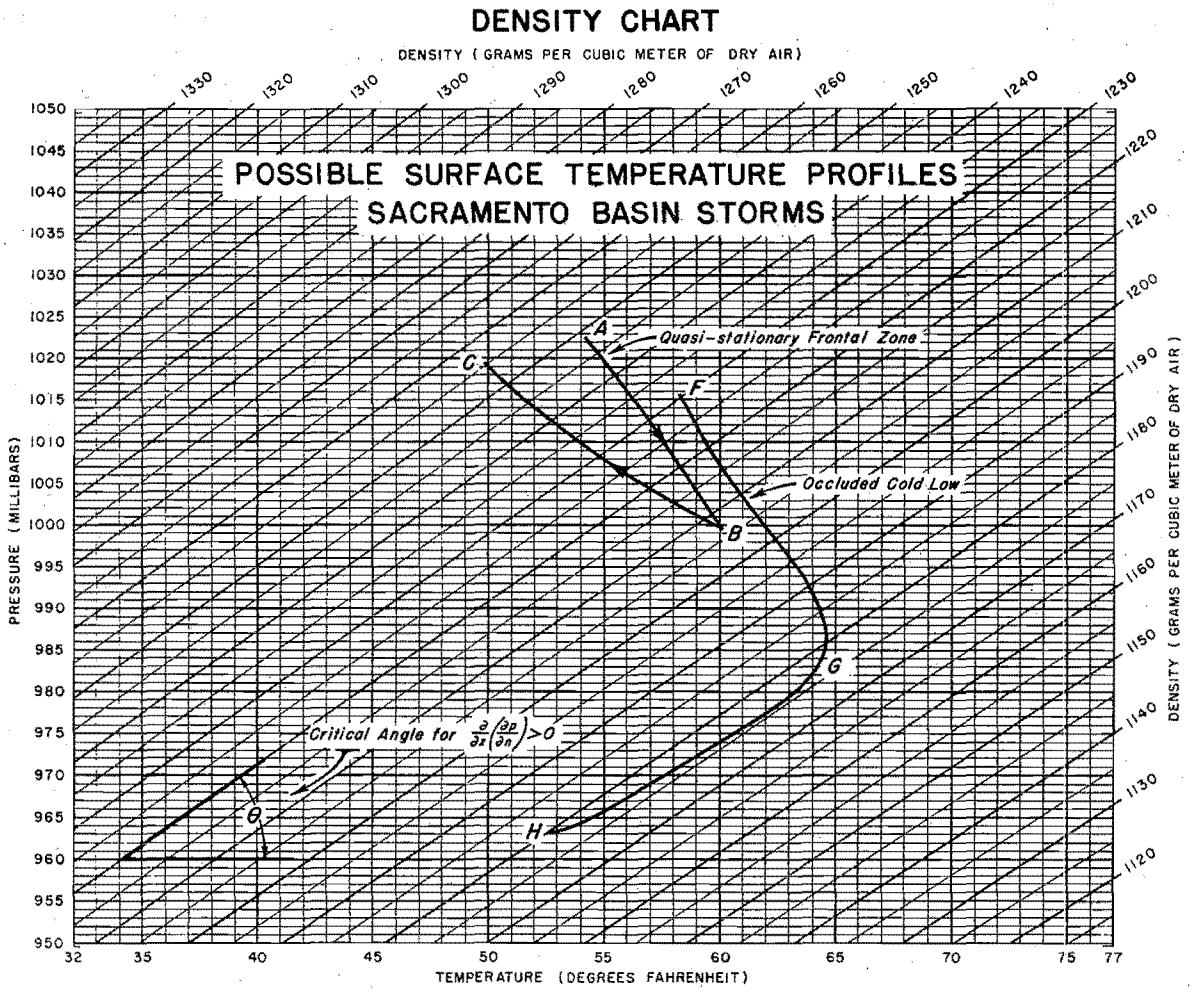

Figure 28

$$(p_c - p_w)_z - (p_c - p_w)_0 = K_2\left(\frac{p_w}{T_w} - \frac{p_c}{T_c}\right)$$

For the pressure gradient to increase with height, the expression $(p_c - p_w)_z$ must be greater than $(p_c - p_w)_0$ and therefore the equation must be positive. However, since p_w the pressure in the warm air is lower than p_c, p_w/T_w is always less than p_c/T_c, which means that the right side of the equation is always negative. It is therefore impossible for the pressure gradient to increase with height in this case. In the second case, with a deep Low over the ocean such as occurred in the

December 1937 storm (cold air in low pressure and warm air in high pressure — curve FGH, Figure 28)

$$(p_w - p_c)_z - (p_w - p_c)_0 = K_2\left(\frac{p_c}{T_c} - \frac{p_w}{T_w}\right)$$

Here, also, the equation must be positive, i.e., p_c/T_c must be greater than p_w/T_w for the pressure gradient to increase with height. However, the steep gradients necessary for strong winds require that p_w (the higher pressure being in the warmer air) be considerably greater than p_c per unit distance. The denominators T_w and T_c must therefore also differ considerably in the same sense for $p_c/T_c - p_w/T_w$ to be positive. In other words, an extreme temperature gradient must exist to cause the pressure gradient aloft to exceed the pressure gradient at the surface.

146. In Figure 28 the angle θ represents the limiting conditions for an increase of pressure gradient with a small change in height. The curve FGH illustrates a possible surface temperature-pressure profile. A critical examination will show that the indicated conditions are as extreme as can be assumed. In order to have the colder air with lower pressure it is necessary to have an occluding cyclone, which means that the cold air and warm air will both be flowing northeastward. Under such circumstances sharp temperature gradients are not observed even over continental United States; while over the Pacific, due to the tempering effect of the ocean surface, steep temperature gradients are not possible. In the segment GH the maximum temperature difference per 10 mb is slightly in excess of 5 degrees. Figure 29 shows that such a condition could produce a 90% increase in pressure gradient in 10,000 feet if the lapse rate in the cold air were dry adiabatic, and a constant pressure gradient

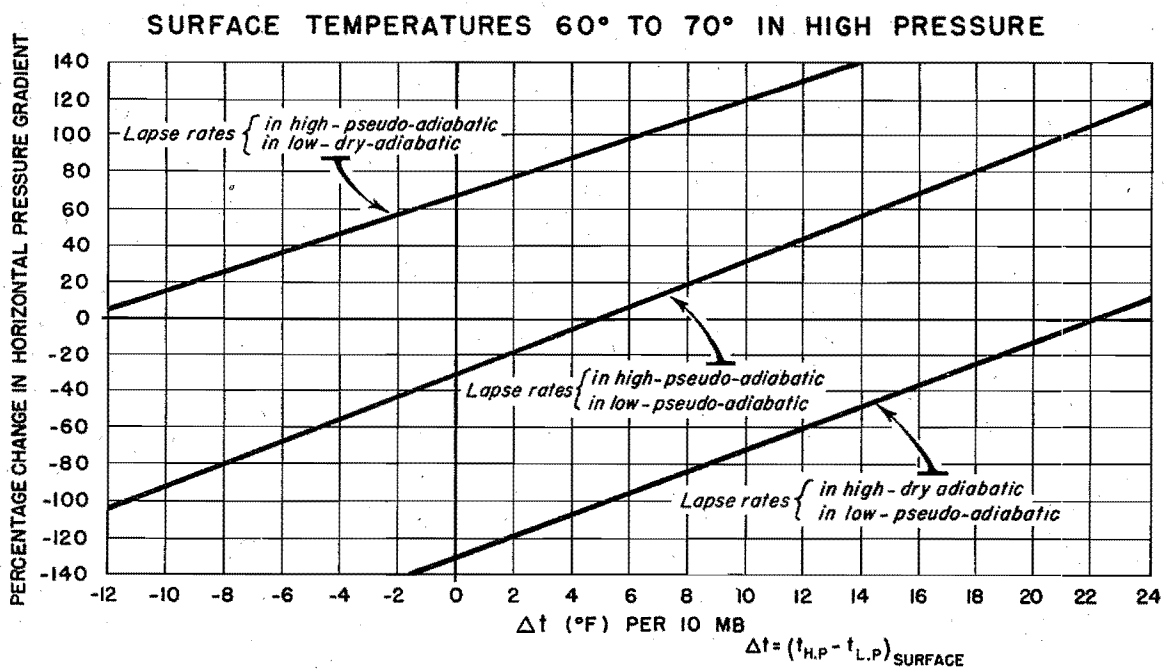

Figure 29

Effect of surface temperature difference on vertical change in pressure gradient in a 10,000 ft. layer

with height for a pseudo-adiabatic lapse rate in the cold air. Since the cold air is assumed to be over the Pacific, it is difficult to postulate a lapse rate steeper than the pseudo-adiabatic in the first 10,000 feet above the surface.

147. The conclusion is that the maximum southwesterly inflow into the Sacramento Basin will occur with a deep occluding Low off the Pacific Coast. The pressure gradient required to produce maximum winds will be so steep that no temperature gradient can exist sufficiently steep to cause the pressure gradient to increase with height in the inflow layer. A constant pressure gradient with height seems to be the limiting assumption.

148. For the maximum possible storm it was assumed that there would

be a convergent cyclonic flow with a radius of curvature of 1200 kilometers at the surface, becoming straight geostrophic flow at 10,000 feet. Assuming pressure gradient constant and density decreasing with height, neglecting surface friction and adjusting for curvature, it was found that the velocity-height curve was practically linear and could be expressed by the equation

$$v = v_o (1 + .06z)$$

where v_o is the frictionless velocity at sea level and z is height in thousands of feet. The density and curvature values are shown below:

	$\rho(gm/m^3)$	:	r(km)
Sea level	1,200	:	1,200
4,000 ft.	1,020	:	2,000
10,000 ft.	880	:	∞
$\frac{\partial p}{\partial x}$	Constant		

149. The strongest southwest wind velocity of record below 5 kilometers in the southwestern United States is 150 mph at Reno, Nevada. This occurred at an elevation of 13,000 feet on June 3, 1939. Adjusting this velocity to the 4000-foot level by the formula

$$v = v_o (1 + .06z)$$

the velocity at 4,000 feet would equal 90 mph. The maximum observed southwest velocity at Point Reyes is 82 mph on March 1, 1902. The maximum observed from any direction at Point Reyes is 91 mph from the northwest on May 30, 1895. Further evidence will be given in a later paragraph that Point Reyes is representative of the 4,000-foot level in the free air. On that basis, adjustment of 91 mph to sea level produces a velocity

of 73 mph, neglecting friction. Under extreme circumstances the observed surface wind may attain approximately 80% of the geostrophic value. Multiplying 73 mph by 80% to correct for friction, the observed maximum surface wind would be 58 mph. The maximum observed 5-minute velocity at San Francisco is 50 mph. There is little security however in attempting to establish values for longer durations by use of observed 5-minute maximum velocities. It was therefore decided to use the wind records at Point Reyes, one of the best exposed points on the Pacific Coast.

150. Figure 30 shows the average wind speed at Point Reyes for May 16-19, 1902. This period includes the greatest wind movement ever observed at Point Reyes. It has already been indicated that the velocity at Point Reyes corresponds to the 4,000-foot free-air velocity in spite of the fact that Point Reyes is only 490 feet high. An examination of a

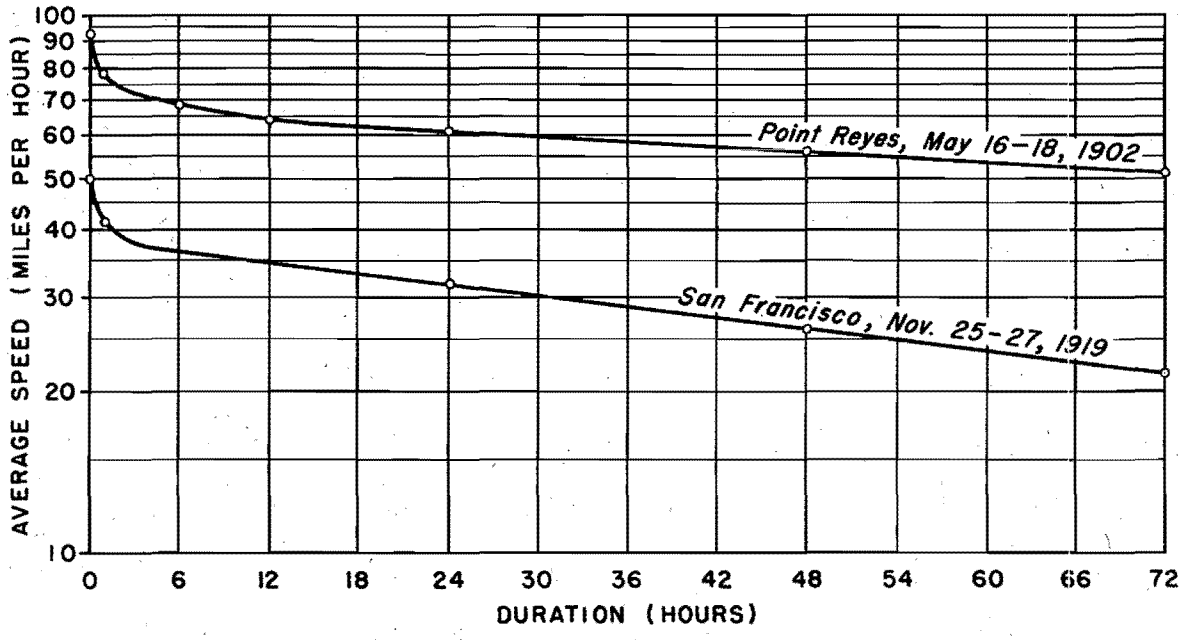

Figure 30

Maximum average wind speed

topographic chart of this station (Figure 31) bears out the hypothesis that a westerly wind is greatly accelerated. The wind-aloft records at Oakland were compared in detail with the anemometer records at Point Reyes, and the conclusion was reached that, under conditions of increasing velocity with height, the hourly wind movement at Point Reyes is actually representative of the 4,000-foot level in the free air. A great many examples could be cited. The following is an illustration:

February 23, 1937, 2 p.m.	
Oakland	Miles per hour
Surface	7
1640 ft.	7
2460 ft.	9
3280 ft.	22
	Point Reyes 26 miles per hour
4920 ft.	36

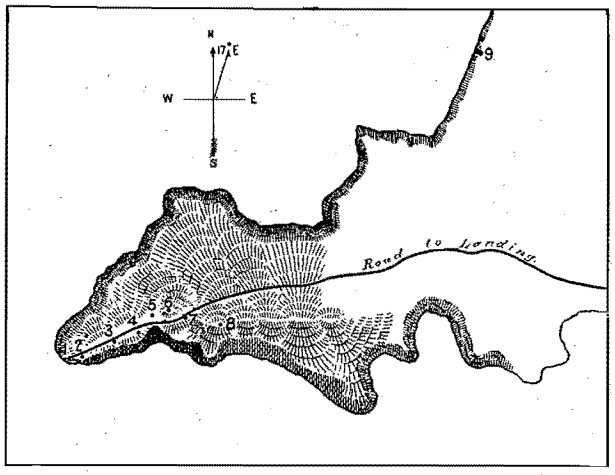

Plan of Point Reyes Peninsula, according to a survey made in 1880 by United States Engineer Corps. 1. Fog signal station; elevation 100 feet. 2. Light-house tower; elevation 250 feet. 3. Steps and chute leading to the light-house and signal stations. 4. Tank; elevation 460 feet. Anemometer on the tank; elevation 490 feet. 5. Weather Bureau building; elevation 490 feet. 6. Location of the new storm-warning tower; the ground at the tower is 540 feet; the peak is 550 feet high; the anemometer on the tower is about 593 feet above sea level. 7. Residences of the keepers. 8. Highest point of the ridge; elevation 597 feet. 9. Life-saving station.

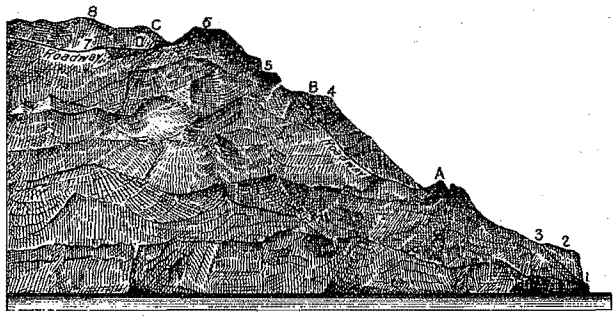

Contour of Point Reyes, as seen from the northwest. 1. Fog signal; elevation 100 feet. 2. Light-house tower; elevation 250 feet. 3. Steps and chute leading to the light-house and signal stations. 4. Water tank; elevation 460 feet. 5. Weather Bureau building; elevation 490 feet. 6. Storm-warning tower; elevation of ground 540 feet. 7. Dwelling of light-house keeper. 8. Highest point of the ridge; elevation 597 feet. A. Point from which photograph C, or fig. 3, was taken. B. Point from which photograph A, or fig. 5, was taken. C. Point from which photograph B, or fig. 6, was taken. D. Former exposure of the anemometer.

Figure 31

Topography of Point Reyes
Extract from Monthly Weather
Review, February, 1903

There is good qualitative evidence that northwest winds are persistently

stronger than southwest winds at Point Reyes. However, the major portion of the Point Reyes wind record is for velocity only and velocity-direction data are too limited and difficult to organize to make a statistical determination of the ratio.

151. It is necessary, next, to compare the synoptic situation which produced the maximum wind movement of record with the synoptic pattern proposed for the maximum possible storm. The strong winds at Point Reyes during May 16-19, 1902 were caused by an intense anticyclone over the Pacific Ocean, with cyclonic conditions inland. The isobars over the ocean showed appreciable anticyclonic curvature but on the average they were approximately straight in the vicinity of Point Reyes. During the maximum possible storm, it has been assumed, the winds at 4,000 ft. will have a cyclonic radius of curvature of 2,000 kilometers. Over the range of velocities considered for the maximum storm such a curvature would reduce the wind to 87% of the geostrophic or straight-isobar value. It was therefore decided to take 87% of the observed maximum northwest straight flow as being representative of the maximum possible cyclonic southwest flow. This leaves two factors of opposite sign unevaluated. The first is that isobaric gradients are generally steeper in cyclones than in anticyclones. During May 16-19, 1902, however, Point Reyes was situated east of the anticyclone and west of the cyclone, and pressure gradients west and northwest of the cyclone are generally steeper than on the eastern side. The second factor is the relative magnitude of the acceleration of northwest and southwest winds at Point Reyes. The maximum observed southwest velocity of 82 mph at Point Reyes is 90% of the observed maximum 5-minute northwest wind of 91 mph. As mentioned

earlier, 5-minute values such as these are not too reliable criteria but at least the order of magnitude is in substantial agreement with the assumed 87% ratio of southwest to northwest winds. To carry the comparison still further, the corrected Point Reyes winds were adjusted to sea level and then reduced 20% as a correction for surface friction. The results, compared to observed maximum winds at San Francisco, follow:

	Mean for			
	12 hrs.	24 hrs.	48 hrs.	72 hrs.
Adjusted Point Reyes	35	32	30	27
Observed San Francisco	34	31	26	22

The following table contains the assumed maximum average wind speeds for various durations at the 4,000-foot level:

TABLE 46

SPEED-DURATION IN THE MAXIMUM STORM

Duration	Average Speed, mph
6 hrs.	61
12 hrs.	58
18 hrs.	55
24 hrs.	53
30 hrs.	52
36 hrs.	51
42 hrs.	50
48 hrs.	49
54 hrs.	48
60 hrs.	47
66 hrs.	46
72 hrs.	45

152. The Maximum Possible Precipitation. With maximum values of v and f determined, it is a simple arithmetical operation to derive the maximum depth-duration values. Table 47 shows the computations for

the various durations of the 72-hour maximum storm in the Sacramento Basin:

TABLE 47

DURATION-DEPTH COMPUTATIONS FOR THE MAXIMUM 72-HOUR STORM

t	v	$f \times 10^4$	R
12	57.8	49.5	3.4
24	52.8	46.6	5.9
36	50.7	43.5	7.9
48	48.7	40.4	9.5
72	44.8	34.2	11.0

t = duration in hours
v = average wind movement, mph
f = moisture index
R = average depth in inches = t X v X f

The values in column R are the maximum possible depths for durations up to and including 72 hours. It may well be that for a storm of greater duration the total depth could exceed 11.0 inches, in which case, however, the average intensities for durations up to 72 hours would probably be less than the values in the above table.

153. The maximum possible precipitation here computed need not be increased by any reliability factor. Four elements entered into the computation. The basin constant was tested in nine major storms and found to require no correction coefficient. The maximum reduced dew point could conceivably be higher but this effect would tend to be cancelled by the consequent decrease in persistence. Since southwest flow was found to be most critical and a continuous southwest direction was assumed for the storm period, no adjustment to higher values was possible in that respect. The maximum wind speed was obtained by reducing the maximum observed northwest wind at Point Reyes by 13% for cycloric curvature.

Any further modification for difference in persistence would tend to reduce the wind speed in the maximum storm. No such modification was made. Since this effect would more than counterbalance any other influences acting to increase the precipitation, the computed values of maximum possible precipitation can be said to contain an adequate reliability factor.

154. The December 1937 storm is a meteorological model of the maximum 72-hour storm. The following adjustments of the 1937 storm would produce the maximum possible storm:

Dew point adjustment	13% increase
Wind adjustment	14.5% increase
Combined adjustment	29.4% increase

155. At this point certain questions may arise which are pertinent to the fundamental theory of the maximum possible storm. If a basin of the same size, shape and location, but with none of the orographic features of the Sacramento Basin, were assumed to exist, what would be its maximum possible 72-hour storm? It would be greater than for the real basin. The purely meteorological factors would be the same but the orographic barrier would be gone. This conclusion seems to be a contradiction of the well-founded notion that the orographic effect is to increase rainfall. The contradiction, however, is not real. In computing the maximum possible storm we have already gone beyond the pure orographic effect. In fact, the maximum efficiency in rain production has been assumed. The necessary mechanism is either a feature of the atmospheric circulation or of the basin. As part of the circulation it can occur over the hypothetical basin by chance; but in the real basin it is an

invariant and ever-present property. The important point is that even though the maximum possible storms are of nearly the same magnitude, the orographic effect will be to increase the frequency of near-maximum storms.

156. Recapitulation of Symbols. For reference purposes the more important symbols used in this chapter are listed below:

A Area of basin (square miles)

D_r Reduced dew point (^oF)

f Moisture index (inches/mile) = KW_E where K applies to Assumption III

H Effective height (ft.)

K Geometric or basin constant ($miles^{-1}$)

L Lift coefficient ($\frac{W_{E_H}}{W_E}$)

M Amount of moisture which can be precipitated out of each unit column (inches)

p Pressure (mb)

q Specific humidity (gm/kg)

R Average depth of precipitation over area (inches)

ρ Density of air (gm/m^3)

T Temperature (^oA)

t Time (hours)

v Wind velocity (miles per hour)

W_E Effective precipitable water (inches)

W_p Precipitable water (inches)

x,y,z Space coordinates (x, y in miles, z in feet)

CHAPTER VII

SNOW MELT

157. Melt Factors. The thermodynamics of snow melt has been discussed in detail in previous reports (1, 2) and in Technical Paper No. 1 (50). Briefly stated, the major factors producing rapid snow melt are considered to be turbulent transfer of heat and moisture between the air and snow surface. An approximate formula, relating the rate of melt over a drainage area to observations of wind velocity, temperature and humidity at standard levels above the surface, is:

$$D = KU\left[.00184(T-32)\ \ 10^{-.0000156h} + .00578\ (e-6.11)\right]$$

where D is melt in inches of water per 6-hour period

U is wind velocity in miles per hour at the 50-foot level

T is temperature in degrees Fahrenheit at the 10-foot level

e is vapor pressure in millibars at the 10-foot level

h is elevation in feet above mean sea level

and K is a regional or basin constant.

The value of K reflects the surface characteristics of the basin or region and is assumed to remain constant for all ranges of wind velocity, temperature, humidity and elevation. Its value is unity when the formula is applied to determine melt over a smooth exposed snow surface. The

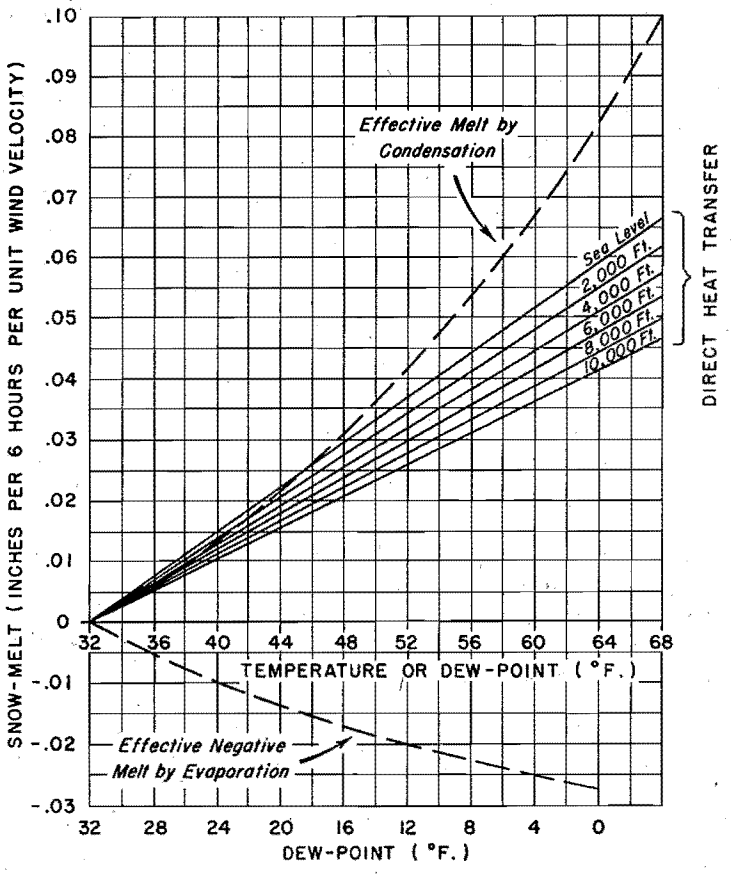

Figure 32

Theoretical rates of snow melt due to atmospheric turbulence

results of such a determination are presented in the form of a graph in Figure 32. Two separate sets of curves are shown; one gives values of equivalent melt (per wind velocity of one mile per hour) caused by sensible heat transfer at various elevations as a function of dry-bulb temperature; the other set, labeled "effective melt by evaporation or condensation," gives the additional gain or loss of melt (per unit wind velocity) as a function of dew point.

158. In the Sacramento study consideration should be given to two distinguishing features of the basin: rugged topography and forest cover. Melting rates decrease with increase of elevation because of the decrease in the air density with height, and also because of the normal decrease of temperature and dew point with height. As melting progresses, the snow line recedes to higher elevations and the percentage of snow-covered area, over which the melting rates are effective, decreases.

Melting proceeds at a rapid rate near the snow line and decreases to zero at some limiting elevation. If a sufficient depth of snow exists below the zero level of melting effect, melt water may be stored in the snow blanket. Therefore, another factor tending to regulate areal melting rates in the region is the normal increase of snow depth with elevation which may confine the runoff contribution from melt to the lower elevation zones above the snow line. During abnormal conditions, however, some melt may occur at all elevations in the basin when shallow depths of snow fail to hold back rapid contribution of melt water and rainfall to runoff.

159. Most of the region above an altitude of 2,500 feet is densely forested. The major portion of snow melt contribution occurs in that area but the application of the melting formula to melt underneath dense forest stands is questionable because of the reduction of wind velocity inside the forest. However, since the diffusion of heat is also greatly reduced in the forest interior by virtue of the protective covering of foliage, branches, etc., most of the melting that does occur within a forested area must occur in the numerous openings, parks, and other cleared spaces where the heat exchange would be governed by the turbulence regime, and where melting would be proportional to the melt over a fully exposed area. The assumption implied in the use of a basin constant is that a constant ratio exists between melts in various portions of the basin area during periods of warm moist winds. Thus, although the portion of the basin area occupied by dense clumps of trees is essentially noncontributing during such periods, the use of a single basin constant and the melting formula is still adequate as a tool for extrapolating

melting rates from moderate wind velocities to the strong winds characteristic of the maximum storm.

160. Determination of Constant. The basin constant is determined by correlation of snow melt values obtained by analysis of runoff records from past periods of rapid melt with corresponding values computed from meteorological observations. In the Sacramento Basin it is probable that the most rapid melting has occurred during storm periods in the winter season. Unusually high temperatures and dew points have occurred during a number of storms of record and produced rapid depletion of the existing snow cover. However, the analysis of such situations is fruitless because of the difficulty of separating snow melt from rainfall through the use of stream-flow records. Another complicating factor is the fluctuation of the 32° isotherm with elevation during the progress of a storm. This signifies that at certain elevations the precipitation may alternate between snowfall and rainfall and the contribution to runoff from various elevation zones may be extremely complex.

161. During the late spring or early summer, meteorological situations may occur when warm moist air flows in at moderate velocity to produce fairly high rates of melt at intermediate and upper elevations in the basin with little or no accompanying rainfall. Flooding of upstream tributaries may take place at such times and discharge records may furnish a convenient source of data for estimating the total volume and time distribution of melt. However, calculations of theoretical melt for such periods offer greater difficulty because radiation usually exerts a significant influence and has to be evaluated from limited data.

162. The following table lists ten snow melt floods of this type

for the Feather, Yuba and American Basins, arranged in descending order of magnitude of flood peaks:

TABLE 48

SNOW-MELT FLOODS -- FEATHER, YUBA AND AMERICAN BASINS

Basin	Date of Flood Peak	Runoff in Inches Max. Day
American River at Fair Oaks	May 15, 1938	.52
	June 12, 1911	.49
	June 1, 1922	.41
	April 21, 1938	.37
	June 1, 1938	.34
	May 6, 1916	.33
	May 16, 1927	.33
	May 1, 1919	.31
	May 14, 1937	.31
	May 10, 1923	.29
Yuba River at Smartville	May 15, 1938	.64
	June 2, 1922	.54
	April 14, 1904	.48
	May 6, 1916	.47
	May 14, 1904	.46
	June 5, 1911	.45
	May 14, 1917	.45
	May 15, 1927	.44
	June 11, 1911	.42
	April 21, 1938	.39
Feather River at Oroville	April 14, 1904	.41
	May 15, 1938	.37
	April 27, 1922	.26
	March 19, 1914	.26
	May 13, 1904	.25
	June 3, 1911	.23
	May 31, 1922	.22
	May 9, 1917	.21
	May 5, 1914	.21
	June 1, 1938	.20

163. From the above list, the May 1938 flood in the Yuba Basin was selected for detailed study because of the large volume and peak rate of snow melt runoff during a single rise of the hydrograph, absence of rainfall as a contributing factor to runoff, and relative sufficiency of

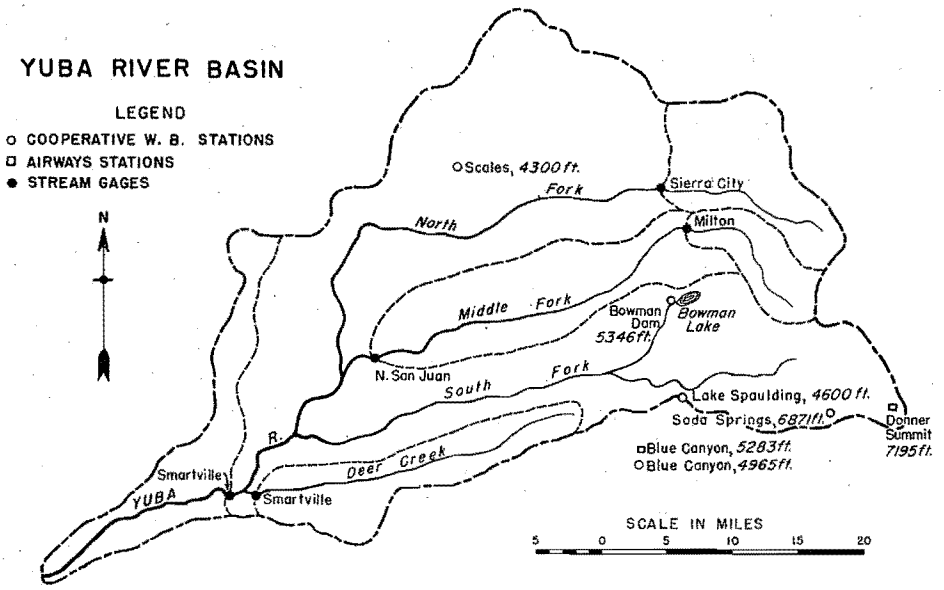

Figure 33

basic data. The locations of observation stations in the vicinity of the basin are shown in Figure 33, and the data are summarized below:

TABLE 49

SOURCES OF DATA - YUBA BASIN - MAY 1938

Runoff Data

Basin	Area	Type of Data
Middle Fork of Yuba at Milton	41	Continuous Hydrograph
North Fork of Yuba at Sierra City	91	Mean Daily Discharge
Middle Fork of Yuba near N. San Juan	207	" " "

Meteorological Data

Station	Elevation, Feet	Type of Data
Donner Summit (Airways)	7195	Hourly temperatures, dew points, wind velocities, cloudiness, and 6-hourly snow depth measurements
Blue Canyon (Airways)	5283	Same as above
Soda Springs	6871	Daily precipitation and snow depth
Bowman Dam	5346	" " " " "
Blue Canyon	4965	" " " " "
Lake Spaulding	4600	" " " " "
Scales	4300	" " " " "

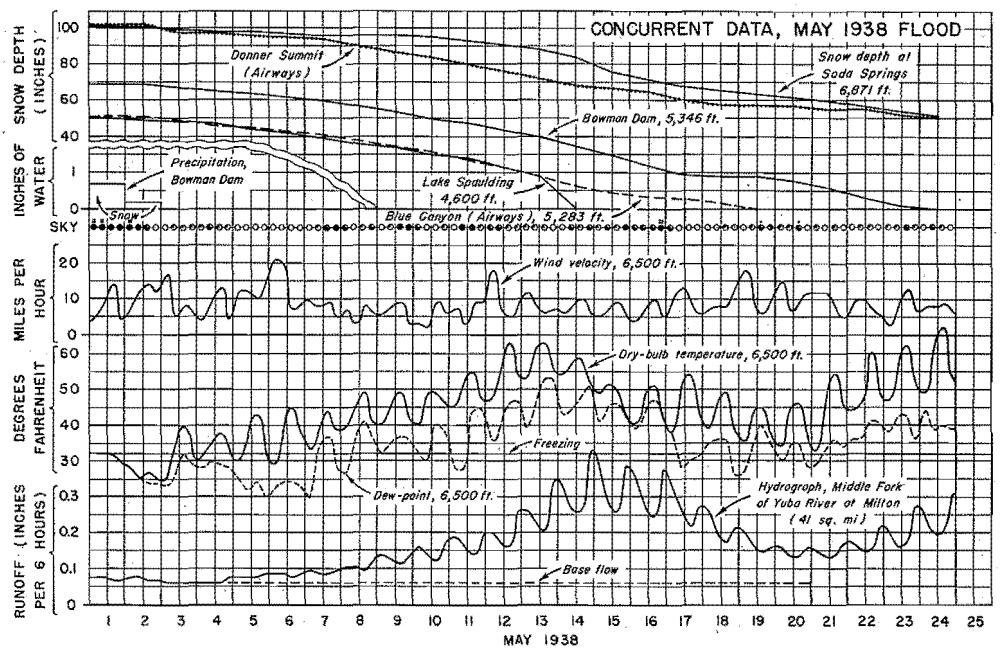

Figure 34

Concurrent meteorological and precipitation observations pertinent to the analysis are plotted in Figure 34, for the period of study May 1-24, together with the hydrograph of discharge for the entire Middle Fork of the Yuba based on the combined records of the Milton gaging station and the diversion through the Milton-Bowman tunnel. The curves for wind, temperature, dew point and runoff are based on 6-hourly observations. The analysis of the data shown in the figure is composed of two sections: computations of the theoretical point melting effect from meteorological observations and determination of over-all basin melt from discharge records.

164. The computations of theoretical melt were based on the assumption of a horizontal smooth exposed snow surface. Melt due to atmospheric turbulence had to be determined separately from melt caused by radiation. In computing the effect of heat transfer from the air by turbulence, the

graph of Figure 32 was applied to observations of temperature, dew point and wind velocity at Blue Canyon Airways Station. Observations at Donner Summit were not considered representative for the region because the station is located in a narrow pass that tends to restrict the air flow to an east-west direction. The net melting effect of incoming and outgoing radiation was estimated from observations of cloudiness and dew point. A graphical procedure developed by Wilson (110) was employed, using a modified albedo for melting snow of 60%. Adjustments of melt for percentage of area covered with snow were made according to the procedure shown in Figure 35. It was assumed that, on the date the snow disappears at a particular station, the station elevation represents the mean elevation of the snow line. Accordingly, the percentages of snow-covered area were read off the area-elevation curves from available dates of snow disappearance and then plotted against time to determine the snow-cover area-time curves. The daily increments of computed melt were next multiplied by

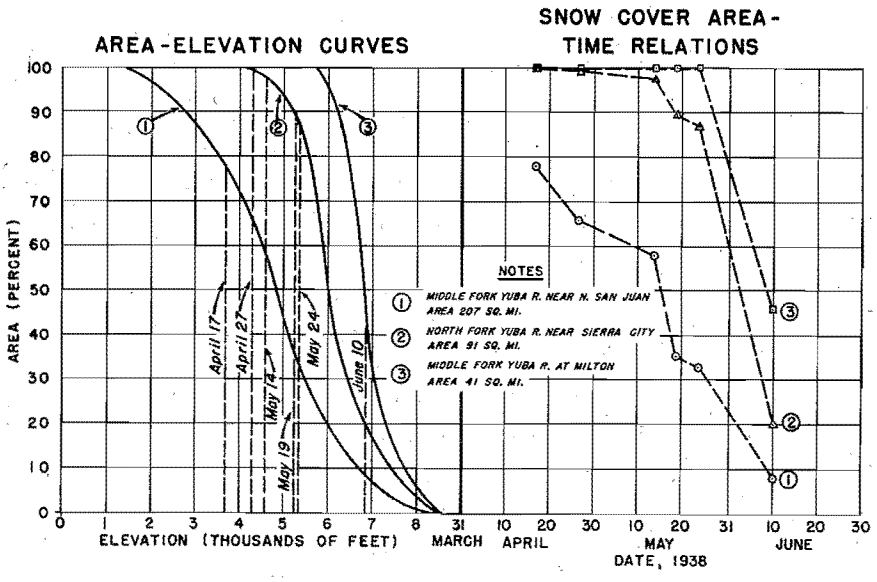

Figure 35

the appropriate area factors to obtain average depths of melt for each successive time interval.

165. The hydrographs for the three sub-basins listed in the data summary (Table 49) were analyzed in detail to determine the approximate volume and distribution of melt for the period May 4-19, inclusive. Sub-freezing weather occurred prior to May 4 and it was assumed that discharge on that date was entirely base flow, the excessive value of the flow indicating near-saturated soil. A value of ground water recharge was estimated from uniform base flow and added to direct runoff to give the entire volume of snow-melt runoff during the period. The time distribution of melt was obtained by correcting the increments of direct runoff for channel storage by the Langbein (48) method involving the use of a storage-discharge curve for the basin. This was developed from the recession hydrograph of the December 1937 flood. The values of channel inflow thus obtained were increased by the ratio of total runoff to direct runoff and accumulated. These accumulated values were plotted against corresponding accumulated values of computed melt in the form of double mass curves shown in Figure 36.

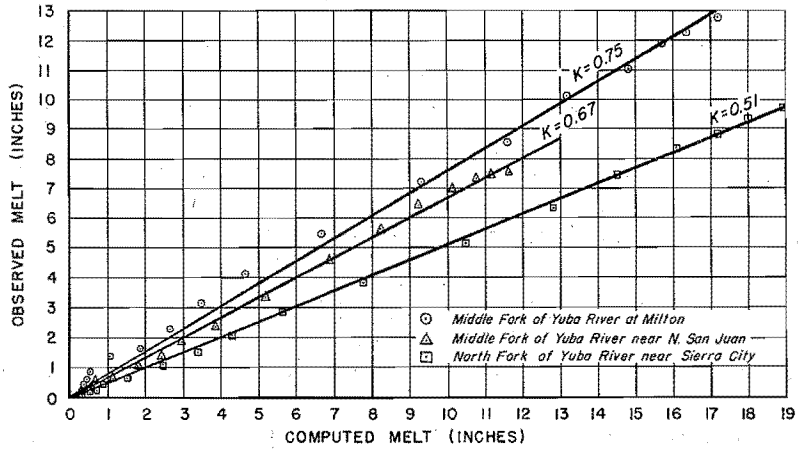

Figure 36

Double mass curve of computed and observed melt, May 1938 flood

166. The following table summarizes the results of runoff and meteorological analysis:

TABLE 50

THEORETICAL AND OBSERVED SNOW MELT

YUBA BASIN — MAY 1938

	Run-off	Turbulence Melt	Radiation Melt	Total Theoretical Melt	K
Middle Fork of Yuba at Milton	12.8	13.0	4.2	17.2	0.75
North Fork of Yuba near Sierra City	9.7	14.9	4.1	19.0	0.51
Middle Fork of Yuba near N.San Juan	7.6	9.2	2.4	11.6	0.67

The constant, K, in each case was obtained from the slopes of lines drawn through the plotted points in Figure 36. The empirical constant to be used for determinations of critical melt, then, has an average value of 0.6. Differences in the value of K can be ascribed to errors involved in runoff analysis and in the estimates of snow-covered area from the meager number of snow depth measurements. Another possibility is that these differences are real and represent variations in basin characteristics. However, in the absence of any detailed information on topography, forest cover, etc., for the three basins in question, it was decided to adopt an average value for the empirical constant and to apply this value throughout the Sacramento watershed.

167. Antecedent Snow Cover. Ordinarily, snow begins to accumulate in the mountains of the Sacramento Basin in the late autumn or early winter and reaches a maximum depth in April. The winter snow pack, within the limits of observation, is usually wedge-shaped in profile, with the snow line located at approximately 4,000 feet. The water equivalent of the normal April snow pack increases with elevation to an

average depth of about 50 inches at 7,000 feet. Above this elevation the observations are inadequate to establish a relation, if any, between seasonal snow accumulation and elevation. Speculation on this subject is rather pointless because only about 4% of the entire basin area is above 7,000 feet.

168. Usually most of the snow melts in the late spring, after the winter season has ended. Table 48 shows that peak rates of streamflow from melting snow alone have been only a fraction of the magnitude of those peaks which include runoff from rain. The great range in elevation and great variation in snow accumulation do not permit uniformly high melting rates to occur over more than a small portion of the Sacramento Basin. Ordinarily, by the time snow is contributing runoff from high elevations, the areas of low elevation have lost their snow.

169. Examination of snow records antecedent to the major flood occurrences reveal deficient amounts of snowfall and snow cover. This seems to support the view that the existence of a normal snow pack of high storage capacity precludes serious floods. The records also show that, except for glacier remnants and scattered patches of snow, the entire Sacramento Basin has been bare of snow at various times in the rainy period. An example of such a situation occurred on February 10, 1918, when the maximum recorded depth of snow on the ground at any of the 54 Weather Bureau stations reporting was 12 inches at Fordyce Dam where the normal accumulated snowfall by February 10 is about 200 inches.

170. Thus far, the discussion of snow has dealt with the ordinary or normal relationship of snow to floods in the Sacramento Basin. However, the conditions leading to a maximum possible storm are not

normal or ordinary. The maximum possible flood will result from a series of abnormal events which can reasonably be expected to occur. The various possibilities are discussed in detail in the final chapter of the report. One possibility is a series of rainstorms, immediately preceding the critical storm, that would saturate the soil and raise all the streams to bankful stage. This would preclude the existence of a snow cover in the valley and foothills of the basin. Since snow does not accumulate at low elevations because of melting between successive snowfalls, another possibility is a single heavy snowfall critically distributed over the basin prior to the maximum possible storm. Such a snowstorm would occur with little or no snow on the ground at upper elevations and produce abnormal snow depths at low elevations. In order to arrive at an optimum snow distribution, an investigation of snowfall and snow-depth records in the basin was made.

171. Critical snow situations are not identified with floods, as heavy rains are, because the snow may not melt at a rate such as to cause a flood commensurate with its potentialities. Therefore the entire period of record at all stations (Weather Bureau since 1893 and California Snow Surveys since their beginning in 1932) was studied. In examining the record it was observed that a snow storm in the valley floor seldom lasted longer than a few hours. The duration increased with elevation, the snowfall at high altitudes frequently lasting for several days. It was determined that a storm lasting 72 hours would be of sufficient duration for the most critical accumulation at elevations below 5,000 feet.

172. Attempts to draw isochion maps for the significant snow

storms were not satisfactory because of the paucity of stations. Depth-elevation curves were therefore plotted for the storm periods identified by the following dates on which the total accumulation during the storm was measured:

January 1, 1899	January 14, 1913
February 7, 1903	January 1, 1916
March 23, 1907	January 18, 1921
January 14, 1910	February 9, 1922
December 5, 1910	January 23, 1933
January 12, 1911	January 27, 1933

Figure 37 shows the elevation-depth curves of water equivalent of snowfall for the storms ending January 12, 1911 and March 23, 1907 in Zone HC_1, the Yuba Basin. Either of these storms could have occurred with negligible antecedent snow cover, followed immediately by a rainstorm. The record shows a number of instances of heavy snow followed by heavy

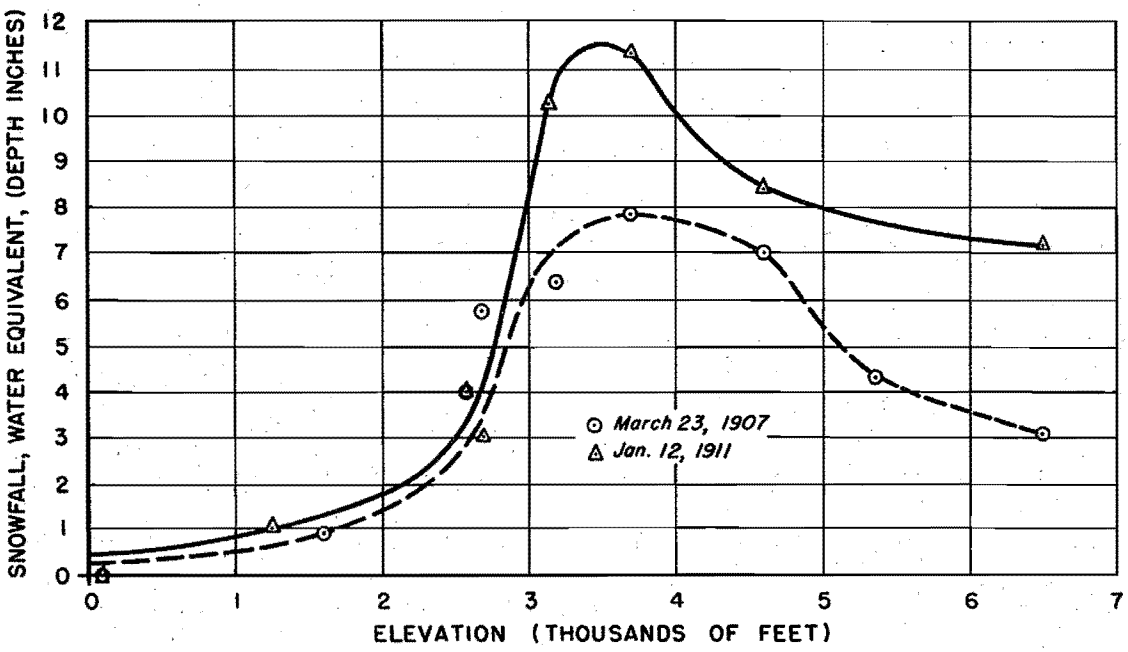

Figure 37

Snow depth-elevation relations, Yuba Basin

rain, as in January 1862 (see Chapter V). Similar studies were carried out for the remaining zones in the basin and the results are listed in the following table:

TABLE 51

DEPTH-ELEVATION RELATIONSHIPS FOR WATER EQUIVALENT OF MAXIMUM RECORD SNOWFALL IN THE SACRAMENTO BASIN

Elevation Thous.Ft.	Average Depth of Snow (Water Equivalent) on Ground							
	Zones AEK	Zone L	Zone P	Zone N	Zone B	Zone M	Zone J	Zones C_1C_2DFGH
0 - 1	2.2	.5	-	-	.5	1.1	-	0.5
1 - 2	4.0	-	-	4.0	-	2.0	-	1.0
2 - 3	3.5	-	.5	3.5	-	3.2	6.0	3.0
3 - 4	2.4	-	.8	2.4	-	6.2	8.0	10.0
4 - 5	2.0	-	1.5	2.0	-	5.2	5.0	8.5
5 - 6	1.4	-	2.1	1.4	-	3.7	5.0	6.0
6 - 7	1.0	-	2.0	1.0	-	3.0	5.0	5.0
7 - 8	-	-	2.0	-	-	2.5	5.0	5.0
8 - 9	-	-	2.0	-	-	2.5	5.0	5.0

(Dash signifies zero area within elevation interval)

The study indicated that a conservative upper limit of critical snow depth and distribution at low elevations has been approached a number of times. The values in the table represent the optimum quantities and distribution that can be assumed to exist on the basin prior to the maximum possible storm. Extrapolation of the critical snow storm to greater depths of snow would be unreasonable because a dew point high enough to produce greater precipitation amounts would cause rain instead of snow at low elevations and raise the elevation of the snow line; and, conversely, a lower dew point would produce less precipitation.

173. Critical Snow Melt. The block diagrams of wind velocity and dew point shown in Figure 38 are obtained from consideration of the

meteorological factors attending the maximum possible storm and represent an index to conditions in the surface layer of the atmosphere during that storm. The arrangement is symmetrical, the maximum wind coinciding with maximum dew point as in the December 1937 storm. This series of meteorological events, in conjunction with the critical snow-cover distribution of Table 51 assumed to exist on the basin prior to the influx of warm air, forms the basis for determination of snow melt contribution to the maximum possible flood. The elevation of Blue Canyon Airways Station, 5,283 feet, was selected as a reference level for wind velocity because the empirical snow melt constant was derived by means of observations at that station. Since Point Reyes is the index station for the wind velocities used in computing maximum possible precipitation, a study was made to determine the relation between wind at Blue Canyon and Point Reyes. This study showed that a fairly constant ratio of 0.64 exists between the wind velocities at the two stations for periods marked by strong winds. Hence the wind velocities used in Chapter VI were multiplied by 0.64 to obtain the values shown in Figure 38.

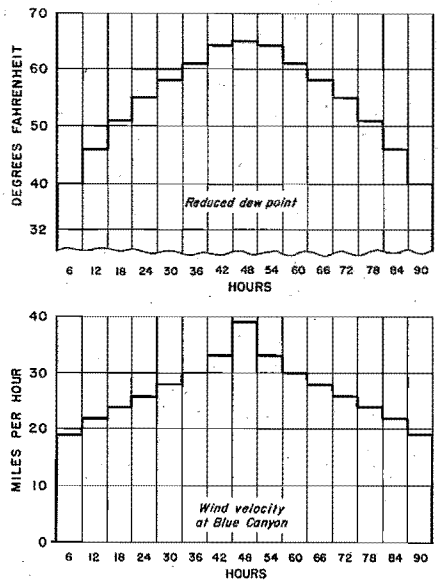

Figure 38

Assumed meteorological sequence for computation of maximum snow melt

174. Since the air mass is approximately homogeneous and saturated at all surface levels during the period of rainfall, dew point is an index both of temperature and vapor pressure for the entire area. The

variation of dew point with elevation, in this case, is governed by the pseudo-adiabatic lapse rate and, for a given wind intensity, the melting effect at any point in the basin can be related to reduced dew point. The question of surface wind velocity distribution over the area offers greater difficulty because of numerous factors affecting wind, such as elevation, aspect, degree of slope, and ground roughness. To simplify the problem, over-all melting rates within a given contour interval were assumed to be constant for all zones, and average melt within an entire zone therefore dependent only on the elevation characteristics of the zone.

175. The increase of geostrophic wind with height in the free air during the critical storm was shown in Chapter VI to be a straight-line function of height. It is an accepted fact that, for a given roughness of ground and anemometer height, surface wind is proportional to geostrophic wind during periods of moderate to strong winds. Therefore, for the purpose of computing critical snow melt, it was assumed that the ratio between surface winds at various elevations is equal to the ratio of geostrophic wind velocities at the same elevations. The graph of Figure 39 has been constructed on that basis and expresses wind velocity at a particular elevation as a percentage of the velocity at a reference level of 5,283 feet, the elevation of

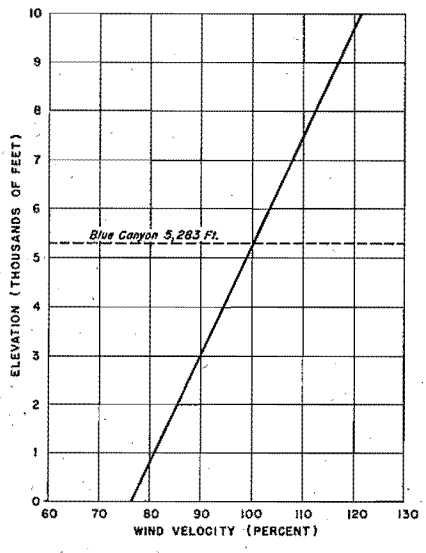

Figure 39

Percentage of Blue Canyon wind velocity vs. elevation

Blue Canyon Airways Station.

176. For convenience of computation of zonal melt, the wind-elevation and dew point-elevation relationships, together with the empirical constant previously derived, have been utilized in developing the graph of Figure 40.

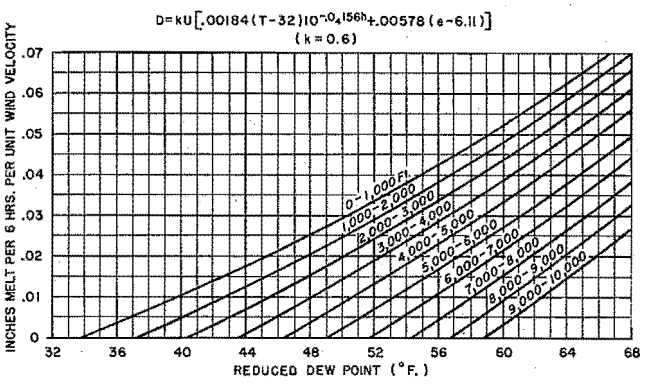

Figure 40

Snow melt due to saturated air per unit wind velocity at Blue Canyon for various elevation intervals

The curves relate values of snow melt during 6-hour periods to reduced dew point for thousand-foot contour intervals and for a unit wind velocity of one mile per hour at the reference station. The process of computation involves first the determination of values of potential melt, or melt that could occur if sufficient snow were available, for each elevation zone from zero to 10,000 feet, using the critical sequence of Figure 38 and the curves of Figure 40. These amounts are then applied to each zone in the following manner: Increments of melt are accumulated up to the maximum depth of snow for each contour interval. The values of accumulated melt are then weighted by the respective areas included within the intervals and totaled to obtain the average accumulated zonal melt. In order to illustrate the method of computation, Tables 52 to 55 are presented. The increments of potential melt per unit wind velocity, applicable to the entire region, are shown in Table 52. In Table 53 the same values are multiplied by the appropriate wind velocities of the meteorological sequence. In Table 54 Zone D is selected as an example.

TABLE 52

INCREMENTS OF POTENTIAL MELT PER UNIT WIND

Unit = Inches x 10^{-3}

Period Ending, Hrs.		6	12	18	24	30	36	42	48	54	60	66	72	78	84	90
Reduced Dewpoint (°F)		40	46	51	55	58	61	64	65	64	61	58	55	51	46	40
Elevation Interval (1000 ft.)	0—1	10	21	32	40	47	55	62	65	62	55	47	40	32	21	10
	1—2	5	16	27	36	43	51	58	61	58	51	43	36	27	16	5
	2—3	0	11	22	31	39	46	54	57	54	46	39	31	22	11	0
	3—4	0	5	17	26	34	41	49	52	49	41	34	26	17	5	0
	4—5	0	0	11	20	28	36	44	47	44	36	28	20	11	0	0
	5—6	0	0	5	14	22	30	38	41	38	30	22	14	5	0	0
	6—7	0	0	0	8	16	24	32	35	32	24	16	8	0	0	0
	7—8	0	0	0	2	10	18	26	29	26	18	10	2	0	0	0
	8—9	0	0	0	0	4	12	20	23	20	12	4	0	0	0	0
	9—10	0	0	0	0	0	6	14	18	14	6	0	0	0	0	0

TABLE 53

INCREMENTS OF POTENTIAL MELT ADJUSTED FOR WIND

Unit = Inches

Period Ending, Hrs.	6	12	18	24	30	36	42	48	54	60	66	72	78	84	90
Wind (mph) Velocity	19	22	24	26	28	30	33	39	33	30	28	26	24	22	19
Elevation Interval (1000 ft.) 0--1	.2	.5	.8	1.0	1.3	1.6	2.0	2.5	2.0	1.6	1.3	1.0	.8	.5	.2
1--2	.1	.4	.6	.9	1.2	1.5	1.9	2.4	1.9	1.5	1.2	.9	.6	.4	.1
2--3	0	.2	.5	.8	1.1	1.4	1.8	2.2	1.8	1.4	1.1	.8	.5	.2	0
3--4	0	.1	.4	.7	1.0	1.2	1.6	2.0	1.6	1.2	1.0	.7	.4	.1	0
4--5	0	0	.3	.5	.8	1.1	1.5	1.8	1.5	1.1	.8	.5	.3	0	0
5--6	0	0	.1	.4	.6	.9	1.3	1.6	1.3	.9	.6	.4	.1	0	0
6--7	0	0	0	.2	.4	.7	1.1	1.4	1.1	.7	.4	.2	0	0	0
7--8	0	0	0	.1	.3	.5	.9	1.1	.9	.5	.3	.1	0	0	0
8--9	0	0	0	0	.1	.4	.7	.9	.7	.4	.1	0	0	0	0
9--10	0	0	0	0	0	.2	.5	.7	.5	.2	0	0	0	0	0

TABLE 54

ACCUMULATED MELT FOR ZONE D

Elevation Interval, Ft.	Snow Depth	Period Ending, Hours 6	12	18	24	30	36	42	48	54	60	66	72
0 --1000	0.5	0.2	0.5	0.5	0.5	0.5	0.5	0.5	0.5	0.5	0.5	0.5	0.5
1000--2000	1.0	0.1	0.5	1.0	1.0	1.0	1.0	1.0	1.0	1.0	1.0	1.0	1.0
2000--3000	3.0	0	0.2	0.7	1.5	2.6	3.0	3.0	3.0	3.0	3.0	3.0	3.0
3000--4000	10.0	0	0.1	0.5	1.2	2.2	3.4	5.0	7.0	8.6	9.8	10.0	10.0
4000--5000	8.5	0	0	0.3	0.8	1.6	2.7	4.2	6.0	7.5	8.5	8.5	8.5
5000--6000	6.0	0	0	0.1	0.5	1.1	2.0	3.3	4.9	6.0	6.0	6.0	6.0
6000--7000	5.0	0	0	0	0.2	0.6	1.3	2.4	3.8	4.9	5.0	5.0	5.0
7000--8000	5.0	0	0	0	0.1	0.4	0.9	1.8	2.9	3.8	4.3	4.6	4.7
8000--9000	5.0	0	0	0	0	0.1	0.5	1.2	2.1	2.8	3.2	3.3	3.3
9000--10000	5.0	0	0	0	0	0	0.2	0.7	1.4	1.9	2.1	2.1	2.1

The values of Table 53 are accumulated for successive 6-hour periods up to the available snow depth for each contour interval. Table 55 shows the same values weighted according to area and summed to obtain average melt in Zone D. The final results of the computation procedure are summarized in Tables 56 and 57 giving accumulated and duration-depth values for each zone and assigned basin. These tables show that the snow-melt contribution ends after the first 66 hours of the melting period. Enveloping duration-depth curves are presented in Figures 41, 42 and 43.

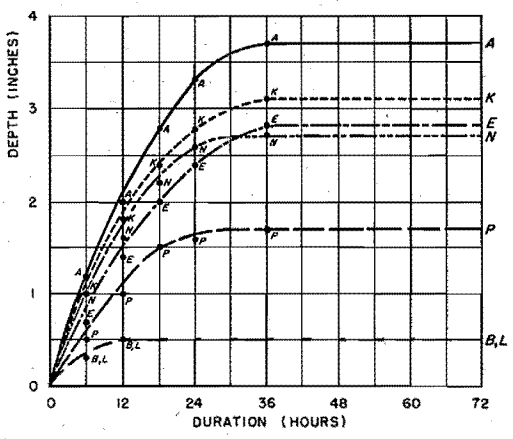

Figure 41

Duration-depth curves of snow melt, Zones A, B, E, K, L, N, P

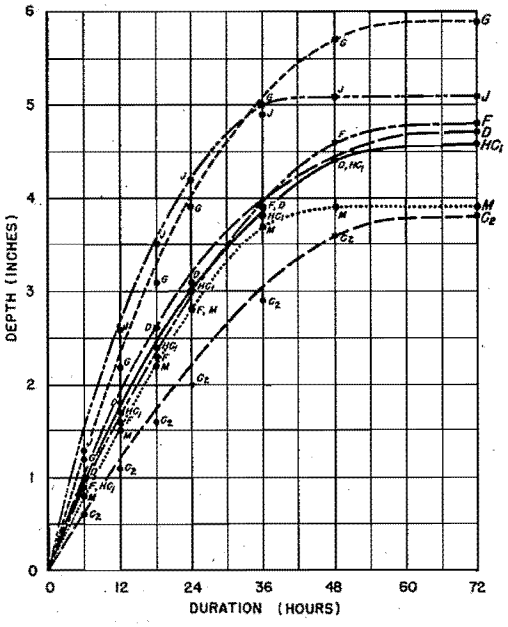

Figure 42. Sierra Nevada Zones

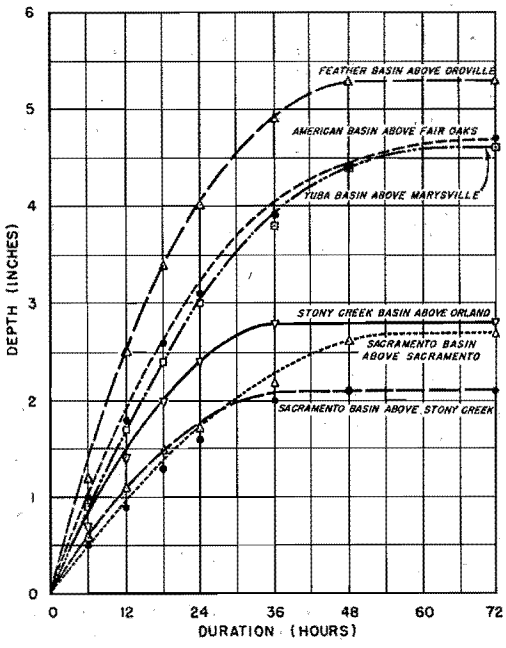

Figure 43. Assigned Basins

Duration-depth curves of snow melt

TABLE 55

WEIGHTED ACCUMULATED MELT FOR ZONE D

Elevation Interval, Ft.	Areal Percentage of Zone	Period Ending, Hours											
		6	12	18	24	30	36	42	48	54	60	66	72
0 --1000	12	0.02	0.06	0.06	0.06	0.06	0.06	0.06	0.06	0.06	0.06	0.06	0.06
1000--2000	15	0.02	0.08	0.15	0.15	0.15	0.15	0.15	0.15	0.15	0.15	0.15	0.15
2000--3000	10	0	0.02	0.07	0.15	0.26	0.30	0.30	0.30	0.30	0.30	0.30	0.30
3000--4000	10	0	0.01	0.05	0.12	0.22	0.34	0.50	0.70	0.86	0.98	1.00	1.00
4000--5000	13	0	0	0.04	0.10	0.21	0.35	0.55	0.78	0.98	1.10	1.10	1.10
5000--6000	16	0	0	0.02	0.08	0.18	0.32	0.53	0.78	0.96	0.96	0.96	0.96
6000--7000	11	0	0	0	0.02	0.07	0.14	0.26	0.42	0.54	0.55	0.55	0.55
7000--8000	10	0	0	0	0.01	0.04	0.09	0.18	0.29	0.38	0.43	0.46	0.47
8000--9000	2	0	0	0	0	0	0.01	0.02	0.04	0.06	0.06	0.07	0.07
9000--10000	1	0	0	0	0	0	0	0.01	0.01	0.02	0.02	0.02	0.02
Accumulated Zonal Melt		0.04	0.17	0.39	0.69	1.19	1.76	2.56	3.53	4.31	4.61	4.67	4.68
Increments of Zonal Melt		0.04	0.13	0.22	0.30	0.50	0.57	0.80	0.97	0.78	0.30	0.06	0.01
Maximum Period		0.97	1.77	2.55	3.12	3.62	3.92	4.22	4.44	4.57	4.63	4.67	4.68

TABLE 56

ACCUMULATED VALUES OF SNOW MELT CONTRIBUTION TO THE MAXIMUM POSSIBLE STORM

Basin	Zone	Period Ending, Hours											
		6	12	18	24	30	36	42	48	54	60	66	72
	A	0.1	0.4	0.9	1.8	2.9	3.7*						
	B	0.2	0.5*										
	C_2	0	0.3	0.7	1.2	1.8	2.3	2.7	3.2	3.6	3.8*		
	F	0	0.2	0.6	1.0	1.6	2.2	2.9	3.8	4.4	4.8*		
	G	0	0.1	0.4	0.9	1.6	2.3	3.3	4.5	5.4	5.8	5.9*	
	J	0	0	0.2	0.6	1.2	2.1	3.4	4.7	5.1*			
	K	0	0.2	0.7	1.4	2.5	3.1*						
	L	0.2	0.5*										
	M	0	0.2	0.6	1.2	1.9	2.6	3.4	3.9*				
	N	0	0.2	0.6	1.2	2.2	2.7*						
	P	0	0	0.1	0.6	1.1	1.6	1.7*					
American	D	0	0.2	0.4	0.7	1.2	1.8	2.6	3.5	4.3	4.6	4.7*	
Stony Creek	E	0.1	0.4	0.9	1.7	2.4	2.8*						
Yuba	HC_1	0	0.2	0.4	0.8	1.3	1.9	2.6	3.5	4.3	4.6*		
Feather	GJ	0	0	0.2	0.6	1.3	2.2	3.4	4.6	5.2	5.3*		
Upper Sacramento	KLMNP	0	0.2	0.4	0.8	1.4	1.9	2.0	2.1*				
Total Sacramento	All	0.1	0.2	0.5	0.9	1.4	1.8	2.1	2.5	2.7*			

* Final period of snow melt.

TABLE 57

DURATION-DEPTH VALUES OF SNOW MELT CONTRIBUTION TO THE MAXIMUM POSSIBLE STORM

Basin	Zone	Hours 6	12	18	24	36	48	72
	A	1.2	2.0	2.8	3.3	3.7	3.7	3.7
	B	0.3	0.5	0.5	0.5	0.5	0.5	0.5
	C_2	0.6	1.1	1.6	2.0	2.9	3.6	3.8
	F	0.9	1.6	2.3	2.8	3.9	4.6	4.8
	G	1.2	2.2	3.1	3.9	5.0	5.7	5.9
	J	1.3	2.6	3.5	4.2	4.9	5.1	5.1
	K	1.0	1.8	2.4	2.8	3.1	3.1	3.1
	L	0.3	0.5	0.5	0.5	0.5	0.5	0.5
	M	0.8	1.5	2.2	2.8	3.7	3.9	3.9
	N	1.0	1.6	2.2	2.6	2.7	2.7	2.7
	P	0.5	1.0	1.5	1.6	1.7	1.7	1.7
American	D	1.0	1.8	2.6	3.1	3.9	4.4	4.7
Stony Creek	E	0.7	1.4	2.0	2.4	2.8	2.8	2.8
Yuba	HC_1	0.9	1.7	2.4	3.0	3.8	4.4	4.6
Feather	GJ	1.2	2.5	3.4	4.0	4.9	5.3	5.3
Upper Sacramento	KLMNP	0.6	1.1	1.4	1.7	2.0	2.1	2.1
Total Sacramento	All	0.5	0.9	1.3	1.6	2.2	2.6	2.7

177. Limitations of the Method. The reliability of the snow melt values is affected, in part, by the inaccuracies inherent in the use and interpretation of meager data. Other sources of error exist because, for the sake of necessary simplification, certain factors affecting melt have been ignored. Some of these factors may be important where normal melting conditions are concerned but represent unjustified refinements in consideration of upper limits. The major sources of error and their significance in the final results are discussed below:

a. The effect of forest cover on melt:

It is assumed that melting rates are directly proportional to wind velocity throughout the basin, including the portion covered by dense forest. This probably overvalues rates of melt at high elevation. At low elevations,

with greater percentage of open land, the derived value of the empirical constant K is too low and therefore melting rates at those elevations are undervalued.

b. Melting effect of rain:

Rainfall as a melting agent was ignored in view of the excessive effect of atmospheric turbulence and because of the unknown value of rain temperature. The effect is significant only in regions of intense rainfall at intermediate elevations and its omission therefore undervalues the melt at those elevations.

c. Negative heat storage in the snow:

During the subfreezing period antecedent to the storm the snow undergoes an indefinite amount of cooling. An equivalent quantity of heat has to be supplied by the air and is unavailable for melting. The effect is to delay melting and decrease the total amount of melt at upper elevations.

d. Storage of water in the snow:

Melt water and rainfall may be stored in the first portion of the melting period and released in the later stages. However, the rate of release is probably controlled by the depletion of snow cover. In addition, maximum rates of melt do not synchronize at various elevations. The over-all effect would be only a slight increase in short-duration melt.

e. Rate of increase of wind with elevation:

Due to vertical convergence and horizontal divergence, up-slope winds increase faster with elevation than indicated. This would tend to increase melt at upper elevations and decrease it at lower elevations in Zones C, D, F, G and H.

f. Cooling and drying of air over snowfield:

The warm air moves transverse to the snow line and crosses a narrow strip of snow before emerging from the basin. At the high velocities assumed, the change of air-mass properties is negligible during most of the melting period. The only significant effect would be to reduce the melting at the upper elevations in the early portion of the storm.

g. Irregular distribution of snow in the valley:

The snow would not form a uniform blanket in the valley. For purposes of simplification it was assumed that snow depth is a function solely of elevation. However, over a large level area considerable regulation of melt would occur because of partial area contribution during the later stages of melting. This effect would tend to reduce short-period melt at the lower elevations.

As indicated in the above analysis, the various factors tend to neutralize each other. After due consideration of the possible effect of all the items listed as sources of error, it was decided that the values as submitted represent safe upper limits. Therefore, in this report, the enveloping duration-depth curves of snow melt are not increased by a factor of reliability.

CHAPTER VIII

THE MAXIMUM POSSIBLE STORM

178. Distribution of the Rainfall. Even in the maximum possible storm a portion of the precipitation at high elevations is in the form of snow. However, the total is relatively small and the area over which it falls a minor percentage of the total basin area. In all computations, therefore, the effect of the snowfall has been neglected and all the precipitation considered as rainfall. The time and areal distribution of the critical precipitation in the maximum possible storm was developed from the duration-depth values assembled in Tables 5, 8, 11, 14, 17, 20, 22, 25 and 28 of Chapter V. These depths are plotted against duration for all the major storms considered in this study, in separate graphs for each zone and assigned basin, Figures 44 to 60. The curves labeled B envelop the duration-depth values of the December 1937 storm. The enveloping curve of maximum possible precipitation for the total basin is shown as curve A in Figure 44 and is determined by the computation procedure discussed in Chapter VI. Corresponding curves A for the individual zones and assigned basins are obtained by adjusting curves B to give the correct volumes of maximum possible precipitation over the whole basin. Tabular values are shown in Table 58.

TABLE 58

DURATION-DEPTH VALUES OF MAXIMUM POSSIBLE RAINFALL -- TOTAL BASIN

Basin	Zone	Hours 6	12	18	24	36	48	72
	A	3.0	5.3	7.3	8.9	11.4	13.2	14.7
	B	0.9	1.7	2.3	2.8	3.8	4.6	5.4
	C_2	1.6	3.0	4.3	5.4	7.4	9.1	10.8
	F	3.3	6.2	8.8	10.8	14.0	16.6	19.2
	G	3.3	6.1	8.7	11.1	15.0	18.0	21.7
	J	1.5	3.0	4.3	5.6	7.7	9.4	11.2
	K	1.8	3.5	4.8	6.0	8.0	9.7	11.4
	L	1.6	2.9	3.9	4.8	6.1	7.1	7.8
	M	3.1	5.6	7.8	9.6	12.3	14.4	16.3
	N	2.4	4.6	6.5	8.1	10.6	12.8	15.0
	P	1.4	2.6	3.8	4.7	6.1	7.1	7.9
American	D	2.3	4.2	5.9	7.4	10.1	12.4	14.9
Stony Creek	E	2.1	3.9	5.3	6.6	8.8	10.6	12.2
Yuba	HC_1	2.2	4.6	6.2	7.8	10.4	12.4	14.6
Feather	GJ	2.2	4.0	5.7	7.3	9.8	11.8	14.1
Upper Sacramento	KLMNP	1.9	3.5	4.9	6.1	8.0	9.3	10.5
Total Sacramento	All	1.8	3.4	4.8	5.9	7.9	9.5	11.0

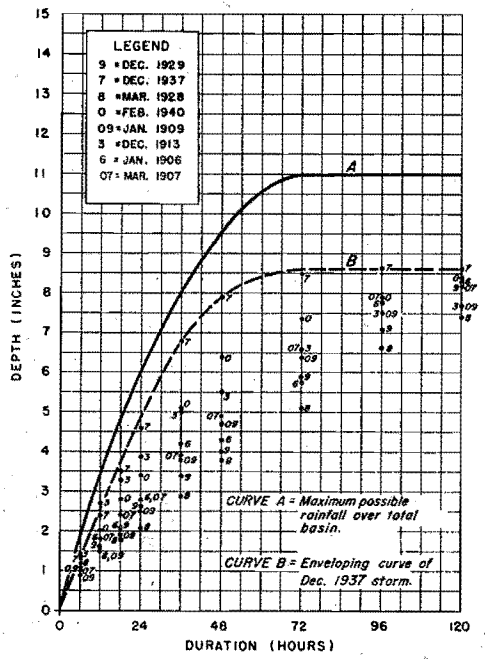

Figure 44. Total basin. Duration-depth values.

It will be noted that in individual zones and sub-basins the values of curve A are occasionally exceeded. It should be remembered that curve A represents the contribution of the individual zone or sub-basin to the maximum possible storm for the total basin. However, the individual zone or sub-basin can have and has had more intense rainfall, but only at the expense of the other subdivisions within the total basin.

Duration-depth values.

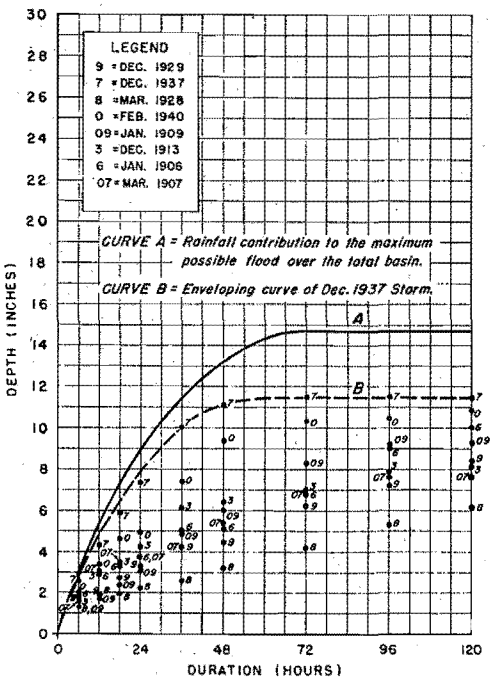

Figure 45. Zone A

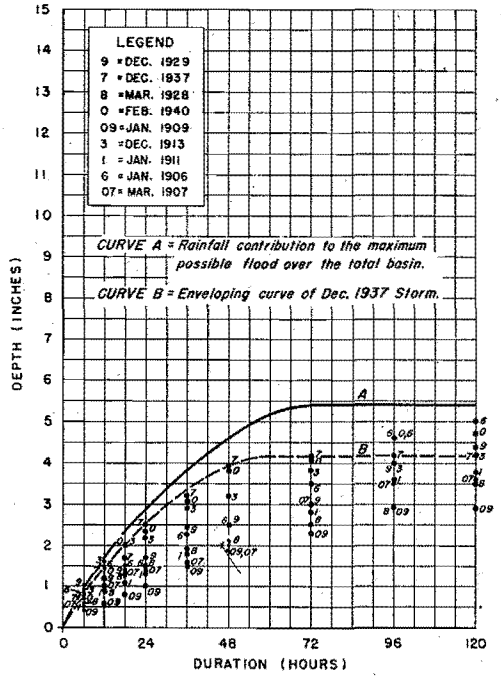

Figure 46. Zone B

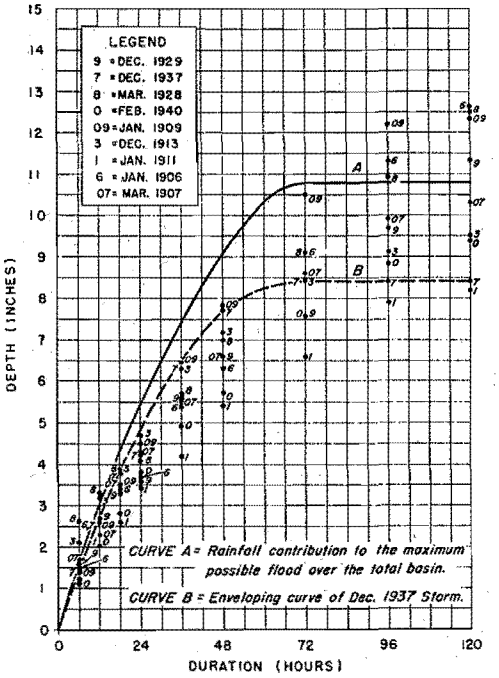

Figure 47. Zone C_2

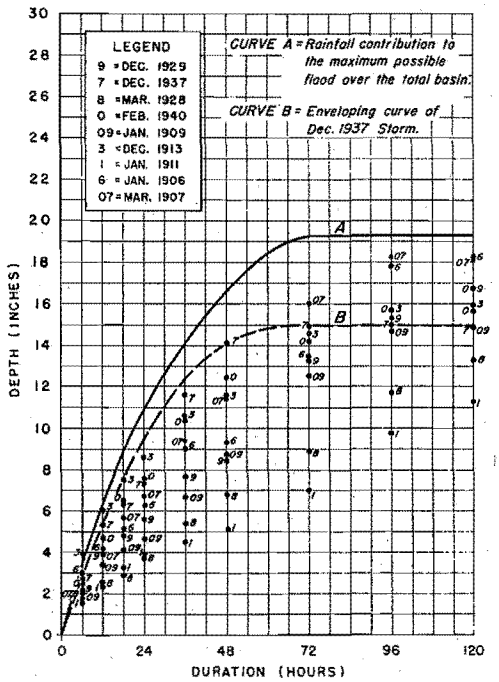

Figure 48. Zone F

Duration-depth values.

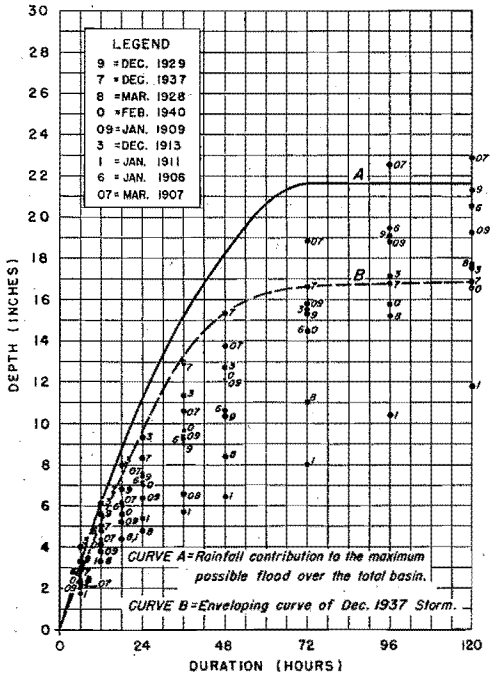

Figure 49. Zone G

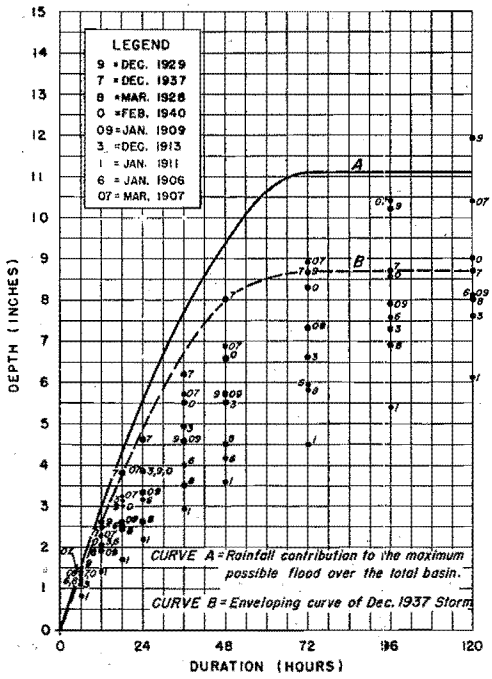

Figure 50. Zone J

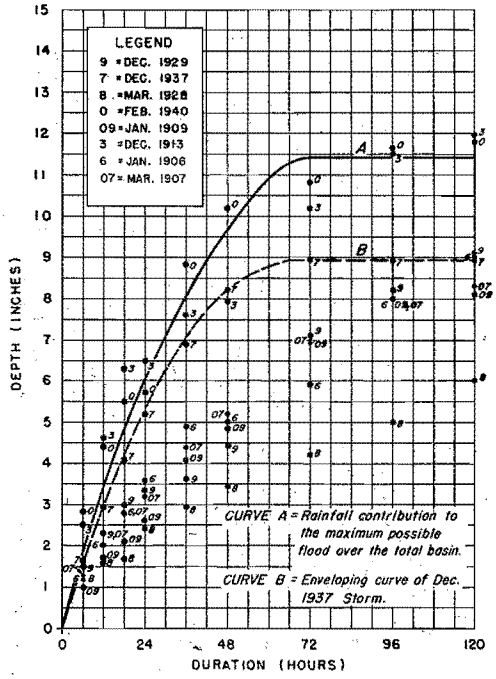

Figure 51. Zone K

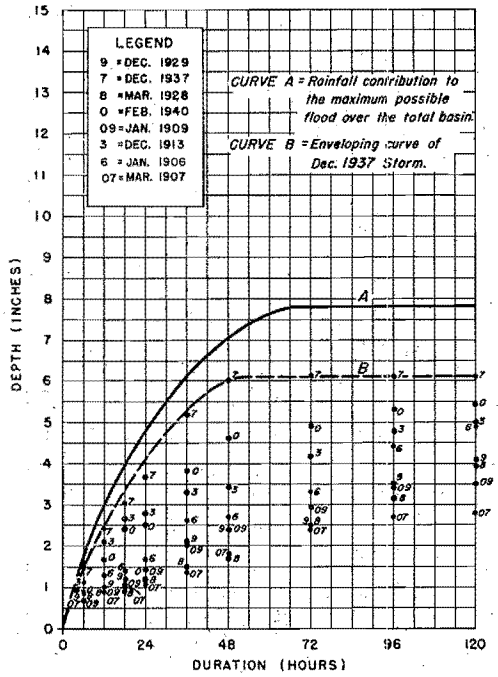

Figure 52. Zone L

Duration-depth values.

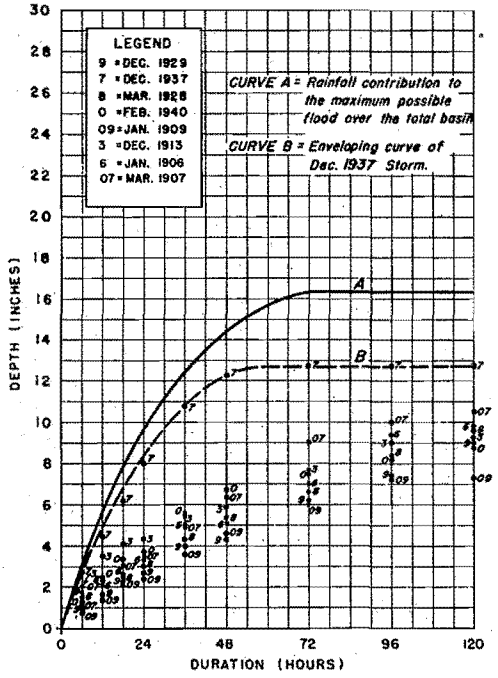

Figure 53. Zone M

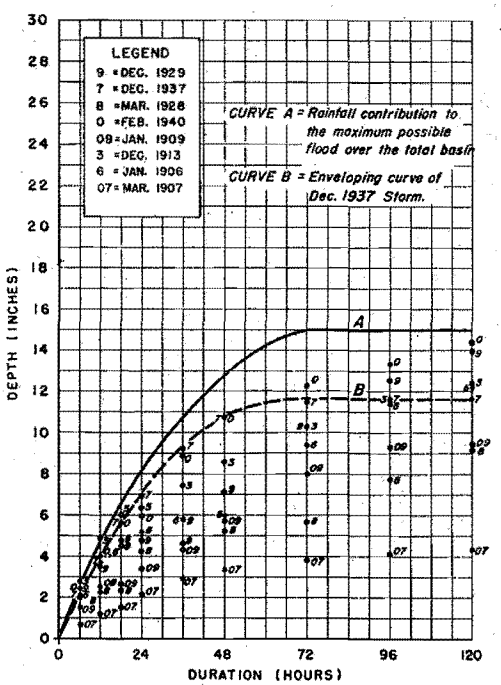

Figure 54. Zone N

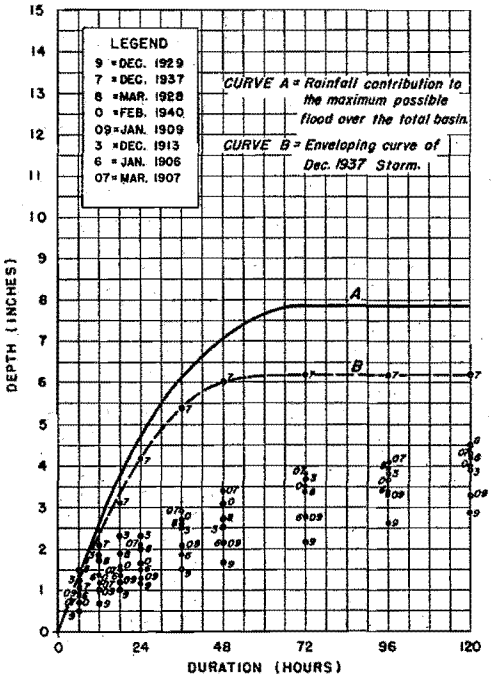

Figure 55. Zone P

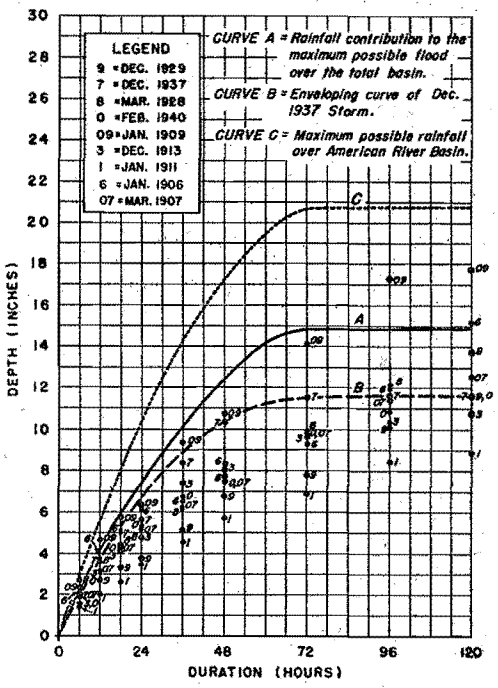

Figure 56
American River Basin, Zone D

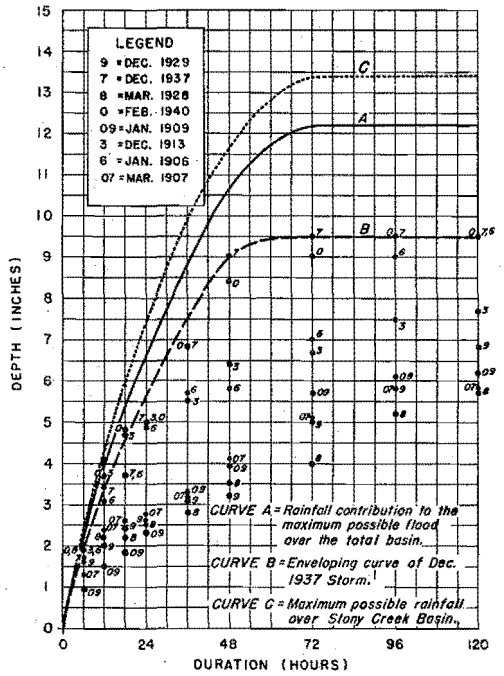

Figure 57
Stony Creek Basin, Zone E

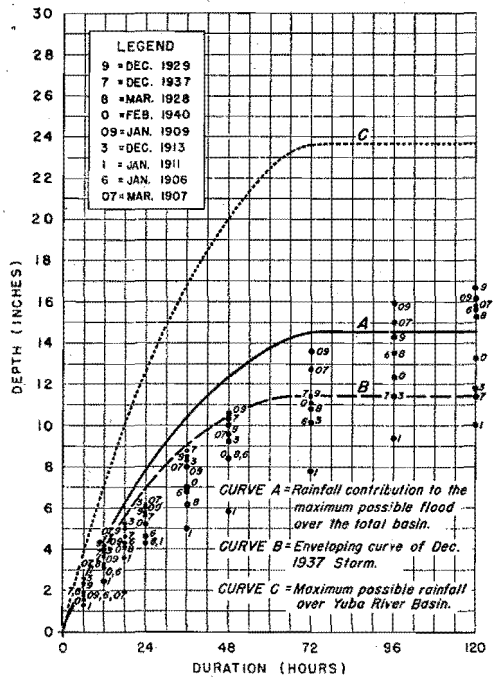

Figure 58
Yuba River Basin, Zone HC_1

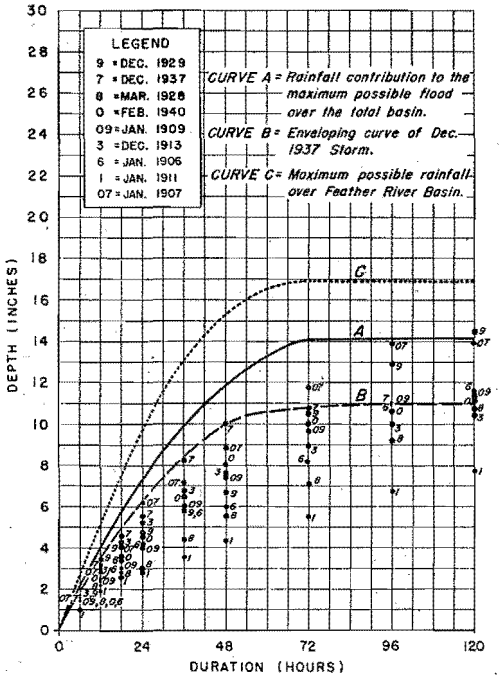

Figure 59
Feather River Basin, Zone GJ

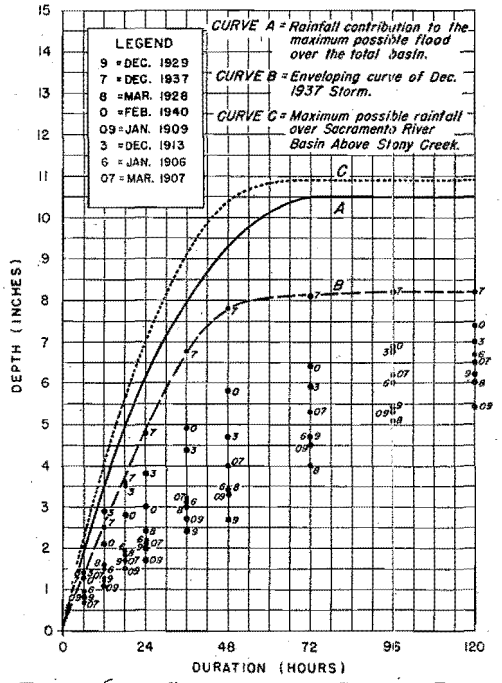

Fig. 60. Sacramento River Basin above Stony Creek, Zone KLMNP

These duration-depth values are enveloped by curves C, shown in Figures 56 to 60, which are for the maximum possible rainfall over the assigned sub-basins. The derivation of curves C will be discussed later.

179. It is evident that the volume of rainfall in the December 1937 storm could have been distributed in a different manner, so that certain portions of the area could have experienced higher intensities than actually occurred. For such a determination of upper limits of rainfall for subdivisions of the basin it was necessary to consider the problem of rainfall transposition within a mountainous area. The ordinary method of transposition involving the use of an area-depth curve fails because the basin's topographic characteristics and location with respect to mountain ranges exert a greater influence on the average rainfall depths than the areal extent of the basin. However, total storm rainfall values can be adjusted to a common base by converting them into percentages of normal seasonal precipitation which presumably are free of the influences of topography and other basin characteristics. For example, the 72-hour zonal rainfall in the December 1937 storm ranges from 4.2 to 16.7 inches while the range in seasonal percentages is only 15.7% to 32.5%. This indicates that seasonal percentages are fairly conservative quantities and that variations in these quantities within a region represent differences in storm intensity over the area.

180. With these facts in mind, the average percentages of normal seasonal precipitation within the maximum 72-hour period of the December 1937 storm were plotted against area in a form similar to an area-depth curve (Figure 61). This storm was selected as a model for distributing rainfall because it gave the greatest percentages for all values of area

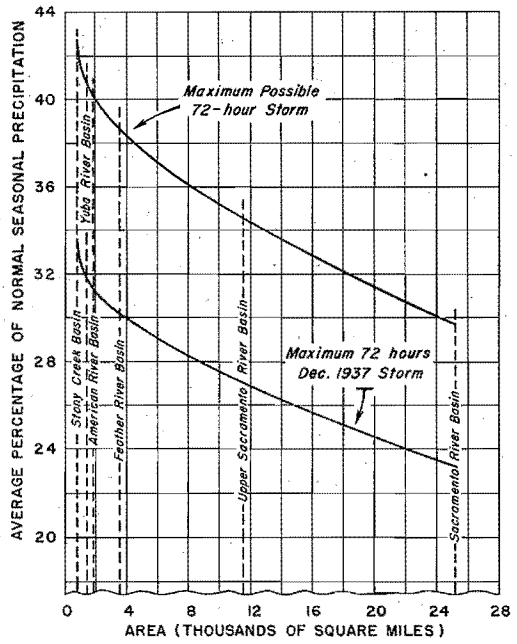

Figure 61

Area-percentage curves of normal seasonal precipitation, Sacramento River Basin

within the Sacramento Basin. For the total basin, the percentage of normal seasonal precipitation is 22.9. The maximum possible storm has a value of 29.7%. Therefore, the curve showing the maximum possible 72-hour percentages was derived by multiplying all the values of the lower curve by the ratio $\frac{29.7}{22.9}$, or 1.30. In applying the upper curve, it is assumed that a storm 30% more intense than the December 1937 storm could occur with the same relative distribution of mean seasonal percentages within the area.

181. The curves of Figures 62, 63 and 64, giving the duration-depth values of maximum possible rainfall for the individual assigned basins were developed from Figure 61. The values are tabulated in Table 59.

TABLE 59

DURATION-DEPTH VALUES OF MAXIMUM POSSIBLE RAINFALL

ASSIGNED SUB-BASINS

	Hours						
Basin	6	12	18	24	36	48	72
American	3.2	5.8	8.2	10.5	14.2	17.2	20.7
Stony Creek	2.3	4.3	6.0	7.4	9.9	11.6	13.4
Yuba	3.9	7.3	10.1	12.7	16.9	20.0	23.6
Feather	2.8	5.2	7.5	9.7	13.2	15.5	16.9
Upper Sacramento	2.2	4.0	5.7	7.0	9.1	10.4	10.9

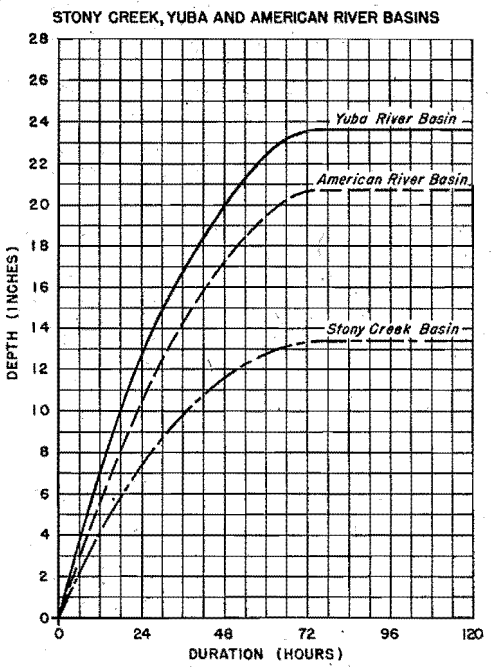

Figure 62

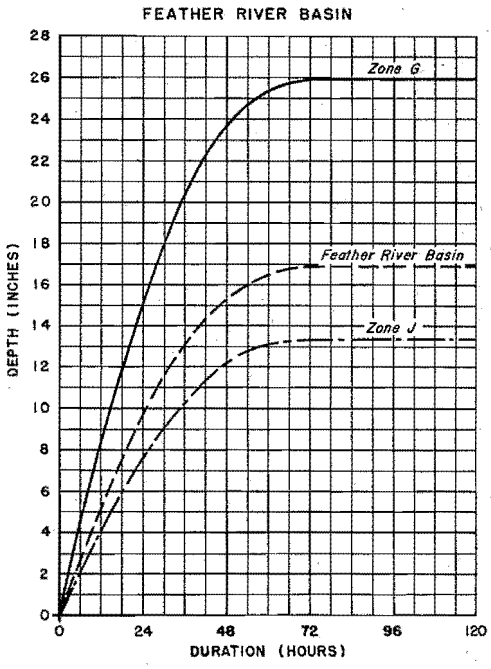

Figure 63

Duration-depth values, maximum possible rainfall

The 72-hour value for a particular basin was established by entering the graph with the area of the basin, reading off the percentage, and multiplying by the normal seasonal precipitation for the basin. The remaining values of duration-depth were then derived by adjusting the curves of Figures 56 to 60, applicable to the total basin, by the ratio of the two 72-hour values. The duration-depth curves of Figures 62 to 64, thus obtained, are the same

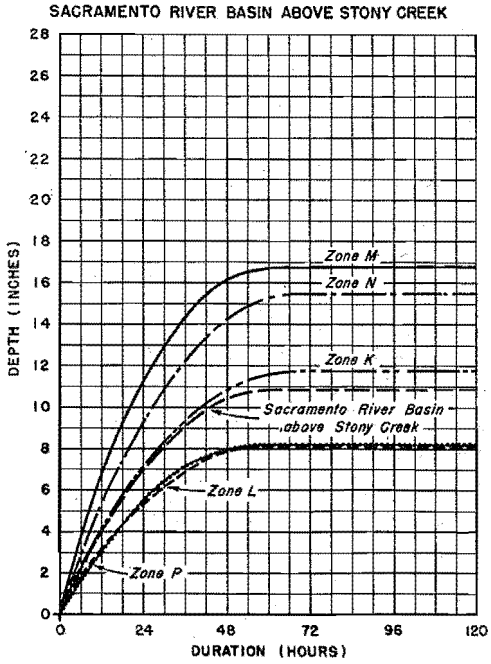

Figure 64

Duration-depth values, maximum possible rainfall

as the curves C of Figures 56 to 60, previously mentioned.

182. In arranging the rainfall increments in a critical chrcnological pattern, certain restrictions must be imposed. Since the maximum possible storm is modeled after the December 1937 storm, the maximum 24-hour rainfall should occur during the second day of the three-day storm period. There are a number of ways of distributing the remaining rainfall, and two possible arrangements of the maximum possible storm over the total basin are shown in Figures 65 and 66. The arrangement of Figure 65, with equal blocks of rainfall on the first and third days of the storm, is based on the symmetrical meteorological pattern of Figure 38. In Figure 66 the second highest 24-hour period of rain occurs on the first day. This is the pattern of the December 1937 storm and would

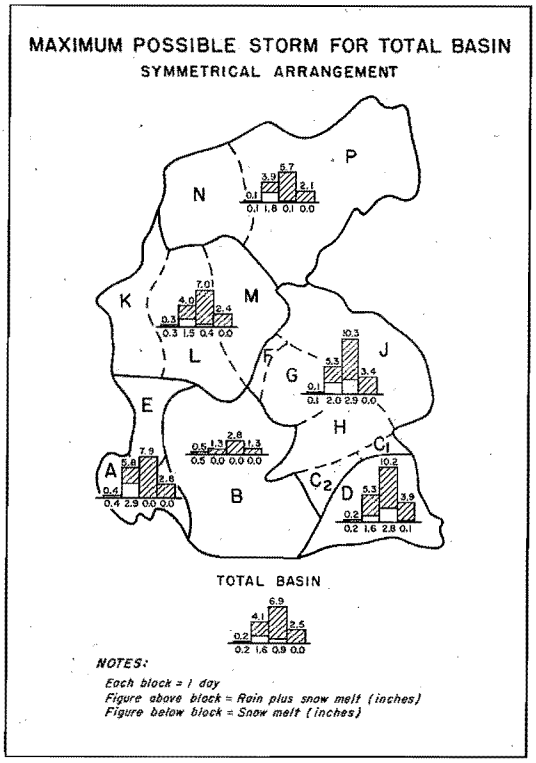

Figure 65

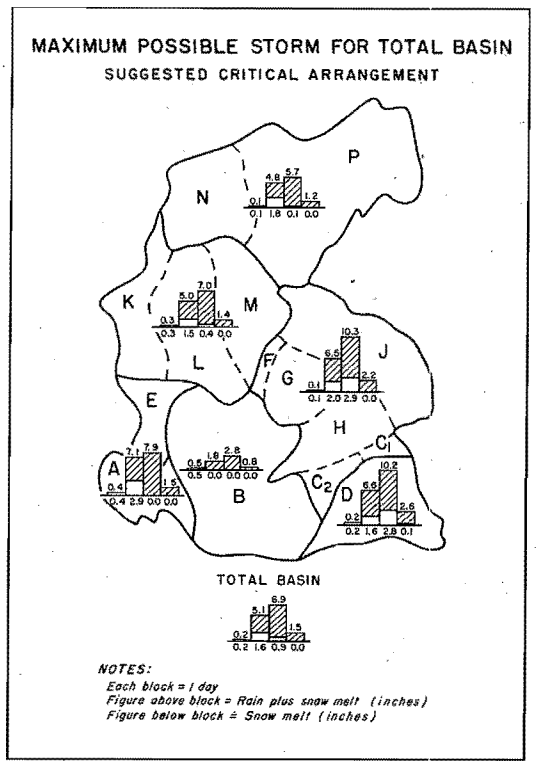

Figure 66

probably produce a higher flood stage at Sacramento. In the figures the basin is subdivided into six sub-areas and daily values of rainfall and snow melt are given for each subdivision. Other arrangements, using other subdivisions and units of time, may be derived from Tables 56 and 58 but, insofar as 24-hour rainfall amounts are concerned the chronological sequence should be the same in every zone. For shorter period breakdowns within the 24-hour interval, a staggering of peak rainfall among the various zones is permissible.

183. Distribution of the Snow Melt. No matter how its increments are arranged, the maximum possible storm melts the optimum snow cover (Chapter VII) that precedes it. A given time sequence of rainfall implies a specific progression in the values of the meteorological elements, such as wind and dew point, which may differ from the pattern, shown in Figure 38, used to compute snow melt. However, the chronological distribution of melting is controlled to a considerable extent by the fixed elevation relationships of the basin, so that a large variation in the meteorological pattern will have only a slight effect on the melt pattern. For that reason, the accumulated values of snow melt in Table 56 are considered practically invariant and should be added to the rainfall values obtained from the duration-depth curve of maximum possible rainfall. This has been done in Figures 65 and 66. However, since the rise in temperature above 32 F occurs approximately 12 hours before the beginning of the 72-hour maximum storm, the increments of rainfall lag 12 hours behind the increments of snow melt.

184. Suggested critical arrangements of maximum possible rainfall and snow melt for each of the assigned basins are given in Figure 67.

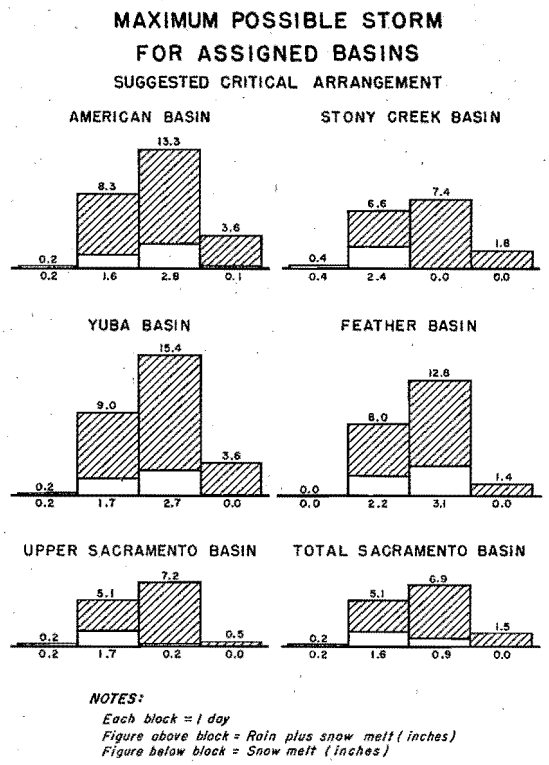

Figure 67

The values were derived from Tables 56 and 59 by the computation method previously described. The restrictions on derivation of rainfall increments and coordination of rain and snow melt were applied.

185. Meteorological Antecedents. Flood rains over the United States are produced by a more or less fortuitous combination of events which brings over the area a deep current of moist air which is potentially unstable. At the same time either the circulation pattern or the local topography must be such as to provide an efficient rain-producing mechanism. In the Sacramento Basin the mechanism is ever-present in the form of fixed mountain barriers, and rains of flood magnitude depend only on the invasion of moist unstable air. Given the proper general circulation pattern, a quasi-permanent frontal zone becomes established normal to the major axis of the basin. From west to east along this frontal zone there moves a series of alternating fluctuations of warm moist and of cold dry air. On the surface weather map they may appear as waves, fronts or cyclones. On charts of the upper air they all appear as tongues of moist and dry air of varying pattern.

186. Such a series constitutes a storm period and, in general,

the greater the intensity of the individual major developments the shorter the duration of the series. The average major storm appears to run its course in approximately five days, after which a repetition may occur. The maximum possible storm has a three-day duration but it cannot be followed as closely by another storm. In considering the storm periods that may precede the maximum storm it has been necessary to compromise between durations short enough to imply major intensity and intensities low enough to permit further developments within a short time. It was decided that in no case would it be logical to assume that the peak activity in two successive storm periods could occur with less than a four-day separation. This should not be confused with recurrent surges of precipitation which are part of the storm and can occur at intervals of 12 hours or less. It is apparent, then, that storm cycles can be repeated frequently enough to warrant the assumption of extremely critical conditions antecedent to the maximum storm. On the other hand, these assumptions must be consistent with the limitation of a four-day interval between peaks of storm activity. In the three sequences which will be here suggested, the critical events preceding the maximum storm are reasonable from a meteorological standpoint. They can occur in the order indicated and within the time intervals specified.

187. In the first suggested sequence the initial event is a period of steady rain which saturates the soil and raises stream and by-pass channels to the bankful stage. The synoptic pattern is of the less intense occluded type -- such as in the major storms of 1909, 1928, or 1929 (see Chapter V). An intense occlusion of the 1937 or 1940 type would inevitably be followed by an invasion of colder polar maritime air

that would not only end the rains but build up the Pacific High to prevent further precipitation for some time. The 1937 storm, for example, was followed by ten days of fair weather. Furthermore, the second event in the sequence requires polar continental rather than polar maritime air in the Sacramento Basin. The cyclonic intensity must be great enough, however, to bring reduced dew points of about 54 F into the valley, so that the temperatures accompanying the rains may be sufficiently high to preclude accumulation of snow at intermediate and high elevations. This first rainy phase lasts four days, with the peak rains occurring about the middle of the period.

188. With the ground bare over most of the area, the second event in the sequence is an invasion of the basin by cold air, cold enough to produce an extensive frost layer in the basin area above 1000 feet elevation and thus limit infiltration during the period of major flood runoff. Such air must come from the continent rather than the Pacific, i.e., it must be polar continental air. For such an influx the quasi-stationary front becomes displaced southward and the cold continental High (which has been seen to be an accompaniment of almost all Sacramento storms) develops a protrusion pushing down into the San Joaquin from Oregon. This occurred in the 1909 storm, and the presence of cold air with northerly winds in the basin has been noted in the 1928 and 1862 storms. For the possibility of temperatures low enough to freeze the soil layer one can cite the polar continental invasion of January 1888 (see Monthly Weather Review of that date), when the ground was frozen hard as far south as Fresno. But so intense an outbreak would delay the subsequent steps in the suggested sequence too long. The postulated freeze would

extend down to only about 1000 feet and would be a dry period of just four-days duration.

189. The third four-day event in the sequence is a snowfall on bare, mostly frozen ground, culminating in the critical distribution described in the previous chapter. The snowfall results from a series of semi-occluded waves on the quasi-stationary front, now being slowly displaced northward. Along that front, out on the Pacific, the major occlusion which is to be the maximum possible storm is developing. The four-day period is followed by a 12-hour interval during which the temperature rises from freezing to the temperature required for the beginning of the maximum storm. The snow melt during those 12 hours is therefore not contemperaneous with the rainfall of the maximum storm which, similar in characteristics to the December 1937 storm, follows and lasts three days. The suggested sequence thus lasts 15-1/2 days. Between the peak of the rainfall intensities of the initial period and the commencement of the maximum storm 10-1/2 days elapse.

190. An alternative sequence, with higher probability of occurrence, is one in which the four-day fair and freezing period is eliminated. There are many precedents for such a combination of events. In 1907 (see Figure 37) a critical snowfall followed directly after the major rain period of March 16-20 had practically cleared all elevations of snow. In 1911 (see Figure 37) a critical type of snowfall distribution was followed by rains, and in 1862 (see Chapters IV and V) heavy snow to within a few miles of Sacramento was followed by heavy rains. The meteorological pattern is again a series of semi-occlusions, a displacement southward and then northward of the major front, winding up

with a major occluded development that is the maximum storm. This alternate sequence lasts 11-1/2 days. Between the peak intensity of the initial rains and the beginning of the maximum storm 6-1/2 days elapse. Between the critical snow cover and the maximum storm there is again the 12-hour period of snow melt which is not coincident with the maximum 72-hour storm.

191. A third possible sequence is one in which both the freezing and snowfall periods are eliminated. In other words, the maximum possible storm follows a period of rain. In postulating such a sequence the four-day interval between peaks of rainfall intensity must still be maintained. Any of the major storms studied in this report can be assumed to occur immediately prior to the maximum possible except the storms of December 1937 and February 1940.

192. The sequences are summarized and their hydrologic consequences indicated in the following table:

TABLE 60

ANTECEDENT CONDITIONS FAVORING CRITICAL RUNOFF OVER THE SACRAMENTO BASIN

		Sequence 1	Sequence 2	Sequence 3
		Rain → Freeze → Snow → MPS*	Rain → Snow → MPS	Rain → MPS
Interval Between Peaks of Antecedent Rainfall and Final Storm		12 days	8 days	4 days
Runoff characteristics immediately preceding MPS	Snow Cover	Optimum	Optimum	None
	Soil Condition	Frozen	Moist	Saturated
	Infiltration Rates	Minimum	Moderate	Minimum to moderate
	Surface and Channel Storage Capacity	Moderate	Minimum to Moderate	Minimum

* Maximum Possible Storm

GLOSSARY

GLOSSARY

Adiabatic Chart. A thermodynamic diagram in which temperature is plotted against pressure (log p or $p^{0.288}$), and on which dry adiabats have been constructed. It is used for the evaluation of an aerological sounding.

Adiabatic or Dry Adiabatic Lapse Rate. The rate of change of temperature of an unsaturated air particle as it is adiabatically raised or lowered in the atmosphere -- equal to approximately 1 C per 100 meters

Adiabatic Process. Atmospheric process in which changes in volume, pressure and temperature occur without the loss or gain of heat.

Air Mass. An extensive body of air approximating horizontal homogeneity in its source region.

Albedo. Percentage of reflected radiation.

Anticyclone. In the Northern Hemisphere, a clockwise circulation around relatively high pressure at the center. Counterclockwise in the Southern Hemisphere.

Back. Verb describing shift of wind in a counterclockwise direction, e.g., from west to south.

Base Flow. Estimated ground-water discharge during period of direct runoff.

Channel Storage. Volume of water in a channel system.

Cold Anticyclone. Anticyclone of chiefly thermal origin, with anticyclonic circulation confined to lower troposphere.

Cold Front. Front at which relatively cold air displaces warmer air.

Cold Front Type Occlusion. Occlusion in which the cold air back of the occluded front is colder than and underruns the cold air in advance of the front.

Conditional Instability. Thermodynamic state which is unstable for saturated air but stable for dry or unsaturated air.

Convective Instability. Thermodynamic state of a layer of air which will become unstable after sufficient lift.

Convective Process. Process, mechanical or thermal, causing the upward or downward movement of a limited portion of the atmosphere. Cumulus type clouds are indicative of the occurrence of convective processes.

Convergence. Generally refers to the condition that exists when the wind distribution within a given area causes a net horizontal inflow into the region. Horizontal convergence is usually accompanied by vertical divergence, which is referred to as stretching. A net horizontal outflow is known as divergence and is generally accompanied by vertical convergence, which is referred to as shrinking.

Cyclone. In the Northern Hemisphere, a counterclockwise circulation around relatively low pressure at the center. Clockwise in the Southern Hemisphere.

Cyclogenesis. Process which creates or develops a new cyclone, or which produces an intensification of an existing one.

Deepening. Decreasing pressure at the center of a pressure system.

Dew Point Temperature. The temperature, at constant pressure, at which saturation occurs in a cooling mass of air.

Divergence. See Convergence.

Double Mass Curve. Two sets of accumulated values plotted against each other.

Duration-Depth Curve. Maximum depths of rainfall or snow melt plotted against the duration required for their accumulation over a selected area in a particular storm or group of storms.

Effective Height (as used in this report). The height to which the base of a column of air must be lifted in order to enter the basin from a given direction.

Effective Precipitable Water. The greatest amount of precipitable water which can be removed from an atmospheric column by convective action.

Equation of State. $\rho = \frac{p}{RT}$ where ρ is density of air, p atmospheric pressure, R the gas constant for air, and T the absolute temperature.

Equivalent Potential Temperature. The potential temperature of an air parcel after all the latent heat of condensation of the contained water vapor has been realized.

Filling. Increasing pressure at the center of a pressure system.

Foehn. A warm dry wind, dynamically heated in descent down mountain slopes.

Front. The line of intersection with the earth of an inclined surface of discontinuity separating two different air masses. When the surface of discontinuity is forced over a third homogeneous air mass, the line of intersection is called an upper front.

Frontogenesis. The process which creates a front or intensifies an existing front.

Frontolysis. The process which tends to weaken or destroy an existing front.

Geostrophic Wind. The wind resulting from the balance of the force due to the pressure gradient and the apparent deflecting force of the earth's rotation, neglecting friction and curvature of path.

Gradient Wind. The wind resulting from a balance (neglecting friction) between the force due to the pressure gradient, the apparent deflecting force of the earth's rotation, and the centrifugal force due to the curvature of path.

Great Basin Anticyclone. A persistent high pressure system frequently found in winter, centered over the plateau between the Sierras and the Rockies.

Ground Water Recharge. Increase in volume of ground water storage due to storm or melting snow.

Hydrograph. Stream discharge plotted against time.

Hydrostatic Equation. $dp = -\rho g dz$ where dp is the change in atmospheric pressure, ρ is air density, g acceleration of gravity, and dz the change in elevation.

Instability. Thermodynamic state in which vertical displacements are favored.

Inversion. An increase of temperature with height.

Isentropic Chart. Synoptic chart of data plotted at a surface of constant potential temperature, which is also a surface of constant entropy for unsaturated air.

Isochion. Line of equal snow depth or equal water equivalent of snow on the ground.

Isopleth. A line connecting equal values on a chart.

k-type Air Mass. An air mass colder than the surface over which it is passing, with stability consequently decreasing in the lower layers.

Lapse Rate. Rate of decrease of temperature in the atmosphere with height.

Lift Coefficient (as used in this report). The ratio of the effective precipitable water remaining in a column of air after lift, to the effective precipitable water before lift.

Mass Curve. Curve representing cumulative values distributed through time.

Mixing Ratio. Ratio of the weight of water vapor to the weight of dry air in a given sample of atmosphere.

Occluded Front. The type of front resulting when a cold front overtakes a warm front, forcing aloft the air in the warm sector.

Occlusion. Process of formation of an occluded front, or a system which has undergone the process.

Orographic Rainfall. Rainfall caused by deflection upwards of moisture-laden winds by mountain slopes.

Polar Front. The line of intersection with the earth of a surface of discontinuity separating air masses of polar origin from those of tropical origin, the line being more or less continuous within each hemisphere.

Potential Temperature. Temperature of air after expansion or compression dry adiabatically to a standard pressure of 1,000 mb.

Precipitable Water. Total water vapor contained in an atmospheric column of unit cross-section area, expressed in terms of a column of liquid water of the same cross-section area.

Pressure Gradient. Decrease in barometric pressure per unit horizontal distance in a direction normal to the isobars.

Pseudo-Adiabatic Chart. The adiabatic chart to which saturation adiabats and lines of constant mixing ratio have been added.

Pseudo-Adiabatic Lapse Rate. The rate at which an ascending body of saturated air will cool during adiabatic expansion. Its value is not constant but approaches the dry adiabatic rate asymptotically as the water vapor content decreases toward zero.

Quasi-Stationary Front. Front along which displacement of warm by cold air, or vice versa, is small and accomplished by minor wave action.

Recession Hydrograph. Portion of hydrograph with no contemporaneous inflow from surface runoff.

Reduced Dew Point (as used in this report). Dew point reduced pseudo-adiabatically to 1,000 mb.

Specific Humidity. Ratio of the weight of water vapor to that of moist air in a given sample of atmosphere.

Stability. Thermodynamic state in which vertical displacements are resisted.

Storage-Discharge Curve. Volume of channel storage plotted against contemporaneous stream discharge.

Strength (of Cyclones and Anticyclones). Steepness of Pressure Gradient. It is synonymous with intensity.

Stretching. See Convergence.

Subsidence. A sinking of air within an air mass.

Synoptic Chart. A chart, such as the ordinary weather map, which shows the distribution of meteorological conditions at a given moment.

Thermal Equator. Line of highest temperatures, near the geographical equator, but displaced to either side of it according to season.

Thiessen Polygon. Geometrical figure drawn by plotting perpendicular bisectors between adjacent precipitation stations. These bisectors bound closed areas around each station and together form a network of contiguous Thiessen polygons, for each of which the enclosed station's rainfall is considered representative.

Tongue. The projecting portion of a large-scale eddy of dry or moist air, as revealed on an isentropic surface.

Trades or Trade Winds. Two belts of winds, one on either side of the equatorial doldrums, in which the winds blow almost constantly from easterly quadrants.

Trough. An elongated area of relatively low barometric pressure.

Veer. Verb describing shift of wind in a clockwise direction, e.g., from south to west.

Vorticity. Rotational component of motion.

Warm Anticyclone. Anticyclone of primarily dynamic origin, with anticyclonic circulation extending to high levels.

Warm Front. Front at which relatively warm air displaces colder air.

Warm Front Type Occlusion. Occlusion where the cold air back of the occluded front is warmer than and overruns the cold air in advance of the front.

Warm Sector. The air bounded by the cold and warm fronts of a cyclone.

Wave. A localized deformation of a front, which travels along the front as a wave-shaped formation, and which may develop into an intense cyclone.

Wet Bulb Temperature. Lowest temperature to which air can be cooled by evaporating water into the air at constant pressure.

w-type Air Mass. An air mass warmer than the surface over which it is passing, with stability consequently increasing in the lower layers.

Zonal Index. Index of average velocity of the westerlies taken as the mean pressure difference between 35° N. and 55° N. latitude for a period, generally, of five days. A high zonal index indicates increased circulation of the westerlies aloft. A low zonal index indicates weak westerly circulation.

BIBLIOGRAPHY

BIBLIOGRAPHY

References to any of the material listed below are indicated in the body of this report by title number, underlined and enclosed within parentheses. The following abbreviations are used: MWR, Monthly Weather Review; BAMS, Bulletin of the American Meteorological Society; TAGU, Transactions, American Geophysical Union; QJ, Quarterly Journal, Royal Meteorological Society.

1. Hydrometeorological Report No. 1: Maximum Possible Precipitation over the Ompompanoosuc Basin above Union Village, Vermont; Hydrometeorological Section, U. S. Weather Bureau, in cooperation with the U. S. Engineer Department, Corps of Engineers, War Department; March 1940

2. Hydrometeorological Report No. 2: Maximum Possible Precipitation over the Ohio River Basin above Pittsburgh, Pa.; Hydrometeorological Section, U. S. Weather Bureau, in cooperation with the U. S. Engineer Department, Corps of Engineers, War Department; June 1941

3. _____ California Cooperative Snow Surveys, Monthly Bulletin of Snow Survey and Precipitation Data, State of California, Department of Public Works, Sacramento. February 1932 through May 1941

4. _____ Sacramento Method of Correlating Storm Precipitation with Normal Seasonal Precipitation and Runoff; War Department, Investigations Division, Sacramento District, Corps of Engineers, U. S. Army. October 1941

5. _____ Supplements A, B and C, Engineer Bulletin R and H, No. 10, 1938; War Department, Office of the Chief of Engineers

6. _____ Sacramento River Basin; Bulletin No. 26, 1931, State

of California, Department of Public Works, Sacramento

7. _____ Flow in California Streams; Bulletin No. 5, 1923, State of California, Department of Public Works, Sacramento

8. Allen, R. A.: Statistical Studies of Certain Characteristics of the General Circulation of the Northern Hemisphere. QJ, Supplement (Canadian Branch), Vol. 66, 1940

9. Alps, H. F.: Foot-Layer Densities of Snow. MWR, Vol. 50, Sept. 1922, pp. 474-475

10. Beals, E. A.: The Northeast Trades of the North Pacific. MWR, Vol. 55, May 1927, pp. 211-221

11. Beals, E. A.: The Semi-Permanent Arizona Low. MWR, Vol. 50, July 1922, pp. 341-347

12. Bjerknes, J.: A Method of Approximate Computation of Orographical Precipitation (unpublished)

13. Blake, Dean: Movement and Effects of an Unstable Tropical Air Mass Aloft over the Far West. BAMS, Vol. 18, Nov. 1937, pp. 360-364

14. Blake, Dean: On the Origin of Tropical Air near the Western American Mainlands. BAMS, Vol. 20, Nov. 1939, pp. 385-389

15. Blake, Dean: Sonora Storms. MWR, Vol. 51, Nov. 1923, pp. 585-588

16. Blochman, L. E.: Five Years of Ocean Mapping and Its Forecast Value. MWR, Vol. 56, Aug. 1928, pp. 315-317

17. Bowie, E. H.: The West Coast Atmospheric Fault. MWR, Vol. 57, Aug. 1929, pp. 332-334

18. Byers, H. R.: The Air Masses of the North Pacific. Scripps Inst. of Oceanography, Tech. Series, Vol. 3, No. 14, pp. 311-354, 1934

19. Byers, H. R.: Characteristic Weather Phenomena of California.

M.I.T., Meteorological Papers, Vol. 1, No. 2, Cambridge, Mass., 1931

20. Byers, H. R.: On the Thermodynamic Interpretation of Isentropic Charts. MWR, Vol. 66, March 1938, pp. 63-68

21. Byers, H. R.: Summer Sea Fogs of the Central California Coast. Univ. of Calif. Geog. Pub., Vol. 3, No. 5, pp. 291-338, 1930

22. Byers, H. R.: Synoptic and Aeronautical Meteorology. McGraw-Hill Co., N.Y., 1937

23. Carpenter, Ford A.: Notes on the Hot Wave in Southern California, June 14-17, 1917. MWR, Vol. 45, Aug. 1917, pp. 408-410

24. Day, John A.: Aviation Wind Forecasts over the Pacific. BAMS, Vol. 20, Oct. 1939, pp. 340-345

25. Dines, W. H.: The Vertical Temperature Distribution in the Atmosphere over England and Some Remarks on the General and Local Circulation. Philos. Trans. Royal Society of London, Series A, Vol. 211, pp. 253-278

26. Fletcher, E. H.: Floods in the Sacramento Valley during April 1935. MWR, Vol. 63, April 1935, pp. 135-137

27. Fletcher, E. H.: Floods in the Sacramento Valley, California, December 1937. MWR, Vol. 65, Dec. 1937, pp. 441-444

28. Fletcher, E. H.: Floods in the Sacramento Valley, California, February 27-March 6, 1940, MWR, Vol. 68, March 1940, pp. 71-74

29. Fletcher, E. H.: Melting Snow as a Flood Factor in the Sierra Nevada. BAMS, Vol. 21, No. 2, Feb. 1940, p. 59

30. French, G. M.: Windstorm in the Los Angeles Area, November 22, 1930 and Some Effects of Wind Flow in a Mountainous Region. MWR, Vol. 59, June 1931, pp. 223-225

31. Glassford, W. A.: Weather Types on the Pacific Coast. Calif. State Society Transactions, 1886, pp. 407-413

32. Gregg, W. R.: The Captive Balloon and Mountain Observations on and near Mt. Whitney, MWR, Vol. 42, July 1914, pp. 419-424

33. Grunsky, C. E.: Tulare Lake, A Contribution to Long Time Weather History. MWR, Vol. 58, July 1930, pp. 288-290

34. Hamrick, A. H.: Cumulus Clouds of Hawaii. MWR, Vol. 46, Sept. 1918, pp. 415-417

35. Harney, P. J.: Note on H. C. Huang's Investigation of Frontogenesis in the North Pacific. MWR, Vol. 65, Sept. 1937, pp. 335-337

36. Henry, A. J.: The Density of Snow. MWR, Vol. 45, March 1917, p. 102

37. Henry, A. J.: Extraordinary April Rains in California. MWR, Vol. 54, April 1926, p. 167

38. Henry, A. J.: The Disappearance of Snow in the High Sierra Nevada of California. MWR, Vol. 44, March 1916, pp. 151-153

39. Henry, A. J.: Increase of Precipitation with Altitude. MWR, Vol. 47, Jan. 1919, pp. 33-41

40. Henry, A. J.: Seasonal Forecasting of Precipitation -- Pacific Coast. MWR, Vol. 49, April 1921, pp. 213-219

41. Henry, A. J.: The Winds of the Middle and Northern California Coast. MWR, Vol. 54, Jan. 1926, pp. 3-5

42. Henry, A. J.: The Winter Anticyclone of the Great Basin. MWR, Vol. 56, April 1928, pp. 125-128

43. Hoge, Wendell P.: Great Rainstorm at Mt. Wilson, December 17-21, 1921. MWR, Vol. 49, Dec. 1921, p. 660

44. Hoyt, W. G.: Factors Influencing Runoff During the Flood of December

1937 in Northern California. TAGU, July 1941, pp. 124-129

45. Hubbard, W. F.: The Relation of Forest to Rainfall. MWR, Vol. 34, Jan. 1906, pp. 24-26

46. Jones, J. M.: Prediction of Seasonal Precipitation in California. MWR, Vol. 59, Feb. 1931, p. 82

47. Knight, W. H.: Handbook Almanac For the Pacific States. An Official Register of Business Directory, 1863. H. H. Bancroft and Co., San Francisco

48. Langbein, W. B.: Some Channel Storage Studies and their Application to the Determination of Infiltration. TAGU, 1938, Part 1, pp. 435-447

49. Lee, Charles H.: Precipitation and Altitude in the Sierra. MWR, Vol. 39, July 1911, pp. 1092-1099

50. Light, P.: Analysis of High Rates of Snow Melting. Technical Paper No. 1, Hydrometeorological Section, Appendix to Pittsburgh Report (2) of Hydrometeorological Section, U. S. Weather Bureau

51. Light, P.: Analysis of High Rates of Snow-Melting. TAGU, July 1941, pp. 195-205

52. Little, D. M.: Some Effects of California Mountain Barriers on Upper Air Winds and Sea-Level Isobars. MWR, Vol. 59, October 1931, pp. 376-380

53. Logan, T. M.: Meteorological Abstract of Observations made during the Years 1853, 1854 and 1855 at Sacramento, Calif. Smithsonian Inst. Annual Report 1855, Washington, 1856

54. McAdie, A. G.: Climatology of California. U. S. Weather Bureau, Bulletin L, 1903

55. McAdie, A. G. and Thomas, W. W.: High Winds at Point Reyes, Calif.

MWR, Vol. 31, May 1903, p. 227

56. McAdie, A. G.: Rainfall of California. U. of California Geographic Pub., Vol. 1, No. 4, Feb. 1914, pp. 127-240

57. McAdie, A. and Thomas, W. W.: Some High Wind Records on the Pacific Coast. MWR, Vol. 31, Feb. 1903, pp. 64-68

58. McAdie, A. G.: Rainfall Variation with Elevation in Sacramento Valley. Principles of Aerography, pp. 211-214, Rand McNally and Co., Chicago, 1917

59. McDonald, W. F. (Editor): Atlas of Climatic Charts of the Oceans. U. S. Weather Bureau, 1938

60. McEwen, G. F.: Ocean Temperatures and Seasonal Rainfall in Southern California. MWR, Vol. 53, Nov. 1925, pp. 483-489

61. McEwen, G. F.: Oceanic Circulation and its Bearing upon Attempts to Make Seasonal Weather Forecasts. Scripps Inst. for Biological Research, Univ. of California, Bulletin No. 7, Nov. 8, 1918

62. McEwen, G. F.: Peculiarities of the California Climate. MWR, Vol. 42, Jan. 1914, pp. 14-23

63. McEwen, G. F.: Quarterly Forecasts of Sea and Air Temperatures. MWR, Vol. 62, Oct. 1934, pp. 361-364

64. McEwen, G. F. and Ritter, W. E.: Ocean Temperatures and Seasonal Weather in Southern California. MWR, Vol. 46, Nov. 1918, p. 512

65. McGlashan, H. D. and Briggs, R. C.: Floods of December 1937 in Northern California. Water Supply Paper 843, U. S. Geological Survey

66. Meyer, O. H.: Flood-routing on the Sacramento River. TAGU, July 1941, pp. 118-124

67. Palmer, A. H.: Fog Along the California Coast. MWR, Vol. 45,

Oct. 1917, pp. 496-499

68. Palmer, A. H.: Region of Greatest Snowfall. MWR, Vol. 43, May 1915, pp. 217-221

69. Paulson, J. B., Jr.: Storm Characteristics of the Sacramento Basin. TAGU, July 1941, pp. 111-117

70. Parsons, W. J., Jr.: Potential Floods in the Sacramento Valley. TAGU, July 1941, pp. 106-110

71. Petterssen, S.: On the Causes and the Forecasting of the California Fog. BAMS, Vol. 19, Feb. 1938, pp. 49-55

72. Petterssen, S.: Weather Analysis and Forecasting. McGraw-Hill Co., New York, 1940

73. Pockels, F.: The Theory of the Formation of Precipitation on Mountain Slopes. MWR, Vol. 29, April 1901; also found in Mechanics of the Earth's Atmosphere, C. Abbe, editor, Smithsonian Institution, Third Collection, 1910

74. Pockels, F.: Supplementary Remarks by Professor Pockels on the Theory of the Formation of Rain on Mountain Slopes. MWR, Vol. 29, July 1901; also found in Mechanics of the Earth's Atmosphere, C. Abbe, editor, Smithsonian Institution, Third Collection, 1910

75. Reed, T. R.: The North American High-Level Anticyclone. MWR, Vol. 61, Nov. 1933, pp. 321-325

76. Reed, T. R.: Further Observations on the North American High-Level Anticyclone. MWR, Vol. 65, Oct. 1937, pp. 364-366

77. Reed, T. R.: Rain-Bearing Winds in the Far Western States. MWR, Vol. 55, May 1927, pp. 228-233

78. Reed, T. R.: Some Aspects of Free-Air Winds in the Far West. MWR,

Vol. 61, Feb. 1933, pp. 42-43

79. Reed, T. R.: Weather Types of the Northeast Pacific Ocean as Related to Weather of the North Pacific Coast. MWR, Vol. 60, Dec. 1932, pp. 246-252

80. Reed, W. G.: Rainfall Data of Berkeley, California. MWR, Vol. 44, March 1916, pp. 123-125

81. Reed, W. G.: The Japan Current and the Climate of California. MWR, Vol. 42, Feb. 1914, pp. 100-101

82. Richardson, R. W.: Winter Air-Mass Convergence over the North Pacific. MWR, Vol. 64, June 1936, pp. 199-203

83. Rossby, C. G.: Scientific Basis of Modern Meteorology. Climate and Man, 1941 Yearbook of Agriculture, U. S. Dept. of Agriculture, pp. 599-655

84. Rugen, O. N.: The Snow Melt Problem as Affecting the Design of Flood Control Works. TAGU, 1940, Part 3, pp. 1033-1046

85. Russell, R. J.: Climate of California. Univ. of California, Geog. Pub., 1926

86. Scarr, J. H.: Flood of March 1907. MWR, Vol. 35, March 1907, pp. 107-108

87. Showalter, A. K.: Frontal Movements Contrary to Indicated Gradient Flow Produced by Minor Waves. MWR, Vol. 68, June 1938, pp. 165-174

88. Showalter, A. K.: Relationship of Low Temperatures Aloft to Precipitation. TAGU, August 1939, pp. 352-353

89. Solot, S. B.: Computation of Depth of Precipitable Water in a Column of Air. MWR, Vol. 67, April 1939, pp. 100-103

90. Sprague, M.: Climate of California. Climate and Man, 1941 Yearbook

of Agriculture, U. S. Department of Agriculture, pp. 783-797

91. Sprague, M.: Monthly and Seasonal Distribution of Snowfall in California. MWR, Vol. 62, Dec. 1934, pp. 438-441

92. Stewart, G. R.: Storm (a novel). Random House, New York, 1941

93. Taylor, G. F.: Aeronautical Meteorology. Pitman Publishing Co., N. Y., 1938

94. Taylor, N. R.: The Rivers and Floods of the Sacramento and San Joaquin Watersheds. U. S. Weather Bureau Bulletin, No. 43, 1913

95. Taylor, N. R.: Floods of March 1928 in the Sacramento Valley. MWR, Vol. 56, March 1928, pp. 100-102

96. Thiessen, A. H.: Precipitation Averages for Large Areas. MWR, Vol. 39, July 1911

97. Thompson and West (Pub.): History of Sacramento County, California; George F. Wright, Ed. Oakland, 1880.

98. Tsukuda, K.: On the Mean Atmospheric Pressure, Cloudiness, and Sea Surface Temperature of the North Pacific Ocean. Memoirs of the Imperial Marine Observatory, Vol. 2, No. 4, Kobe, Japan.

99. U. S. Engineer Dept.: Sacramento River and Valley. Partial Report on Sacramento, San Joaquin, and Kern Rivers, California, covering Navigation, Flood Control, Power Development, and Irrigation, with Bibliography. February 27, 1931. (U. S. 71st Cong., 3d Sess. House Doc. 791. Ser. 9387. Vol. 37)

100. U. S. Engineer Dept.: Sacramento, San Joaquin, and Kern Rivers, California. Letter submitting Final Report, containing General Plan for Improvement of Sacramento, San Joaquin, and Kern Rivers, California, for Purpose of Navigation and Efficient Development of

its Water Power Control of Floods, and Needs of Irrigation. 1934. (U. S. 73d Cong., 2d Sess. House Doc. 191. Ser. 9833. Vol. 29)

101. U. S. Rivers and Harbors Board: Sacramento, San Joaquin, and Kern Rivers, California. Report on Review of Reports heretofore submitted, on Sacramento, San Joaquin, and Kern Rivers, California. March 27, 1934. With Report of Thomas M. Robins. 1934. (Rivers and Harbors Committee, U. S. 73d Cong., 1st Sess. House Doc. 35)

102. U. S. Rivers and Harbors Board: Sacramento River and Tributaries, California (Debris Control). Report on Revision of Reports heretofore submitted on Sacramento River and Tributaries. May 23, 1935. With Report of California Debris Commission, 1935. (Rivers and Harbors Committee, U. S. 74th Cong., 1st Sess. House Doc. 50)

103. Varney, B. M.: Daytime Wind Turbulence in a Mountain Valley. MWR, Vol. 48, June 1920, p. 336

104. Varney, B. M.: Monthly Variations of the Precipitation-Altitude Relation in the Central Sierra Nevada of California. MWR, Vol. 48, Nov. 1920, pp. 648-650

105. Varney, B. M.: Seasonal Precipitation in California and its Variability. MWR, Vol. 53, April 1925, pp. 148-163

106. Ward, R. DeC.: Some Characteristics of the Rainfall of the United States. MWR, Vol. 47, September 1919, pp. 631-632

107. Wexler, H.: Some Causes and Consequences of Dynamic Anticyclones. Paper delivered before the Washington, D. C. Chapter, American Meteorological Society, Jan. 23, 1942 (unpublished)

108. Willett, H. C.: Ground Plan of a Dynamic Meteorology. MWR, Vol. 59, June 1931, pp. 219-223

109. Willis, W. L.: History of Sacramento County, California. Historic Records Co., Los Angeles. 1913

110. Wilson, W. T.: An Outline of the Thermodynamics of Snow Melt. TAGU, July 1941, p. 182

111. Wright, H. H.: Certain Characteristics of the Winds at Mt. Tamalpais. MWR, Vol. 44, Sept. 1916, pp. 512-514

112. Wright, H. H.: Fog in Relation to Wind Direction at Mt. Tamalpais. MWR, Vol. 44, June 1916, pp. 342-344

113. Wyatt, B. H.: Temperature and Humidity of the Upper Air at San Diego. MWR, Vol. 53, August 1925, p. 349

APPENDIX

SYNOPTIC WEATHER CHARTS

SYMBOLS USED ON SYNOPTIC CHARTS

STATION MODEL (SPECIMEN OBSERVATIONS)

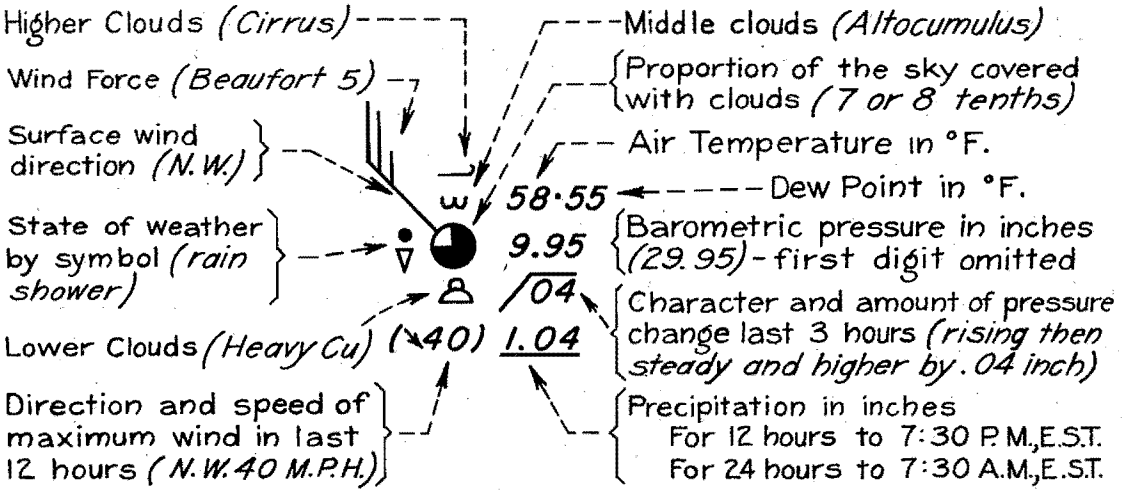

EXCEPTIONS FOR SHIP REPORTS:

Maximum wind not reported.
Dew Point replaced by Wet Bulb Temperature in parenthesis.
Amount of precipitation replaced by Temperature (°F.) of sea surface.

SYMBOLS FOR STATE OF WEATHER

- • *Rain*
- , *Drizzle*
- ✳ *Snow*
- ▲ *Sleet*
- △ *Hail*

Number of symbols indicates relative intensity of precipitation

- ⍱ *Thunderstorm*
- ∞ *Hazy*

- ⛆ *Rain shower*
- ⛇ *Snow shower*
- ∧ *Squally*
- ⩓ *Severe Squalls*
- = *Light to Moderate Fog*
- ≡ *Dense Fog*
- ≡ *Ground Fog*

NOTE:

On maps after June 30, 1939, barometric pressure and amount of pressure change are entered in millibars and tenths; e.g. *1011.2 mbs.* entered as *11.2* and *989.6 mbs.* as *89.6*

BEAUFORT SCALE

FORCE	SYMBOL	M.P.H.	FORCE	SYMBOL	M.P.H.	FORCE	SYMBOL	M.P.H.
0	◎	Less than 1	4		13 to 18	9		47 to 54
1		1 to 3	5		19 to 24	10		55 to 63
2		4 to 7	6		25 to 31	11		64 to 75
3		8 to 12	7		32 to 38	12		above 75
			8		39 to 46			

FIGURE 68 A

UPPER FRONTS

SURFACE FRONTS

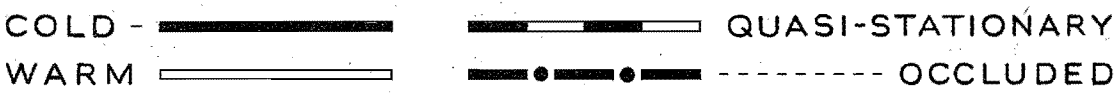

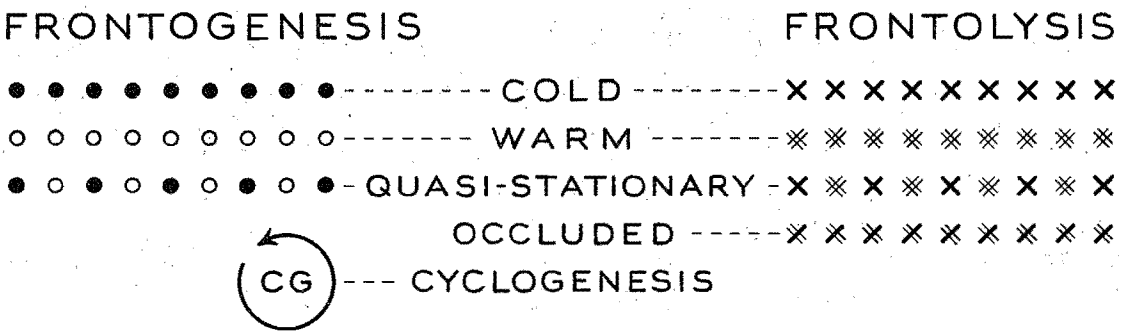

AIR MASSES *

cAw - CONTINENTAL ARCTIC AIR, warmer than the surface over which it lies *(stable in the lower layers).*

cAk - CONTINENTAL ARCTIC AIR, colder than the surface over which it is passing *(steep lapse rate in the lower layers)*

mAk - MARITIME ARCTIC AIR, colder than the surface over which it is passing *(steep lapse rate).*

cPw - CONTINENTAL POLAR AIR, warmer than the surface over which it is passing *(stable in the lower layers).*

cPk - CONTINENTAL POLAR AIR, colder than the surface over which it is passing *(steep lapse rate).*

mPw - MARITIME POLAR AIR, warmer than the surface over which it is passing *(stable in the lower layers).*

mPk - MARITIME POLAR AIR, colder than the surface over which it is passing *(steep lapse rate).*

mTw - MARITIME TROPICAL AIR, warmer than the surface over which it is passing *(stable in the lower layers).*

mTk - MARITIME TROPICAL AIR, colder than the surface over which it lies or is passing *(steep lapse rate).*

S --- SUPERIOR AIR, which includes all air masses that appear warm and very dry because of, principally, subsidence and divergence.

** SEE MONTHLY WEATHER REVIEW, VOL. 67, JULY 1939, pp. 204-218.*

FIGURE 68 B

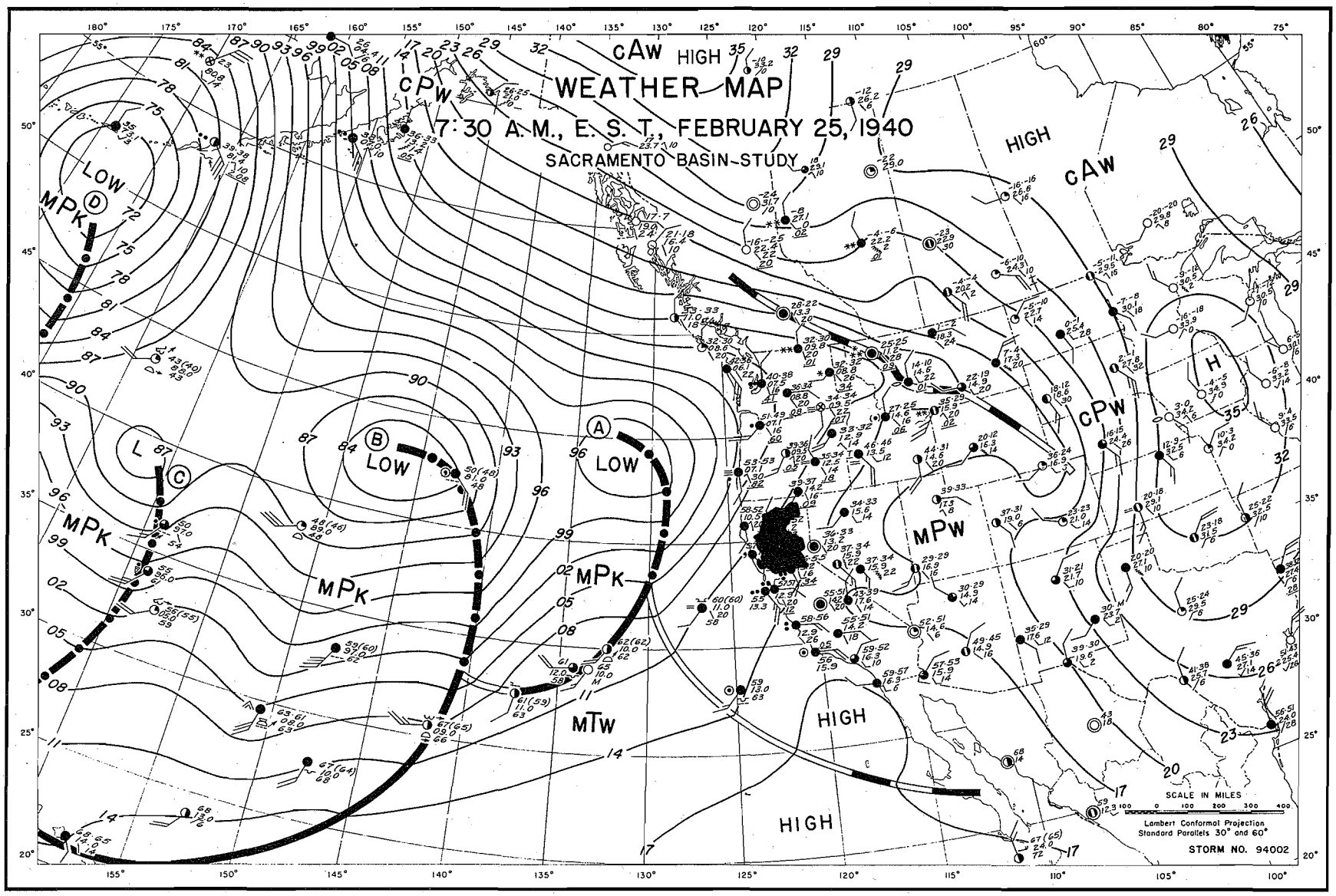
WEATHER MAP
7:30 A.M., E.S.T., FEBRUARY 25, 1940
SACRAMENTO BASIN-STUDY
cAw
HIGH
cPw
LOW
MPk
MPw
MTw
HIGH
SCALE IN MILES
Lambert Conformal Projection
Standard Parallels 30° and 60°
STORM NO. 94002

FIGURE 69

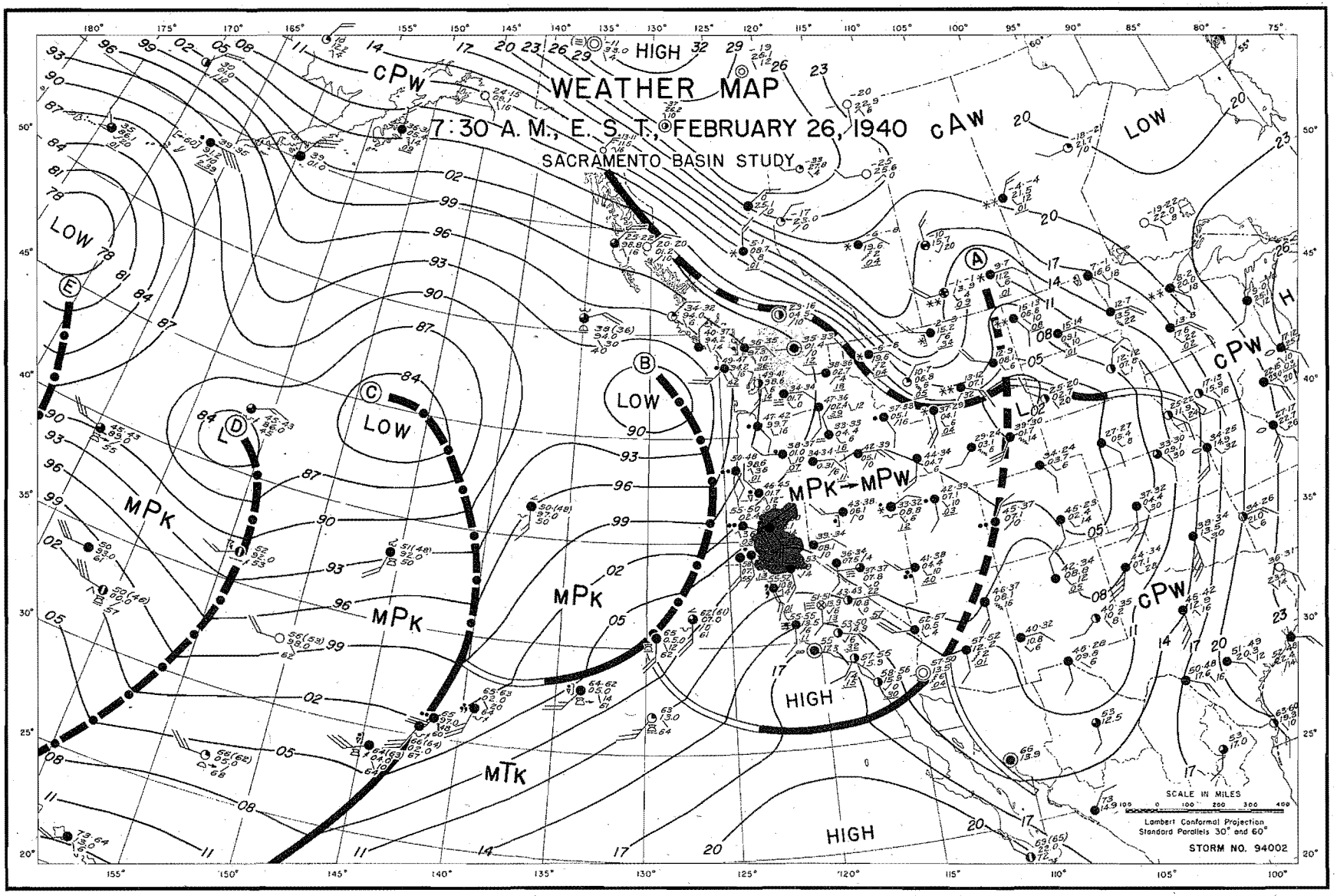
WEATHER MAP
7:30 A. M., E. S. T., FEBRUARY 26, 1940
SACRAMENTO BASIN STUDY
HIGH
LOW
LOW
LOW
LOW
HIGH
HIGH
cPw
cAw
MPk
MPk
MPk
MPk
MPk–MPw
MTk
cPw
cPw
SCALE IN MILES
Lambert Conformal Projection
Standard Parallels 30° and 60°
STORM NO. 94002

FIGURE 70

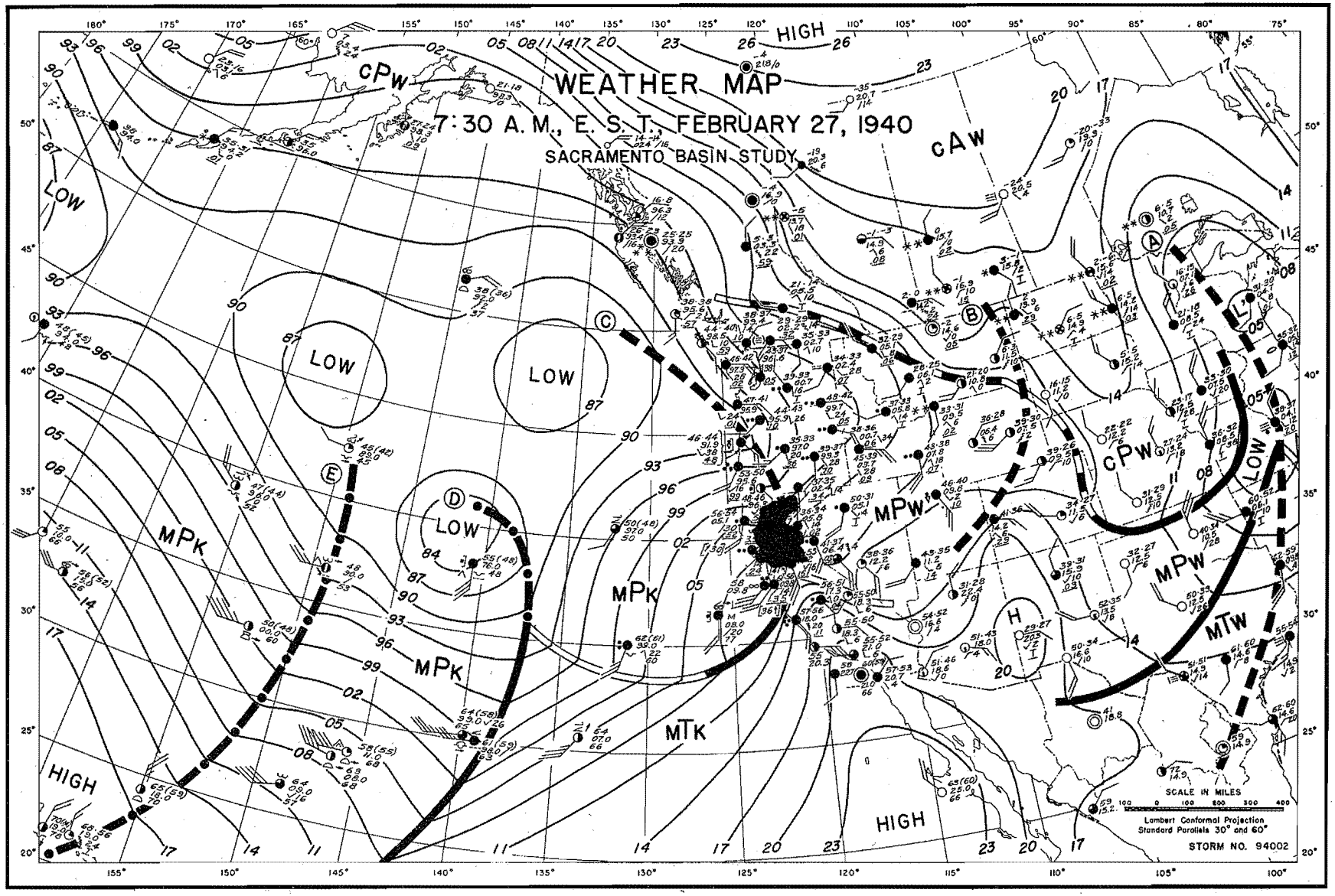
WEATHER MAP
7:30 A. M., E. S. T., FEBRUARY 27, 1940
SACRAMENTO BASIN STUDY
HIGH
LOW
LOW
LOW
LOW
HIGH
HIGH
cPw
cAw
cPw
MPw
MPw
MPw
MPk
MPk
MPk
MTk
MTw
SCALE IN MILES
Lambert Conformal Projection
Standard Parallels 30° and 60°
STORM NO. 94002

FIGURE 71

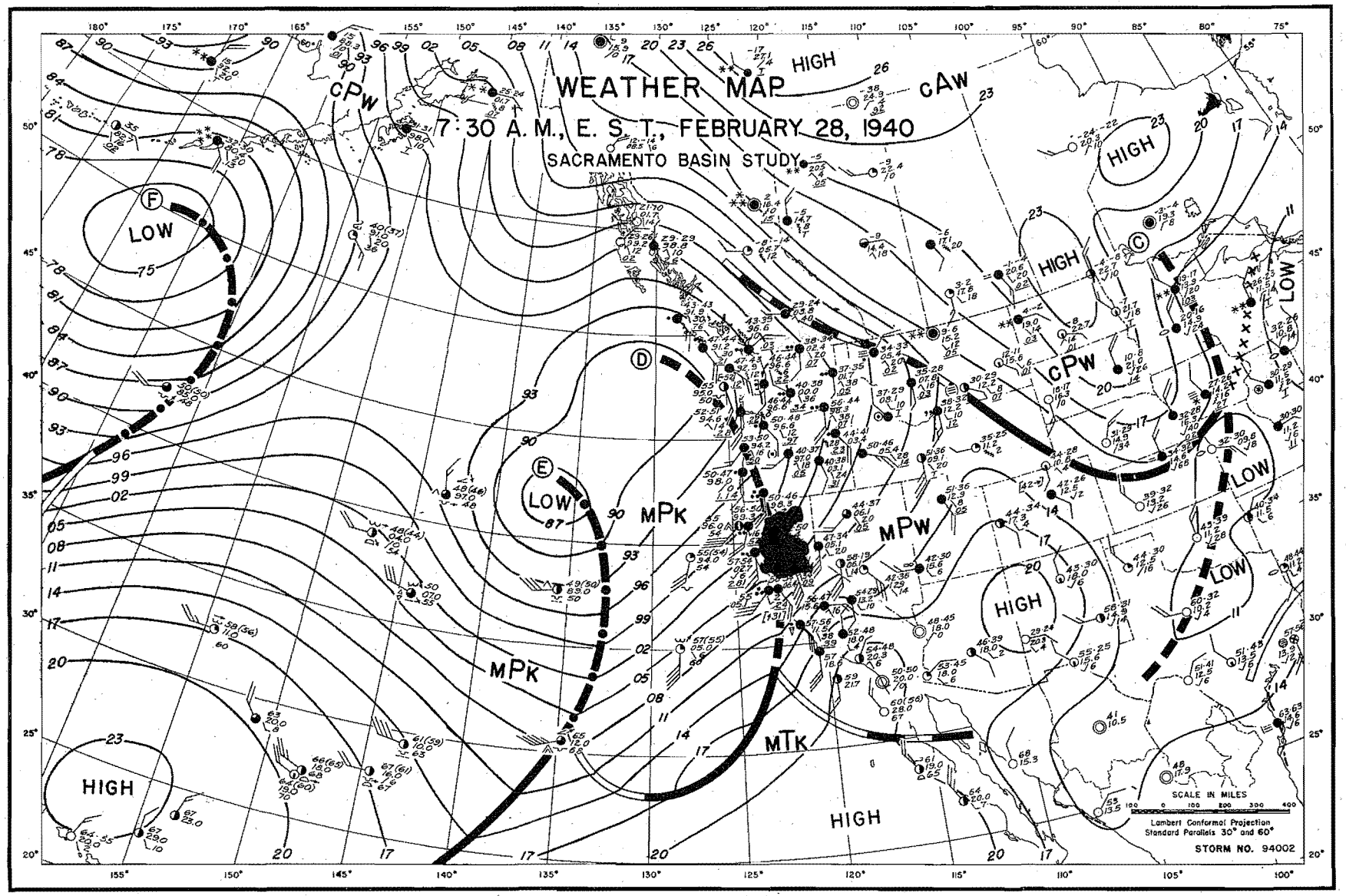
WEATHER MAP
7:30 A.M., E.S.T., FEBRUARY 28, 1940
SACRAMENTO BASIN STUDY
HIGH
cAW
cPW
LOW
MPK
MPW
MTK
SCALE IN MILES
Lambert Conformal Projection
Standard Parallels 30° and 60°
STORM NO. 94002

FIGURE 72

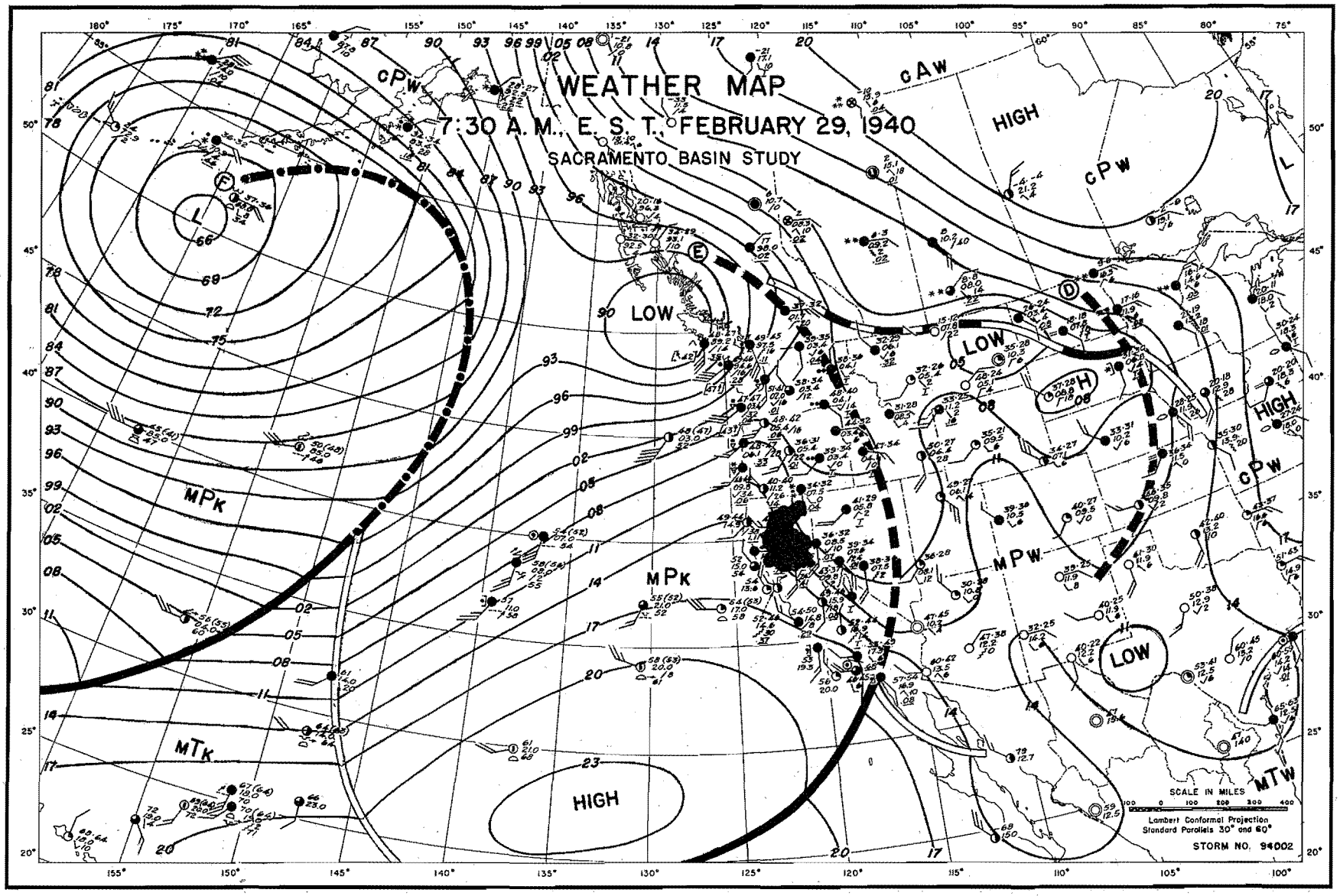
WEATHER MAP
7:30 A. M., E. S. T., FEBRUARY 29, 1940
SACRAMENTO BASIN STUDY
cAW
cPW
HIGH
LOW
MPk
MPw
MTk
MTw
SCALE IN MILES
Lambert Conformal Projection
Standard Parallels 30° and 60°
STORM NO. 94002

FIGURE 73

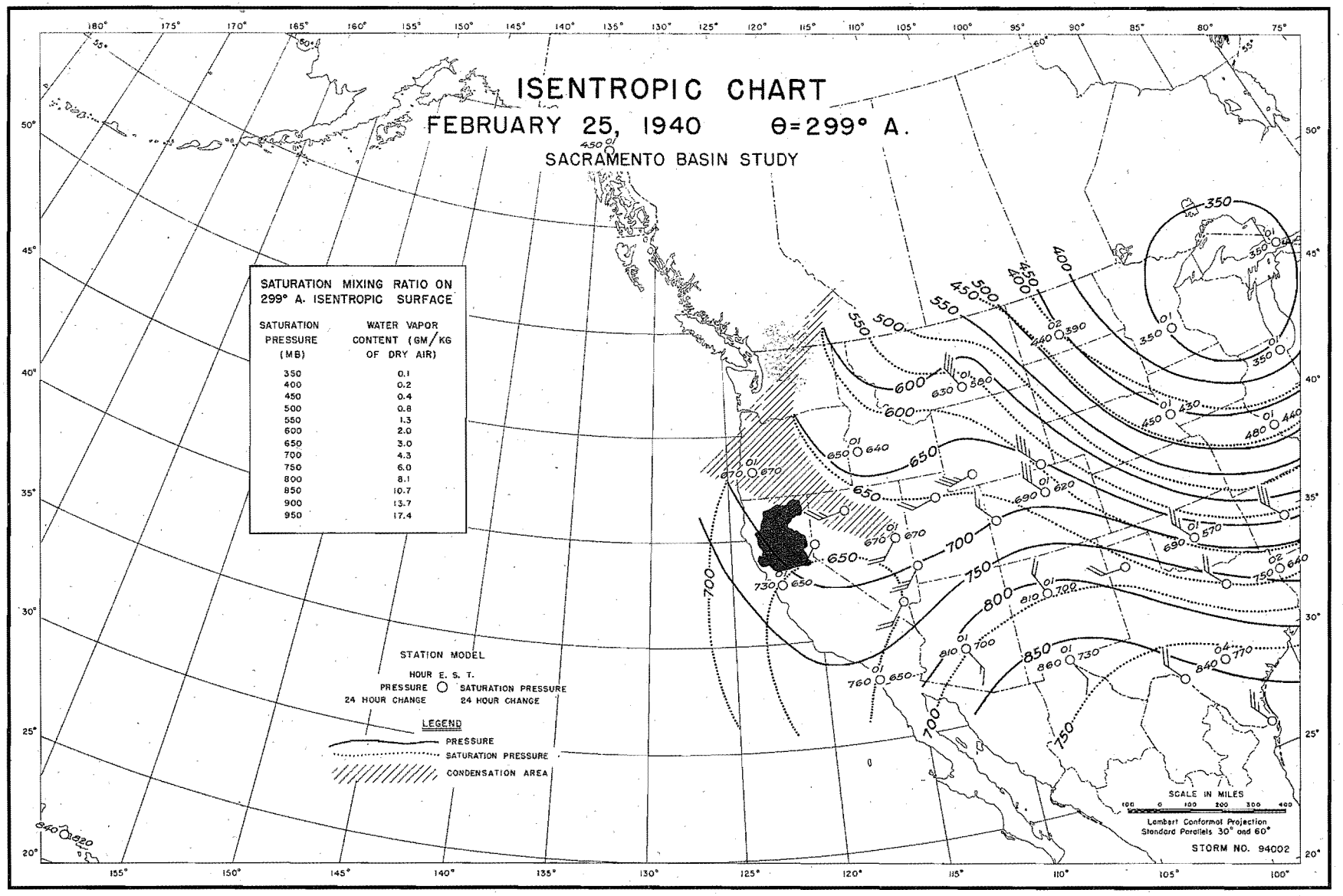
ISENTROPIC CHART
FEBRUARY 25, 1940 θ=299° A.
SACRAMENTO BASIN STUDY
SATURATION MIXING RATIO ON 299° A. ISENTROPIC SURFACE
SATURATION PRESSURE (MB) | WATER VAPOR CONTENT (GM/KG OF DRY AIR)
350 0.1
400 0.2
450 0.4
500 0.8
550 1.3
600 2.0
650 3.0
700 4.3
750 6.0
800 8.1
850 10.7
900 13.7
950 17.4
STATION MODEL
HOUR E. S. T.
PRESSURE ○ SATURATION PRESSURE
24 HOUR CHANGE 24 HOUR CHANGE
LEGEND
PRESSURE
SATURATION PRESSURE
CONDENSATION AREA
SCALE IN MILES
Lambert Conformal Projection
Standard Parallels 30° and 60°
STORM NO. 94002

FIGURE 74

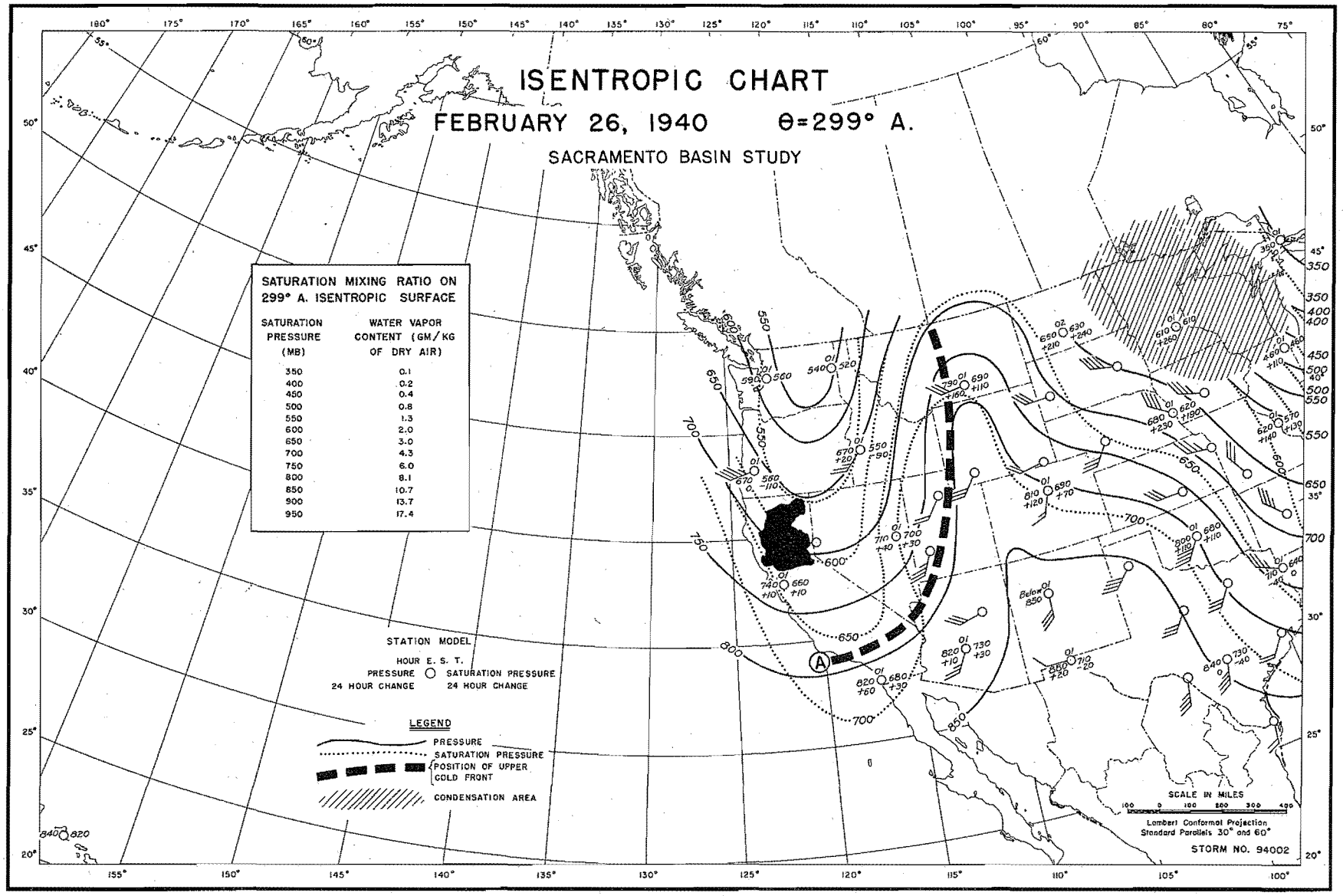
ISENTROPIC CHART
FEBRUARY 26, 1940 θ=299° A.
SACRAMENTO BASIN STUDY
SATURATION MIXING RATIO ON 299° A. ISENTROPIC SURFACE
SATURATION PRESSURE (MB) | WATER VAPOR CONTENT (GM/KG OF DRY AIR)
350 0.1
400 0.2
450 0.4
500 0.8
550 1.3
600 2.0
650 3.0
700 4.3
750 6.0
800 8.1
850 10.7
900 13.7
950 17.4
STATION MODEL
HOUR E. S. T.
PRESSURE ○ SATURATION PRESSURE
24 HOUR CHANGE 24 HOUR CHANGE
LEGEND
PRESSURE
SATURATION PRESSURE
POSITION OF UPPER COLD FRONT
CONDENSATION AREA
SCALE IN MILES
Lambert Conformal Projection
Standard Parallels 30° and 60°
STORM NO. 94002

FIGURE 75

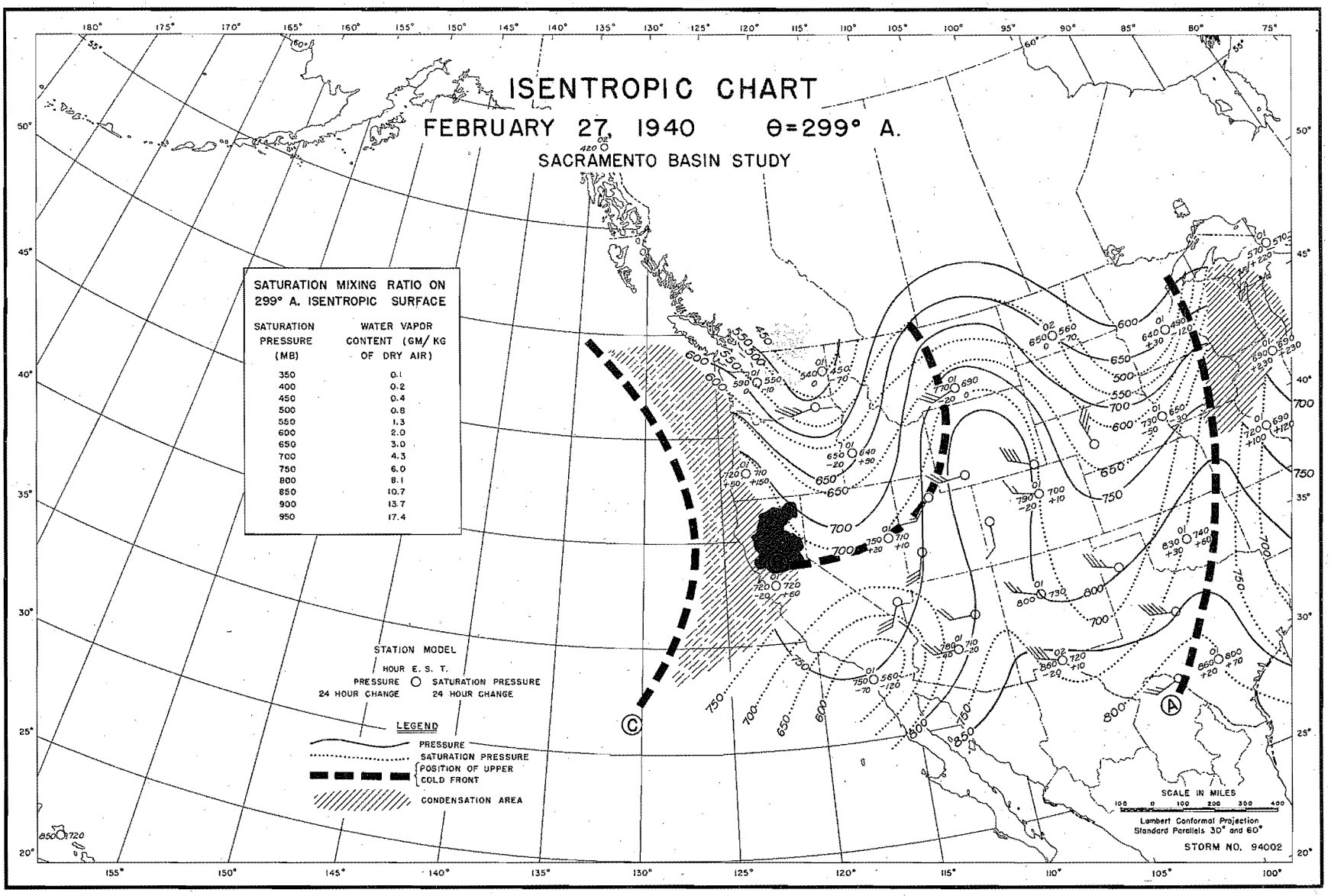
ISENTROPIC CHART
FEBRUARY 27, 1940 θ=299° A.
SACRAMENTO BASIN STUDY
SATURATION MIXING RATIO ON 299° A. ISENTROPIC SURFACE
SATURATION PRESSURE (MB) | WATER VAPOR CONTENT (GM/KG OF DRY AIR)
350 0.1
400 0.2
450 0.4
500 0.8
550 1.3
600 2.0
650 3.0
700 4.3
750 6.0
800 8.1
850 10.7
900 13.7
950 17.4
STATION MODEL
HOUR E. S. T.
PRESSURE SATURATION PRESSURE
24 HOUR CHANGE 24 HOUR CHANGE
LEGEND
PRESSURE
SATURATION PRESSURE
POSITION OF UPPER COLD FRONT
CONDENSATION AREA
SCALE IN MILES
100 0 100 200 300 400
Lambert Conformal Projection
Standard Parallels 30° and 60°
STORM NO. 94002

FIGURE 76

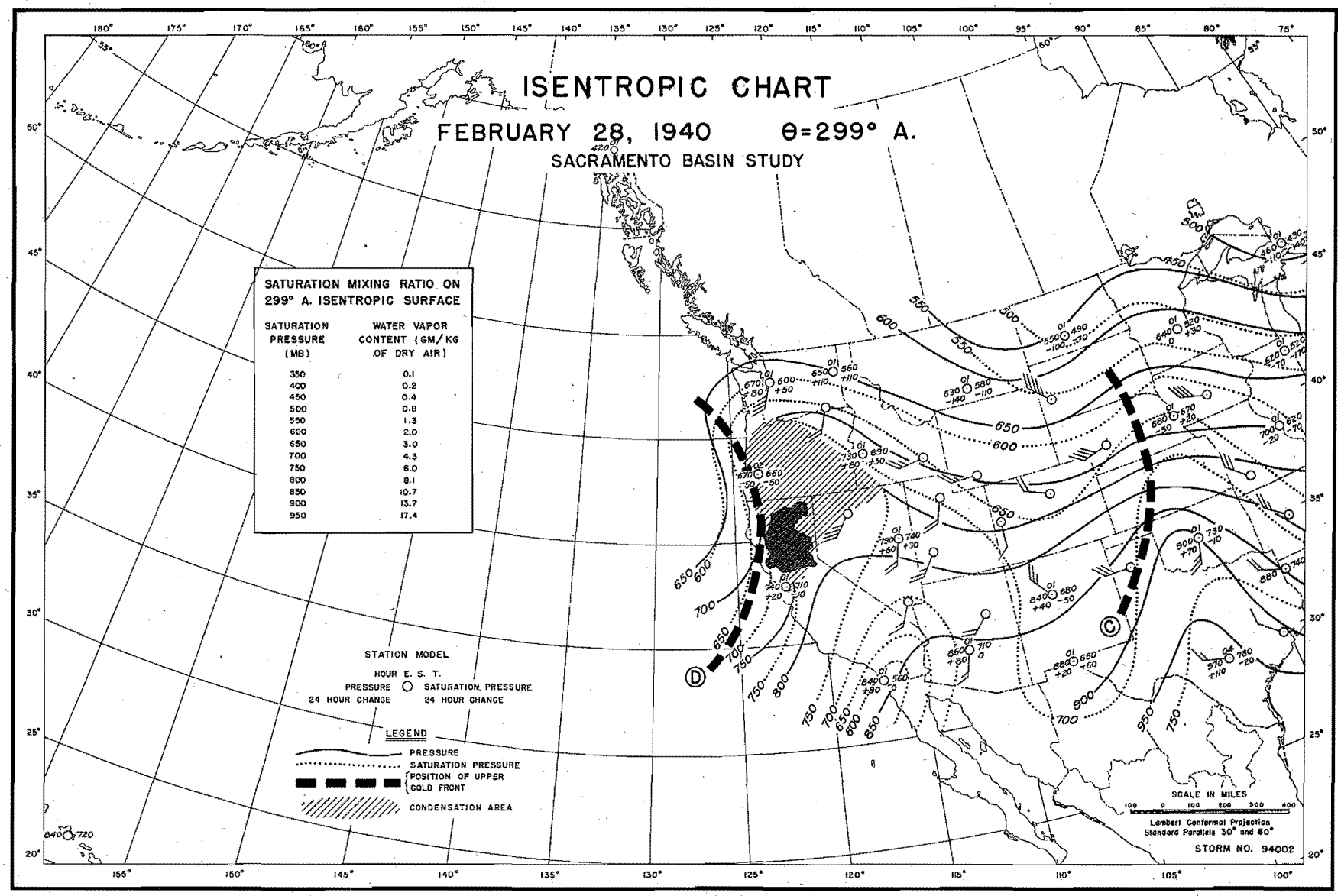
ISENTROPIC CHART
FEBRUARY 28, 1940 θ=299° A.
SACRAMENTO BASIN STUDY
SATURATION MIXING RATIO ON 299° A. ISENTROPIC SURFACE
SATURATION PRESSURE (MB)
WATER VAPOR CONTENT (GM/KG OF DRY AIR)
350 0.1
400 0.2
450 0.4
500 0.8
550 1.3
600 2.0
650 3.0
700 4.3
750 6.0
800 8.1
850 10.7
900 13.7
950 17.4
STATION MODEL
HOUR E. S. T.
PRESSURE
24 HOUR CHANGE
SATURATION PRESSURE
24 HOUR CHANGE
LEGEND
PRESSURE
SATURATION PRESSURE
POSITION OF UPPER COLD FRONT
CONDENSATION AREA
SCALE IN MILES
100 0 100 200 300 400
Lambert Conformal Projection
Standard Parallels 30° and 60°
STORM NO. 94002

FIGURE 77

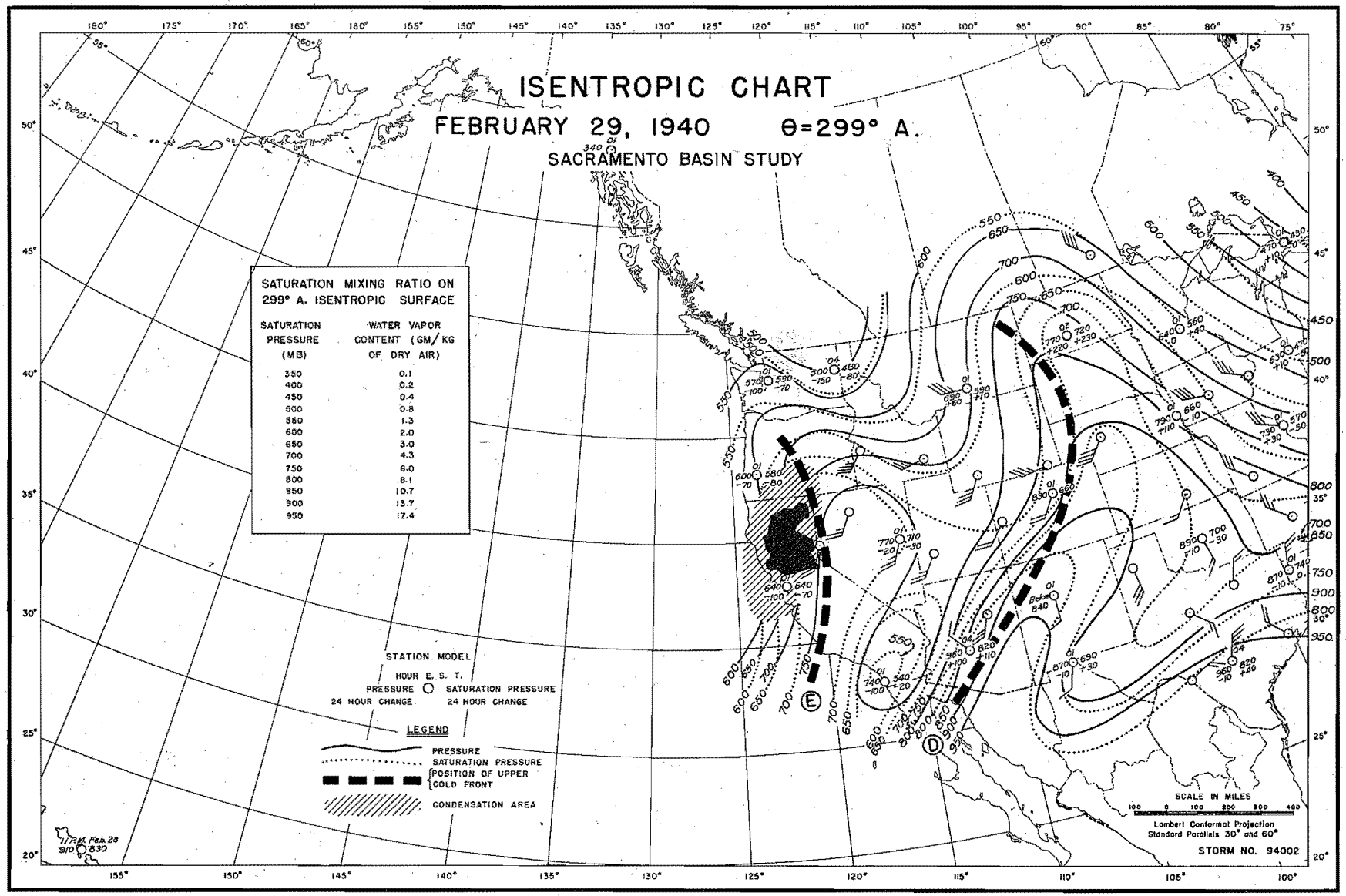
ISENTROPIC CHART
FEBRUARY 29, 1940 θ=299° A.
SACRAMENTO BASIN STUDY
SATURATION MIXING RATIO ON 299° A. ISENTROPIC SURFACE
SATURATION PRESSURE (MB) | WATER VAPOR CONTENT (GM/KG OF DRY AIR)
350 0.1
400 0.2
450 0.4
500 0.8
550 1.3
600 2.0
650 3.0
700 4.3
750 6.0
800 8.1
850 10.7
900 13.7
950 17.4
STATION MODEL
HOUR E. S. T.
PRESSURE ○ SATURATION PRESSURE
24 HOUR CHANGE 24 HOUR CHANGE
LEGEND
PRESSURE
SATURATION PRESSURE
POSITION OF UPPER COLD FRONT
CONDENSATION AREA
SCALE IN MILES
100 0 100 200 300 400
Lambert Conformal Projection
Standard Parallels 30° and 60°
STORM NO. 94002

FIGURE 78

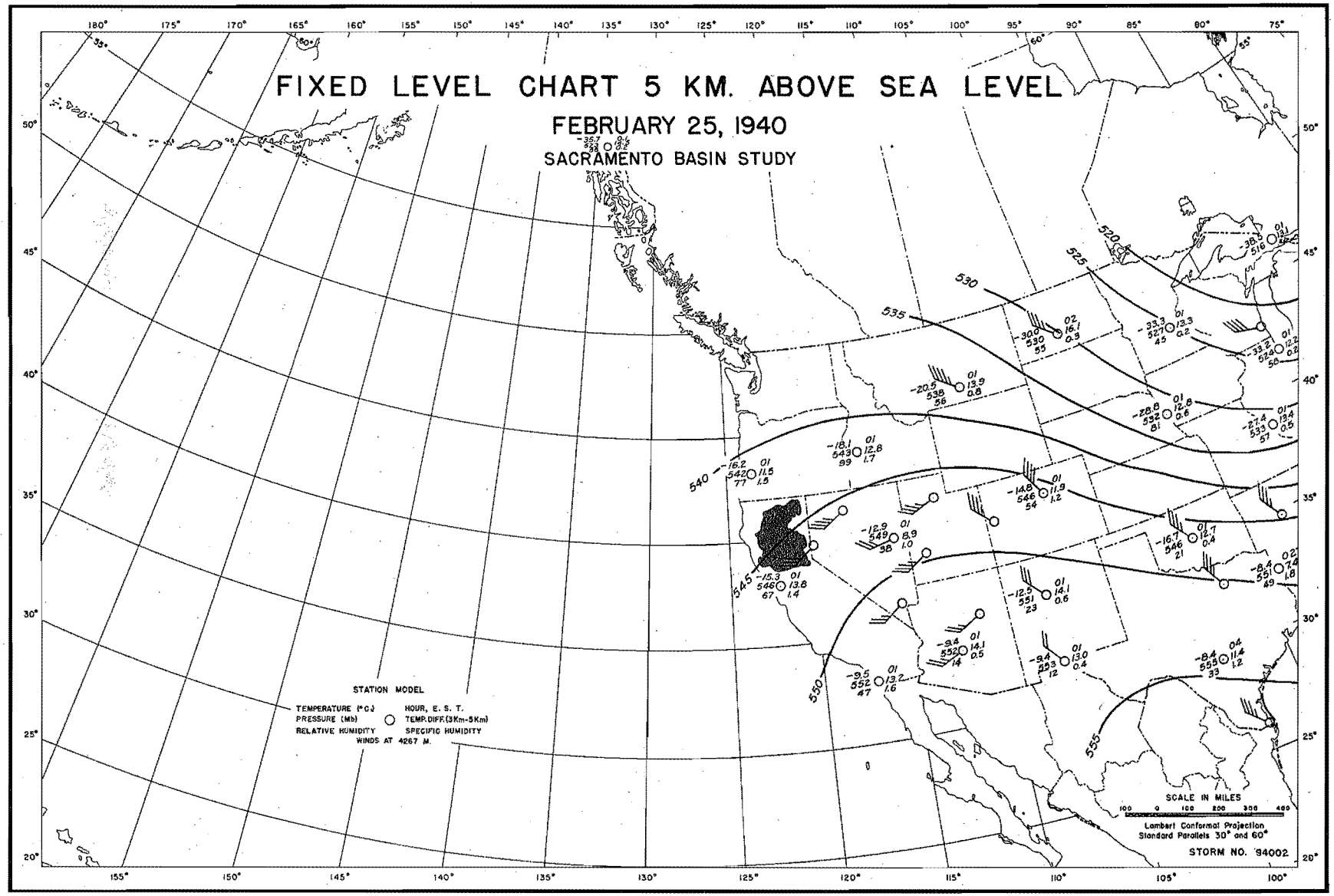
FIXED LEVEL CHART 5 KM. ABOVE SEA LEVEL
FEBRUARY 25, 1940
SACRAMENTO BASIN STUDY
STATION MODEL
TEMPERATURE (°C)
PRESSURE (Mb)
RELATIVE HUMIDITY
HOUR, E. S. T.
TEMP. DIFF. (3Km-5Km)
SPECIFIC HUMIDITY
WINDS AT 4267 M.
SCALE IN MILES
Lambert Conformal Projection
Standard Parallels 30° and 60°
STORM NO. 94002

FIGURE 79

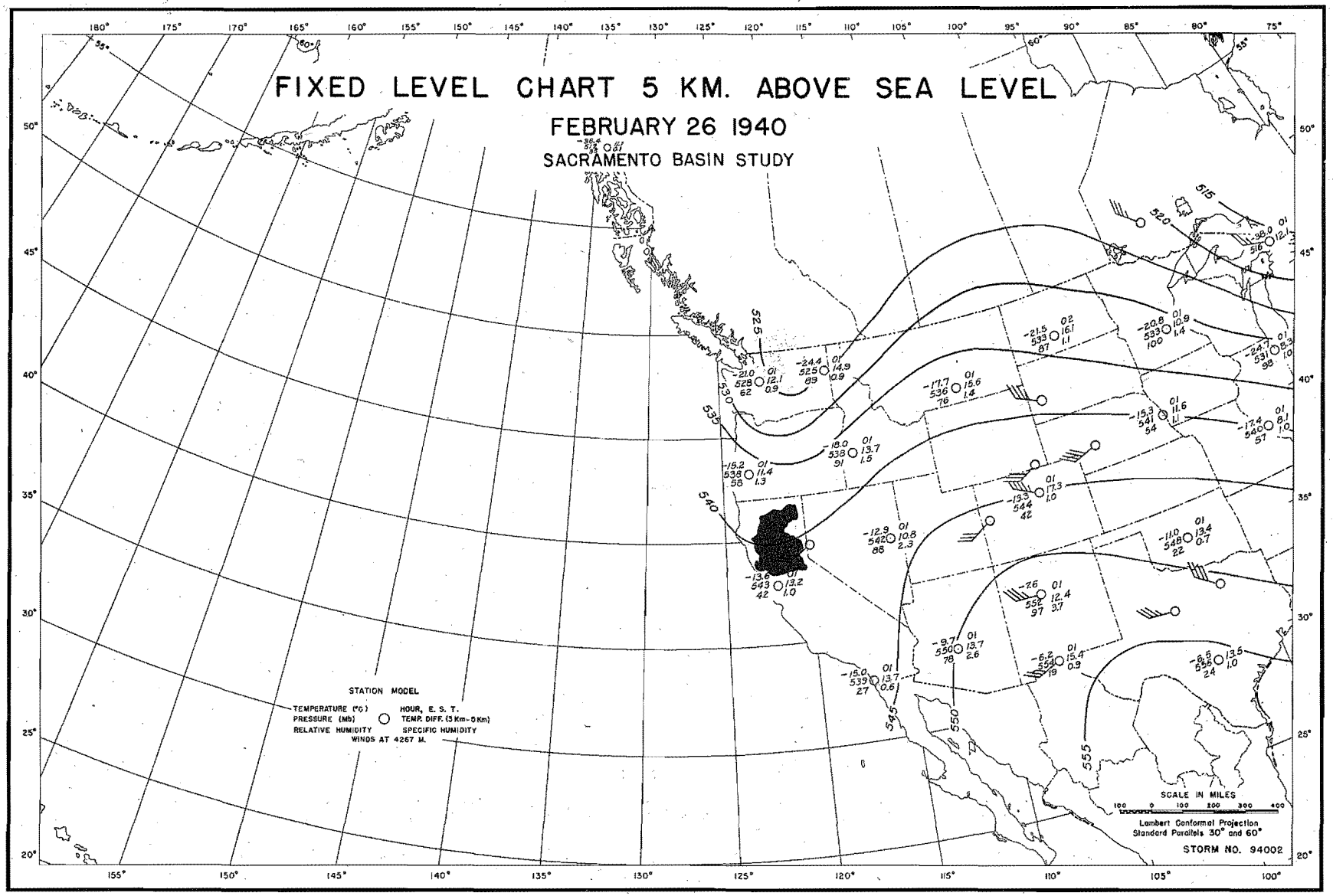
FIXED LEVEL CHART 5 KM. ABOVE SEA LEVEL
FEBRUARY 26 1940
SACRAMENTO BASIN STUDY
STATION MODEL
TEMPERATURE (°C)
PRESSURE (Mb)
RELATIVE HUMIDITY
HOUR, E. S. T.
TEMP. DIFF. (5 Km - 0 Km)
SPECIFIC HUMIDITY
WINDS AT 4267 M.
SCALE IN MILES
100 0 100 200 300 400
Lambert Conformal Projection
Standard Parallels 30° and 60°
STORM NO. 94002

FIGURE 80

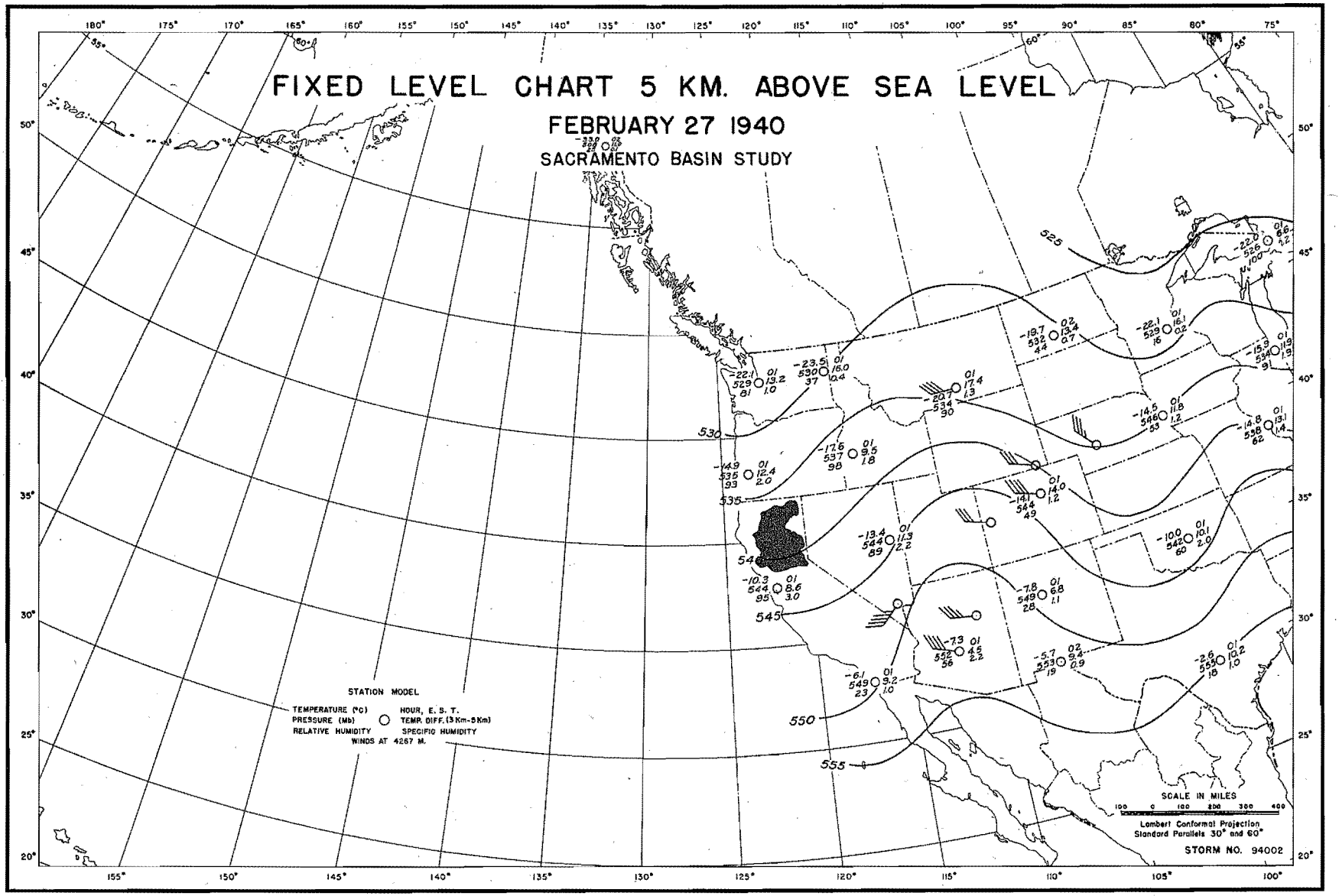
FIXED LEVEL CHART 5 KM. ABOVE SEA LEVEL
FEBRUARY 27 1940
SACRAMENTO BASIN STUDY
525
530
535
540
545
550
555
STATION MODEL
TEMPERATURE (°C)
PRESSURE (Mb)
RELATIVE HUMIDITY
HOUR, E. S. T.
TEMP. DIFF. (3 Km-5 Km)
SPECIFIC HUMIDITY
WINDS AT 4267 M.
SCALE IN MILES
100 0 100 200 300 400
Lambert Conformal Projection
Standard Parallels 30° and 60°
STORM NO. 94002

FIGURE 81

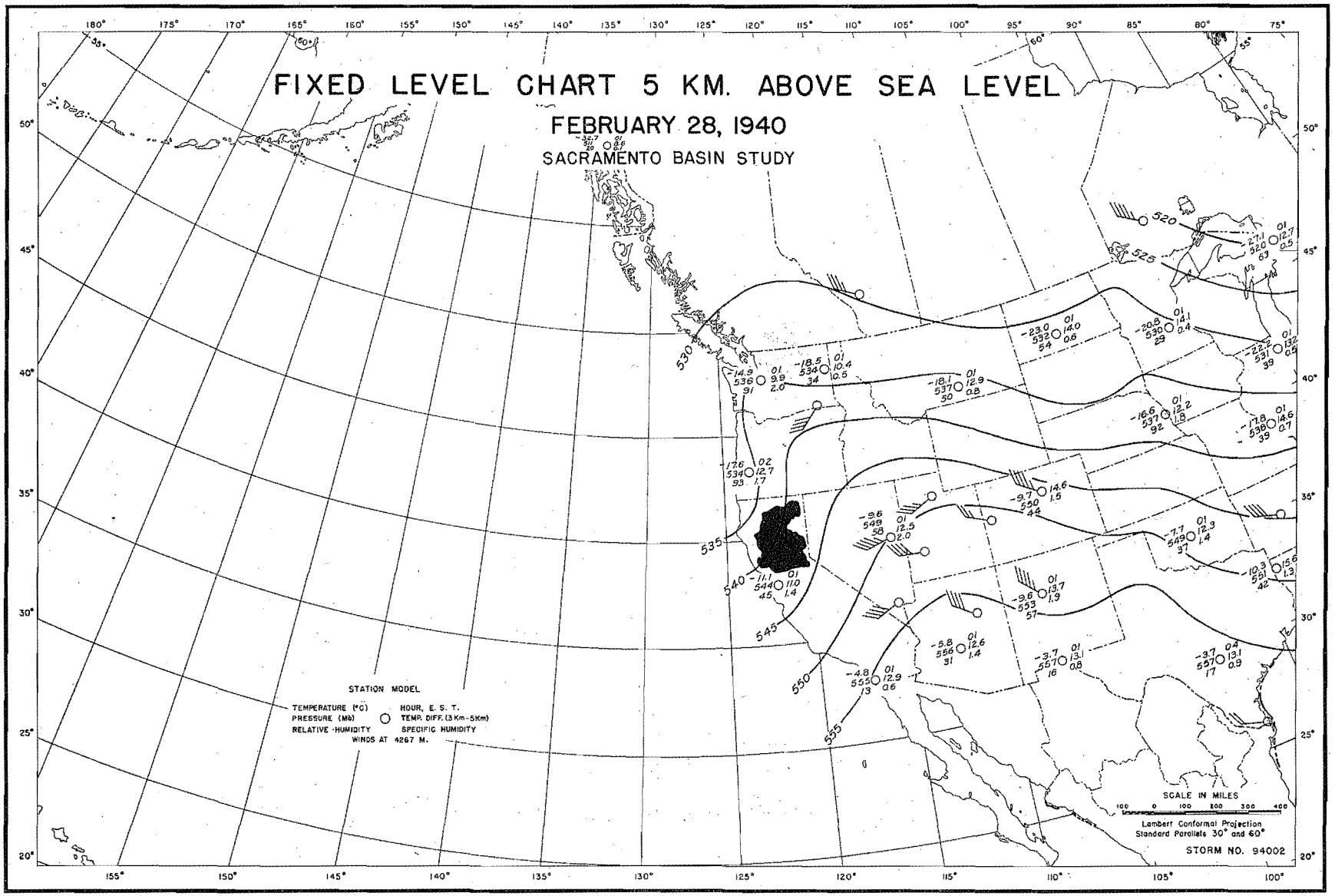
FIXED LEVEL CHART 5 KM. ABOVE SEA LEVEL
FEBRUARY 28, 1940
SACRAMENTO BASIN STUDY
STATION MODEL
TEMPERATURE (°C)
PRESSURE (MB)
RELATIVE HUMIDITY
HOUR, E. S. T.
TEMP. DIFF. (5 Km - SKm)
SPECIFIC HUMIDITY
WINDS AT 4267 M.
SCALE IN MILES
100 0 100 200 300 400
Lambert Conformal Projection
Standard Parallels 30° and 60°
STORM NO. 94002

FIGURE 82

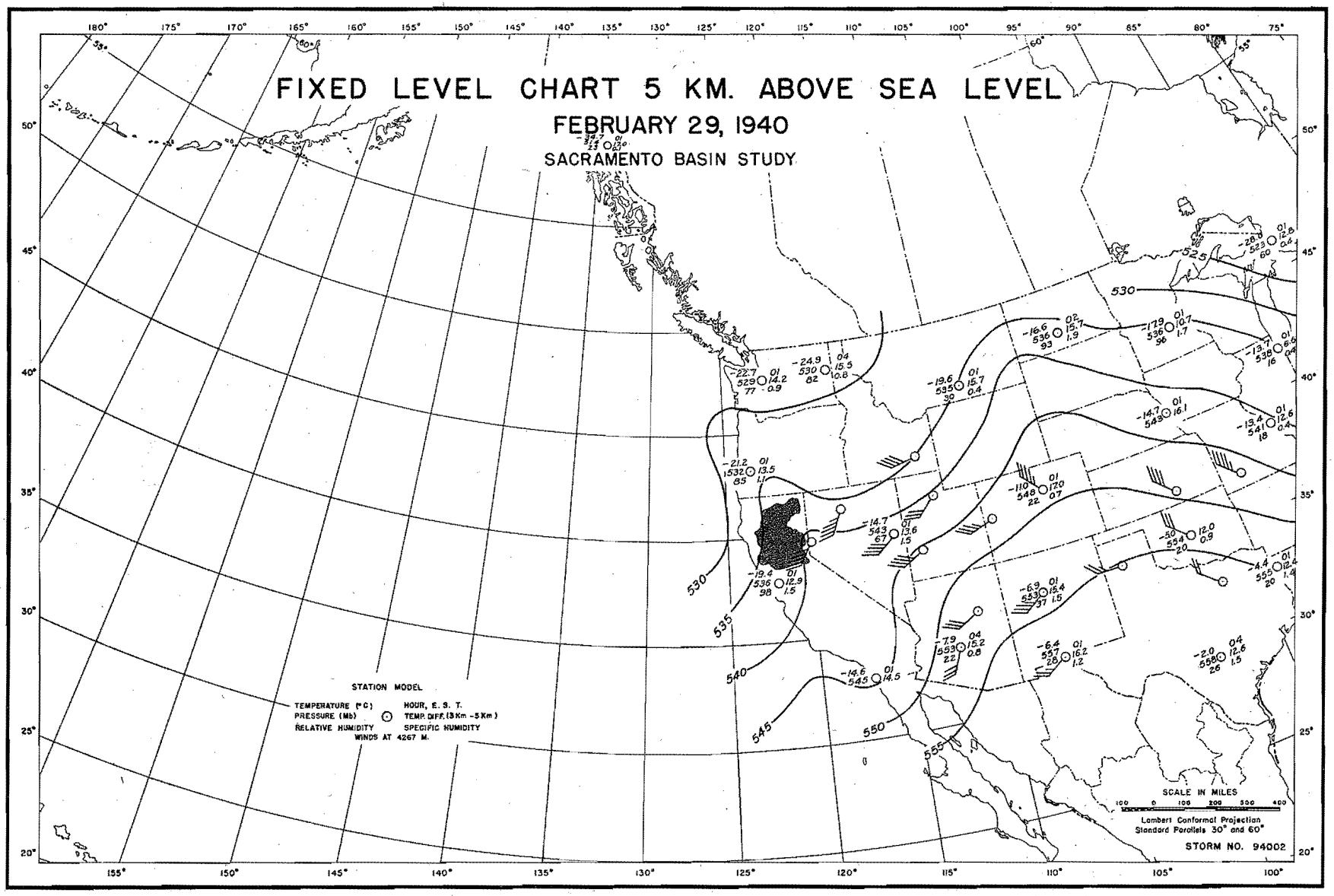
FIXED LEVEL CHART 5 KM. ABOVE SEA LEVEL
FEBRUARY 29, 1940
SACRAMENTO BASIN STUDY
STATION MODEL
TEMPERATURE (°C)
PRESSURE (Mb)
RELATIVE HUMIDITY
HOUR, E. S. T.
TEMP. DIFF. (3 Km - 5 Km)
SPECIFIC HUMIDITY
WINDS AT 4267 M.
SCALE IN MILES
Lambert Conformal Projection
Standard Parallels 30° and 60°
STORM NO. 94002

FIGURE 83

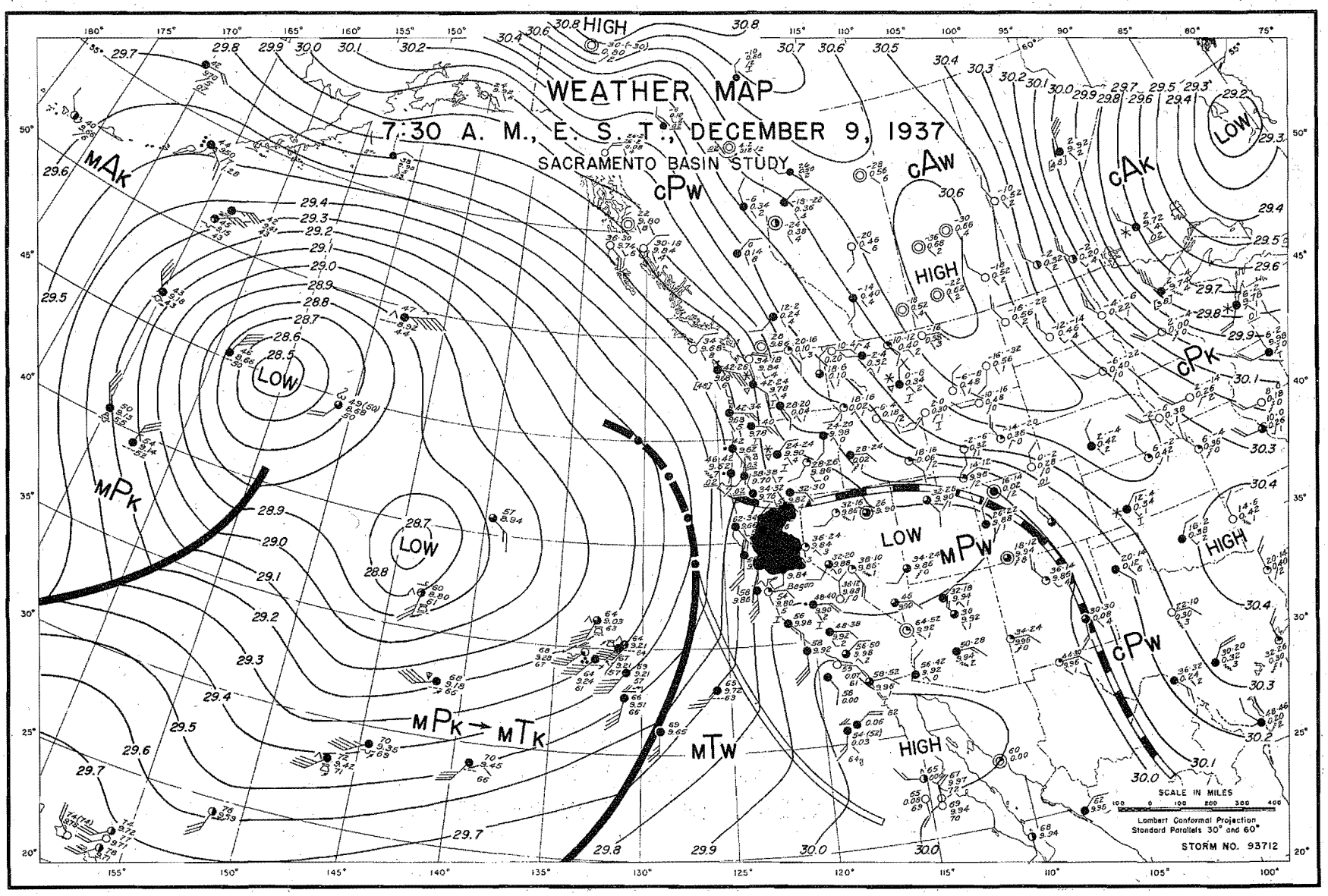
WEATHER MAP
7:30 A. M., E. S. T., DECEMBER 9, 1937
SACRAMENTO BASIN STUDY
HIGH
LOW
cPw
cAw
cAk
cPk
mAk
mPk
mPw
mPk → mTk
mTw
SCALE IN MILES
Lambert Conformal Projection
Standard Parallels 30° and 60°
STORM NO. 93712

FIGURE 84

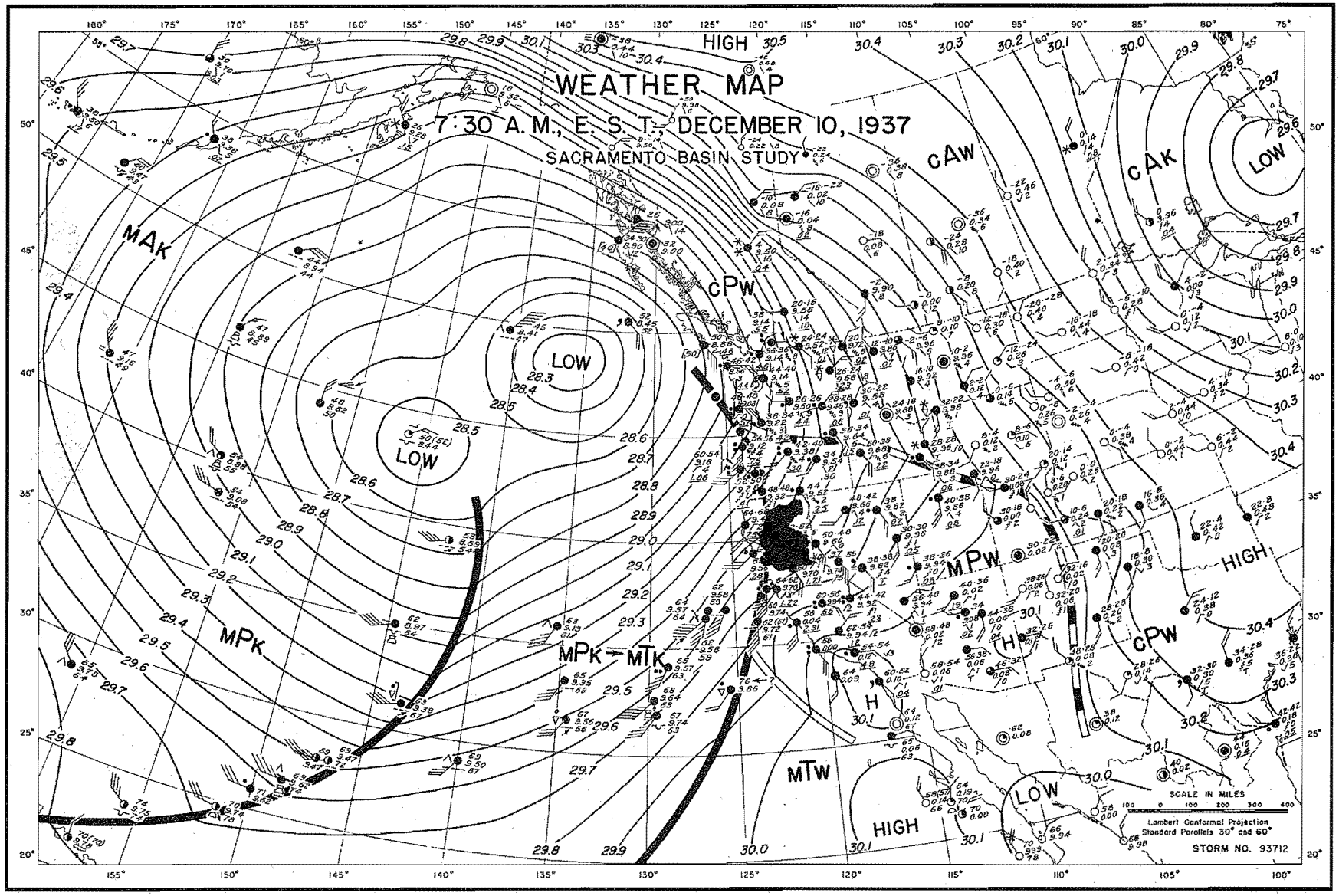
WEATHER MAP
7:30 A.M., E.S.T., DECEMBER 10, 1937
SACRAMENTO BASIN STUDY
HIGH
LOW
LOW
LOW
HIGH
HIGH
cAw
cAk
cPw
MAk
MPk
MPk → MTk
MPw
cPw
MTw
SCALE IN MILES
0 100 200 300 400
Lambert Conformal Projection
Standard Parallels 30° and 60°
STORM NO. 93712

FIGURE 85

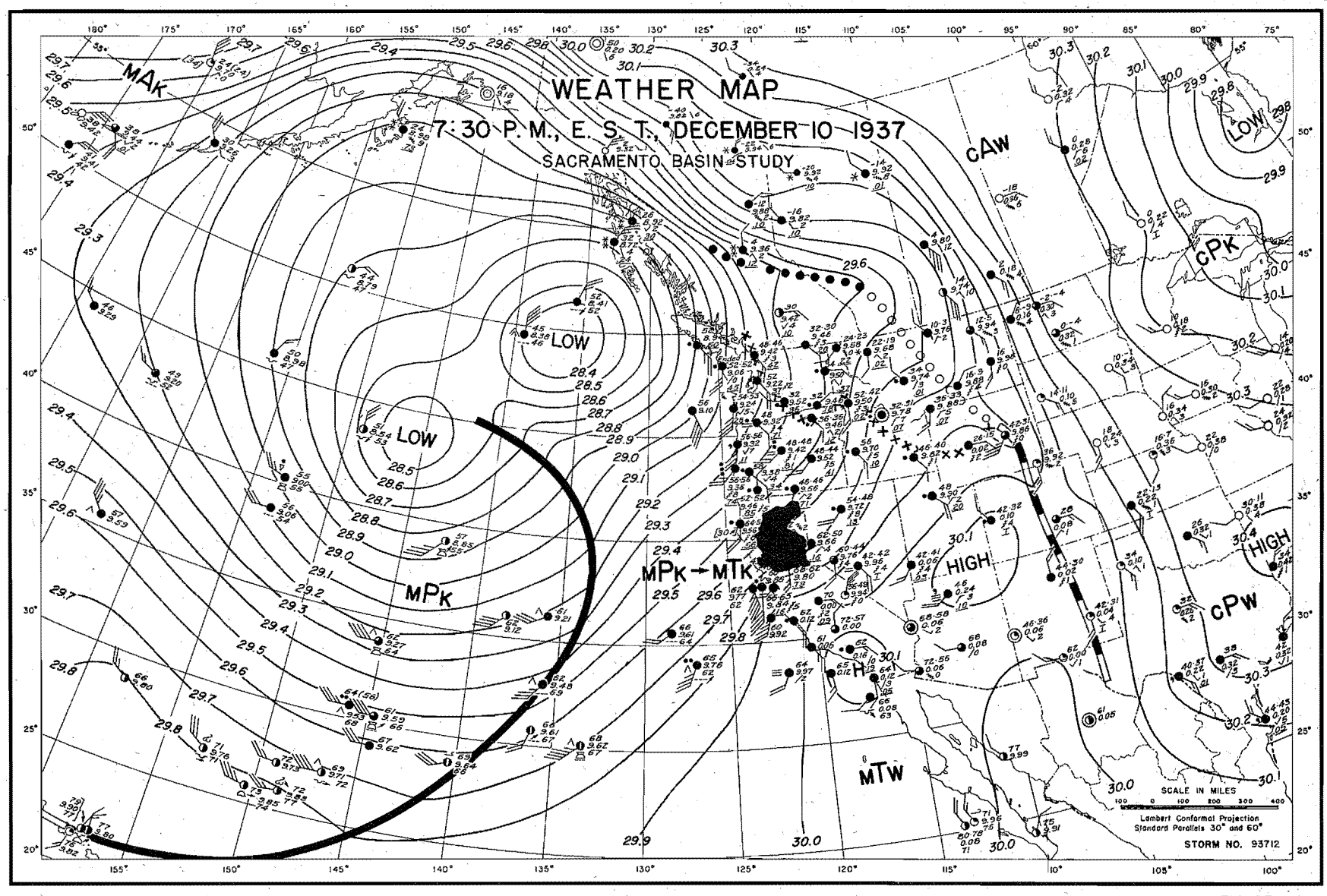
WEATHER MAP
7:30 P. M., E. S. T., DECEMBER 10 1937
SACRAMENTO BASIN STUDY
MAK
LOW
LOW
LOW
cAw
cPK
cPw
MPk
MPk → MTk
MTW
HIGH
HIGH
H
SCALE IN MILES
100 0 100 200 300 400
Lambert Conformal Projection
Standard Parallels 30° and 60°
STORM NO. 93712

FIGURE 86

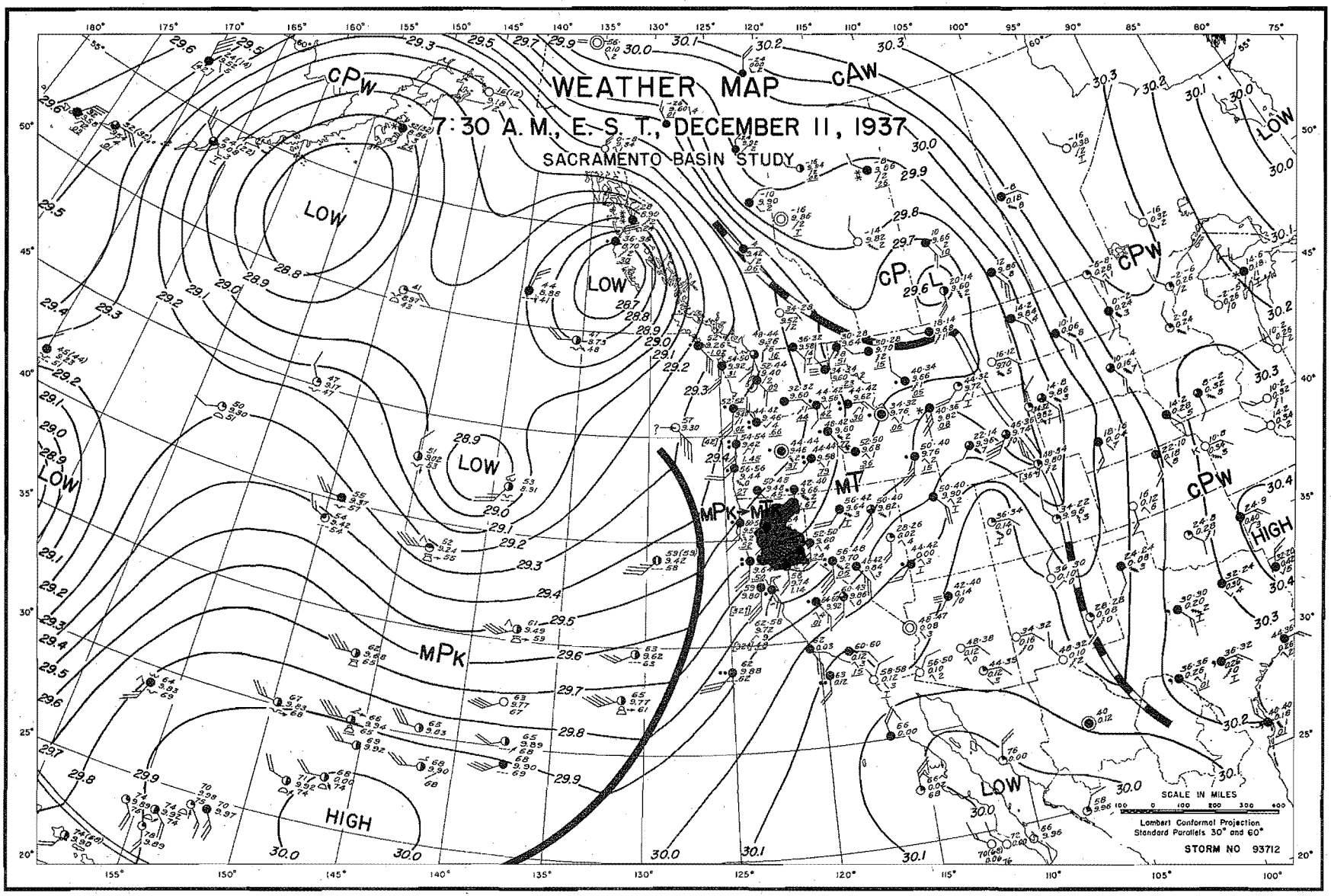
WEATHER MAP
7:30 A.M., E.S.T., DECEMBER 11, 1937
SACRAMENTO BASIN STUDY
LOW
LOW
LOW
LOW
HIGH
HIGH
cPw
cAw
cP
MPk
MT
MPk-MT
SCALE IN MILES
Lambert Conformal Projection
Standard Parallels 30° and 60°
STORM NO 93712

FIGURE 87

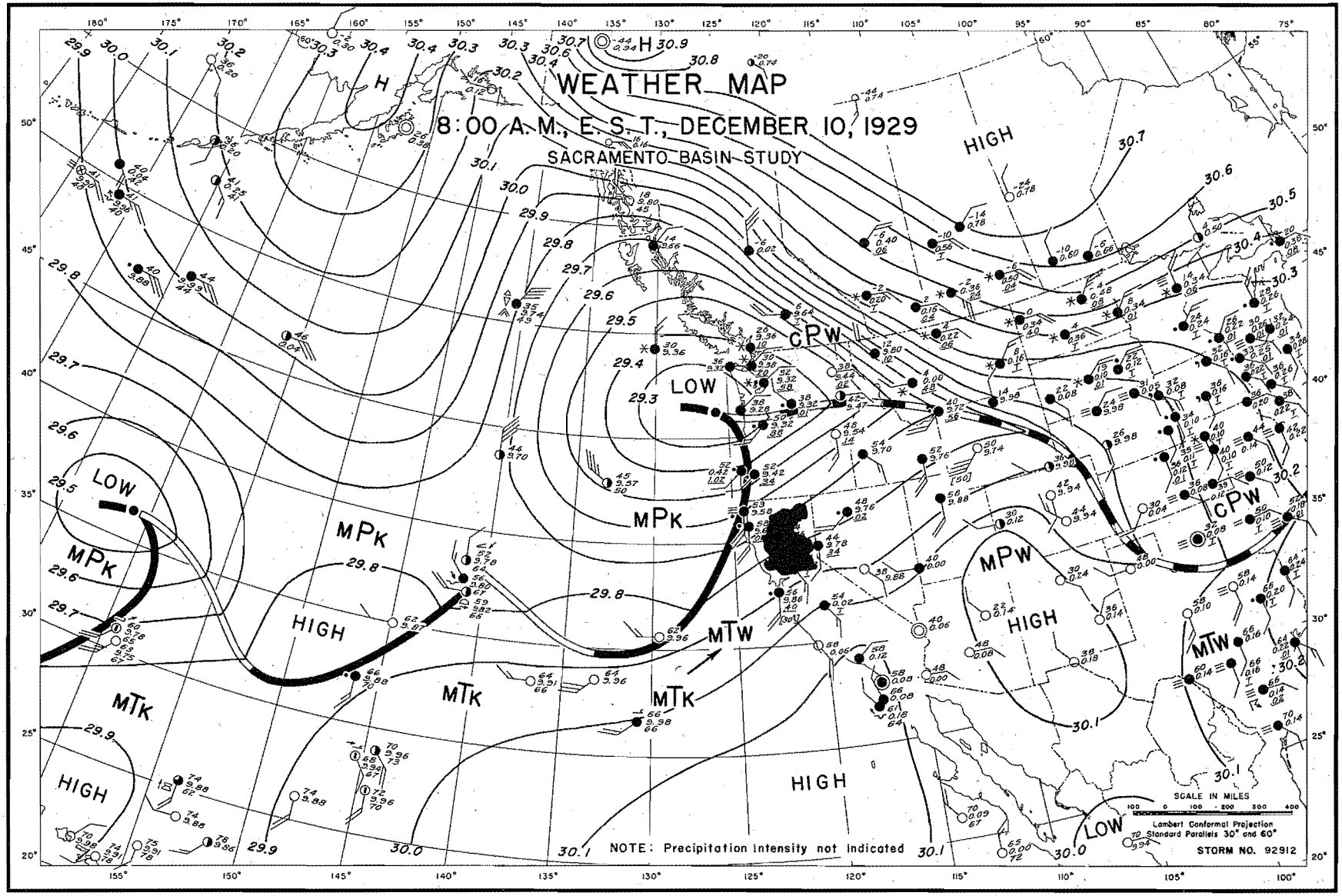
WEATHER MAP
8:00 A.M., E.S.T., DECEMBER 10, 1929
SACRAMENTO BASIN STUDY
HIGH
LOW
MPK
MTW
MTK
CPW
MPW
NOTE: Precipitation intensity not indicated
SCALE IN MILES
Lambert Conformal Projection
Standard Parallels 30° and 60°
STORM NO. 92912

FIGURE 88

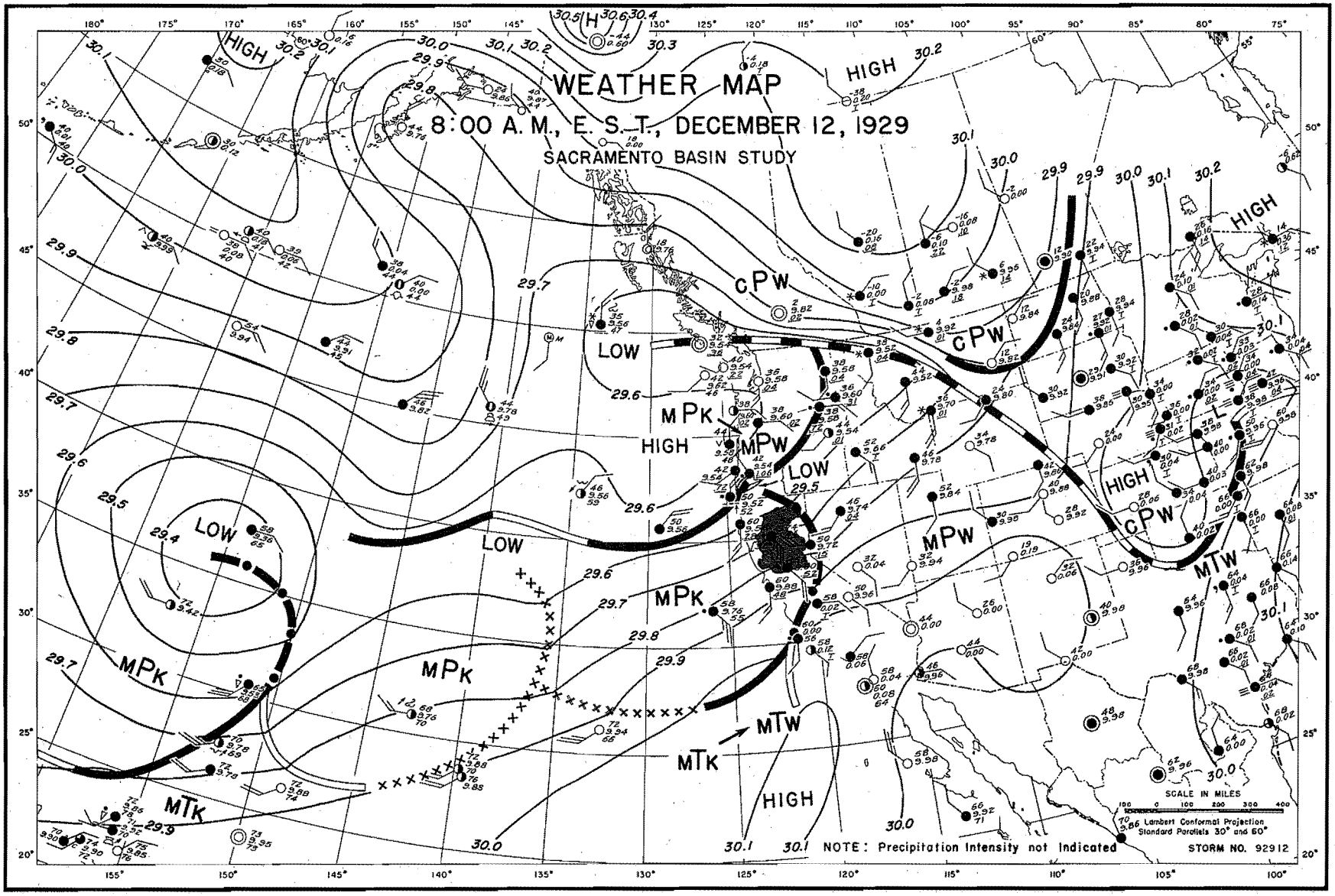
WEATHER MAP
8:00 A. M., E. S. T., DECEMBER 12, 1929
SACRAMENTO BASIN STUDY
HIGH
LOW
cPW
MPK
MPW
MTK
MTW
SCALE IN MILES
Lambert Conformal Projection
Standard Parallels 30° and 60°
NOTE: Precipitation Intensity not Indicated
STORM NO. 92912

FIGURE 89

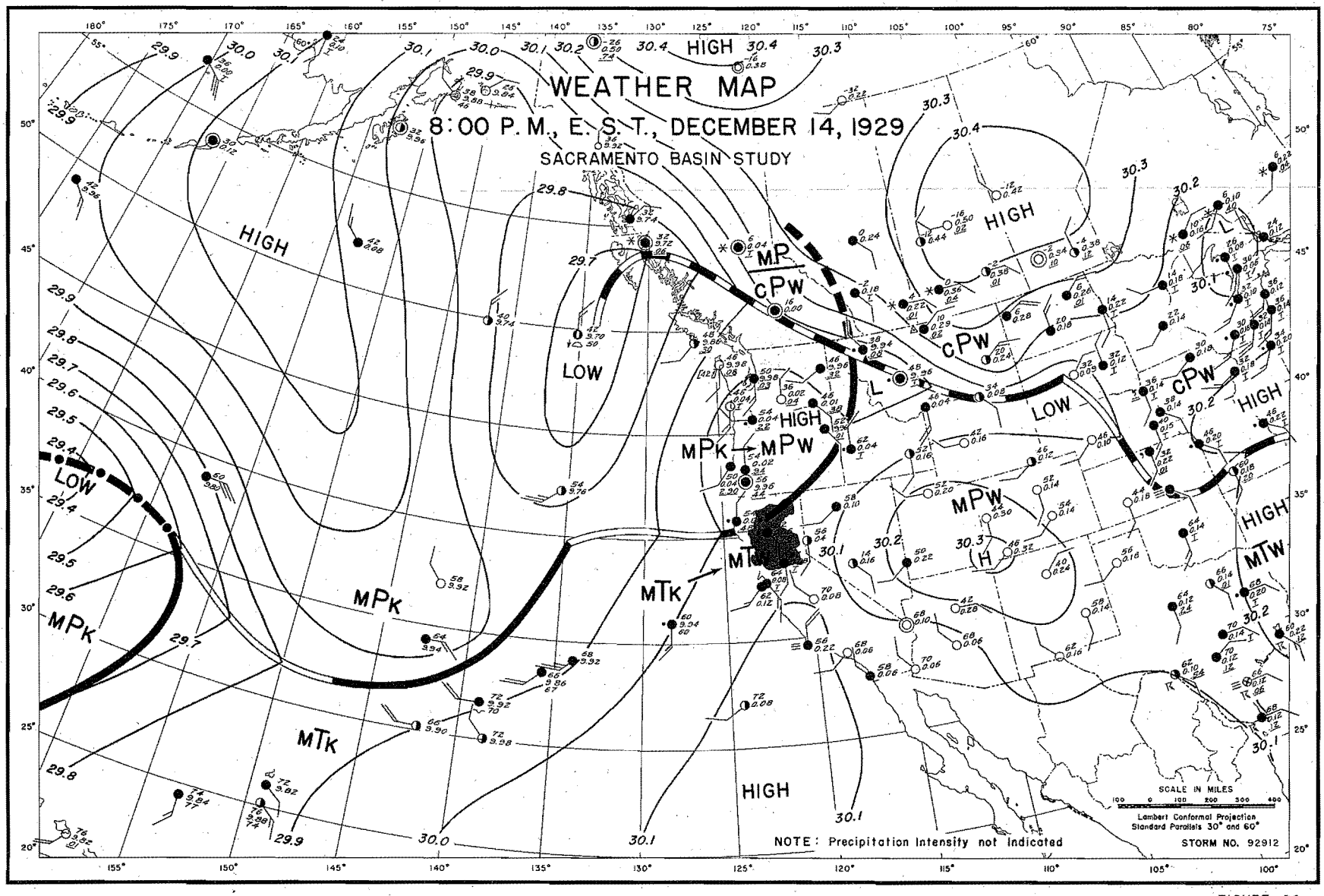
WEATHER MAP
8:00 P.M., E.S.T., DECEMBER 14, 1929
SACRAMENTO BASIN STUDY
HIGH
LOW
MPk
MPW
cPw
MP
MTk
MTW
SCALE IN MILES
Lambert Conformal Projection
Standard Parallels 30° and 60°
NOTE: Precipitation Intensity not Indicated
STORM NO. 92912

FIGURE 90

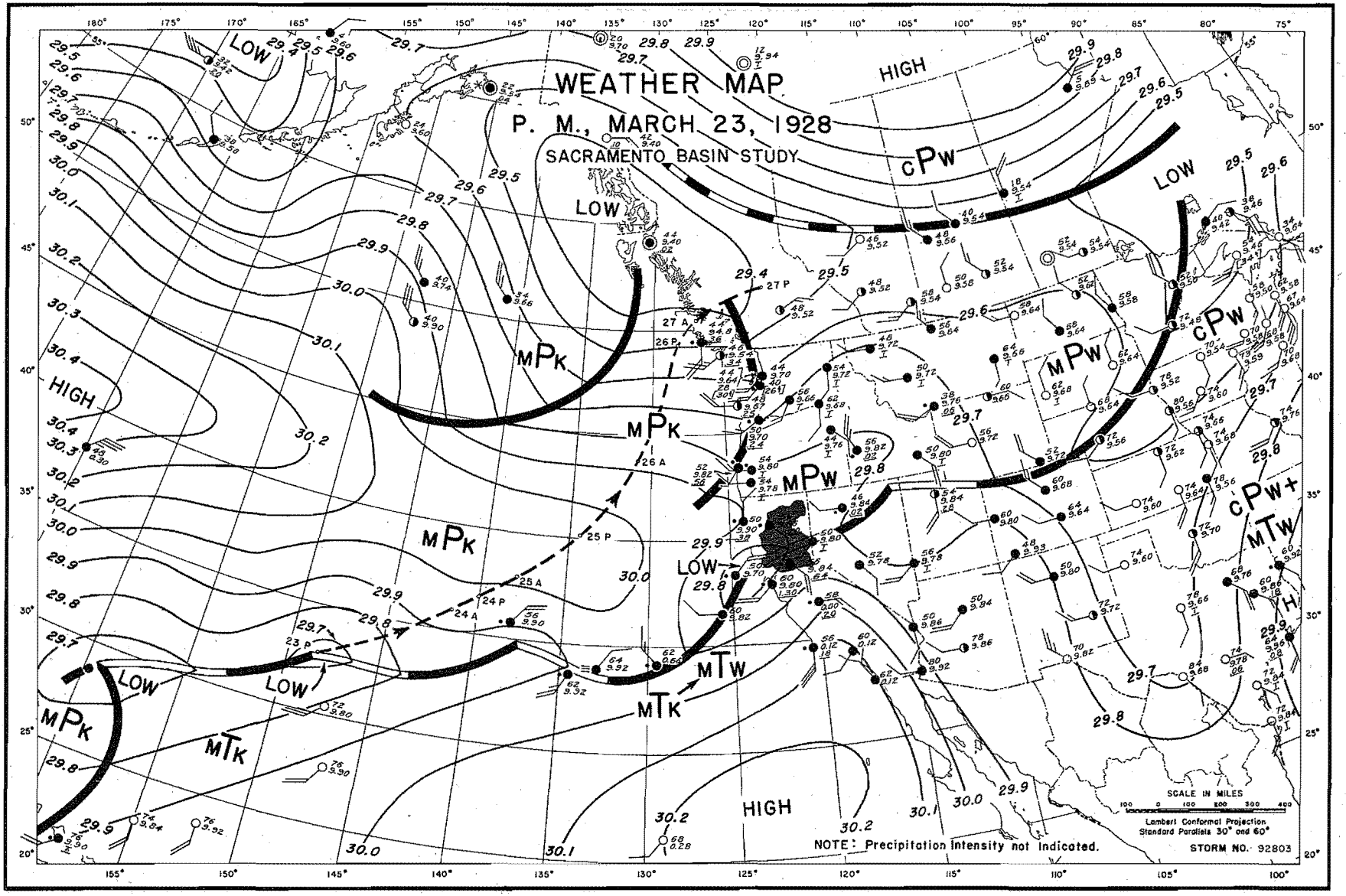
WEATHER MAP
P. M., MARCH 23, 1928
SACRAMENTO BASIN STUDY
HIGH
LOW
cPw
mPw
mPk
mTw
mTk
cPw+
HIGH
LOW
LOW
LOW
HIGH
27 P
27 A
26 P
26 A
25 P
25 A
24 P
24 A
23 P
SCALE IN MILES
100 0 100 200 300 400
Lambert Conformal Projection
Standard Parallels 30° and 60°
NOTE: Precipitation intensity not indicated.
STORM NO. 92803

FIGURE 91

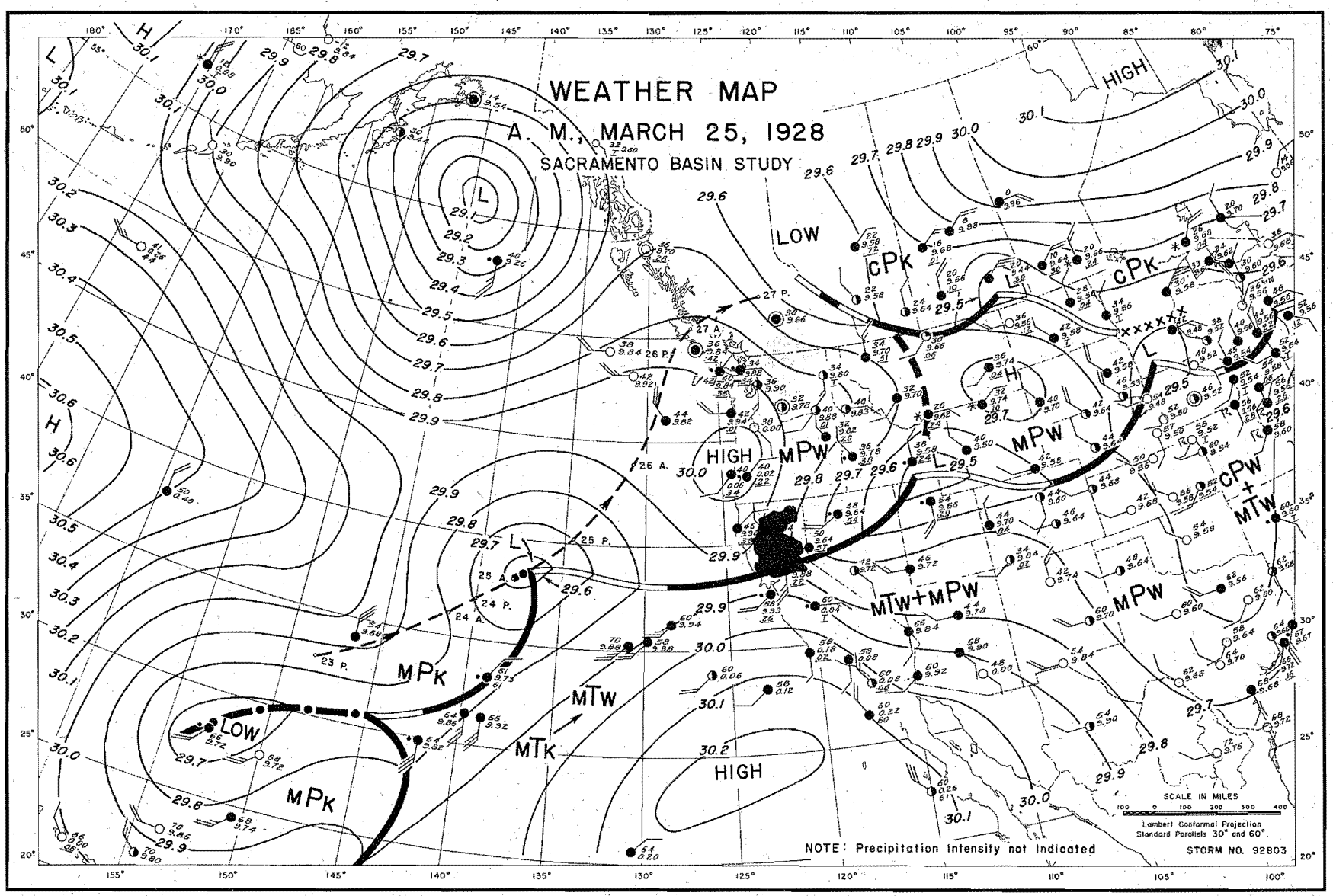
WEATHER MAP
A. M., MARCH 25, 1928
SACRAMENTO BASIN STUDY
HIGH
LOW
CPk
MPw
MPk
MTw
MTk
MTw+MPw
cPw + MTw
HIGH
LOW
HIGH
27 P.
27 A.
26 P.
26 A.
25 P.
25 A.
24 P.
24 A.
23 P.
SCALE IN MILES
100 0 100 200 300 400
Lambert Conformal Projection
Standard Parallels 30° and 60°.
NOTE: Precipitation Intensity not Indicated
STORM NO. 92803

FIGURE 92

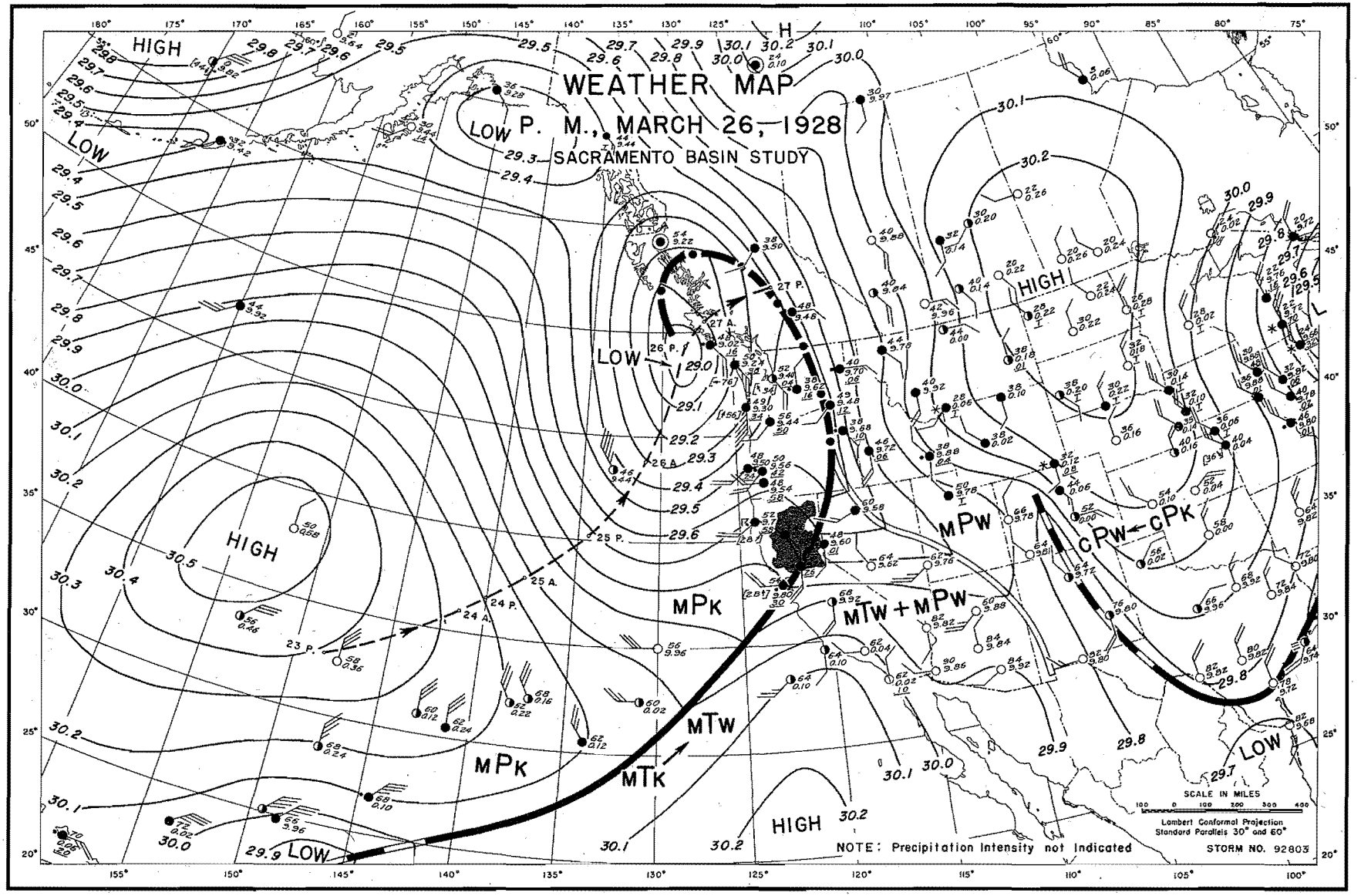
WEATHER MAP
P. M., MARCH 26, 1928
SACRAMENTO BASIN STUDY
HIGH
LOW
MPw
cPw—cPk
MPk
MTw + mPw
MTw
MTk
SCALE IN MILES
Lambert Conformal Projection
Standard Parallels 30° and 60°
NOTE: Precipitation Intensity not Indicated
STORM NO. 92803

FIGURE 93